The Role of the NHERF-1 and NHERF-2 Adapter Proteins in Intestinal Ion Transport Regulation

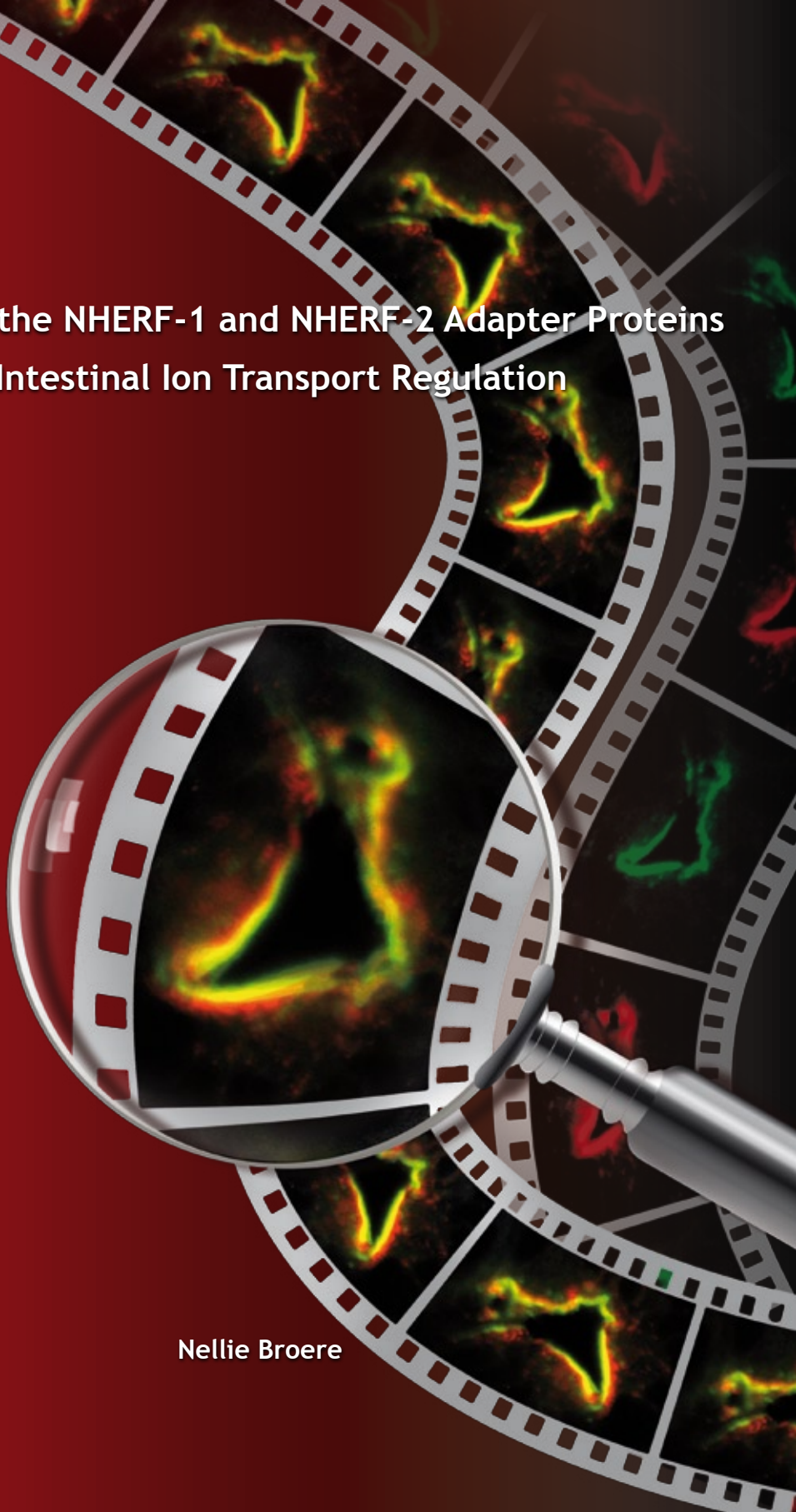

Nellie Broere

The Role of the NHERF-1 and NHERF-2 Adapter Proteins in Intestinal Ion Transport Regulation

Nellie Broere

ISBN/EAN: 978-90-9023073-3

Cover, layout and graphical assistance: Tom de Vries Lentsch

Printed by: PrintPartners Ipskamp, Enschede

The Role of the NHERF-1 and NHERF-2 Adapter Proteins in Intestinal Ion Transport Regulation

De rol van de adapter eiwitten NHERF-1 en NHERF-2
in de regulatie van ionentransport in darmepitheel

Proefschrift

ter verkrijging van de graad van doctor aan de
Erasmus Universiteit Rotterdam
op gezag van de
rector magnificus

Prof.dr. S.W.J. Lamberts

en volgens besluit van het College voor Promoties.

De openbare verdediging zal plaatsvinden op
woensdag 11 juni 2008 om 11.45 uur

door

Neeltje Broere
geboren te Rotterdam

ERASMUS UNIVERSITEIT ROTTERDAM

Promotiecommissie

Promotor:	Prof.dr. C.P. Verrijzer
Overige leden:	Prof.dr. M. Donowitz
	Prof.dr. J.A. Grootegoed
	Prof.dr. J.P.T.M. van Leeuwen
Copromotoren:	Dr. B.M. Hogema
	Dr. H.R. de Jonge

Table of contents

List of abbreviations 7

Chapter 1 General introduction 9

- Intestinal ion and fluid transport 11
- Key transporters involved in transepithelial ion transport 13
- CFTR and cystic fibrosis 15
- Na^+/H^+ exchanger 3 (NHE3) 19
- PDZ domain proteins 22
- The NHERF family of proteins 23
- Regulation of CFTR by PDZ domain interactions 26
- Regulation of NHE3 inhibition by PDZ proteins 28
- NHERF deficient mice 30
- cGMP-dependent protein kinase anchoring proteins (GKAPs) 31
- Scope of this thesis 32

Chapter 2 Cystic fibrosis transmembrane conductance regulator activation is reduced in the small intestine of Na^+/H^+ exchanger 3 regulatory factor 1 (NHERF-1) but not NHERF-2 deficient mice 41

Chapter 3 Defective jejunal and colonic salt absorption and altered NHE3 regulation in PDZ-adapter protein NHERF-1 deficient mice 61

Chapter 4 NHERF-2 is required for cyclic GMP-dependent inhibition of NHE3 but not for cGMP-dependent stimulation of CFTR 81

Chapter 5 Proteome of murine brush border membrane vesicles 93

Chapter 6 Identification of glial fibrillary acidic protein (GFAP) as binding partner of cGMP-dependent protein kinase II 117

Chapter 7 Discussion 135

Summary 149

Samenvatting 153

Curriculum vitae 159

Dankwoord 161

Color figures 164

List of abbreviations

ABC transporter	ATP-binding cassette transporter
AC	Adenylate cyclase
AKAP	Protein kinase A anchoring protein
β_2AR	β_2-adrenergic receptor
BBMV	Brush border membrane vesicle
Caco-2/bbe	Human colon adenocarcinoma derived cells, subclone BBE
CAL	CFTR-associated ligand
cAMP	Adenosine 3',5'-cyclic-monophosphate
CF	Cystic fibrosis
CFTR	Cystic fibrosis transmembrane conductance regulator
cGKI	cGMP-dependent protein kinase isoform I
cGKII	cGMP-dependent protein kinase isoform II
cGMP	Guanosine 3',5'-cyclic monophosphate
CT	Cholera toxin
DRA	Downregulated in adenoma
E3KARP	NHE3 kinase A regulatory protein (also named NHERF-2)
EBP50	Ezrin-moesin-radixin binding protein of 50 kDa (also named NHERF-1)
ENaC	Epithelial Na^+ channel
EPAC	Exchange protein directly activated by cAMP
ERM domain	Ezrin / Radaxin / Moesin binding domain
F508del	Deletion of phenylalanine at amino acid position 508 of CFTR
GFAP	Glial fibrillary acidic protein
GKAP	cGMP-dependent protein kinase anchoring protein
GST	Glutathione-S-transferase
GC-C	Guanylate cyclase C
IEC-CF7	Intestinal epithelial cell line from rat (stably expressing human CFTR)
IF	Intermediate filament
IKEPP	Intestine and kidney enriched PDZ protein (also named NHERF-4)
I_{sc}	Short-circuit current
MDCK	Madin-Darby canine kidney cells
MSD	Membrane spanning domain
NBD	Nucleotide binding domain
NHE	Na^+/H^+ exchanger
NHERF	Na^+/H^+ exchanger 3 regulatory factor
OK	Opossum kidney
PAT1	Putative anion transporter 1
PDZ	acronym of: postsynaptic density protein (PSD95/SAP90) / Discs lagre protein (Dlg) / tight junction protein ZO-1
PDZK1	PDZ domain protein from kidney 1 (also named CAP70 or NHERF-3)
PKA	Protein kinase A
PKC	Protein kinase C
R domain	Regulatory domain of CFTR
Shank2	SH3 and multiple ankyrin repeat domains 2
siRNA	Small interfering RNA
STa	Heat stable enterotoxin from *Escherichia coli*

CHAPTER 1

General Introduction

Intestinal ion and fluid transport

An important function of the human intestinal tract is the absorption of water and electrolytes. Daily, approximately 9 L of fluid enters the intestinal tract; on average 2 L from ingested food and drinks and 7 L from secretion of salivary, gastric, biliary, pancreatic and intestinal fluids. Of the 9 L, only 1 L passes into the colon, implying that 8 L is absorbed across the small intestinal epithelium (1).

The intestinal tract consists of two anatomically and functionally different compartments, the small and large intestine. The small intestine is further subdivided into duodenum, jejunum and ileum, while the large intestine is separated into cecum and colon. The gastrointestinal tract digests and absorbs nutrients from the ingested food that passes through the lumen. All segments of the intestine, from duodenum to distal colon, have mechanisms for absorbing and secreting water and electrolytes (3). Along the entire length of the intestine, mucus secreting goblet cells are present to lubricate the passage of food and to protect the gut from digestive enzymes. Tiny finger-like structures, called villi, protrude from the wall of the intestine and increase the absorptive area. The villi are lined by a single layer of epithelial cells, that contain extrusions at the luminal side, called microvilli. Together, the microvilli form the brush border (Figure 1) (4). The microvilli further increase the surface area of the intestine to 200-500 m^2, which is a 600-fold increase over the projected surface area of the human bowels (5). The entire lining of the intestine is continuously replaced by newly generated epithelial cells. The new epithelial cells divide from stem cells that lie in the crypts beneath the villi (see Figure 1 for the position of the crypts). These stem cells produce precursor cells, that go through four to six divisions before they stop dividing and differentiate into mature epithelial cells (4). In mice, the cells reach the tips of the villi within 2–5 days after emerging from the crypts. At the tips the cells undergo the initial stages of apoptosis and are finally discarded into the gut lumen (6, 7). The cells in the crypts fulfill a major role in the secretion of ions and water, whereas the epithelial cells that line the villi display a high rate of ion and water absorption.

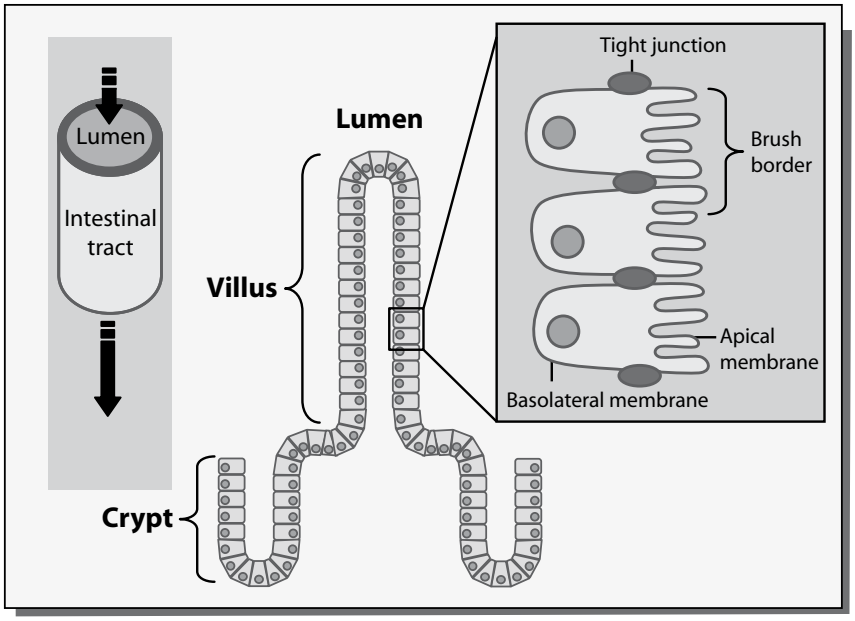

Figure 1. Schematic illustration of the intestinal morphology. Overview of the localization of crypt, villus, brush borders, apical- and basal-lateral membranes and tight junctions in the small intestine. Figure is adapted from Nelson *et al.*, 2004 (8).

The mechanisms leading to absorption and secretion of ions in the gut are interconnected, but in the 1960s they were discovered separately (3). In those days, it was found that the sodium gradient is the driving force for absorption of amino acids, oligopeptides and sugars (glucose and galactose) (9). Na^+ coupling permits organic solutes to be transported uphill (from low luminal concentrations to higher intracellular concentrations), because the Na^+ gradient is opposite to that of the organic solutes (10). During transport of organic solutes and ions, water follows the osmotic gradient. Water can be transported through the cell membrane, via water channel proteins (aquaporins) (11), or paracellularly through a complex network of proteins called the tight junction.

Initial knowledge about ion and water secretion mechanisms in the intestine originates from ion transport studies in rabbit ileum. In rabbit ileum, cyclic AMP (cAMP) and agents that increase cAMP levels in the cell (e.g. cholera toxin) stimulate chloride and water secretion and inhibit NaCl absorption (12-14). Since these observations in the early seventies, the knowledge about intestinal ion and water transport, and the transporters that are involved in these processes, has expanded rapidly.

Key transporters involved in transepithelial ion transport

Disruption of the balance between absorption and secretion of fluids and ions may lead to pathological states. Reduced salt and water absorption from the lumen, or excessive secretion, results in diarrhea. Diarrheal diseases cost millions of lives every year (mostly of children), especially in developing countries. But also traveler's diarrhea is a common problem, affecting more than 15 million travelers worldwide every year (15). Insufficient secretion of ions and water, on the other hand, can result in intestinal obstruction, as exemplified by the occurrence of meconium ileus in a subgroup of cystic fibrosis (CF) patients (as will be discussed later in this chapter).

Toxins from enterotoxigenic *Escherichia coli* strains (STa) and cholera toxin both enhance intestinal Cl^- secretion and inhibit Na^+ absorption, resulting in osmotic flow of water into the lumen of the gut (12, 13). The key intestinal Cl^- transporter, located in the apical membrane and targeted by these toxins, has been identified as CFTR (cystic fibrosis transmembrane conductance regulator). CFTR is a channel that permits the flow of chloride (and bicarbonate) from the epithelial cells into the lumen. The previously mentioned toxins override the tight and complex control normally imposed on CFTR function. As shown in Figure 2, cholera toxin irreversibly increases intracellular levels of cAMP, inducing prolonged hyperactivation of CFTR. STa, on the other hand, overstimulates the cGMP-dependent pathway. The cGMP-dependent pathway is endogenously regulated by the paracrine hormone guanylin (secreted by goblet cells) (16). Guanylin (or STa) binds to the receptor GC-C (guanylate cyclase C) and induces the production of cGMP at the cell interior. The increased levels of cGMP result in activation of the cGMP dependent protein kinase II (cGKII), which phosphorylates and activates CFTR (see Figure 2, *left panel*).

Concomitantly with the activation of CFTR, increased levels of cAMP and/or cGMP lead to the inhibition of Na^+/H^+ exchanger type 3 (NHE3) activity. NHE3 is an antiporter that absorbs Na^+ in exchange for H^+ secretion. Inhibition of NHE3 results in a reduction of sodium and water absorption (Figure 2, *right panel*). Prolonged inhibition of NHE3, induced by STa or cholera toxin, increases diarrheal water loss. The involvement of NHE3 in intestinal water transport is clearly demonstrated in mice lacking NHE3, which suffer from chronic diarrhea (17). Also patients with a defect Na^+/H^+ exchange in the jejunum develop secretory diarrhea (18, 19).

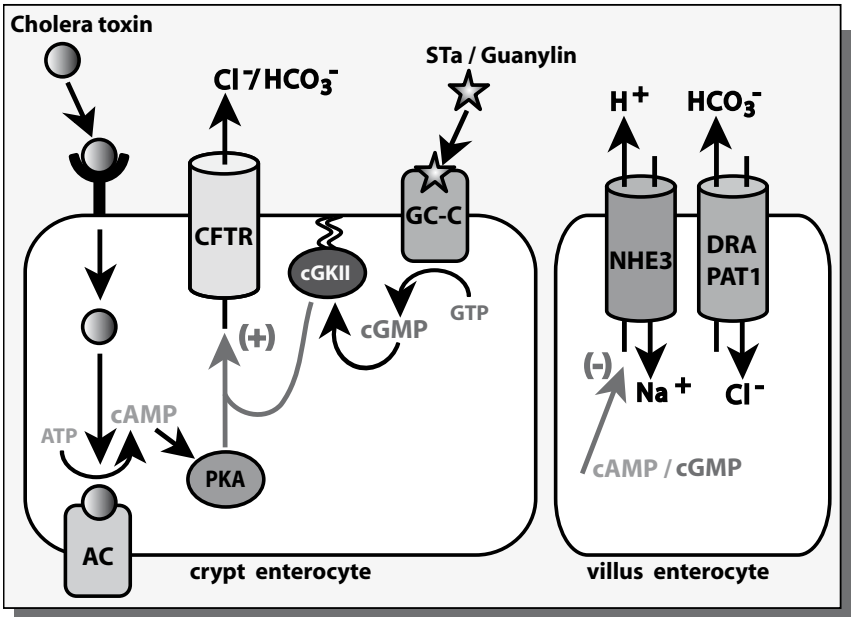

Figure 2. Overview of cAMP- and cGMP-dependent phosphorylation of the key transporters involved in transepthelial ion transport. *Left panel (depicting a crypt enterocyte)* - Under normal conditions, CFTR activity is stimulated by the phosphorylation of the chloride channel by PKA (cAMP-dependent protein kinase) and/or cGKII (cGMP-dependent protein kinase). Bacterial toxins (cholera toxin and STa) induce endured increased levels of cAMP and cGMP respectively, leading to hypersecretion of chloride (and water) from the enterocyte into the lumen of the gut, resulting in diarrhea. *Right panel (depicting a villus enterocyte)* - NHE3 is phosphorylated by cAMP- and/or cGMP-activated kinases in a similar way as CFTR. Phosphorylation of NHE3 inhibits its activity. Increased cAMP and/or cGMP levels result in inhibition of electroneutral NaCl absorption and, as a consequence, of fluid absorption. Prolonged, toxin-induced inhibition of NHE3 results in the absence of fluid absorption from the lumen of the gut, enhancing diarrhea. AC, adenylate cyclase; GC-C, guanylate cyclase C; DRA, downregulated in adenoma; PAT1, putative anion transporter 1.

Two other exchangers linked to diarrheal disorders, are the Cl^-/HCO_3^- antiporters DRA (down regulated in adenoma or SLC26A3) and PAT1 (putative anion transporter 1 or SLC26A6), it is dependent of the intestinal segment which of these two antiporters is involved (Figure 2, *right panel*). Severe diarrhea in patients with congenital chloride diarrhea (CLD) was shown to be caused by mutations in the DRA gene (17, 20). NHE3 and the Cl^-/HCO_3^- antiporters are functionally linked and take part in electroneutral NaCl absorption (21, 22). In cultured cells, DRA and PAT1 were also found to be linked to CFTR. In HEK293 cells, activation of CFTR stimulates the chloride/bicarbonate exchange by the SLC26 transporters (23), and binding of DRA to the phosphorylated R domain of CFTR increases CFTR activity (24, 25).

Until now, diarrhea is mostly treated with antibiotics and/or antimotility agents, but these therapeutics do not target the primary cause of secretory diarrhea. Further study of antisecretory agents and compounds that enhance absorption may improve

pharmacologic therapy of diarrhea. Pharmacological targeting of both the Cl^- secretory and Na^+ absorptive pathway would be an effective approach to limit the excessive salt and water loss typifying diarrheal diseases. Further exploring the regulation of CFTR and NHE3 activity by cAMP and cGMP-dependent pathways in epithelial cells of the intestine was the main purpose of the research described in this thesis.

CFTR and cystic fibrosis

The cystic fibrosis transmembrane conductance regulator (CFTR) acts both as a chloride channel and as a regulator of other transporters. CFTR is most prominently expressed in epithelia lining the airways, secretory glands, epididymis, bile ducts and intestine. The genetic disease cystic fibrosis (CF) is caused by mutations in the *CFTR* gene (26).

Cystic fibrosis is a life-threatening autosomal recessive disease, affecting one in 2500 newborn children in the western world. Although the disease remained unknown until the middle of the 20th century, a poem from the 18th century already referred to cystic fibrosis stating that "the child will soon die whose brow tastes salty when kissed", meaning that children with a salty taste suffered from a deadly disease (27). Indeed, elevated sweat salt concentration became the prime diagnostic criterion for the diagnosis of CF. The majority of the CF patients have elevated sweat electrolytes (chloride concentrations above 60 mEq/l). In 1938, CF was called "cystic fibrosis of the pancreas" because most of the clinical features associated with CF were related to abnormal functioning of the pancreas at that time (27). Later on, when pancreatic problems were treated more successfully, patients survived longer and the disease phenotype was also found to affect other mucus-secreting glands and tissues, including the intestinal tract, the intrahepatic bile ducts, the gall bladder and in particular the lungs. Because of these findings, the name was changed to the more general term "cystic fibrosis". Nowadays, 1550 mutations in the *CFTR* gene have been described (Cystic fibrosis Mutation Database: http://www.genet.sickkids.on.ca/cftr/). CF patients show highly variable clinical symptoms, even if they harbor identical mutations (28).

Although CF infants are born with unaffected lungs, lung disease forms the most life-threatening symptom of cystic fibrosis. CFTR chloride channels in lung epithelium ensure the secretion of chloride ions and, as a consequence, of water in the airway fluid. In CF airway epithelia, chloride secretion is decreased and sodium absorption is increased, resulting in the formation of dry and thick mucus (29). Because of this thick mucus, CF patients display an impaired mucus clearance and an enhanced sensitivity to infection by pathogenic bacteria (*Pseudomonas aeruginosa* and *Staphylococcus aureus*), resulting in inflammatory responses that leads to the formation of even more rigid mucus and irreversible lung damage. Approximately 85 percent of the CF patients display pancreatic insufficiency as a result of cyst formation and obstruction of the pancreatic ducts. Dysfunction of CFTR in the pancreas of CF patients reduces the secretory activity of the

tubular duct cells, which leads to blockage of the ductal system and eventually to fibrosis of the whole gland (30). Pancreatic insufficiency can be treated by oral supplementation of pancreatic enzymes.

Due to reduced water secretion in the gut, approximately 15% of the CF patients suffers from obstruction of the distal ileum or proximal colon in the neonatal period (meconium ileus). Adult patients may suffer from intestinal obstruction, known as DIOS (distal intestinal obstruction syndrome) (31). The majority of the male CF patients have reduced fertility, or infertility, due to congenital bilateral absence of the vas deferens (32, 33).

The cystic fibrosis transmembrane conductance regulator (CFTR) gene was cloned in 1989 (34-37). It consists of 27 exons and is located on the long arm of chromosome 7 (7q31). The CFTR gene encodes a 1480 amino acid chloride channel that consists of 2 membrane spanning domains (MSD1 and MSD2, each consisting of 6 transmembrane helices), two nucleotide-binding domains (NBD1 and NBD2) and a hydrophilic regulatory domain (R-domain) (38). The membrane spanning domains together form the chloride-selective pore. The fourth extracellular loop in MSD2 contains two glycosylation sites (39). Both the N-terminus and the C-terminus of CFTR are localized at the cytosolic side (see Figure 3).

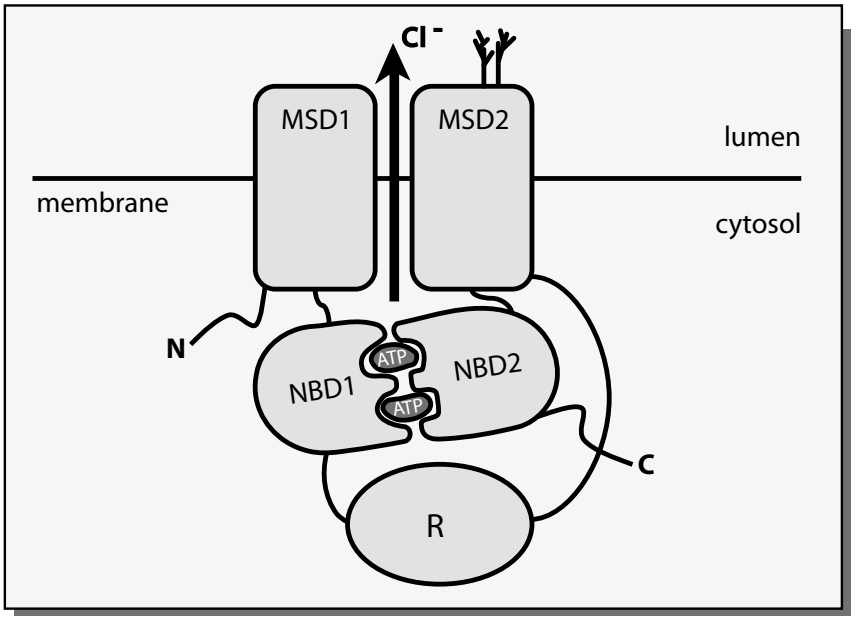

Figure 3. Domain organization of the cystic fibrosis transmembrane conductance regulator (CFTR). CFTR has the typical structure of an ABC transporter with two membrane spanning domains (MSD) and two nucleotide binding domains (NBD) at the cytoplasmic side. The regulatory domain (R) is unique for CFTR. Glycosylation of the fourth extracellular loop (of MSD2) is indicated.

CFTR is a member of the superfamily of ATP-binding cassette transporters (ABC transporters). The ABC transporters form a large superfamily of proteins that share extensive sequence similarity and a common structural organization. They consist in general of two cytoplasmatic ATP-binding domains with ATPase activity, and two membrane-spanning domains each composed of six or more transmembrane segments (40, 41). Although the general architecture of CFTR resembles the structure of most ABC transporters, the presence of the regulatory (R) domain is unique. CFTR is the sole ABC transporter that functions as a chloride channel (42). The transporters are relatively specific for a single substrate (or a group of related substrates), which can be a small molecule such as an amino acid or sugar, or a large molecule such as a polysaccharide or peptide. The human genome contains 49 ABC transporter encoding genes, and over 40 ABC family proteins have been characterized (42). The ABC transporter family includes the P-glycoprotein that is associated with multi drug resistance in tumors (MDR). MDR transporters are frequently expressed at high levels in cancer cells where they export a variety of drugs out of cells, rendering the tumor resistant to a broad spectrum of chemotherapeutic agents and posing a major obstacle to successful cancer treatment (43). Another member of the ABC transporter family is MRP4 (multidrug resistance protein 4, also named ABCC4), which was very recently found to be functionally coupled to CFTR via NHERF-3 (44).

The regulation of the CFTR chloride channel is complex and not fully understood. Opening and closing of the channel is controlled by the activity of kinases and phosphatases, the ATP levels in the cell, intermolecular interactions between the CFTR domains, and interactions with other proteins (45). Multiple kinases (e.g. PKA, cGKII and PKC) can activate the CFTR chloride channel, although the activation by protein kinase A (PKA) has been described most extensively (46). After phosphorylation of multiple serine residues in the R domain, the channel gating is regulated via ATP hydrolysis by the NBDs. The R domain contains multiple consensus PKA phosphorylation sites, of which 6 are known to be used *in vivo* (position 660, 700, 737, 768, 795 and 813). The channel is restored to its resting state after dephosphorylation of the R-domain by protein phosphatases, such as PP2A and PP2C (26, 47, 48).

Mutations in the CFTR gene can result in different structural and functional defects of the CFTR protein. Based on these differences, the CFTR-mutations have been subdivided in six classes, as shown in Figure 4 (49-51). **Class I** includes mutations that leads to premature degradation of the CFTR protein (e.g. nonsense mutations or frameshift mutations). Most of the mutations that are found in CF patients are classified in **Class II**. These mutations affect the folding of the CFTR protein. A large amount of the misfolded proteins remains associated with molecular chaperones and is targeted for degradation by the proteasomes or lysosomes (52, 53). This class also includes the most common F508del (deletion of phenylalanine at position 508) mutation. More than 90% of the CF patients carries this F508del mutation on at least one allele and these patients suffer from a severe form of CF (http://www.genet.sickkids.on.ca) (35). The third class of mutations (**Class III**)

gives rise to a CFTR protein that is normally sorted to the apical membrane, but displays an impaired phosphorylation or ATP hydrolysis, resulting in reduced activity of the channel. **Class IV** mutations affect the amino acids in the membrane spanning domains of the CFTR protein and result in a reduced Cl^- conductance. Because the CFTR cannel can still function partially, these Class IV mutations results in a mild clinical phenotype of CF (54). The fifth class of mutations (**Class V**) are often found in splice sites of the CFTR gene and cause a reduction in the production of normal CFTR protein. Atypical (non-CF) diseases associated with the CFTR gene are commonly caused by Class V and/or Class IV mutations. Examples are patients with congenital bilateral absence of the vas deferens (CBAVD) (55), obstructive azoospermia (56), disseminated bronchiectasis (57, 58) and hypertrypsinaemia (59). **Class VI** mutations harbors nucleotide alterations that affect the turnover of CFTR at the apical membrane. CF patients that harbor C-terminal truncations are classified in this class (28, 51).

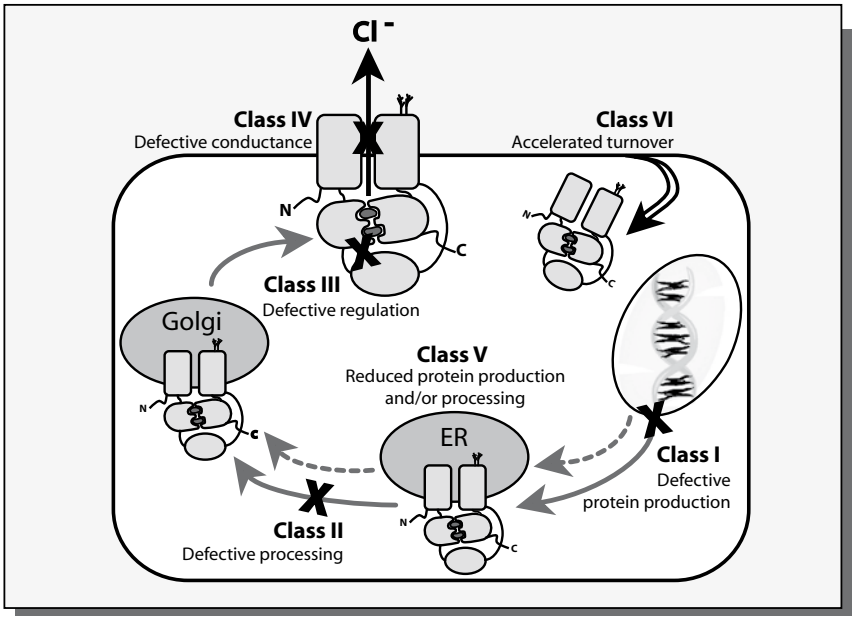

Figure 4. Schematic presentation of the different classes of CFTR mutations. Figure modified from Vankeerberghen *et al.*, 2002 (27) and Rowe *et al.*, 2005 (51).

Some mutations affect CFTR function in more than one way and therefore belong to more than one mutation class. The F508del mutation, for example, causes an arrest in maturation (Class II), slightly reduces the gating of the F508del channel (Class III) and destabilizes the protein in the plasma membrane (Class VI).

Several domains of CFTR interact, intra-molecularly, with another domain. The N-terminus of CFTR directly binds to the R domain, thereby controlling the PKA-dependent channel gating (60). In addition, the R domain can bind distal regions of CFTR, promoting R domain phosphorylation and CFTR activation (61).

As mentioned previously, apart from its role as a chloride channel, CFTR also regulates other channels and transporters. The amiloride-sensitive Na^+ channel ENaC is more active in the airways CF patients, resulting in an enhanced dehydration of the mucus layer due to increased sodium absorption (62, 63). The presence of CFTR in the kidney enhances the sensitivity of the renal potassium channel ROMK2 to the ATP-sensitive K^+-channel blocker glibenclamide (64, 65). Other proteins that are regulated by CFTR are ORCC (outwardly rectifying chloride channel), NHE3 (Na^+/H^+ exchanger 3), Kir6.1 (inwardly rectifying K^+ channel 6.1), DRA (downregulated in adenoma) and PAT-1 (putative anion transporter 1) (23, 66-71).

Besides its presence in the apical membrane, CFTR is also localized in the membranes of intracellular compartments, including the Golgi-network, pre-lysosomes and endosomes, where it is involved in the maintenance of the pH. It is still unclear by which mechanism CFTR is able to affect the pH of these compartments, but it is known that changes in vacuolar pH (alkalization or acidification) result in altered (undersialylated) glycosylation patterns (72, 73). In the lungs of CF patients *Pseudomonas aeruginosa* preferentially attaches to these undersialylated glycoproteins (74).

The role of CFTR in intestinal chloride secretion has been demonstrated by bioelectric measurements of transepithelial chloride currents in rectal biopsies from CF patients and intestinal fragments from CFTR deficient mice. Intestinal current measurements (ICM) on rectal suction biopsies in Ussing chambers were introduced more than a decade ago as new *ex vivo* diagnostic method for CF (75, 76). The Ussing chamber technique is an established method for measuring electrogenic ion transport across epithelial surfaces. This technique takes advantage of the fact that electric charge over a biological membrane leads to a shift in the transmembrane potential difference (PD). These changes in PD can be measured, allowing quantitative, real-time assessment of the activity of such electrogenic ion transport system (77). Rectal biopsies from CF patients show a reduced cAMP- and calcium-mediated chloride secretion (75, 76). In the study described in Chapter 2 of this thesis, we used the Ussing Chamber technique to measure both cAMP- and cGMP-stimulated CFTR-mediated chloride currents in different segments of the mouse intestine.

Na^+/H^+ exchanger 3 (NHE3)

Electroneutral salt absorption (followed by osmotically coupled uptake of water) in the intestinal tract and kidney is mediated, and highly regulated, by proteins from the Na^+/

H^+ exchanger (NHE) family (3). The NHEs transport Na^+ into the cells in exchange for intracellular H^+ with a stoichiometry of 1:1 (78).

In 1989, the first mammalian Na^+/H^+ exchanger was cloned by Sardet *et al*. and named NHE (79). The mammalian NHE family consists of nine isoforms that are primarily localized in the plasma membrane (NHE1-5 and -8) or reside in the intracellular organelles (NHE6, -7 and -9) (78, 80-83). All the mammalian NHE isoforms have two structurally and functionally distinct domains: an N-terminal domain consisting of 10-12 transmembrane helices and a long cytoplasmatic C-terminal domain (see Figure 5 for a schematic overview of NHE3).

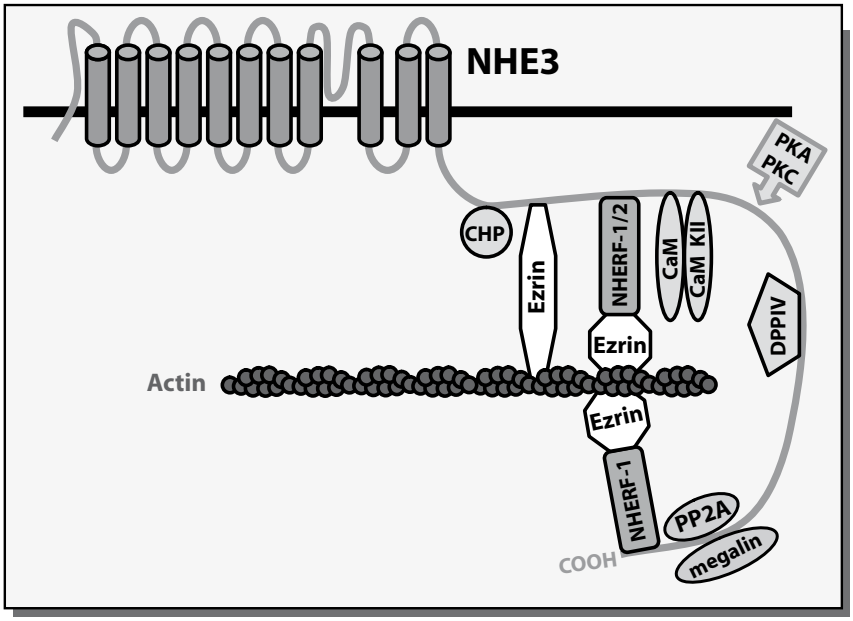

Figure 5. Schematic overview NHE3 and its C-terminal binding partners. NHE3 associating proteins and the area of their binding sites on the C terminus of NHE3 are depicted. The site of acute inhibition of NHE3 by PKA and PKC is indicated by the arrow. CHP, calcineurin B homologous protein; NHERF, NHE3 regulatory factor; CaM, Ca^{2+} calmodulin; CaM KII, CaM kinase 2; DPPIV, dipeptidyl peptidase IV; PP2A, type 2 protein serine/threonine phosphatase. Figure is modified from Donowitz *et al.*, 2007 (2).

The first Na^+/H^+ exchanger found in the intestine, NHE1, is present in the basolateral membrane of epithelial cells, where it is required for the regulation of cell volume and intracellular pH (81, 84). NHE2 and NHE3 are both expressed in the small intestine and colon and are localized in the apical membrane (85). The physiological function of NHE2 in the intestinal tract is not yet resolved. Colon from NHE2 null mice displays normal histology and absorptive function, however, the NHE3 expression level is twice as high in NHE2 deficient mice as compared to wild-type littermates (86).

NHE3, the NHE isoform focused on in this thesis, is an 89 kD protein that has been cloned from numerous species, including rat (87) and human (88). NHE3 can be found in the apical membrane of epithelial cells in the small and large intestine, the gallbladder, pancreatic ducts and the kidney proximal tubule (86, 89-93).

In conjunction with the Cl^-/HCO_3^- exchangers DRA and PAT-1, NHE3 is responsible for the majority of electroneutral NaCl absorption in the intestine and kidney (see Figure 2, *right panel*) (94-96). The Cl^-/HCO_3^- exchanger involved in the NaCl absorption process varies between intestinal segments; PAT-1 dominates in Na^+ absorptive cells in the duodenum and jejunum, while DRA is the major anion exchanger in ileum and colon (although this is species dependent) (2, 90). In the kidney, the anion exchanger involved in bicarbonate secretion appears to be PAT-1 (97).

Regulation of NHE3 activity occurs at two interrelated levels. First, the presence of NHE3 in the apical membrane is coordinated by endo- and exocytosis, and secondly the activity of the individual NHE3 molecules in the membrane is regulated by phosphorylation and dephosphorylation (98-100). In the intestinal tract, the amount of NHE3 present in the membrane is increased by end-products of digestion, like glucose and short-chain fatty acids (2). Glucose induces, via the Na^+-glucose co-transporter SGLT1, a signaling pathway that results in the stimulation of NHE3 exocytosis and lead to an increased NHE3 activity (101, 102). Apart from regulation via endo- and exocytosis, the activity of NHE3 is directly affected by phosphorylation catalyzed by cAMP-, cGMP- and Ca^+-dependent kinases (PKA, cGKII and PKC respectively). The major phosphorylation of NHE3 by these kinases is on serine, with a minor phosphorylation on threonine (103). Phosphorylation of NHE3 results in inhibition of the transporter (104-106). In contrast, phosphorylation of NHE3 by the serum- and glucocorticoid-induced protein kinase (SGK1) results in stimulation of the antiporter. The C-terminal binding partner of NHE3, NHERF-2, anchors SGK1 to NHE3 and is required for SGK1-mediated phosphorylation and activation of NHE3 (107). NHERF-2 is a member of the NHERF family of proteins (NHERF-1, -2, -3 and 4-) which will be discussed thoroughly later in this thesis.

The C terminus of NHE3 is important for the regulation of its activity because it is phosphorylated by several kinases and this phosphorylation alters the activity of the channel. Furthermore, the C terminus of NHE3 is involved in multiple interactions with other proteins (108, 109). A schematic overview of NHE3, including the known C-terminal binding partners, is shown in Figure 5.

The PDZ proteins NHERF-1 and NHERF-2 (NHE3 regulatory factor 1 and 2) were shown to bind NHE3 and are required for its phosphorylation by PKA, cGKII, PKC and SGK1 (110-112). Furthermore, the NHERF proteins link NHE3 to the cytoskeleton via ezrin binding, thereby associating NHE3 with the actin cytoskeleton and decreasing its lateral mobility (105, 113). In addition to binding ezrin indirectly (via the NHERF proteins) NHE3 can also directly bind to ezrin (114). The presence of, and connection to, an intact cytoskeleton is required for optimal trafficking and function of NHE3 (114-116). The role of the NHERF

proteins in regulation of NHE3 phosphorylation and inhibition will be discussed in more detail later in this introduction.

NHE3 activity is also regulated via dephosphorylation by phosphatases. The phosphatase PP2A (type 2 protein serine/threonine phosphatase) binds to the C terminus of NHE3 and possibly inhibits NHE3 activity. NHE3 activity was stimulated after inhibition of PP2A phosphatase activity by okadiaic acid (a PP2A inhibitor) in rabbit fibroblasts (108).

Other proteins that, so far, have been reported to directly interact with the C-terminus of NHE3 are CHP (calcineurin B homologous protein), CaM (Ca^{2+} calmodulin), CaM kinase II, DPPIV (dipeptidyl peptidase IV), megalin and Shank2 (SH3 and multiple ankyrin repeat domains 2) (see Figure 5) (2). CHP binding is required for basal NHE activity, because mutants of NHE1, NHE2 and NHE3 that can not bind to CHP showed a ~90% reduced Na^+/H^+ activity (117). The binding partners CaM and CaM kinase II are present in ileum and kidney and (Ca^{2+}-depenently) inhibit basal NHE3 activity (118, 119). DPPIV was identified as a binding partner for NHE3 via immunoprecipitation studies in OK cells. DPPIV inhibitors inhibited NHE3 activity, indicating that DPPIV activity is required for NHE3 activity (120, 121). Megalin was shown to bind NHE3, but the function of this binding has not been studied yet (122).

The most recently found C-terminal binding partner of NHE3 is Shank2. Shank2 increases the abundance and basal activity of NHE3 in the membrane of PS120 cells, whereas downregulation of native Shank2 decreased NHE3 protein expression and NHE3 activity in Caco-2 cells. Together these results suggest that Shank2 is important for NHE3 abundance and activity (123).

Consistent with its association with multiple binding partners, density gradient centrifugation indicates that NHE3 exists in ~400-900kD protein complexes. NHE3 is present in protein complexes in early endosomes and in the brush border membrane (BBM). The phosphorylation state of NHE3 affects the amount of NHE3 present in the complexes and therefore the size of the complexes (124, 125). Exposure of rabbit ileum to carbachol (which increases intracellular $Ca2^+$ levels resulting in PKC-mediated phosphorylation and inhibition of NHE3) decreases the amount of NHE3 present in the BBM and increases the amount of NHE3 in the early endosomes. In addition, the size of NHE3 complexes in the BBM increased in carbachol-exposed ileum, suggesting that carbachol treatment enhanced the association of proteins with NHE3. Indeed, NHERF-2, α-actinin-4 and PKC were co-immunoprecipitated more efficiently from BBM after carbachol treatment (126).

PDZ domain proteins

PDZ domains are one of the most commonly found protein-protein interaction domains in organisms ranging from bacteria to mammals. In humans, 1163 PDZ domains have been identified in 484 different proteins (127, 128). PDZ proteins can be found at any location in the cell and serve a key role in the formation of functional protein complexes (129, 130).

PDZ is an acronym of the first letter of the three proteins in which these modules were originally characterized: the postsynaptic density protein PSD95/SAP90, its *Drosophila* homologue Discs-large and the tight junction protein ZO-1. PDZ domains are globular structures consisting of two α-helixes and six β-sheets, with a length of 90-100 amino acids (131). Because many PDZ domains have been crystallized with their corresponding ligands, the structural basis for PDZ interaction is well understood. The PDZ domain forms a groove with a structurally conserved Gly-Leu-Gly-Phe (GLGF) sequence between their second α-helix and their second β-sheet. These residues form hydrogen bonds with a short piece of the target protein, usually the extreme C-terminal residues (127). Some PDZ domains, however, are able to interact with internal sequences, e.g. the PDZ protein NHERF-1 binds to an internal sequence of NHE3 (111). The PDZ domains are subdivided into three classes, based on the amino acids at position 0 (the last amino acid of the C-terminus) and -2 of the ligand protein: Class I (S/T-X-Φ), Class II (Φ-X-Φ) and Class III (Ψ-X-Φ), where Φ represents a hydrophobic amino acid, Ψ a negatively charged residue and X can be any amino acid (132). However, other data has suggested that these designations are too restrictive, therefore additional classes have been proposed (133, 134). A recent study characterized the binding selectivity of 157 mouse PDZ domains with respect to 217 C-terminal peptides. In this study, the above mentioned classes were recognized, but there was much overlap between the classes. Therefore, it was concluded that PDZ domains do not fall into discrete classes, but are optimized across the proteome (135).

Binding partners of PDZ proteins are of many categories and include growth factor receptors, G protein-coupled receptors, neurotransmitter receptors, transport proteins, adhesion molecules, cytoskeletal elements and transcription factors (129, 131, 132). The organizational capacity of a PDZ protein in clustering and anchoring transmembrane proteins, was for the first time shown in case of the PDZ protein PSD-95 and the Shaker K^+ channel. Expression of both proteins in a heterologous cell type resulted in the formation of a complex containing the PDZ protein and its ligand on the cell surface. This clustering was eliminated when the PDZ-binding motif in the K^+ channel was mutated (136).

The binding affinity of the ligand protein and the PDZ domain can be influenced by phosphorylation (137-141). For example, phosphorylation of the PDZ binding motif of the multidrug resistance protein 2 (MRP2) significantly increases binding of MRP2 to the PDZ proteins NHERF-1 and NHERF-4 (137).

The NHERF family of proteins

The NHE3 regulatory factor (NHERF) family of PDZ proteins consists of four members: NHERF-1, NHERF-2, NHERF-3 and NHERF-4. The NHERF proteins are expressed in numerous tissues, including the small intestine, colon and renal proximal tubules. One important function of the NHERF proteins is the regulation of CFTR and NHE3 activity (142-147). An overview of the NHERF family members is shown in Figure 6.

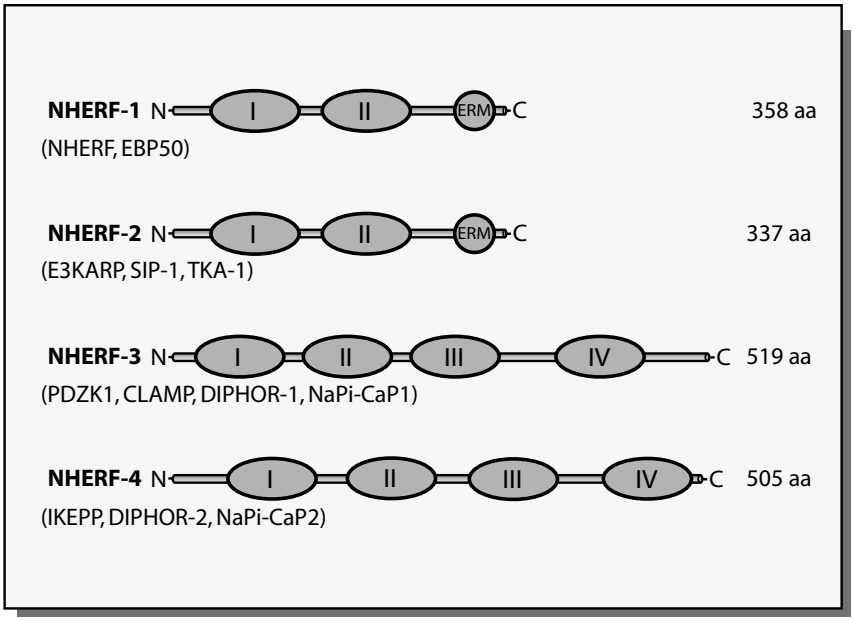

Figure 6. Overview of the NHERF family members. The N- and C-termini, PDZ domains (I, II, III and IV), the number of amino acid residues (aa), and the presence of ERM domains (ezrin-radixin moesin binding domain) are indicated. Modified from Donowitz *et al.*, 2007 (2).

NHERF-1 (also named NHERF and EBP50) was first cloned as a cofactor required for PKA-mediated inhibition of NHE3, whereas NHERF-2 (also named E3KARP, SIP-1 or TKA1) was identified as a protein that binds to the C-terminus of NHE3 in yeast two-hybrid screens (142, 143, 148). NHERF-1 and NHERF-2 are highly homologous proteins (~52% sequence identity for the human orthologs). They both contain two PDZ domains and a C-terminal ezrin-radixin-moesin (ERM) binding domain which anchors the proteins (via ezrin) to the actin cytoskeleton (149). Although several binding partners interact exclusively with NHERF-1 or NHERF-2, numerous others are capable of binding both NHERF proteins, including CFTR and NHE3 (111, 143, 147, 150). NHERF-1, in contrast to NHERF-2, is a phosphoprotein (151) and can be phosphorylated by GRK6A (G protein-coupled receptor kinase 6A), PKA, PKC and cdc2 (cyclin dependent kinase 2) (152, 153). Protein phosphatase 1 (PP1) and PP2A are able to dephosphorylate NHERF-1 (154). Phosphorylation of NHERF-1 can affect its affinity for binding to other proteins. For example, parathyroid hormone (PTH)-induced phosphorylation of Ser77 in PDZ domain I of NHERF-1 by PKA or PKC results in the dissociation of NHERF-1/Npt2a complexes. Infection of renal proximal tubule cells from NHERF-1 -/- mice with mutated NHERF-1 (Ser77 substituted with Ala) resulted in increased Npt2a-mediated phosphate transport, indicating that inhibition of renal phosphate transport is affected by NHERF-1 phosphorylation and the dissociation of

NHERF-1/Npt2a complexes (155). Very recently, it was demonstrated that phosphorylation of the C terminus of NHERF-1 (at Ser339 and 340) by PKC results in a conformational change of NHERF-1 and a abolishment of autoinhibitory intramolecular interactions. The phosphorylated NHERF-1 showed an increased binding affinity for CFTR, indicating that PKC phosphorylation might affect the ability of NHERF-1 to assemble macromolecular complexes (156).

NHERF-1 and NHERF-2 are both able to form homo- and heteromultimers via PDZ domain-mediated interactions (152, 157, 158). NHERF-1/NHERF-1 association has a low affinity, but the binding of a ligand protein can increase this affinity. For example, binding of the β_2-adrenergic receptor or the platelet-derived growth factor receptor to NHERF-1 facilitates oligomerization of NHERF-1. NHERF-2/NHERF-2 association, on the other hand, has a relatively high affinity and is hardly affected by interaction with ligand proteins (152). NHERF-1 was also shown to form heterodimers with NHERF-2 or NHERF-3, thereby facilitating the formation of protein complexes that contain binding partners of both PDZ proteins (152, 159).

The expression levels of the NHERF proteins differ per tissue. Western blots revealed a high expression level of NHERF-1 in kidney and small intestine of mice, whereas lower levels of expression were detected in liver and stomach. NHERF-1 is also expressed (often mutated) in several breast cancer tumors and has been indicated to function as a tumor suppressor in mammary epithelial cells (160, 161). NHERF-2 expression in mice is most abundant in the lung, while its expression in kidney, small intestine, liver and stomach is considerably lower (162).

NHERF-3 was first discovered as a protein that is upregulated in rats kept on a low phosphate diet and was called diphor-1 (dietary Pi-regulated RNA-1) (144). Other names for NHERF-3 are: PDZK1, CLAMP, CAP70 and NaPi-Cap1. NHERF-3 is localized in or near the apical membrane of epithelial cells in the kidney, the pancreas, the liver and the intestinal tract (159, 163, 164). NHERF-3 contains four PDZ domains but no other interaction domains and is phosphorylated at serine 509 by PKA (165). The closest homologue of NHERF-3 is NHERF-4 (IKEPP), their 4 PDZ domains share an identity of ~30-50% (145). More than 20 binding partners of NHERF-3 have been identified thus far, including CFTR, ClC-3B (chloride channel 3B) and the transmembrane mucin MUC17 (166-169).

NHERF-4 is the most recently discovered member of the NHERF family. It was found in a search for interactors of GC-C (guanylate cyclase C) (170). GC-C is the intestinal receptor for guanylin and heat-stable enterotoxin (STa). As shown in Figure 2, binding of guanylin or STa to the receptor stimulates GC-C and increases intracellular cGMP levels (171). NHERF-4 was originally named intestinal and kidney enriched PDZ domain protein (IKEPP), based on domain organization and mRNA distribution (145). Other names for NHERF-4 are: DIPHOR-2 and NaPi-CaP2 (172). Interaction of NHERF-4 with GC-C significantly reduced STa-induced GC-C activation in heterologous overexpression systems (145). The mechanism by which NHERF-4 inhibits the production of cGMP by GC-C is unknown. It has

been suggested that NHERF-4 fulfills a role in recruiting inhibitory factors to the activated GC-C receptor (170). NHERF-4 is also reported to interact with the type IIa sodium-phosphate co-transporter (NaPi IIa) (172) and the multidrug resistance protein MRP2 (137). Based on these interactions, NHERF-4 is predicted to regulate epithelial transport and signaling similar to the other NHERF proteins.

Regulation of CFTR by PDZ domain interactions

Several mechanisms were found by which the NHERF family of PDZ proteins are capable of regulating the CFTR chloride channel. These mechanisms include: regulation of CFTR phosphorylation, anchoring to the actin cytoskeleton, dimerization of CFTR, targeting to and/or retention in the apical membrane, and linking CFTR to other NHERF binding partners (45). An overview of the putative PDZ protein mediated mechanisms involved in regulating CFTR activity is given in Figure 7.

PDZ proteins and phosphorylation of CFTR – NHERF-1 and/or NHERF-2 are thought to be involved in the regulation of phosphorylation of the regulatory (R) domain of CFTR, thereby affecting the activation of the channel. NHERF-1 and/or NHERF-2 can bind both the C terminus of CFTR and indirectly also to the kinase protein. As shown in panel A of Figure 7, the NHERF proteins may serve as bridging proteins for the coupling of PKA (bound to ezrin) and CFTR (149, 173-175). The mechanism for the activation of CFTR by the Ca^{+}-dependent kinase PKC (protein kinase C) is similar: NHERF binds to the PKC-interacting protein RACK1 (receptor for activated C kinase), bringing this protein complex in close proximity of CFTR (176).

Shank2 is a PDZ protein introduced earlier as a binding partner of NHE3 (page 22). It competes with NHERF-1 for the binding of CFTR and negatively regulates CFTR activity. Shank2 is a member of the Shank family of synaptic proteins, which contain multiple domains for protein-protein interaction, including ankyrin repeats, a SH3 domain and a PDZ domain (177). An association between Shank2 and CFTR was found in yeast two-hybrid studies and verified by co-immunoprecipitation in mammalian cells (178). Shank2 functions as a bridging protein for the phosphodiesterase PDE4D and CFTR. It brings PDE4D in close proximity of CFTR, thereby decreasing the local cAMP concentration near CFTR and reducing CFTR-mediated chloride currents (178, 179). Recently, it was found that NHERF-3 might reduce the cAMP-dependent phosphorylation of CFTR by a comparable mechanism: via coupling of CFTR and MRP4. As mentioned before, MRP4 is a cAMP transporter which transports cAMP out of the cell. NHERF-3 was shown to bring MRP4 in close proximity of CFTR, resulting in reduced CFTR activity, probably via a reduction in local cAMP levels (44). However, the CFTR-dependent short circuit current and bicarbonate secretion in the jejunum of NHERF3 null mice were reduced rather than increased (180), suggesting that this mechanism is not important for CFTR regulation in the murine intestine.

Dimerization of CFTR – NHERF-1 and NHERF-3 are able to bind 2 CFTR molecules

simultaneously (Figure 7a) (140, 181). Patch clamp studies showed that CFTR dimers were more active upon PKA stimulation than monomers (167).

Linking of CFTR to other NHERF binding partners – Linking CFTR to various NHERF binding partners, including NBC3 (Na^+/HCO_{3-} cotransporter 3) (182), NHE3 (183) and Kir1.1 (inward rectifier potassium channel 1.1) (184) may contribute to regulation of ion transport. In airway epithelial cells, CFTR is coupled physically and functionally to the β_2-adrenergic receptor (see Figure 7b) by NHERF-1. Deletion of the PDZ motif from CFTR resulted in reduced CFTR activity (185). Furthermore, it was shown that the long acting β_2AR-agonist salmeterol, in a cAMP/PKA independent way, increased the amount of CFTR expressed in the membrane of human airway epithelial cells (HAEC) (186).

Anchoring of CFTR to the actin cytoskeleton – By binding CFTR and ezrin, NHERF-1 and NHERF-2 were shown to anchor CFTR to the actin cytoskeleton (149, 173, 174) (see also Figure 7). Coupling of CFTR to the actin cytoskeleton may limit the lateral mobility of CFTR in the membrane (187). CFTR was shown to have a strongly reduced half-life and in increased mobility in the cell membrane after deletion of the PDZ binding site (187-189).

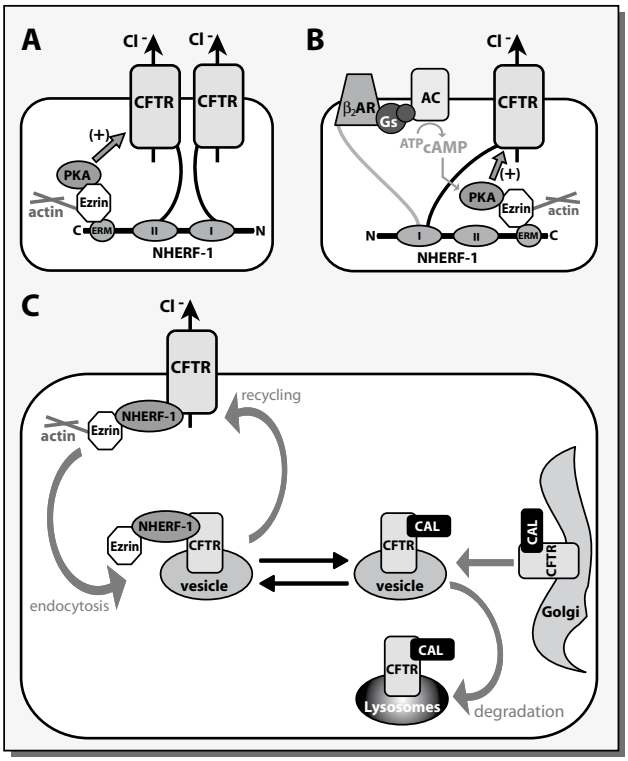

Figure 7. Model depicting the various mechanisms of NHERF-mediated regulation of CFTR activity. *A*. NHERF binds to the C-terminus of CFTR and indirectly (via ezrin) to PKA (protein kinase A). Phosphorylation by PKA stimulates CFTR activity. NHERF-1 might function as a bridging protein to bring PKA and CFTR together. NHERF-1 and NHERF-3 (the latter is not indicated in the figure) are able to bind 2 molecules of CFTR simultaneously, and dimerization of CFTR enhances the open probability of the channels. *B*. Activation of the β_2-adrenergic receptor (β_2AR) leads to G_s-mediated activation of adenylate cyclase (AC). Increased levels of cAMP subsequently stimulate PKA-mediated activation of CFTR. β_2AR, PKA and CFTR might be kept in the same signaling complex by binding to NHERF-1. *C*. The PDZ proteins NHERF-1 and CAL compete for binding to CFTR. Binding of CFTR to NHERF-1 anchors the channel (via ezrin) to the actin cytoskeleton, thereby reducing its lateral mobility in the apical membrane. However, binding of CFTR to CAL (CFTR associated ligand) can stimulate its degradation by targeting CFTR to the lysosomes. Figure is modified from Guggino *et al.*, 2006 (45).

Targeting of CFTR to, and retention in, the apical membrane – The role of the C-terminal PDZ binding domain for trafficking of CFTR to the apical membrane has been subject to debate and remains controversial. Several studies, using CFTR proteins with a mutated C-terminus indicated that interaction of CFTR with PDZ domain proteins is required for correct sorting (targeting) of CFTR to the apical membrane because these mutants were also localized in the basolateral membrane of MDCK and airway cells (190-192). However, these results were not confirmed in several very similar other studies. (188, 193, 194). A major disadvantage of the use of C-terminally mutated CFTR is that the interaction with all PDZ domain proteins is lost and the role of individual binding partners could not be studied. The first studies of CFTR function in mice lacking individual PDZ domain proteins were therefore eagerly awaited.

CFTR is endocytosed and recycled back to the membrane continuously and the NHERF proteins may affect these processes. It has been suggested that the PDZ protein CAL (CFTR associated ligand) competes with NHERF-1 for CFTR binding and thereby negatively regulates the amount of CFTR in the membrane (Fig. 7c). CAL (also named PIST or FIG) contains one PDZ domain and is most abundantly localized in the Golgi apparatus. CAL expression can reduce the total and cell-surface protein expression of CFTR by targeting CFTR for degradation in the lysosomes (195).

It has been found that NHERF-1 might not only affect the targeting of CFTR, but also the targeting of F508del-CFTR to the apical membrane. Over-expression of NHERF-1 in CF airway cells resulted in redistribution of F508del-CFTR from the cytoplasm to the apical membrane and increased the PKA-dependent chloride secretion (196). Furthermore, it was recently shown that β-estradiol upregulates NHERF-1 expression and increases functional expression of F508del-CFTR in cultured cells (197). Rescue of functional F508del-CFTR is of clinical relevance to CF patients.

Regulation of NHE3 inhibition by PDZ proteins

Regulation of NHE3 via the NHERF proteins was first studied in several cell lines. Studies with a PS120 cell line (stably transfected with NHE3) demonstrated that neither NHERF-1 nor NHERF-2 are required for basal NHE3 activity (143), but (as shown in Figure 8) the NHERF proteins are required for the cAMP-, cGMP-, and Ca^{2+}-dependent inhibition of NHE3.

NHERF-1 or NHERF-2 enable the formation of a complex containing NHE3 and ezrin, bringing PKA (bound to ezrin) in close proximity to NHE3, resulting in inhibition of NHE3 via its direct phosphorylation (Figure 8a) (111, 198, 199). In contrast, cGMP-mediated regulation of NHE3 is exclusively NHERF-2 dependent. NHERF-2 binds both NHE3 and the cyclic GMP dependent kinase II (cGKII), which phosphorylates NHE3, leading to its inhibition (Figure 8b). NHERF-1 is not able to bind cGKII and therefore can not facilitate the cGMP-dependent inhibition of NHE3 (105, 112). As shown in Figure 8c, in response to increased intracellular Ca^{2+}-levels a complex is formed, including NHE3, PKC, NHERF-2 and

α-actinin-4. This complex may be involved in the endocytosis of NHE3 (200). Stimulation of NHE3 activity can occur as a consequence of competition of NHE3 and the β_2-adrenergic receptor for NHERF-1 binding. Because only activated β_2AR interacts with NHERF-1, activation of the receptor can lead to the disruption of NHERF-1/NHE3 interactions and reduced PKA-mediated NHE3 inhibition (201, 202).

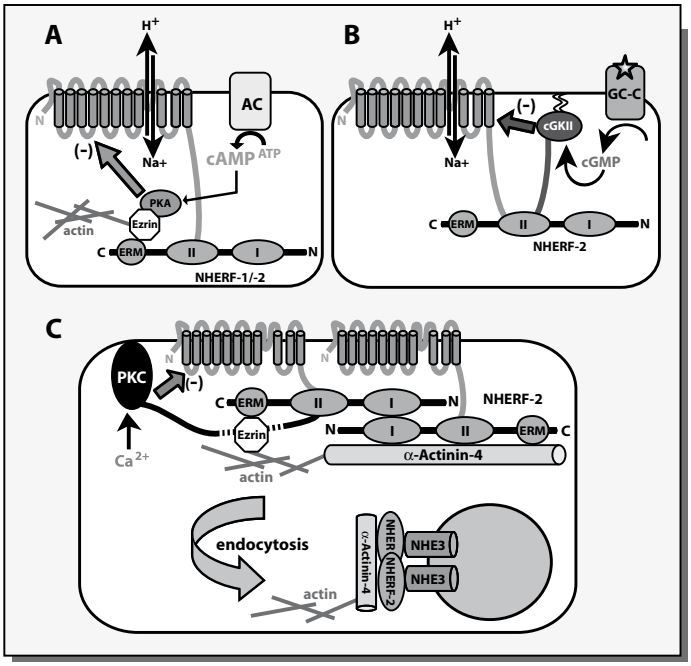

Figure 8. Model of putative NHE3 complexes promoting NHERF-mediated inhibition of NHE3. *A*. NHERF-1 or NHERF-2 links NHE3 via ezrin to PKA and actin. cAMP activates PKA which phosphorylates NHE3 resulting in its inhibition. *B*. NHERF-2 binds both NHE3 and cGKII and is required for the cGMP-mediated inhibition of NHE3. cGMP levels are increased after activation of guanylate cyclase C (GC-C). Ezrin is not necessary for the cGMP-dependent inhibition of NHE3, perhaps because the complex is fixed to the apical membrane by myristoylation of cGKII. *C*. Ca^{2+}-activated PKC phosphorylates and inhibits NHE3. Complex formation of NHE3, NHERF-2, α-Actinin-4 and PKC may induce endocytosis of NHE3. Figure is modified from Donowitz *et al.*, 2007 (2).

Recently, it has become clear that cAMP-mediated inhibition of NHE3 is regulated via different mechanisms in kidney and ileum of mice (203). As mentioned before, increased levels of cAMP stimulate PKA, but they also activate EPAC (exchange protein directly activated by cAMP). EPAC acts as a GDP/GTP exchange factor (GEF) for the small GTPases Rap1 and Rap2 and activates these proteins (204). EPAC is involved in various processes, including cAMP-regulated insulin secretion, regulation of the H^+/K^+-ATPase in the kidney cortical collecting duct and NHE3 inhibition in OK cells (205-207). The EPAC-mediated inhibition of NHE3 is phosphorylation independent (208). In the proximal tubule of mice, NHE3 activity is inhibited by cAMP via both PKA and EPAC, and both inhibitory pathways are NHERF-1 dependent. In contrast, cAMP inhibits ileal NHE3 only by a PKA-dependent pathway, which unexpectedly was independent of NHERF-1 (203). A final mechanism whereby one of the NHERF proteins affect NHE3 regulation is the NHERF-2-dependent NHE3 stimulation by LPA (lysophosphatidic acid). In opossum kidney (OK) cells expressing NHERF-2, LPA treatment increased the surface expression of NHE3. Most likely, NHERF-2 is required to increase LPA-induced phospholipase C (PLC) activity in these cells, resulting in PLC-dependent Ca^{2+} elevation and increased exocytosis of NHE3 (209, 210).

NHERF deficient mice

Different mouse strains that are deficient for NHERF-1, NHERF-2 or NHERF-3 have been generated. For NHERF-1 two independently generated knockout models have been described. The first NHERF-1-deficient mouse model was generated by Shenolikar *et al.*(2002), by using homologous recombination targeting exon 1 of the mouse NHERF-1 gene. These NHERF-1-deficient mice displayed increased secretion of phosphate in the urine, due to a redistribution of Npt2a in the proximal tubule (211). Decreased membrane abundance of Npt2a in the absence of NHERF-1 resulted in reduced Na^+-dependent phosphate reabsorption compared to wild-type controls (155, 212, 213). NHERF-1 was not only required for the apical targeting of Npt2a, but also for the rapid reduction of Npt2a membrane abundance that is induced by PTH. NHERF-1 phosphorylation at Ser 77 (by PKC) was recently shown to lead to dissociation of the Npt2a/NHERF-1 complex and resulted in internalization of Npt2a in the membrane of the proximal tubule cells (155).

Female NHERF-1 null mice exhibited a lower body weight and a reduced lifespan. Some of these NHERF-1-deficient females suffered from severe osteoporosis and bone fractures, whereas other female NHERF-1 null littermates looked normal. These “normal” NHERF-1-deficient females (i.e. not suffering from osteoporosis) were used to establish a NHERF-1 null mouse colony (211, 214).

The level of NHE3 protein and its localization were unaltered in the NHERF-1 null mice, both in the proximal tubule and in enterocytes. However, the cAMP-dependent inhibition of NHE3 in the proximal tubule was strongly reduced and the cAMP-stimulated phosphorylation of NHE3 was no longer observed, confirming the model in which NHERF-1 facilitates the formation of a complex containing NHE3 and PKA (211, 215).

The second NHERF-1-deficient mice strain, generated by Morales *et al.* (2004), did not suffer from increased mortality, but (as in the first mentioned NHERF-1 null mice) serum phosphate was decreased. The animals demonstrated a strong down-regulation of ezrin protein levels and had disorganized intestinal microvilli, dispersed actin-rich terminal webs and an increased number of goblet cells in the small intestine (216).

NHERF-2-deficient mice were generated in our lab and are described for the first time in this thesis (see Chapter 2).

NHERF-3 null mice were generated by Kocher *et al*, (2003), they developed normally and did not display any gross phenotypic abnormalities (146). However, reduced expression of the HDL receptor SR-B1 in the liver resulted in two-fold increased plasma cholesterol levels (217). Furthermore, similar to NHERF-1-deficient mice, NHERF-3 null mice demonstrated a reduced level of Npt2a in the apical membrane leading to increased renal phosphate excretion when fed on a high-phosphate diet, but in contrast to NHERF-1 null mice the downregulation of Npt2a by PTH was normal (218). Levels of CFTR mRNA expression were unaltered in the NHERF-3 null mice, but the small intestine displayed a mild reduction in maximal CFTR-mediated chloride currents (180). Furthermore, the forskolin-mediated duodenal anion secretion (reflecting CFTR activity) was slightly

decreased in these mice, whereas in jejunum the basal and forskolin-inhibited NHE3-mediated sodium absorption was profoundly reduced (180, 219). NHE3 mRNA expression level was significantly increased in small intestinal mucosa of NHERF-3 null mice. However, total enterocyte and BBM abundance of NHE3 was not significantly different, suggesting an increased NHE3 turnover (180).

cGMP-dependent protein kinase anchoring proteins (GKAPs)

cGKII is bound to the plasma membrane via a N-terminal myristoyl group. This insertion in the membrane is required for cGKII to cGMP-dependently phosphorylate and stimulate CFTR (220, 221). Various GKAPs (cGMP-dependent protein kinase anchoring proteins) are known that bind to cGKI and target it to the proper substrate proteins. It was unknown whether protein interactions were also required to target cGKII to its substrates until it was observed that NHERF-2 is required for the cGMP-dependent inhibition of NHE3. By acting as a GKAP, NHERF-2 is required to bring cGKII in close proximity of NHE3 and to allow cGMP-mediated phosphorylation of NHE3 (105, 112)(Chapter 4 of this thesis). To learn more about the functions of cGKII and to find novel binding partners for this kinase we used cGKII as a bait in a yeast two-hybrid screen, and identified glial fibrillary acidic protein (GFAP) as a new interaction partner.

GFAP is an intermediate filament (IF) protein expressed in glial cells and belongs to the type III subclass of IF proteins. Intermediate filament proteins are composed of an amino-terminal head domain, a central rod domain and a carboxy terminal tail domain. Multimerization of GFAP is regulated by phosphorylation and dephosphorylation of the head domain (222). Various protein kinases are known to phosphorylate the N-terminus of GFAP, including PKA, Ca^{2+}/calmodulin-dependent protein kinase II (CaMK II), protein kinase C (PKC) and cdc-2 kinase (223, 224). Dephosphorylation of GFAP has received less attention. In the rat hippocampus GFAP dephosphorylation is mainly catalyzed by protein phosphatase 1 (PP1) (225). GFAP is mainly expressed in astrocytes in the central nervous system (226). Intriguingly, hardly any specific function has been attributed to GFAP. Mice lacking GFAP develop normally and show no obvious anatomical abnormalities in their central neural system, behavior or memory. However, they display post-traumatic reactive gliosis, a deficiency in long-term depression and exhibit a significant impairment of eyeblink conditioning (227-229). Furthermore, glutamate transport activity is reduced in GFAP null mice (230). Formation of a complex containing GFAP and the glutamate transporter GLAST (as well as NHERF-1 and ezrin) was recently observed and co-expression of GFAP and NHERF-1 was shown to increase the transport of the glutamate analogue D-aspartate (231). Regulation of glutamate transporters, including GLAST, is important to protect the brain against glutamate-mediated excitotoxicity and the regulation of GLAST is the first function of GFAP identified at the molecular level (231).

cGKII has several known functions in the brain (232). cGKII deficient mice display changes in the resetting of the circadian clock in the suprachiasmatic nucleus (SCN) at the base of the hypothalamus (233). Furthermore, cGKII deficient mice display a strong increase in anxiety-like behavior and a reduced sensitivity to the hypnotic effect of ethanol (234). Although a physiological role of binding of GFAP to cGKII remains to be determined, we observed that the amount of GFAP protein is increased in cells expressing active cGKII (Chapter 6).

Scope of this thesis

The present study was inspired by the research reviewed in this introduction. Whereas the knowledge about the function of PDZ proteins based on studies in numerous cell lines has expanded rapidly, their physiological function in native intestinal epithelia was never studied before. A major goal of our research was to fill in this gap of knowledge by focusing on the possible roles of the NHERF proteins in intestinal ion transport, using mice lacking one or more of the NHERF proteins. We exploited NHERF-1 and generated NHERF-2 and NHERF-1/-2 double deficient mice to investigate the roles of these proteins in the cyclic nucleotide dependent regulation of both CFTR and NHE3. CFTR and NHE3 are the key transporters of Cl^- and Na^+ across the intestinal epithelial layer (**Chapter 2 and 3** respectively). By this approach we attempted to avoid some major disadvantages of cultured cell studies, i.e. the use of over-expression models and/or poorly polarized cells (often of non-epithelial origin) and to gain a better understanding of the physiological mechanisms of intestinal ion transport.

In our studies we were especially interested in the function of the PDZ proteins NHERF-1 and NHERF-2, as previous research in cultured cells had indicated that these proteins could play a role in the regulation of both CFTR and NHE3, and therefore might affect both secretion and absorption processes in the gut. Another new approach in our studies on the roles of the NHERF proteins in the regulation of CFTR and NHE3 activity was to downregulate NHERF-1 and/or NHERF-2 expression in polarized epithelial cells and to examine the consequences for CFTR-mediated chloride efflux and NHE3 activity in these cells (**Chapter 4**).

To better understand the unique aspects of the system biology of the gastro-intestinal epithelia we also considered it important to know the structural composition of the apical region of these epithelial cells. To this aim we started off by identifying the proteome of the murine jejunal brush border (**Chapter 5**). Knowledge of the brush border proteome of wild-type mice is a prerequisite for future comparisons with the proteome of NHERF deficient mice, which will learn us more about the function of NHERF proteins in the expression, localization and stabilization of brush border membrane proteins.

Finally, we were interested to identify novel binding partners and/or substrates for the cGMP-dependent kinase II (cGKII). cGMP-dependent protein kinase anchoring proteins

(GKAPs) can improve the efficiency and specificity of target protein phosphorylation. To date, most of the GKAPs known are specific for cGKI (the cytosolic cGK), whereas binding of cCKII to anchoring proteins has received less attention. Membrane anchoring of cGKII via an N-terminal myristoyl-group was previously found to be a prerequisite for the efficient phosphorylation of both NHE3 and CFTR. In addition, cGMP-mediated phosphorylation of NHE3 requires expression of NHERF-2 as GKAP. Because it is still unclear if cGKII binding partners are essential to allow cGMP-dependent phosporylation and activation of CFTR, we searched for novel cGKII binding partners using the yeast two-hybrid system (**Chapter 6**).

References

1. Saunders, D. R., Rubin, C. E., and Ostrow, J. D. (2007) The Gut. In. *Chapter V Small bowel*
2. Donowitz, M., and Li, X. (2007) *Physiol Rev* **87**(3), 825-872
3. Field, M. (2003) *J Clin Invest* **111**(7), 931-943
4. Alberts, B., Johnson, A., Lewis, J., Raff, M., Roberts, K., and Walter, P. (2002) **fourth edition**, Chapter 22
5. Madara, J. L. (1991) The gastrointestinal system. In. *Handbook of physiology*
6. Potten, C. S., and Loeffler, M. (1990) *Development* **110**(4), 1001-1020
7. Pitari, G. M., Li, P., Lin, J. E., Zuzga, D., Gibbons, A. V., Snook, A. E., Schulz, S., and Waldman, S. A. (2007) *Clin Pharmacol Ther* **82**(4), 441-447
8. Nelson, W. J. (2004) *Nature* **428**(6978), 28-29
9. Schultz, S. G., Fuisz, R. E., and Curran, P. F. (1966) *J Gen Physiol* **49**(5), 849-866
10. Ganapathy, and Leibach, F. H. (1985) *Am J Physiol* **249**(2 Pt 1), G153-160
11. Ma, T., and Verkman, A. S. (1999) *J Physiol* **517 (Pt 2)**, 317-326
12. Field, M. (1971) *Am J Physiol* **221**(4), 992-997
13. Kimberg, D. V., Field, M., Johnson, J., Henderson, A., and Gershon, E. (1971) *J Clin Invest* **50**(6), 1218-1230
14. Field, M., Fromm, D., al-Awqati, Q., and Greenough, W. B., 3rd. (1972) *J Clin Invest* **51**(4), 796-804
15. Al-Abri, S. S., Beeching, N. J., and Nye, F. J. (2005) *Lancet Infect Dis* **5**(6), 349-360
16. Li, Z., Taylor-Blake, B., Light, A. R., and Goy, M. F. (1995) *Gastroenterology* **109**(6), 1863-1875
17. Schultheis, P. J., Clarke, L. L., Meneton, P., Miller, M. L., Soleimani, M., Gawenis, L. R., Riddle, T. M., Duffy, J. J., Doetschman, T., Wang, T., Giebisch, G., Aronson, P. S., Lorenz, J. N., and Shull, G. E. (1998) *Nat Genet* **19**(3), 282-285
18. Booth, I. W., Stange, G., Murer, H., Fenton, T. R., and Milla, P. J. (1985) *Lancet* **1**(8437), 1066-1069
19. Fell, J. M., Miller, M. P., Finkel, Y., and Booth, I. W. (1992) *J Pediatr Gastroenterol Nutr* **15**(2), 112-116
20. Kere, J., Lohi, H., and Hoglund, P. (1999) *Am J Physiol* **276**(1 Pt 1), G7-G13
21. Seidler, U., Rottinghaus, I., Hillesheim, J., Chen, M., Riederer, B., Krabbenhoft, A., Engelhardt, R., Wiemann, M., Wang, Z., Barone, S., Manns, M. P., and Soleimani, M. (2007) *Pflugers Arch*
22. Melvin, J. E., Park, K., Richardson, L., Schultheis, P. J., and Shull, G. E. (1999) *J Biol Chem* **274**(32), 22855-22861
23. Ko, S. B., Shcheynikov, N., Choi, J. Y., Luo, X., Ishibashi, K., Thomas, P. J., Kim, J. Y., Kim, K. H., Lee, M. G., Naruse, S., and Muallem, S. (2002) *Embo J* **21**(21), 5662-5672
24. Shcheynikov, N., Ko, S. B., Zeng, W., Choi, J. Y., Dorwart, M. R., Thomas, P. J., and Muallem, S. (2006) *Novartis Found Symp* **273**, 177-186; discussion 186-192, 261-174
25. Ko, S. B., Zeng, W., Dorwart, M. R., Luo, X., Kim, K. H., Millen, L., Goto, H., Naruse, S., Soyombo, A., Thomas, P. J., and Muallem, S. (2004) *Nat Cell Biol* **6**(4), 343-350
26. Sheppard, D. N., and Welsh, M. J. (1999) *Physiol Rev* **79**(1 Suppl), S23-45

27. Vankeerberghen, A., Cuppens, H., and Cassiman, J. J. (2002) *J Cyst Fibros* **1**(1), 13-29
28. Zielenski, J., and Tsui, L. C. (1995) *Annu Rev Genet* **29**, 777-807
29. Knowles, M. R., Stutts, M. J., Spock, A., Fischer, N., Gatzy, J. T., and Boucher, R. C. (1983) *Science* **221**(4615), 1067-1070
30. Gray, M. A., Winpenny, J. P., Verdon, B., McAlroy, H., and Argent, B. E. (1995) *Biosci Rep* **15**(6), 531-541
31. Ledson, M. J., Tran, J., and Walshaw, M. J. (1998) *J R Soc Med* **91**(1), 7-9
32. Osborne, L. R., Lynch, M., Middleton, P. G., Alton, E. W., Geddes, D. M., Pryor, J. P., Hodson, M. E., and Santis, G. K. (1993) *Hum Mol Genet* **2**(10), 1605-1609
33. Collins, F. S. (1992) *Science* **256**(5058), 774-779
34. Kerem, B., Rommens, J. M., Buchanan, J. A., Markiewicz, D., Cox, T. K., Chakravarti, A., Buchwald, M., and Tsui, L. C. (1989) *Science* **245**(4922), 1073-1080
35. Riordan, J. R., Rommens, J. M., Kerem, B., Alon, N., Rozmahel, R., Grzelczak, Z., Zielenski, J., Lok, S., Plavsic, N., Chou, J. L., and et al. (1989) *Science* **245**(4922), 1066-1073
36. Rommens, J. M., Iannuzzi, M. C., Kerem, B., Drumm, M. L., Melmer, G., Dean, M., Rozmahel, R., Cole, J. L., Kennedy, D., Hidaka, N., and et al. (1989) *Science* **245**(4922), 1059-1065
37. Zielenski, J., Rozmahel, R., Bozon, D., Kerem, B., Grzelczak, Z., Riordan, J. R., Rommens, J., and Tsui, L. C. (1991) *Genomics* **10**(1), 214-228
38. Chang, X. B., Hou, Y. X., Jensen, T. J., and Riordan, J. R. (1994) *J Biol Chem* **269**(28), 18572-18575
39. Chen, M., and Zhang, J. T. (1996) *Mol Membr Biol* **13**(1), 33-40
40. Higgins, C. F. (2001) *Res Microbiol* **152**(3-4), 205-210
41. Klein, I., Sarkadi, B., and Varadi, A. (1999) *Biochim Biophys Acta* **1461**(2), 237-262
42. Kaminski, W. E., Piehler, A., and Wenzel, J. J. (2006) *Biochim Biophys Acta* **1762**(5), 510-524
43. Sharom, F. J. (2006) *Biochem Cell Biol* **84**(6), 979-992
44. Li, C., Krishnamurthy, P. C., Penmatsa, H., Marrs, K. L., Wang, X. Q., Zaccolo, M., Jalink, K., Li, M., Nelson, D. J., Schuetz, J. D., and Naren, A. P. (2007) *Cell* **131**(5), 940-951
45. Guggino, W. B., and Stanton, B. A. (2006) *Nat Rev Mol Cell Biol* **7**(6), 426-436
46. Gadsby, D. C., and Nairn, A. C. (1999) *Physiol Rev* **79**(1 Suppl), S77-S107
47. Travis, S. M., Berger, H. A., and Welsh, M. J. (1997) *Proc Natl Acad Sci U S A* **94**(20), 11055-11060
48. Luo, J., Pato, M. D., Riordan, J. R., and Hanrahan, J. W. (1998) *Am J Physiol* **274**(5 Pt 1), C1397-1410
49. Welsh, M. J., and Smith, A. E. (1993) *Cell* **73**(7), 1251-1254
50. Estivill, X. (1996) *Nat Genet* **12**(4), 348-350
51. Rowe, S. M., Miller, S., and Sorscher, E. J. (2005) *N Engl J Med* **352**(19), 1992-2001
52. Jilling, T., and Kirk, K. L. (1997) *Int Rev Cytol* **172**, 193-241
53. Kalin, N., Claass, A., Sommer, M., Puchelle, E., and Tummler, B. (1999) *J Clin Invest* **103**(10), 1379-1389
54. Koch, C., Cuppens, H., Rainisio, M., Madessani, U., Harms, H., Hodson, M., Mastella, G., Navarro, J., Strandvik, B., and McKenzie, S. (2001) *Pediatr Pulmonol* **31**(1), 1-12
55. Cuppens, H., Lin, W., Jaspers, M., Costes, B., Teng, H., Vankeerberghen, A., Jorissen, M., Droogmans, G., Reynaert, I., Goossens, M., Nilius, B., and Cassiman, J. J. (1998) *J Clin Invest* **101**(2), 487-496
56. Jarvi, K., Zielenski, J., Wilschanski, M., Durie, P., Buckspan, M., Tullis, E., Markiewicz, D., and Tsui, L. C. (1995) *Lancet* **345**(8964), 1578
57. Pignatti, P. F., Bombieri, C., Marigo, C., Benetazzo, M., and Luisetti, M. (1995) *Hum Mol Genet* **4**(4), 635-639
58. Girodon, E., Cazeneuve, C., Lebargy, F., Chinet, T., Costes, B., Ghanem, N., Martin, J., Lemay, S., Scheid, P., Housset, B., Bignon, J., and Goossens, M. (1997) *Eur J Hum Genet* **5**(3), 149-155
59. Castellani, C., Bonizzato, A., and Mastella, G. (1997) *J Med Genet* **34**(4), 297-301
60. Naren, A. P., Cormet-Boyaka, E., Fu, J., Villain, M., Blalock, J. E., Quick, M. W., and Kirk, K. L. (1999) *Science* **286**(5439), 544-548
61. King, S. A., and Sorscher, E. J. (2000) *Biochemistry* **39**(32), 9868-9875
62. Stutts, M. J., Rossier, B. C., and Boucher, R. C. (1997) *J Biol Chem* **272**(22), 14037-14040
63. Quinton, P. M. (1990) *Faseb J* **4**(10), 2709-2717
64. McNicholas, C. M., Guggino, W. B., Schwiebert, E. M., Hebert, S. C., Giebisch, G., and Egan, M. E. (1996) *Proc Natl Acad Sci U S A* **93**(15), 8083-8088

65. McNicholas, C. M., Nason, M. W., Jr., Guggino, W. B., Schwiebert, E. M., Hebert, S. C., Giebisch, G., and Egan, M. E. (1997) *Am J Physiol* **273**(5 Pt 2), F843-848
66. Gabriel, S. E., Clarke, L. L., Boucher, R. C., and Stutts, M. J. (1993) *Nature* **363**(6426), 263-268
67. Schwiebert, E. M., Morales, M. M., Devidas, S., Egan, M. E., and Guggino, W. B. (1998) *Proc Natl Acad Sci U S A* **95**(5), 2674-2679
68. Clarke, L. L., and Harline, M. C. (1996) *Am J Physiol* **270**(2 Pt 1), G259-267
69. Bagorda, A., Guerra, L., Di Sole, F., Hemle-Kolb, C., Cardone, R. A., Fanelli, T., Reshkin, S. J., Gisler, S. M., Murer, H., and Casavola, V. (2002) *J Biol Chem* **277**(24), 21480-21488
70. Ishida-Takahashi, A., Otani, H., Takahashi, C., Washizuka, T., Tsuji, K., Noda, M., Horie, M., and Sasayama, S. (1998) *J Physiol* **508 (Pt 1)**, 23-30
71. Mount, D. B., and Romero, M. F. (2004) *Pflugers Arch* **447**(5), 710-721
72. Barasch, J., Kiss, B., Prince, A., Saiman, L., Gruenert, D., and al-Awqati, Q. (1991) *Nature* **352**(6330), 70-73
73. Poschet, J. F., Timmins, G. S., Taylor-Cousar, J. L., Ornatowski, W., Fazio, J., Perkett, E., Wilson, K. R., Yu, H. D., de Jonge, H. R., and Deretic, V. (2007) *Am J Physiol Lung Cell Mol Physiol* **293**(3), L712-719
74. Di, A., Brown, M. E., Deriy, L. V., Li, C., Szeto, F. L., Chen, Y., Huang, P., Tong, J., Naren, A. P., Bindokas, V., Palfrey, H. C., and Nelson, D. J. (2006) *Nat Cell Biol* **8**(9), 933-944
75. Veeze, H. J., Halley, D. J., Bijman, J., de Jongste, J. C., de Jonge, H. R., and Sinaasappel, M. (1994) *J Clin Invest* **93**(2), 461-466
76. Veeze, H. J., Sinaasappel, M., Bijman, J., Bouquet, J., and de Jonge, H. R. (1991) *Gastroenterology* **101**(2), 398-403
77. De Jonge, H. R., Ballmann, M., Veeze, H., Bronsveld, I., Stanke, F., Tummler, B., and Sinaasappel, M. (2004) *J Cyst Fibros* **3 Suppl 2**, 159-163
78. Wakabayashi, S., Shigekawa, M., and Pouyssegur, J. (1997) *Physiol Rev* **77**(1), 51-74
79. Sardet, C., Franchi, A., and Pouyssegur, J. (1989) *Cell* **56**(2), 271-280
80. Orlowski, J., and Grinstein, S. (2004) *Pflugers Arch* **447**(5), 549-565
81. Orlowski, J., and Grinstein, S. (1997) *J Biol Chem* **272**(36), 22373-22376
82. Brett, C. L., Wei, Y., Donowitz, M., and Rao, R. (2002) *Am J Physiol Cell Physiol* **282**(5), C1031-1041
83. Brett, C. L., Donowitz, M., and Rao, R. (2005) *Am J Physiol Cell Physiol* **288**(2), C223-239
84. Putney, L. K., Denker, S. P., and Barber, D. L. (2002) *Annu Rev Pharmacol Toxicol* **42**, 527-552
85. Hoogerwerf, W. A., Tsao, S. C., Devuyst, O., Levine, S. A., Yun, C. H., Yip, J. W., Cohen, M. E., Wilson, P. D., Lazenby, A. J., Tse, C. M., and Donowitz, M. (1996) *Am J Physiol* **270**(1 Pt 1), G29-41
86. Bachmann, O., Riederer, B., Rossmann, H., Groos, S., Schultheis, P. J., Shull, G. E., Gregor, M., Manns, M. P., and Seidler, U. (2004) *Am J Physiol Gastrointest Liver Physiol* **287**(1), G125-133
87. Orlowski, J., Kandasamy, R. A., and Shull, G. E. (1992) *J Biol Chem* **267**(13), 9331-9339
88. Brant, S. R., Yun, C. H., Donowitz, M., and Tse, C. M. (1995) *Am J Physiol* **269**(1 Pt 1), C198-206
89. Furukawa, O., Bi, L. C., Guth, P. H., Engel, E., Hirokawa, M., and Kaunitz, J. D. (2004) *Am J Physiol Gastrointest Liver Physiol* **286**(1), G102-109
90. Maher, M. M., Gontarek, J. D., Bess, R. S., Donowitz, M., and Yeo, C. J. (1997) *Gastroenterology* **112**(1), 174-183
91. Collins, J. F., Xu, H., Kiela, P. R., Zeng, J., and Ghishan, F. K. (1997) *Am J Physiol* **273**(6 Pt 1), C1937-1946
92. Colombani, V., Silviani, V., Marteau, C., Lerique, B., Cartouzou, G., and Gerolami, A. (1996) *Clin Sci (Lond)* **91**(2), 209-212
93. Lee, M. G., Ahn, W., Choi, J. Y., Muallem, S., and Kim, K. H. (2000) *J Korean Med Sci* **15 Suppl**, S29-30
94. Jacob, P., Rossmann, H., Lamprecht, G., Kretz, A., Neff, C., Lin-Wu, E., Gregor, M., Groneberg, D. A., Kere, J., and Seidler, U. (2002) *Gastroenterology* **122**(3), 709-724
95. Lamprecht, G., Heil, A., Baisch, S., Lin-Wu, E., Yun, C. C., Kalbacher, H., Gregor, M., and Seidler, U. (2002) *Biochemistry* **41**(41), 12336-12342
96. Zachos, N. C., Tse, M., and Donowitz, M. (2005) *Annu Rev Physiol* **67**, 411-443
97. Aronson, P. S. (2006) *J Nephrol* **19 Suppl 9**, S3-S10
98. Janecki, A. J., Montrose, M. H., Zimniak, P., Zweibaum, A., Tse, C. M., Khurana, S., and Donowitz, M. (1998) *J Biol Chem* **273**(15), 8790-8798

99. Bobulescu, I. A., Dwarakanath, V., Zou, L., Zhang, J., Baum, M., and Moe, O. W. (2005) *Am J Physiol Renal Physiol* **289**(4), F685-691
100. Cavet, M. E., Akhter, S., Murtazina, R., Sanchez de Medina, F., Tse, C. M., and Donowitz, M. (2001) *Am J Physiol Cell Physiol* **281**(6), C2039-2048
101. Turner, J. R., and Black, E. D. (2001) *Am J Physiol Cell Physiol* **281**(5), C1533-1541
102. Zhao, H., Shiue, H., Palkon, S., Wang, Y., Cullinan, P., Burkhardt, J. K., Musch, M. W., Chang, E. B., and Turner, J. R. (2004) *Proc Natl Acad Sci U S A* **101**(25), 9485-9490
103. Yip, J. W., Ko, W. H., Viberti, G., Huganir, R. L., Donowitz, M., and Tse, C. M. (1997) *J Biol Chem* **272**(29), 18473-18480
104. Moe, O. W., Amemiya, M., and Yamaji, Y. (1995) *J Clin Invest* **96**(5), 2187-2194
105. Cha, B., Kim, J. H., Hut, H., Hogema, B. M., Nadarja, J., Zizak, M., Cavet, M., Lee-Kwon, W., Lohmann, S. M., Smolenski, A., Tse, C. M., Yun, C., de Jonge, H. R., and Donowitz, M. (2005) *J Biol Chem* **280**(17), 16642-16650
106. Moe, O. W. (1999) *J Am Soc Nephrol* **10**(11), 2412-2425
107. Yun, C. C., Chen, Y., and Lang, F. (2002) *J Biol Chem* **277**(10), 7676-7683
108. Levine, S. A., Nath, S. K., Yun, C. H., Yip, J. W., Montrose, M., Donowitz, M., and Tse, C. M. (1995) *J Biol Chem* **270**(23), 13716-13725
109. Yun, C. H., Tse, C. M., and Donowitz, M. (1995) *Proc Natl Acad Sci U S A* **92**(23), 10723-10727
110. Weinman, E. J., Wang, Y., Wang, F., Greer, C., Steplock, D., and Shenolikar, S. (2003) *Biochemistry* **42**(43), 12662-12668
111. Yun, C. H., Lamprecht, G., Forster, D. V., and Sidor, A. (1998) *J Biol Chem* **273**(40), 25856-25863
112. Donowitz, M., Cha, B., Zachos, N. C., Brett, C. L., Sharma, A., Tse, C. M., and Li, X. (2005) *J Physiol* **567**(Pt 1), 3-11
113. Kurashima, K., D'Souza, S., Szaszi, K., Ramjeesingh, R., Orlowski, J., and Grinstein, S. (1999) *J Biol Chem* **274**(42), 29843-29849
114. Cha, B., Tse, M., Yun, C., Kovbasnjuk, O., Mohan, S., Hubbard, A., Arpin, M., and Donowitz, M. (2006) *Mol Biol Cell* **17**(6), 2661-2673
115. Szaszi, K., Grinstein, S., Orlowski, J., and Kapus, A. (2000) *Cell Physiol Biochem* **10**(5-6), 265-272
116. Chalumeau, C., du Cheyron, D., Defontaine, N., Kellermann, O., Paillard, M., and Poggioli, J. (2001) *Am J Physiol Renal Physiol* **280**(2), F283-290
117. Pang, T., Su, X., Wakabayashi, S., and Shigekawa, M. (2001) *J Biol Chem* **276**(20), 17367-17372
118. Cohen, M. E., Reinlib, L., Watson, A. J., Gorelick, F., Rys-Sikora, K., Tse, M., Rood, R. P., Czernik, A. J., Sharp, G. W., and Donowitz, M. (1990) *Proc Natl Acad Sci U S A* **87**(22), 8990-8994
119. Emmer, E., Rood, R. P., Wesolek, J. H., Cohen, M. E., Braithwaite, R. S., Sharp, G. W., Murer, H., and Donowitz, M. (1989) *J Membr Biol* **108**(3), 207-215
120. Girardi, A. C., Degray, B. C., Nagy, T., Biemesderfer, D., and Aronson, P. S. (2001) *J Biol Chem* **276**(49), 46671-46677
121. Girardi, A. C., Knauf, F., Demuth, H. U., and Aronson, P. S. (2004) *Am J Physiol Cell Physiol* **287**(5), C1238-1245
122. Biemesderfer, D., Nagy, T., DeGray, B., and Aronson, P. S. (1999) *J Biol Chem* **274**(25), 17518-17524
123. Han, W., Kim, K. H., Jo, M. J., Lee, J. H., Yang, J., Doctor, R. B., Moe, O. W., Lee, J., Kim, E., and Lee, M. G. (2006) *J Biol Chem* **281**(3), 1461-1469
124. Li, X., Galli, T., Leu, S., Wade, J. B., Weinman, E. J., Leung, G., Cheong, A., Louvard, D., and Donowitz, M. (2001) *J Physiol* **537**(Pt 2), 537-552
125. Murtazina, R., Kovbasnjuk, O., Donowitz, M., and Li, X. (2006) *J Biol Chem* **281**(26), 17845-17855
126. Li, X., Zhang, H., Cheong, A., Leu, S., Chen, Y., Elowsky, C. G., and Donowitz, M. (2004) *J Physiol* **556**(Pt 3), 791-804
127. Jelen, F., Oleksy, A., Smietana, K., and Otlewski, J. (2003) *Acta Biochim Pol* **50**(4), 985-1017
128. van Ham, M., and Hendriks, W. (2003) *Mol Biol Rep* **30**(2), 69-82
129. Nourry, C., Grant, S. G., and Borg, J. P. (2003) *Sci STKE* **2003**(179), RE7
130. Fanning, A. S., and Anderson, J. M. (1999) *J Clin Invest* **103**(6), 767-772
131. Harris, B. Z., and Lim, W. A. (2001) *J Cell Sci* **114**(Pt 18), 3219-3231
132. Hung, A. Y., and Sheng, M. (2002) *J Biol Chem* **277**(8), 5699-5702
133. Bezprozvanny, I., and Maximov, A. (2001) *FEBS Lett* **509**(3), 457-462
134. Song, E., Gao, S., Tian, R., Ma, S., Huang, H., Guo, J., Li, Y., Zhang, L., and Gao, Y. (2006) *Mol Cell Proteomics* **5**(8), 1368-1381

135. Stiffler, M. A., Chen, J. R., Grantcharova, V. P., Lei, Y., Fuchs, D., Allen, J. E., Zaslavskaia, L. A., and MacBeath, G. (2007) *Science* **317**(5836), 364-369
136. Kim, E., Niethammer, M., Rothschild, A., Jan, Y. N., and Sheng, M. (1995) *Nature* **378**(6552), 85-88
137. Hegedus, T., Sessler, T., Scott, R., Thelin, W., Bakos, E., Varadi, A., Szabo, K., Homolya, L., Milgram, S. L., and Sarkadi, B. (2003) *Biochem Biophys Res Commun* **302**(3), 454-461
138. Chetkovich, D. M., Chen, L., Stocker, T. J., Nicoll, R. A., and Bredt, D. S. (2002) *J Neurosci* **22**(14), 5791-5796
139. Leonard, A. S., Yermolaieva, O., Hruska-Hageman, A., Askwith, C. C., Price, M. P., Wemmie, J. A., and Welsh, M. J. (2003) *Proc Natl Acad Sci U S A* **100**(4), 2029-2034
140. Li, J., Dai, Z., Jana, D., Callaway, D. J., and Bu, Z. (2005) *J Biol Chem* **280**(45), 37634-37643
141. Peterson, F. C., Penkert, R. R., Volkman, B. F., and Prehoda, K. E. (2004) *Mol Cell* **13**(5), 665-676
142. Weinman, E. J., Steplock, D., Wang, Y., and Shenolikar, S. (1995) *J Clin Invest* **95**(5), 2143-2149
143. Yun, C. H., Oh, S., Zizak, M., Steplock, D., Tsao, S., Tse, C. M., Weinman, E. J., and Donowitz, M. (1997) *Proc Natl Acad Sci U S A* **94**(7), 3010-3015
144. Custer, M., Spindler, B., Verrey, F., Murer, H., and Biber, J. (1997) *Am J Physiol* **273**(5 Pt 2), F801-806
145. Scott, R. O., Thelin, W. R., and Milgram, S. L. (2002) *J Biol Chem* **277**(25), 22934-22941
146. Kocher, O., Pal, R., Roberts, M., Cirovic, C., and Gilchrist, A. (2003) *Mol Cell Biol* **23**(4), 1175-1180
147. Shenolikar, S., Voltz, J. W., Cunningham, R., and Weinman, E. J. (2004) *Physiology (Bethesda)* **19**, 362-369
148. Weinman, E. J., Steplock, D., and Shenolikar, S. (1993) *J Clin Invest* **92**(4), 1781-1786
149. Sun, F., Hug, M. J., Lewarchik, C. M., Yun, C. H., Bradbury, N. A., and Frizzell, R. A. (2000) *J Biol Chem* **275**(38), 29539-29546
150. Ladias, J. A. (2003) *J Membr Biol* **192**(2), 79-88
151. Hall, R. A., Spurney, R. F., Premont, R. T., Rahman, N., Blitzer, J. T., Pitcher, J. A., and Lefkowitz, R. J. (1999) *J Biol Chem* **274**(34), 24328-24334
152. Lau, A. G., and Hall, R. A. (2001) *Biochemistry* **40**(29), 8572-8580
153. Deliot, N., Hernando, N., Horst-Liu, Z., Gisler, S. M., Capuano, P., Wagner, C. A., Bacic, D., O'Brien, S., Biber, J., and Murer, H. (2005) *Am J Physiol Cell Physiol* **289**(1), C159-167
154. He, J., Lau, A. G., Yaffe, M. B., and Hall, R. A. (2001) *J Biol Chem* **276**(45), 41559-41565
155. Weinman, E. J., Biswas, R. S., Peng, Q., Shen, L., Turner, C. L., E, X., Steplock, D., Shenolikar, S., and Cunningham, R. (2007) *J Clin Invest* **117**(11), 3412-3420
156. Li, J., Poulikakos, P. I., Dai, Z., Testa, J. R., Callaway, D. J., and Bu, Z. (2007) *J Biol Chem* **282**(37), 27086-27099
157. Fouassier, L., Yun, C. C., Fitz, J. G., and Doctor, R. B. (2000) *J Biol Chem* **275**(32), 25039-25045
158. Shenolikar, S., Minkoff, C. M., Steplock, D. A., Evangelista, C., Liu, M., and Weinman, E. J. (2001) *FEBS Lett* **489**(2-3), 233-236
159. Gisler, S. M., Pribanic, S., Bacic, D., Forrer, P., Gantenbein, A., Sabourin, L. A., Tsuji, A., Zhao, Z. S., Manser, E., Biber, J., and Murer, H. (2003) *Kidney Int* **64**(5), 1733-1745
160. Pan, Y., Weinman, E. J., and Dai, J. (2008) *Breast Cancer Res* **10**(1), R5
161. Pan, Y., Wang, L., and Dai, J. L. (2006) *Breast Cancer Res* **8**(6), R63
162. Ingraffea, J., Reczek, D., and Bretscher, A. (2002) *Eur J Cell Biol* **81**(2), 61-68
163. Kocher, O., Comella, N., Tognazzi, K., and Brown, L. F. (1998) *Lab Invest* **78**(1), 117-125
164. Ikemoto, M., Arai, H., Feng, D., Tanaka, K., Aoki, J., Dohmae, N., Takio, K., Adachi, H., Tsujimoto, M., and Inoue, K. (2000) *Proc Natl Acad Sci U S A* **97**(12), 6538-6543
165. Nakamura, T., Shibata, N., Nishimoto-Shibata, T., Feng, D., Ikemoto, M., Motojima, K., Iso, O. N., Tsukamoto, K., Tsujimoto, M., and Arai, H. (2005) *Proc Natl Acad Sci U S A* **102**(38), 13404-13409
166. Yesilaltay, A., Kocher, O., Rigotti, A., and Krieger, M. (2005) *Curr Opin Lipidol* **16**(2), 147-152
167. Wang, S., Yue, H., Derin, R. B., Guggino, W. B., and Li, M. (2000) *Cell* **103**(1), 169-179
168. Gentzsch, M., Cui, L., Mengos, A., Chang, X. B., Chen, J. H., and Riordan, J. R. (2003) *J Biol Chem* **278**(8), 6440-6449
169. Malmberg, E. K., Pelaseyed, T., Petersson, A., Seidler, U. E., de Jonge, H., Riordan, J. R., and Hansson, G. C. (2007) *Biochem J*
170. Thelin, W. R., Hodson, C. A., and Milgram, S. L. (2005) *J Physiol* **567**(Pt 1), 13-19
171. Schulz, S., Green, C. K., Yuen, P. S., and Garbers, D. L. (1990) *Cell* **63**(5), 941-948

172. Gisler, S. M., Stagljar, I., Traebert, M., Bacic, D., Biber, J., and Murer, H. (2001) *J Biol Chem* **276**(12), 9206-9213
173. Sun, F., Hug, M. J., Bradbury, N. A., and Frizzell, R. A. (2000) *J Biol Chem* **275**(19), 14360-14366
174. Short, D. B., Trotter, K. W., Reczek, D., Kreda, S. M., Bretscher, A., Boucher, R. C., Stutts, M. J., and Milgram, S. L. (1998) *J Biol Chem* **273**(31), 19797-19801
175. Huang, P., Trotter, K., Boucher, R. C., Milgram, S. L., and Stutts, M. J. (2000) *Am J Physiol Cell Physiol* **278**(2), C417-422
176. Liedtke, C. M., Yun, C. H., Kyle, N., and Wang, D. (2002) *J Biol Chem* **277**(25), 22925-22933
177. Sheng, M., and Kim, E. (2000) *J Cell Sci* **113 (Pt 11)**, 1851-1856
178. Kim, J. Y., Han, W., Namkung, W., Lee, J. H., Kim, K. H., Shin, H., Kim, E., and Lee, M. G. (2004) *J Biol Chem* **279**(11), 10389-10396
179. Lee, J. H., Richter, W., Namkung, W., Kim, K. H., Kim, E., Conti, M., and Lee, M. G. (2007) *J Biol Chem* **282**(14), 10414-10422
180. Hillesheim, J., Riederer, B., Tuo, B., Chen, M., Manns, M., Biber, J., Yun, C., Kocher, O., and Seidler, U. (2007) *Pflugers Arch* **454**(4), 575-586
181. Raghuram, V., Mak, D. D., and Foskett, J. K. (2001) *Proc Natl Acad Sci U S A* **98**(3), 1300-1305
182. Park, M., Ko, S. B., Choi, J. Y., Muallem, G., Thomas, P. J., Pushkin, A., Lee, M. S., Kim, J. Y., Lee, M. G., Muallem, S., and Kurtz, I. (2002) *J Biol Chem* **277**(52), 50503-50509
183. Ahn, W., Kim, K. H., Lee, J. A., Kim, J. Y., Choi, J. Y., Moe, O. W., Milgram, S. L., Muallem, S., and Lee, M. G. (2001) *J Biol Chem* **276**(20), 17236-17243
184. Yoo, D., Flagg, T. P., Olsen, O., Raghuram, V., Foskett, J. K., and Welling, P. A. (2004) *J Biol Chem* **279**(8), 6863-6873
185. Naren, A. P., Cobb, B., Li, C., Roy, K., Nelson, D., Heda, G. D., Liao, J., Kirk, K. L., Sorscher, E. J., Hanrahan, J., and Clancy, J. P. (2003) *Proc Natl Acad Sci U S A* **100**(1), 342-346
186. Taouil, K., Hinnrasky, J., Hologne, C., Corlieu, P., Klossek, J. M., and Puchelle, E. (2003) *J Biol Chem* **278**(19), 17320-17327
187. Haggie, P. M., Kim, J. K., Lukacs, G. L., and Verkman, A. S. (2006) *Mol Biol Cell* **17**(12), 4937-4945
188. Swiatecka-Urban, A., Duhaime, M., Coutermarsh, B., Karlson, K. H., Collawn, J., Milewski, M., Cutting, G. R., Guggino, W. B., Langford, G., and Stanton, B. A. (2002) *J Biol Chem* **277**(42), 40099-40105
189. Haggie, P. M., Stanton, B. A., and Verkman, A. S. (2004) *J Biol Chem* **279**(7), 5494-5500
190. Moyer, B. D., Duhaime, M., Shaw, C., Denton, J., Reynolds, D., Karlson, K. H., Pfeiffer, J., Wang, S., Mickle, J. E., Milewski, M., Cutting, G. R., Guggino, W. B., Li, M., and Stanton, B. A. (2000) *J Biol Chem* **275**(35), 27069-27074
191. Milewski, M. I., Mickle, J. E., Forrest, J. K., Stafford, D. M., Moyer, B. D., Cheng, J., Guggino, W. B., Stanton, B. A., and Cutting, G. R. (2001) *J Cell Sci* **114**(Pt 4), 719-726
192. Moyer, B. D., Denton, J., Karlson, K. H., Reynolds, D., Wang, S., Mickle, J. E., Milewski, M., Cutting, G. R., Guggino, W. B., Li, M., and Stanton, B. A. (1999) *J Clin Invest* **104**(10), 1353-1361
193. Benharouga, M., Sharma, M., So, J., Haardt, M., Drzymala, L., Popov, M., Schwapach, B., Grinstein, S., Du, K., and Lukacs, G. L. (2003) *J Biol Chem* **278**(24), 22079-22089
194. Ostedgaard, L. S., Randak, C., Rokhlina, T., Karp, P., Vermeer, D., Ashbourne Excoffon, K. J., and Welsh, M. J. (2003) *Proc Natl Acad Sci U S A* **100**(4), 1937-1942
195. Cheng, J., Wang, H., and Guggino, W. B. (2004) *J Biol Chem* **279**(3), 1892-1898
196. Guerra, L., Fanelli, T., Favia, M., Riccardi, S. M., Busco, G., Cardone, R. A., Carrabino, S., Weinman, E. J., Reshkin, S. J., Conese, M., and Casavola, V. (2005) *J Biol Chem* **280**(49), 40925-40933
197. Fanelli, T., Cardone, R. A., Favia, M., Guerra, L., Zaccolo, M., Monterisi, S., De Santis, T., Riccardi, S. M., Reshkin, S. J., and Casavola, V. (2008) *Biol Cell*
198. Lamprecht, G., Weinman, E. J., and Yun, C. H. (1998) *J Biol Chem* **273**(45), 29972-29978
199. Zizak, M., Lamprecht, G., Steplock, D., Tariq, N., Shenolikar, S., Donowitz, M., Yun, C. H., and Weinman, E. J. (1999) *J Biol Chem* **274**(35), 24753-24758
200. Kim, J. H., Lee-Kwon, W., Park, J. B., Ryu, S. H., Yun, C. H., and Donowitz, M. (2002) *J Biol Chem* **277**(26), 23714-23724
201. Weinman, E. J., Steplock, D., and Shenolikar, S. (2001) *Kidney Int* **60**(2), 450-454
202. Hall, R. A., Premont, R. T., Chow, C. W., Blitzer, J. T., Pitcher, J. A., Claing, A., Stoffel, R. H., Barak, L. S., Shenolikar, S., Weinman, E. J., Grinstein, S., and Lefkowitz, R. J. (1998) *Nature* **392**(6676), 626-630
203. Murtazina, R., Kovbasnjuk, O., Zachos, N. C., Li, X., Chen, Y., Hubbard, A., Hogema, B. M., Steplock, D., Seidler, U., Hoque, K. M., Tse, C. M., De Jonge, H. R., Weinman, E. J., and Donowitz, M. (2007) *J Biol Chem* **282**(34), 25141-25151

204. Bos, J. L. (2006) *Trends Biochem Sci* **31**(12), 680-686
205. Nakazaki, M., Crane, A., Hu, M., Seghers, V., Ullrich, S., Aguilar-Bryan, L., and Bryan, J. (2002) *Diabetes* **51**(12), 3440-3449
206. Kang, G., Joseph, J. W., Chepurny, O. G., Monaco, M., Wheeler, M. B., Bos, J. L., Schwede, F., Genieser, H. G., and Holz, G. G. (2003) *J Biol Chem* **278**(10), 8279-8285
207. Laroche-Joubert, N., Marsy, S., Michelet, S., Imbert-Teboul, M., and Doucet, A. (2002) *J Biol Chem* **277**(21), 18598-18604
208. Honegger, K. J., Capuano, P., Winter, C., Bacic, D., Stange, G., Wagner, C. A., Biber, J., Murer, H., and Hernando, N. (2006) *Proc Natl Acad Sci U S A* **103**(3), 803-808
209. Lee-Kwon, W., Kawano, K., Choi, J. W., Kim, J. H., and Donowitz, M. (2003) *J Biol Chem* **278**(19), 16494-16501
210. Choi, J. Y., Muallem, D., Kiselyov, K., Lee, M. G., Thomas, P. J., and Muallem, S. (2001) *Nature* **410**(6824), 94-97
211. Shenolikar, S., Voltz, J. W., Minkoff, C. M., Wade, J. B., and Weinman, E. J. (2002) *Proc Natl Acad Sci U S A* **99**(17), 11470-11475
212. Capuano, P., Bacic, D., Roos, M., Gisler, S. M., Stange, G., Biber, J., Kaissling, B., Weinman, E. J., Shenolikar, S., Wagner, C. A., and Murer, H. (2007) *Am J Physiol Cell Physiol* **292**(2), C927-934
213. Cunningham, R., Steplock, D., E, X., Biswas, R. S., Wang, F., Shenolikar, S., and Weinman, E. J. (2006) *Am J Physiol Renal Physiol* **291**(4), F896-901
214. Weinman, E. J., Cunningham, R., and Shenolikar, S. (2005) *Pflugers Arch* **450**(3), 137-144
215. Weinman, E. J., Steplock, D., and Shenolikar, S. (2003) *FEBS Lett* **536**(1-3), 141-144
216. Morales, F. C., Takahashi, Y., Kreimann, E. L., and Georgescu, M. M. (2004) *Proc Natl Acad Sci U S A* **101**(51), 17705-17710
217. Kocher, O., Yesilaltay, A., Cirovic, C., Pal, R., Rigotti, A., and Krieger, M. (2003) *J Biol Chem* **278**(52), 52820-52825
218. Capuano, P., Bacic, D., Stange, G., Hernando, N., Kaissling, B., Pal, R., Kocher, O., Biber, J., Wagner, C. A., and Murer, H. (2005) *Pflugers Arch* **449**(4), 392-402
219. Lamprecht, G., and Seidler, U. (2006) *Am J Physiol Gastrointest Liver Physiol* **291**(5), G766-777
220. Vaandrager, A. B., Ehlert, E. M., Jarchau, T., Lohmann, S. M., and de Jonge, H. R. (1996) *J Biol Chem* **271**(12), 7025-7029
221. Vaandrager, A. B., Smolenski, A., Tilly, B. C., Houtsmuller, A. B., Ehlert, E. M., Bot, A. G., Edixhoven, M., Boomaars, W. E., Lohmann, S. M., and de Jonge, H. R. (1998) *Proc Natl Acad Sci U S A* **95**(4), 1466-1471
222. Inagaki, M., Nakamura, Y., Takeda, M., Nishimura, T., and Inagaki, N. (1994) *Brain Pathol* **4**(3), 239-243
223. Arcuri, C., Bocchini, V., Guerrieri, P., Fages, C., and Tardy, M. (1995) *J Neurosci Res* **40**(5), 622-631
224. Tsujimura, K., Tanaka, J., Ando, S., Matsuoka, Y., Kusubata, M., Sugiura, H., Yamauchi, T., and Inagaki, M. (1994) *J Biochem (Tokyo)* **116**(2), 426-434
225. Vinade, L., and Rodnight, R. (1996) *Brain Res* **732**(1-2), 195-200
226. Pekny, M., and Pekna, M. (2004) *J Pathol* **204**(4), 428-437
227. Pekny, M., Leveen, P., Pekna, M., Eliasson, C., Berthold, C. H., Westermark, B., and Betsholtz, C. (1995) *Embo J* **14**(8), 1590-1598
228. Gomi, H., Yokoyama, T., Fujimoto, K., Ikeda, T., Katoh, A., Itoh, T., and Itohara, S. (1995) *Neuron* **14**(1), 29-41
229. Shibuki, K., Gomi, H., Chen, L., Bao, S., Kim, J. J., Wakatsuki, H., Fujisaki, T., Fujimoto, K., Katoh, A., Ikeda, T., Chen, C., Thompson, R. F., and Itohara, S. (1996) *Neuron* **16**(3), 587-599
230. Hughes, E. G., Maguire, J. L., McMinn, M. T., Scholz, R. E., and Sutherland, M. L. (2004) *Brain Res Mol Brain Res* **124**(2), 114-123
231. Sullivan, S. M., Lee, A., Bjorkman, S. T., Miller, S. M., Sullivan, R. K., Poronnik, P., Colditz, P. B., and Pow, D. V. (2007) *J Biol Chem*
232. Hofmann, F., Ammendola, A., and Schlossmann, J. (2000) *J Cell Sci* **113 (Pt 10)**, 1671-1676
233. Oster, H., Werner, C., Magnone, M. C., Mayser, H., Feil, R., Seeliger, M. W., Hofmann, F., and Albrecht, U. (2003) *Curr Biol* **13**(9), 725-733
234. Werner, C., Raivich, G., Cowen, M., Strekalova, T., Sillaber, I., Buters, J. T., Spanagel, R., and Hofmann, F. (2004) *Eur J Neurosci* **20**(12), 3498-3506

CHAPTER 2

CFTR activation is reduced in the small intestine of NHERF-1, but not NHERF-2, deficient mice

Nellie Broere[1], Jutta Hillesheim[2], Biguang Tuo[2], Huub Jorna[1], Adriaan B. Houtsmuller[3], Shirish Shenolikar[4], Edward J. Weinman[5], Mark Donowitz[6], Ursula Seidler[2], Hugo R. de Jonge[1], and Boris M. Hogema[1]

[1]Department of Biochemistry, Erasmus University Medical Center, Rotterdam, The Netherlands
[2]Department of Gastroenterology, Hepatology and Endocrinology, Hannover Medical School, Hannover, Germany
[3]Optical Image Center, Josephine Nefkens Institute, Erasmus University Medical Center, Rotterdam, The Netherlands
[4]Department of Pharmacology and Cancer Biology, Duke University Medical Center, Durham, North Carolina (Current address: Pfizer Global Research and Development, Ann Arbor, Michigan, USA
[5]Departments of Medicine and Physiology, University of Maryland School of Medicine and the Medical service, Department of Veterans Affairs Medical Center, Baltimore, Maryland, USA
[6]Departments of Medicine and Physiology, Gastrointestinal Division, The Johns Hopkins University School of Medicine, Baltimore, Maryland, USA

The Journal of Biological Chemistry 2007 Dec; 282: 37575-37584.

Abstract

Binding of the cystic fibrosis transmembrane conductance regulator (CFTR) chloride channel to the Na^+/H^+ exchanger 3 regulatory factor 1 (NHERF-1) and NHERF-2 scaffolding proteins has been shown to affect its localization and activation.We have for the first time studied the physiological role of these proteins in CFTR regulation in native tissue by determining CFTR-dependent chloride current in NHERF-1- and NHERF-2-deficient mice. The cAMP- and cGMP-activated chloride current and the basal chloride current in basolaterally permeabilized jejunum were reduced by ~30% in NHERF-1-deficient mice but not in NHERF-2-deficient mice. The duodenal bicarbonate secretion was affected in a similar way, whereas no significant differences in CFTR activity were observed in ileum. CFTR abundance as determined by Western blotting was unaltered in jejunal epithelial cells and brush border membranes of NHERF-1 and NHERF-2 mutant mice. However, semi-quantitative detection of CFTR by confocal microscopy showed that the level of apically localized CFTR in jejunal crypts was reduced by ~35% in NHERF-1-deficient and NHERF-1/2 double deficient mice but not in NHERF-2 null mice. Together our results indicate that NHERF-1 is required for full activation of CFTR in murine duodenal and jejunal mucosa and that NHERF-1 affects the local distribution of CFTR in or near the plasma membrane. These studies provide the first evidence in native intestinal epithelium that NHERF-1 but not NHERF-2 is involved in the formation of CFTR-containing functional complexes that serve to position CFTR in the crypt apical membrane and/or to optimize its function as a cAMP- and cGMP-regulated anion channel.

Introduction

Cystic fibrosis, the most common inherited lethal disorder among Caucasians, is caused by mutations in the gene encoding the cystic fibrosis transmembrane conductance regulator (CFTR) chloride channel, resulting in abnormal electrolyte transport in epithelial tissues, most notably in airways, pancreas, and intestine (1). CFTR is the major cAMP- and cGMP-activated anion transporter in various epithelia including intestinal crypt cells, where it is essential for electrolyte and fluid secretion, as is apparent from the occurrence of life-threatening intestinal obstruction in ~10% of newborn cystic fibrosis patients. On the other hand, overstimulation of CFTR by bacterial enterotoxins causes secretory diarrhea, leading to the death of millions of children per year in the developing world (2).

The abbreviations used are: CFTR, cystic fibrosis transmembrane conductance regulator; BBMV, brush border membrane vehicles; I_{sc}, short circuit current; NHE3, Na^+/H^+ exchanger 3; PDZ, Postsynaptic Density 95/Drosophila Disks large/Zonula Occludens I binding domain; NHERF, NHE3 regulatory factor; PDZK1, PDZ domain protein kidney 1; WT, wild type.

The C terminus of CFTR can bind to several PDZ domain containing proteins (3–5). PDZ domains are protein-protein interaction modules that bind to short stretches of amino acids, usually at the extreme C terminus of their target proteins. Most PDZ domain proteins contain more than one PDZ domain or other protein interacting modules, thereby facilitating the formation of macromolecular complexes, which is important for targeting, trafficking, and multi-protein complex formation of their binding partners.

Several studies have indicated that binding of CFTR to members of the NHERF family of PDZ domain proteins may be important for regulation of activity and for maintaining correct localization in the apical membrane where the NHERF proteins as well as CFTR are localized. Three of the four members of the NHERF family of PDZ proteins present in the intestinal brush border are known to bind to CFTR (5, 6). NHERF-1 (also named NHERF and EBP50) and NHERF-2 (also named E3KARP, SIP-1, and TKA-1) share a structural homology; they contain tandem PDZ domains and a C-terminal ezrin-radixin-moesin binding domain, which anchors the proteins to the actin cytoskeleton. PDZK1 (also known as CAP70, NaPi-CAP1, and more recently as NHERF-3) contains four PDZ domains but no ezrin-radixin-moesin binding domain (7–9).

The multiple (potential) roles of the CFTR C terminus in the regulation of its function have recently been reviewed and are still controversial (10). These roles include: 1) increasing cAMP-dependent activation of CFTR by positioning the cAMP-dependent protein kinase in the vicinity of CFTR where it can efficiently phosphorylate its substrate (11, 12). This corresponds to the mechanism whereby NHERF-1 and NHERF-2 facilitate formation of a NHE3/NHERF/ezrin/cAMP-dependent protein kinase complex, which is required for inhibition of NHE3 (Na^+/H^+ exchanger 3) (9, 13, 14). 2) Coupling of CFTR to the cytoskeleton (via NHERF-1 or NHERF-2 binding to ezrin), resulting in a strong reduction in the lateral mobility of CFTR in the membrane (15, 16). 3) NHERF-1-or PDZK1-induced CFTR dimerization by binding of two CFTR molecules to either NHERF-1 or PDZK1, which allosterically enhances the open probability of the channel (17, 18). 4) Targeting of CFTR to the apical membrane and/or its retention in the membrane was shown to require PDZ domain interactions in several studies (19—21); however, various highly similar studies failed to show this effect (12, 22); 5) Linking CFTR to various NHERF binding partners (which include many channels, transporters, and G protein-coupled receptors) may contribute to temporal and spatial specificity and efficiency of signal transduction.

Whether CFTR-NHERF interactions are exploited as a mechanism for CFTR regulation in native tissue has not been studied yet. All of the previous studies were performed using cell culture systems expressing different amounts and members of the NHERF family proteins (endogenously or using overexpressing systems) or recombinant proteins (*e.g.* C-terminally truncated CFTR or CFTR fragments), which may have contributed to the different outcomes of similar experiments.

To further investigate the role of the NHERF proteins as regulators of CFTR in a physiological context and to study the functions of the isoforms separately, we have

studied CFTR regulation in native intestinal epithelia from mice lacking NHERF-1, NHERF-2, or both. We demonstrate that NHERF-1, but not NHERF-2, is essential for full activation of transepithelial chloride and bicarbonate secretion by cAMP and cGMP and that the immunostaining intensity of CFTR in the jejunal crypts of NHERF-1 deficient mice is reduced.

Experimental procedures

Animals - Using a previously described retroviral trapping method (23), Lexicon Genetics generated NHERF-2-deficient mice using Omnibank clone OST2298. The retroviral gene trap cassette pVICTR22, containing an optimal splice acceptor sequence that causes mis-splicing of the targeted gene and puromycin resistance as a selectable marker was found to be inserted 157 bp 3' of the second exon (see Fig. 1*A*). The mice were genotyped by two-allele three-primer PCR, using genomic DNA isolated from tail clips; primers 1 (5'-TTCTATAAGCCTCCATTTCCTCT-3') and 3 (5'-CCCACCCCCATCGCTGCTC- 3') were used for detection of the wild type (WT) allele. Primer 2 (5'-GCGCCAGTCCTCCGATTGA-3') is complementary to a sequence in the 5' long terminal repeat of the retroviral insert and serves to amplify the mutant allele in combination with primer 1. PCR of tail clips was performed using 0.4 μM of each primer, 1 mM $MgCl_2$, 0.2 mM dNTPs (Promega), 0.3 units of RedTaq DNA polymerase (Sigma), and the supplied buffer. The sizes of the PCR products were 303 bp for the wild type and 231 bp for the mutant allele (see Fig. 1*C*).

NHERF-1-deficient mice were originally generated at the Duke University Medical Center and have been described before (24). NHERF-1 and NHERF-2 mice were backcrossed for at least five generations into the FVB/n genetic background. Furthermore, NHERF-1-deficient mice were crossed with NHERF-2-deficient mice and with mice carrying a targeted disruption in the CFTR gene described previously (also from the FVB genetic background) (25). In contrast to previous reports (24), the viability and fertility of female NHERF-1 null mice was not different from wild type, probably because of breeding into the FVB/n genetic background.

The mice were housed in the animal facilities of the Erasmus Medical Centre of Rotterdam and the Medical School of Hannover under standardized light and climate conditions and *ad libitum* access to water and chow. All of the animal experiments were approved by the Dutch Animal Welfare Committee and followed the protocols at the Hannover Medical School and the local authorities for the regulation of animal welfare (Regierungspräsidium). Both male and female animals were used for studies at 12–20 weeks of age. The mice were anesthetized with ketamine and xylazine (100 and 20 mg/kg respectively, intraperitoneally) and euthanized by cervical dislocation after removal of tissue.

Bioelectric Measurements - Short circuit currents (I_{sc}) of muscle-stripped ileal and jejunal sheets mounted in Ussing chambers were measured as described previously (26). Transepithelial PD was clamped at 0 mV, and I_{sc} was measured using a DVC-1000 voltage/current clamp (World Precision Instruments), digitized by a Digidata 1320, and analyzed using AxoScope 9.2 software (Axon Instruments). After stabilization of the base-line current or the previous response the following agents were added: 8-Br-cGMP (serosal, 200 μM), forskolin (serosal, 10 μM), and D-glucose (mucosal, 10 mM). To determine whether the observed changes in the NHERF-1-deficient mice (see "Results")

were the direct consequence of reduced CFTR activity or whether NHERF-1 deficiency affects activity of basolateral ion transporters and/or the driving force for chloride secretion, the basolateral membrane was permeabilized to monovalent ions using nystatin during the I_{sc} measurements (27). After stabilization of the base-line current, an inward transepithelial chloride gradient was generated by iso-osmotic replacement of chloride in the serosal bath by mannitol. The ionophore nystatin was added at the serosal side at 0.36 g/ml. Forskolin (serosal, 10 μM) and glucose (mucosal, 10 mM) were subsequently added after stabilization of the current.

Bicarbonate Secretion - Isolated proximal duodenum was stripped of external serosal and muscle layers. Duodenal mucosa was mounted in a gas-lifted Ussing chamber and maintained at 37 °C. The mucosal side was bathed with unbuffered bicarbonate-free Ringer's solution, and the serosal side was bathed with buffered gassed Ringer's solution (pH 7.4) containing 22 mM HCO_3^-. Under control of a pH-stat system (PHM290, pH-Stat Controller, Radiometer Copenhagen), the luminal pH was maintained at 7.4 by continuous infusion of 1 mM HCl. The amount infused/time unit was used to quantitate HCO_3^- secretion (μmol/cm^2/h^{-1}). After measuring basal secretion for 30 min, forskolin (10 μM) or 8-Br-cGMP (200 μM) was added at the serosal side, and changes in bicarbonate secretion were determined during a 40-min period.

Isolation of Intestinal Epithelial Cells and Brush Border Membrane Vesicles (BBMVs) - Mechanical high frequency vibration was used to isolate epithelial cells from mouse jejunum in isotonic buffer as described before (28). BBMVs were isolated from epithelial cell homogenates by differential magnesium precipitation (29). Epithelial tissue and BBMVs were resuspended in SDS-PAGE loading buffer containing protease inhibitors (Complete; Roche Applied Science) and homogenized by brief sonication on ice. The protein concentrations were determined using the *RC DC* protein assay kit (Bio-Rad).

Western Blot Analysis - For quantitative analysis of the relevant proteins in epithelial cells and BBMVs, samples from at least two mice were pooled. Crude extracts from other tissues were prepared by snap-freezing and homogenization in Laemmli sample buffer (containing Complete protease inhibitor) followed by brief sonication on ice. The samples were separated by SDS-PAGE and transferred to Protean nitrocellulose membrane (Schleicher & Schuell Bioscience Hybond-P) or polyvinylidene difluoride membrane (Amersham Biosciences). The membranes were blocked with 2.5% nonfat dried milk for 1 h at room temperature and incubated overnight with primary antibody at 4 °C. The primary antibodies used were anti-CFTR antibody R3195 (dilution 1:1000) (30), anti-NHERF-1 antibody (dilution 1:3000) (31), anti-NHERF-2 antibody R2570 (dilution 1:1000) (32), and anti-actin antibody MAB1501 (Chemicon; dilution, 1:15000). An antibody against PDZK1 was generated in rabbit against a peptide (amino acids 339–354 of mouse PDZK1), and serum was affinity-purified on peptide-bound agarose beads. The signal on Western blots was completely blocked by the peptide (0.5 mM; data not shown). After incubation with primary antibody and washing, the membranes were incubated with secondary antibody. Horseradish peroxidase-conjugated donkey anti-rabbit IgG-horseradish peroxidase (Amersham Biosciences; dilution, 1:3000) was employed for detection of all primary antibodies except anti-actin, which was detected using horseradish peroxidase-conjugated goat antimouse IgG (BIOSOURCE International; dilution, 1:5000). The secondary antibody was detected by chemiluminescence (Supersignal West Pico substrate; Pierce) by exposing to light sensitive imaging film (Biomax MR film; Kodak). The imaged bands

were quantified using a calibrated GS-800 densitometer (Bio-Rad) and analyzed using Quantity-one software (version 4.2.1; Bio-Rad).

Immunohistochemistry and Confocal Microscopy - Formalin-fixed, paraffin-embedded tissue sections (5 μm) from mice of different genotypes were prepared on the same slide. After deparaffinization with xylene and treatment with 0.01 M sodium citrate solution, endogenous peroxidase activity was blocked with 0.6 %H_2O_2 and 0.12% sodium azide. Sections were incubated with anti-CFTR (R3195, 1:100) or anti-NHERF-1 (1:500) antibodies in phosphate-buffered saline with 2% bovine albumin for 1.5 h at room temperature. The sections stained with monoclonal anti-villin antibody (Santa Cruz; SC-58897; dilution, 1:50) were incubated overnight. The slides were subsequently incubated for 2 h with fluorescein isothiocyanate labeled anti-rabbit secondary antibody and/or Cy3-labeled anti-mouse IgG (1:100, both secondary antibodies were from Jackson Immunoresearch Laboratory, West Grove, PA) and mounted with Vectashield (Vector Laboratories Inc., Burlingame, CA). Immunofluorescence micrographs were captured using a Zeiss LSM510 confocal microscope equipped with a 25 milliwatt argon laser. Fluorescence emission after excitation (488 nm for CFTR, 543 nm for villin) was detected using 10x/0.3 or 40x/1.3 numerical aperture oil immersion lenses, a dichroic beam splitter reflecting 488-nm excitation light, and a 505–530 bandpass emission filter (560–615 nm for villin). The images were scanned using a 75-μm pinhole. Initial analysis of images was performed double-blind by at least two investigators. For (semi) quantification of signal from jejunal crypts, images from longitudinal sections at Z-steps of 0.5 μm were analyzed by determining total background-subtracted fluorescent signal using KS400 Zeiss software. The same threshold was utilized for all images from one slide. Three individual crypts from three age- and sex-matched mice of each genotype were analyzed.

Data Analysis - The data are the means ± S.E. Statistical significance was established using Student's unpaired two-tailed *t* test.

Results

Generation and Characterization of NHERF-2-deficient Mice – NHERF-2-deficient mice were generated as described under "Experimental Procedures". Insertion of the retroviral cassette resulted in a complete absence of NHERF-2 protein in all tissues studied (kidney, lung, stomach, heart, brain, and colon; a representative example of a Western blot is shown in Fig. 1*B*). NHERF-2 null mice developed normally and were born at Mendelian ratios. They showed no obvious alterations in gross morphology, body size, and fertility. No abnormal behavior or signs of distress were apparent. Histological analysis of various tissues (lung, kidney, jejunum, ileum and colon, and nasal and tracheal epithelium) displayed comparable morphology in wild type and NHERF-2-deficient mice (data not shown).

cAMP- and cGMP-dependent Activation of CFTR-mediated Ion Transport in NHERF-1- and NHERF-2-deficient Mice - Several studies using cultured cells have indicated an important role for the NHERF proteins in the activation of CFTR (10). By using mice deficient in NHERF-1, NHERF-2, or both, we were able to analyze native epithelia *ex vivo*, avoiding potential artifacts introduced by using overexpression systems or recombinant proteins. First, cAMP- and cGMP-activated CFTR transepithelial short circuit currents (I_{sc})

were measured in mice of the different genotypes. As shown in Fig. 2*A* (*panel 1*), the response to the adenylyl cyclase activator forskolin was significantly reduced in jejunum of NHERF-1-deficient mice (34% reduction, $p<0.05$), whereas the response in NHERF-2-deficient mice was not altered. The response to forskolin in NHERF-1/2 double deficient mice was reduced by 37% ($p<0.05$) compared with wild type. Thus, additional absence of NHERF-2 did not result in a stronger effect or different characteristics of transepithelial current in response to cAMP, suggesting that an absence of NHERF-1 was not compensated by NHERF-2.

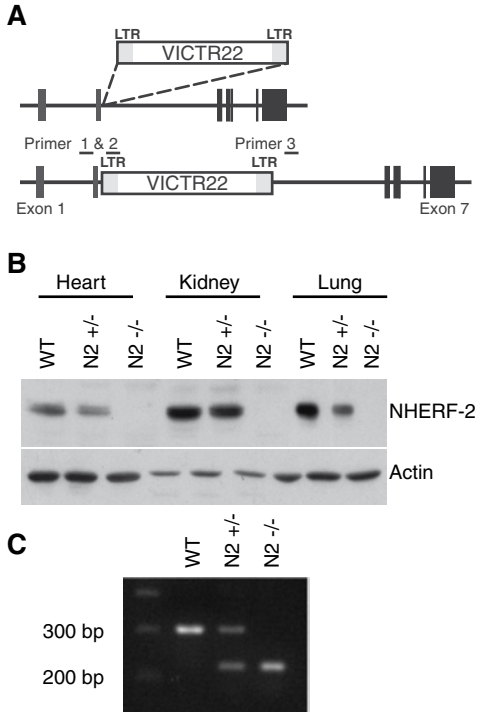

Figure 1. Disruption of the NHERF-2 gene and characterization of the NHERF-2-deficient mice. *A*, schematic representation of the integration of retroviral construct VICTR22 between exons 2 and 3 of the NHERF-2 gene. *LTR*, long terminal repeat. *B*, Western blot analysis of NHERF-2 in different tissues: heart (15 μg/lane), kidney (15 μg/lane), and lung (2.5 μg/lane). NHERF-2 is absent in tissues from the NHERF-2-deficient (N2-/-) mice and reduced in heterozygote (N2+/-) mice. Actin was used as loading control (10 μg/lane). *C*, genotyping of NHERF-2-deficient mice. PCR products generated by amplification of genomic DNA from WT, heterozygous (N2+/-), and NHERF-2 null mice (N2-/-). The location of primers used for the genotyping PCR is schematically shown in *A*.

We subsequently examined whether cGMP-dependent regulation of CFTR was affected similarly. As shown in a previous study, cGMP-dependent inhibition of another intestinal ion transporter in the apical membrane, NHE3, is selective in its requirement for the NHERF proteins in comparison with cAMP-dependent inhibition. Whereas NHERF-1 and NHERF-2 were interchangeable as mediators of cAMP-mediated inhibition of NHE3, only NHERF-2 could act as a cofactor for cGMP-mediated inhibition (33). In contrast, our results show that CFTR activation by cAMP and cGMP in the jejunum was reduced to a similar extent in NHERF-1-deficient mice (Fig. 2). Stimulation of I_{sc} by the membrane-permeable analog 8-Br-cGMP was significantly decreased (31%, $p<0.05$) in NHERF-1-deficient mice as compared with wild type, whereas no change was observed in NHERF-2-deficient mice.

Again, the phenotype of NHERF-1/2 null mice was similar to that of NHERF-1-deficient mice (32% reduction in I_{sc} compared with NHERF-2 deficient mice, $p<0.05$).

To compare the relative functional quality of the various sheets of muscle stripped epithelia, stimulation of the short circuit current by glucose (monitoring sodium transport mediated by the Na^+/glucose cotransporter SGLT1) was determined as a measure for CFTR-independent electrogenic transport. The response to glucose was not significantly different in mice lacking NHERF-1 or NHERF-2, with the exception of the NHERF-1/2 double-mutant mice, in which the response in jejunum was increased by 25% ($p<0.05$) (Fig. 2*A*, *panel 3*).

An identical series of experiments was performed using ileal tissue. In contrast to jejunum, the response to forskolin or 8-BrcGMP was not significantly reduced in epithelium from ileum of mice lacking NHERF-1, NHERF-2, or both (Fig. 2*B*). Finally, the glucose-stimulated I_{sc} was not affected by NHERF-1 or NHERF-2 deficiency (Fig. 2*A*, *panel 3*).

To test whether cAMP- and cGMP-dependent responses in NHERF-1-deficient mice were entirely CFTR-dependent, as they are in wild type mice, short circuit current measurements were performed in mice lacking both NHERF-1 and CFTR. As shown in Fig. 2, the response to forskolin and 8-Br-cGMP was completely abolished in both jejunum and ileum of these mice, demonstrating that the currents measured in NHERF-1 null mouse intestine were fully CFTR-mediated and that no compensatory anion channel is active. Altogether, these results demonstrate that NHERF-1, but not NHERF-2, is required for full cAMP- and cGMP-dependent activation of CFTR-dependent anion transport in jejunum but not in ileum.

The reduced forskolin- and 8-Br-cGMP-activated CFTR-dependent chloride current in NHERF-1 null mice could either result from a direct effect on the amount and/or gating of CFTR in the apical membrane or by reduction of the required driving force for chloride secretion, which is generated by several basolateral ion transport proteins (34). To discriminate between these possibilities, nystatin was used to permeabilize the basolateral membrane during short circuit current measurements. First, an inwardly directed chloride gradient was generated by iso-osmotic replacement of chloride to mannitol at the serosal side. Subsequent permeabilization of the basolateral membrane to monovalent ions by addition of nystatin generates a condition in which the Cl^- concentration gradient is the sole driving force for chloride transport when the voltage is clamped to zero. This will result in chloride influx (*i.e.* a negative current) upon activation of apical anion channels. As shown in Fig. 3, the response of jejunal epithelium to the addition of nystatin was reduced by ~40% ($p<0.05$) in the NHERF-1-deficient mice compared with wild type controls. This suggests that prior to CFTR stimulation by cAMP-induced phosphorylation, a large pool of CFTR is already present in the membrane in the active state and that either the size of the pool or the activity is reduced in the NHERF-1-deficient mice. In contrast, the subsequent activation of the current by forskolin was not significantly different between NHERF-1 and wild type mice. The measured currents were almost completely CFTR-dependent as evidenced by its virtual absence in CFTR null mice. Stimulation of the I_{sc} by glucose was

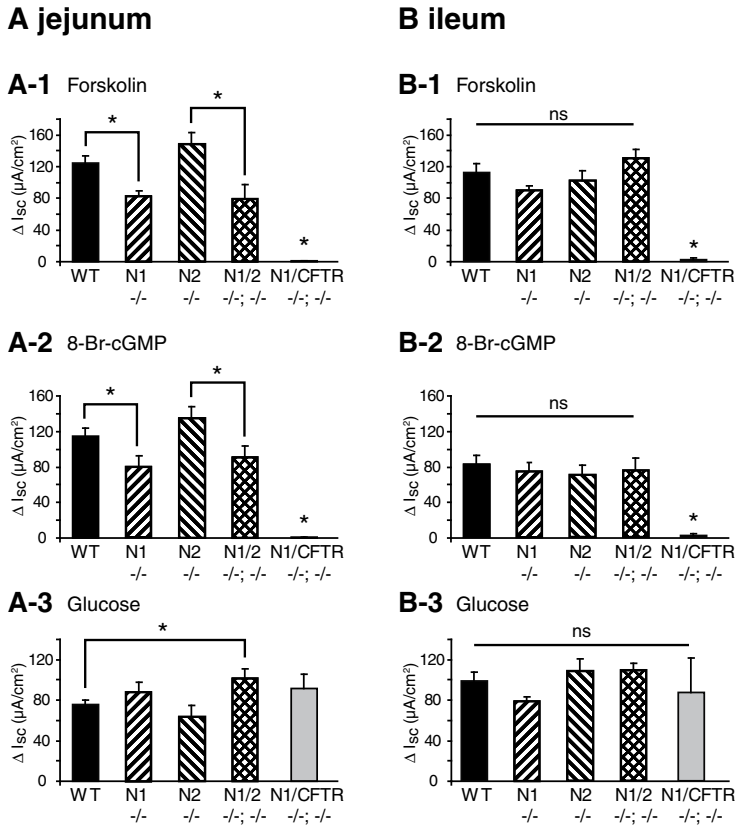

Figure 2. ***Ex vivo*** **CFTR-mediated short circuit current (I_{sc}) measurement in Ussing chambers using jejunal (*A*, *panels 1-3*) and ileal (*B*, *panels 1-3*) tissue.** Activation of short circuit current by forskolin (10μM) (*panels 1*), 8-Brc-GMP (200 μM) (*panels 2*), and glucose (10 mM) (*panels 3*) was measured in WT and NHERF-1-deficient (N1-/-), NHERF-2-deficient (N2-/-), NHERF-1/2 double deficient (N1/2-/-), and NHERF-1/CFTR double deficient (N1/CFTR-/-) mice. The data represent average values from at least seven mice/genotype and are expressed as the means ± S.E. Forskolin-stimulated I_{sc} is significantly reduced in jejunum of NHERF-1- and NHERF-1/2-deficient mice, but not in NHERF-2 null mice. The near absence of CFTR activity in NHERF-1/CFTR double deficient mice shows that no alternative anion channel is active in NHERF-1 null mice. Stimulation of I_{sc} by glucose showed full preservation of this marker of villus function in the NHERF-1- and NHERF-2-deficient mice. The glucose-stimulated I_{sc} was actually slightly higher in the jejunum from NHERF-1/2-deficient mice (25%) compared with wild type mice (*A*, *panel 3*). Identical experiments were performed using ileal intestinal epithelial tissue (*B*, *panels 1-3*). *ns*, not significant. *, $p<0.05$.

comparable in wild type (28.4 ± 4.9), NHERF-1-deficient (28.1 ± 3.8), and CFTR-deficient (27.0 ± 9.6) mice, demonstrating that the functional quality of the tissues examined was similar during nystatin treatment.

Duodenal Bicarbonate Secretion in NHERF-1 and NHERF-2 Null Mice - It is estimated that 50% of bicarbonate secretion in mouse duodenum is directly mediated by CFTR (8, 35, 36). The role of NHERF-1 and NHERF-2 in the regulation of bicarbonate secretion was determined by measuring stimulation of the HCO_3^- secretory rate (J_{HCO3^-}) by

forskolin and 8-Br-cGMP in duodenal epithelium of control and NHERF-1- and NHERF-2-deficient mice. Forskolin- and cGMP-stimulated bicarbonate secretion in NHERF-1-deficient mice was reduced by 35 and 30% compared with wild type, respectively (p<0.05; Fig. 4). The response in NHERF-2 null mice on the other hand was not altered. Together these results suggest that CFTR activation in duodenum is in part dependent on NHERF-1, as it is in jejunum.

Expression and Localization of CFTR in the Intestine of NHERF-1- and NHERF-2-deficient Mice - CFTR expression and localization in mice lacking NHERF-1, NHERF-2, or both were studied in isolated jejunal enterocytes and BBMVs. No significant difference was observed in the level of CFTR protein in mice from the various genotypes (Fig. 5*A*). The maturation of CFTR also appeared to be unaffected in NHERF-1- and NHERF-2-deficient mice, because there was no difference in the ratio of mature, complex-glycosylated (*band C*) and immature, core-glycosylated CFTR (*band B*) in epithelial cell extracts. Furthermore, staining of an SDS-PAGE gel loaded with total jejunal epithelial cell homogenate or BBMVs by Coomassie Brilliant Blue did not display obvious differences in the overall protein composition of enterocytes of NHERF-1 or NHERF-2 mice (data not shown). We subsequently analyzed the immunostaining pattern of CFTR in jejunal crypts of the NHERF-1-, NHERF-2-, and NHERF-1/2-deficient mice by confocal microscopy. Importantly, CFTR staining remained confined to the apical border in all mice examined, and no evidence was found

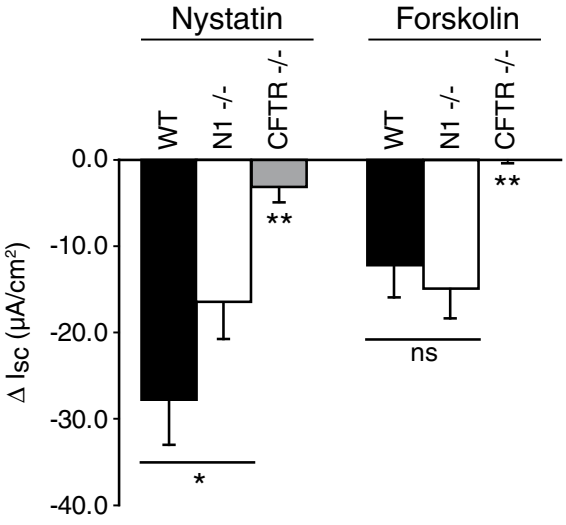

Figure 3. ***Ex vivo*** **CFTR-mediated short circuit current (I_{sc}) measurement in jejunal epithelium during basolateral membrane permeabilization by nystatin in WT, NHERF-1-deficient (N1-/-), and CFTR null (CFTR-/-) mice.** The data represent the average values from at least three mice per genotype and are expressed as the means ± S.E. The CFTR-dependent chloride current prior to forskolin stimulation was reduced in NHERF-1-deficient mice, whereas the response to stimulation by forskolin was not altered in NHERF-1 null mice. *, p<0.05 *versus* wild type; **, p<0.05 *versus* N1-/-; *ns*, not significant.

for redistribution to a perinuclear area or the basolateral membrane (Fig. 5*B*). However, the intensity of CFTR staining at or near the apical membrane was reduced in NHERF-1 and NHERF-1/2 double deficient mice, but not in NHERF-2 null mice. The absence of staining in CFTR null mice proved that the antibody is specific for CFTR. (Semi)quantitative image analysis in crypts from NHERF-1 and NHERF-1/2 null mice showed the reduction in both

mean and total fluorescence intensity in the surface area in which signal was detected was ~35% (p<0.05; Fig. 5*C*).

Double staining of CFTR and the microvillus marker villin was performed to more accurately determine whether the subcellular localization of CFTR was altered in NHERF-1 null mice. Colocalization with villin confirmed that CFTR was confined mostly to the microvilli both in WT and NHERF-1 null mice (Fig. 5*D*). Image analysis of sections from five age and sex-matched couples from WT and NHERF-1 mutant mice showed no evidence for a relocalization of CFTR in jejunal crypts at the resolution obtained by confocal microscopy.

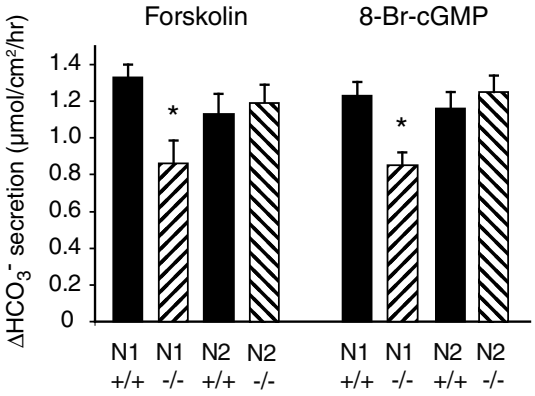

Figure 4. Stimulation of the HCO_3^- secretory rate (J_{HCO3^-}) by forskolin and 8-Br-cGMP in duodenal epithelium of control (N1+/+ and N2+/+),NHERF-1-deficient (N1-/-), and NHERF-2-deficient (N2-/-) mice. Stimulation of net bicarbonate secretion by forskolin (10 μM) and 8-Br-cGMP (200 μM) was reduced by 35 and 30%, respectively, in NHERF-1-deficient mice (p<0.05), whereas no difference was detected in NHERF-2-deficient mice.

Combined with the observation that the total amount of CFTR in BBMVs is not altered, these data suggest that CFTR localization at the apical cell surface in jejunal crypts of NHERF-1- and NHERF-1/2-deficient mice has become more diffuse (see "Discussion").

Expression and Localization of NHERF Proteins in Jejunal Epithelial Cells of Wild Type and NHERF-1- and NHERF-2-deficient Mice - Because many functions of the NHERF proteins are redundant, we determined whether absence of NHERF-1 and/or NHERF-2 causes compensatory overexpression, down-regulation, or mislocalization of the other NHERF proteins, including PDZK1 (NHERF-3), the third NHERF protein known to bind to CFTR. As shown in Fig. 6*A*, the localization of NHERF-1 in epithelial cells lining the jejunal crypts and villi was very similar in wild type and NHERF-2 null mice. NHERF-1 is expressed along the entire crypt-villus axis, with the most abundant NHERF-1 staining in the villus tips. No compensatory overexpression of NHERF-1 was detected in jejunal epithelial cell extracts and BBMVs from NHERF-2-deficient mice (Fig. 6*B*). We were not able not detect any NHERF-2 protein by confocal microcopy or by Western blotting using 10 μg of BBMV sample from wild type or NHERF-1-deficient mice, employing the frequently used R2570 antibody. Under our conditions, the detection threshold of this NHERF-2 antibody in Western blots is ~0.1 ng of purified His-tagged NHERF-2 protein. We conclude that the amount of NHERF-2 is less than 0.001% of the total protein content in BBMVs and that no

up-regulation of NHERF-2 to a level beyond the detection limit has taken place in NHERF-1-deficient mice (data not shown; see also "Discussion"). Unexpectedly, PDZK1 protein levels in extracts from jejunal epithelial cells and BBMVs of NHERF-1-deficient mice were reduced by 80 and 40%, respectively (Fig. 7), whereas no change was detected in NHERF-2 null mice.

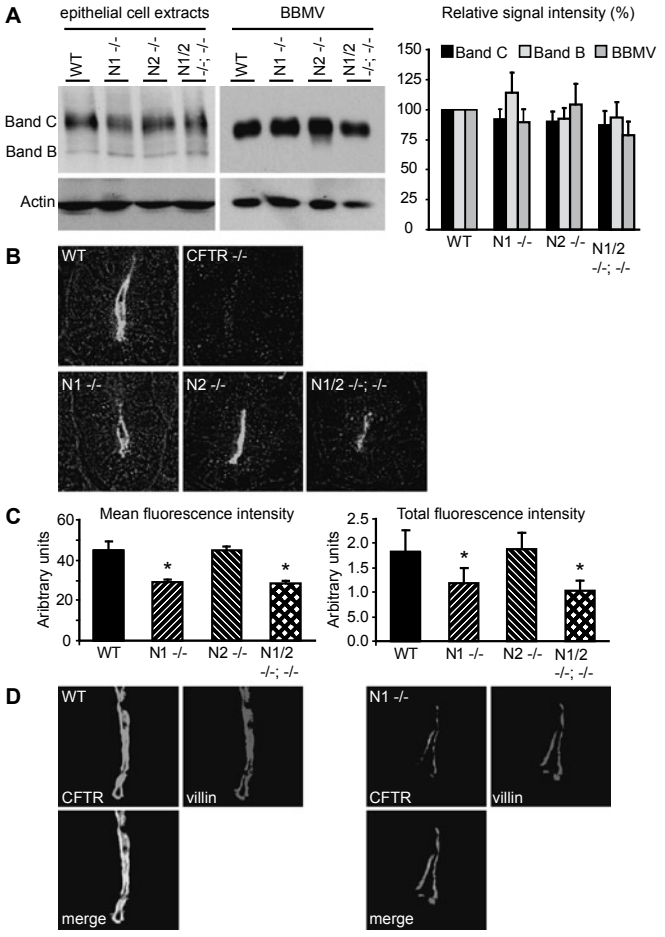

Figure 5. Western blot analysis of CFTR expression in jejunal epithelium and immunocytochemical detection of CFTR in jejunal crypt cells from WT, NHERF-1-deficient (N1-/-), NHERF-2-deficient (N2-/-), and NHERF-1/2-deficient (N1/2-/-) mice. *A*, Western blot analysis of CFTR in jejunal epithelial cell extracts (20 μg/lane) and BBMVs from jejunum (5 μg/lane) displayed no significant difference in the amounts of CFTR protein among mice of the different genotypes. The positions of *band B* (immature CFTR) and *band C* (mature, complex glycosylated CFTR) are indicated. Actin was used as a loading control. Representative Western blots from at least five independently isolated samples are shown at the *left*, and the average amounts of CFTR levels relative to wild type mice are shown in the *right panel*. The data represent relative signal intensity of at least eight Western blots. The *error bars* indicate the S.E. *B*, confocal microscopic analysis of CFTR abundance and localization in jejunal crypts of wild type, NHERF-1-deficient, NHERF-2-deficient, NHERF-1/2-deficient, and CFTR-deficient (CFTR-/-) mice. CFTR-dependent fluorescence was significantly ($p<0.05$) reduced in NHERF-1-and NHERF-1/2-deficient mice. No signal was detected in sections from CFTR-deficient mice, demonstrating the high specificity of the antibody. *C*, quantitative analysis of confocal microscope datasets of three sex- and age-matched couples of wild type, NHERF-1-, NHERF-2-, and NHERF-1/2-deficient mice. Three jejunal crypts from each section were analyzed, and the total and average intensities from all Z-stacks with detectable CFTR signal were calculated for each individual crypt. The average intensity was significantly lower in NHERF-1 and NHERF-1/2 null mice compared with wild type (*left panel*). Likewise, the total intensity per crypt was reduced in NHERF-1 and NHERF-1/2 but not in NHERF-2-deficient mice (*right panel*). *, $p<0.05$ *versus* wild type. *D*, CFTR and villin abundance in jejunal crypts was studied by confocal microscopy in wild type (*left three images*) and NHERF-1-deficient mice(*right three images*). CFTR (shown in *green*) colocalization with villin (shown in *red*) in the apical border is unaltered in NHERF-1 null mice compared with wild type control. *(Color figure on page 164.)*

Discussion

The exploitation of NHERF-1- and NHERF-2-deficient and NHERF-1/2 double-mutant mice in this study has enabled us to investigate, for the first time, the role of these PDZ domain proteins in CFTR expression and regulation in native small intestinal epithelium. Because most previous studies used NHERF overexpression systems and because the level of endogenous expression of the different NHERF proteins varies widely among different cell lines, little is known about the relative contribution of each individual CFTR-binding PDZ protein to CFTR regulation in native epithelia. In addition to NHERF-1 and NHERF-2, PDZK1 and the single PDZ domain proteins CAL (CFTR-associated ligand) and Shank2 are known binding partners of CFTR and candidate PDZ proteins binding to CFTR *in vivo* in enterocytes (37). Each of these PDZ domain proteins may affect CFTR function in different ways in epithelial cells from different tissues (18, 37, 38).

Our study demonstrated clearly that NHERF-1 is required for full activation of the CFTR-dependent chloride current by cAMP- and cGMP-linked agonists. Forskolin-activated duodenal bicarbonate secretion, CFTR-dependent short circuit current (I_{sc}) in jejunum, and basically active chloride current in nystatin-permeabilized jejunum were all significantly reduced in NHERF-1 null mice. In contrast, ablation of NHERF-2 had no effect on bicarbonate secretion and short circuit current, and NHERF-1 deficiency did not affect the CFTR-dependent short circuit current in the ileum. The normal response to glucose in the NHERF-1-deficient mice (Fig. 2, *A* and *B*, *panels 3*) showed that the altered response to forskolin and 8-pCPT-cGMP is CFTR-specific and that no general changes in ion transport capacity have occurred.

The observed reduction (approximately 30%) in cAMP- and cGMP-stimulated transepithelial current in jejunum of NHERF-1-deficient mice could be caused either by a functional loss of CFTR in the apical membrane or by a direct or indirect effect of NHERF-1 deficiency on the electrochemical driving force for chloride exit across the apical membrane. This was further investigated by measuring macroscopic currents through apical CFTR channels at a fixed electrochemical gradient for chloride in short circuit measurements of jejunal tissue permeabilized by nystatin. Basolateral permeabilization was found to induce, or unmask, a basically active pool of CFTR in wild type mice that amounted to ~70% of the total activity in the presence of forskolin (Fig. 3). This implies that a significant fraction of the total CFTR pool is already in the open state, a situation similar to that observed in the sweat gland and nasal epithelium (39, 40). Furthermore, it suggests that under non-stimulated conditions the basolateral chloride entry in the cell limits the transcellular chloride current. Surprisingly, the basically active pool, but not the cAMP-activated fraction of CFTR was strongly reduced (~40%) in nystatin-permeabilized jejunum from NHERF-1-deficient mice. Because cAMP activation of chloride current under nystatin conditions more directly reflects the ability of cAMP to activate CFTR channels in the apical membrane than activation under nonpermeabilized conditions, the outcome of these experiments argues against a major role of NHERF-1 in positioning cAMP-dependent

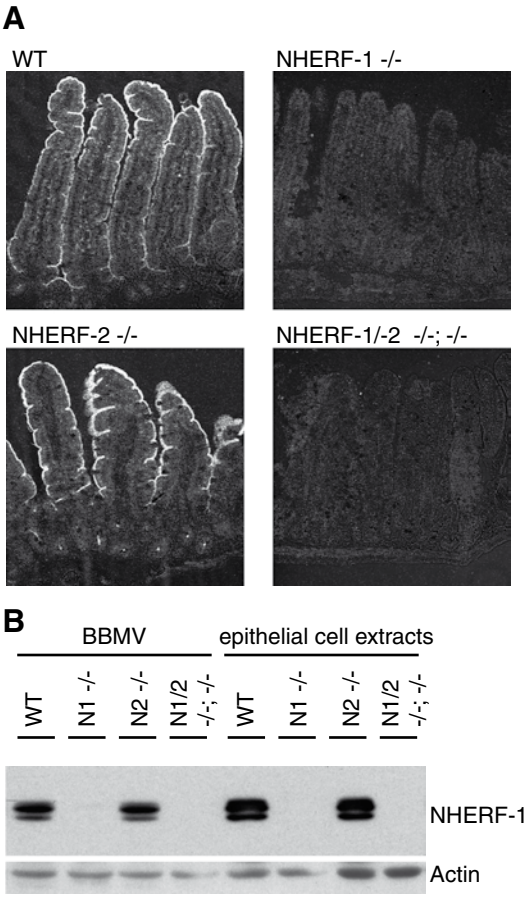

Figure 6. Localization and quantification of NHERF-1 in jejunum by immunocytochemical and Western blot analysis. *A*, immunocytochemical staining shows that NHERF-1 lines the apical border of epithelial cells along the entire crypt-villus axis. No alterations were observed in NHERF-2-deficient (N2-/-) mice. No staining was detected in tissue sections from NHERF-1-deficient (N1-/-) and NHERF-1/2 double deficient (N1/2-/-) mice. *B*, Western blot analysis of NHERF-1 in pooled BBMV extracts from jejunum (5 μg/lane) and pooled jejunal epithelial cell extracts (10 μg/lane). NHERF-1 expression was not significantly altered in NHERF-2-deficient mice. Actin was used as a loading control.
(Color figure on page 165.)

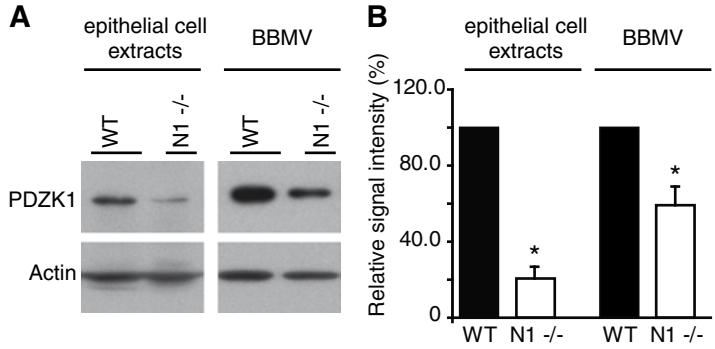

Figure 7. *A*, Western blot analysis of PDZK1 in jejunal epithelial cell extracts (20 μg/lane) and jejunal BBMVs (2.5 μg/lane) of WT and NHERF-1-deficient (N1-/-) mice. NHERF-1-deficient mice displayed reduced PDZK1 abundance in both jejunal cell extracts and BBMVs. A representative Western blot is shown. Actin was used as a loading control. *B*, quantification of PDZK1 abundance relative to wild type. The data are the means ± S.E. from at least five Western blots using five independently isolated pools of enterocytes or BBMVs. *, $p < 0.05$ *versus* wild type.

protein kinase in the vicinity of CFTR and improving CFTR phosphorylation and activation. This differs from the functional role of NHERF-1 and NHERF-2 in the regulation of NHE3 in PS120 and OK cell lines and the role of NHERF-1 in the kidney brush border. Both NHERF-1 and NHERF-2 are able to mediate cAMP-dependent inhibition of NHE3 by facilitating formation of a NHERF/NHE3/ezrin complex. Ezrin then acts as AKAP (cAMP dependent protein kinase anchoring protein) and tethers cAMP-dependent protein kinase near its phosphorylation target (13,14, 41).

The role of NHERF-1 and NHERF-2 in the cGMP-dependent regulation of CFTR has not been described previously. Our results indicate that absence of NHERF-1 affected cGMP-dependent activation of CFTR to a similar extent as cAMP-dependent activation in jejunal epithelial cells (Fig. 2). NHERF-2 ablation on the other hand did not affect CFTR stimulation by cGMP. This is a second line of evidence suggesting that the mechanism of regulation by the NHERF proteins differs between CFTR and NHE3, because cGMP-dependent inhibition of NHE3 in PS120 and OK cell lines requires NHERF-2 but not NHERF-1 (33).

The major controversial issue concerning the function of the NHERF proteins as CFTR regulators is their possible involvement in apical targeting or retention. Our results demonstrate that the total amount of CFTR present in the brush borders of epithelial cells as measured by Western blotting was unaltered, arguing against a key role of NHERF-1 and NHERF-2 in targeting CFTR to the apical membrane in native intestinal tissue. The ratio of CFTR band B to band C was also unaltered, suggesting that CFTR maturation and glycosylation were not grossly affected by NHERF-1 ablation. Furthermore, confocal microscopy showed no evidence for an alteration in the localization of CFTR in jejunal crypts of NHERF-1 -/- mice, but it should be added that not all CFTR present in the cell is detected by this technique; in general, even the best CFTR antibodies fail to detect CFTR in the endoplasmic reticulum and Golgi, although it is known to be present there as well (42). Based on analysis of CFTR abundance in jejunal crypts by confocal microscopy, we estimate that the mean fluorescence intensity and the total level of fluorescence per crypt were reduced by ~35% in NHERF-1- and NHERF-1/2-deficient mice. This differs from the result obtained by Western blotting. To account for both seemingly paradoxical results, we assume that not the amount but the distribution of CFTR in the apical membrane and/or the subapical compartment is altered in NHERF-1 null mice. CFTR is known to be continuously endocytosed and recycled back to the plasma membrane, and interaction with PDZ proteins has been shown to increase endocytic recycling in MDCK cells (21, 43). NHERF-1 deficiency could therefore lead to a redistribution of CFTR between apical and subapical compartments, possibly resulting in a more diffuse pattern and reduced local fluorescence levels that may drop below the detection limit. Attempts to reduce this limit by increasing the pinhole size caused overexposure in areas where the fluorescence was the most intense. Unfortunately, the resolution of the microscope was not sufficient to clearly distinguish between CFTR localized in the apical membrane and in submembrane vesicles.

Various recent investigations have shown that C-terminally mutated CFTR has a higher mobility in the membrane, as measured by fluorescence recovery after photobleaching of GFP-labeled CFTR and by single particle tracking of individual CFTR molecules labeled with quantum dots (15, 16, 44). The lateral mobility of CFTR was also increased by overexpression of dominant-negative NHERF-1 lacking the ezrin-binding domain, suggesting that coupling of CFTR to the cytoskeleton limits its mobility (15). Importantly, a reduction in the amount of ezrin and phospho-ezrin was reported in the brush border membrane of kidney and intestinal homogenates from a different line of NHERF-1 null mice (45). Uncoupling of CFTR from the cytoskeleton and an altered migration pattern could potentially explain relocalization and a more diffuse distribution.

Alternatively, it may be that the changes in CFTR immunostaining and activity reflect a loss of NHERF-1-driven CFTR dimerization. Possibly, CFTR dimers are more readily detected by immunostaining (because of the higher local density of the signal), and the formation of dimers by the action of NHERF-1 (or PDZK1) is known to increase the open probability of the CFTR channel. Future CFTR crosslinking studies on native intestinal epithelium may help to further evaluate this model.

Whereas our data indicate that NHERF-1 is an important factor for regulation of CFTR activity in jejunal epithelial cells, we could not identify a similar role for NHERF-2. This may be indicative for a functional difference between these sister proteins or, alternatively, might be explained by the low levels of NHERF-2 protein in murine small intestinal epithelium. Unexpectedly, we failed to detect NHERF-2 in jejunal BBMVs by Western blot despite previous claims of NHERF-2 protein expression in rabbit small intestine and more recently also in the small intestine of CD1 mice (46, 47). Although we did observe a prominent band in our NHERF-2 blots of jejunal BBMVs isolated from FVB and CD1 mice, it was attributed to a cross-reactivity of the antibody with abundantly expressed NHERF-1, based on its higher molecular weight and its detection in BBMVs from NHERF-2-deficient but not NHERF-1-deficient mice (data not shown).

The reduced PDZK1 abundance that we observed in NHERF-1-deficient mice (Fig. 7) suggests that NHERF-1 may be important for the stabilization of PDZK1. In contrast, NHERF-1 RNA and protein abundance were not altered in the jejunum of PDZK1-deficient mice (48). Most plausibly, NHERF-1 and PDZK1 form a complex *in vivo*, in line with the observation that the proteins can form heterodimers *in vitro* (49). The notion that expression and/or stability of PDZK1 and NHERF-1 are interconnected is supported by the observation that the NHERF-1 abundance in proximal kidney tubules of PDZK1-deficient mice was increased by ~50%, but only when mice were kept on a high phosphate diet (50). This might be a compensatory mechanism to counteract the reduced Npt2a abundance in the membrane, which has been observed in both NHERF-1- and PDZK1-deficient mice (24, 50). Our data indicates that PDZK1 and NHERF-1 function also overlaps in the duodenum, where the bicarbonate secretion was recently shown to be reduced (by approximately 20%) in the PDZK1-deficient mice (48). In contrast, the jejunal forskolin-activated anion

secretion was not affected in PDZK1-deficient mice compared with wild type controls (48), suggesting that in this segment PDZK1 is not required for normal CFTR function or that NHERF-1 is able to fully compensate for PDZK1 loss. Because a total absence of PDZK1 does not affect I_{sc}, we conclude that the reduction in CFTR-dependent activation of anion transport in the NHERF-1 null mice (Fig. 2) is the direct consequence of NHERF-1 ablation and not secondary to the lowered PDZK1 abundance in these mice.

In summary, we have shown that NHERF-1 is important for full activity of CFTR in native duodenal and jejunal epithelial tissue as well as in nystatin-permeabilized epithelium. Whereas NHERF-1 is not required for targeting CFTR to the apical membrane (as evidenced by normal CFTR levels in the brush borders), it is responsible for placing or keeping more active CFTR in the apical membrane, most likely by affecting the local distribution of CFTR and/or by linking CFTR to the actin cytoskeleton. Our observations provide new insight into the role of NHERF-1 in the formation of CFTR-containing functional complexes in the apical membrane of jejunal enterocytes and in the pathophysiology of cystic fibrosis in patients expressing C-terminally truncated CFTR. Interestingly, it was reported recently that small molecules fitting in the binding pocket of PDZ domains can be used to disrupt interactions with peptide ligands. By using a newly developed reversible inhibitor, a reduction of CFTR activation by CPT-cAMP in bronchial airway cells was achieved (51). In line with our finding that CFTR interaction with NHERF-1 is important for its full activation in native epithelium, this suggests that a novel class of anti-diarrheal drugs could potentially be developed that targets interactions of NHERF-1 with its binding partners. This would possibly lead not only to reduced chloride secretion by CFTR but also to enhanced salt absorption by NHE3.

Acknowledgment

The authors are grateful for the assistance of Brigitta Riederer and Pim van Schalkwijk with breeding and genotyping of mice and Western blots, and Mingmin Chen for help with measuring bicarbonate secretion. Chris Yun and Chris Marino generously provided the NHERF-1, NHERF-2 and CFTR antibodies.

These studies were financially supported by the Sophia Foundation grant 506-2006 (H. de J.); the DFG grants Se 460/13-1/2, DFG Se 460/17-1, and Sonderforschungsbereich SFB 621/project C9 (U.S.);. MLDS grant MWO 03-15 (H. de J.); NIH grant DK55881 (E.J.W. and S.S.); Research Service, Department of Veteran Affairs (E.J.W.); NIH NIDDK Grants RO1DK26523, RO1 DK61765, PO1 DK072084 and R24 DK64388 (M.D.) and the Hopkins Basic Research Digestive Diseases Development Core Center (M.D.).

References

1. Collins, F. S. (1992) *Science* **256**, 774-779
2. Field, M. (2003) *J. Clin. Invest.* **111**, 931-943
3. Karthikeyan, S., Leung, T., and Ladias, J. A. (2001) *J. Biol. Chem.* **276**, 19683-19686
4. Short, D. B., Trotter, K. W., Reczek, D., Kreda, S. M., Bretscher, A., Boucher, R. C., Stutts, M. J., and Milgram, S. L. (1998) *J. Biol. Chem.* **273**, 19797-19801
5. Wang, S., Raab, R. W., Schatz, P. J., Guggino, W. B., and Li, M. (1998) *FEBS Lett.* **427**, 103-108
6. Thelin, W. R., Hodson, C. A., and Milgram, S. L. (2005) *J. Physiol.* **567**, 13-19
7. Raghuram, V., Hormuth, H., and Foskett, J. K. (2003) *Proc. Natl. Acad. Sci. USA* **100**, 9620-9625
8. Schreiber, R., Boucherot, A., Murle, B., Sun, J., and Kunzelmann, K. (2004) *J. Membr. Biol.* **199**, 85-98
9. Donowitz, M., Cha, B., Zachos, N. C., Brett, C. L., Sharma, A., Tse, C. M., and Li, X. (2005) *J. Physiol.* **567**, 3-11
10. Guggino, W. B., and Stanton, B. A. (2006) *Nat Rev Mol Cell Biol* **7**, 426-436
11. Sun, F., Hug, M. J., Bradbury, N. A., and Frizzell, R. A. (2000) *J. Biol. Chem.* **275**, 14360-14366
12. Benharouga, M., Sharma, M., So, J., Haardt, M., Drzymala, L., Popov, M., Schwapach, B., Grinstein, S., Du, K., and Lukacs, G. L. (2003) *J. Biol. Chem.* **278**, 22079-22089
13. Dransfield, D. T., Bradford, A. J., Smith, J., Martin, M., Roy, C., Mangeat, P. H., and Goldenring, J. R. (1997) *EMBO J.* **16**, 35-43
14. Yun, C. H., Oh, S., Zizak, M., Steplock, D., Tsao, S., Tse, C. M., Weinman, E. J., and Donowitz, M. (1997) *Proc. Natl. Acad. Sci. USA* **94**, 3010-3015
15. Haggie, P. M., Kim, J. K., Lukacs, G. L., and Verkman, A. S. (2006) *Mol. Biol. Cell* **17**, 4937-4945
16. Bates, I. R., Hebert, B., Luo, Y., Liao, J., Bachir, A. I., Kolin, D. L., Wiseman, P. W., and Hanrahan, J. W. (2006) *Biophys. J.* **91**, 1046-1058
17. Wang, S., Yue, H., Derin, R. B., Guggino, W. B., and Li, M. (2000) *Cell* **103**, 169-179
18. Raghuram, V., Mak, D. D., and Foskett, J. K. (2001) *Proc. Natl. Acad. Sci. USA* **98**, 1300-1305
19. Moyer, B. D., Denton, J., Karlson, K. H., Reynolds, D., Wang, S., Mickle, J. E., Milewski, M., Cutting, G. R., Guggino, W. B., Li, M., and Stanton, B. A. (1999) *J. Clin. Invest.* **104**, 1353-1361
20. Milewski, M. I., Mickle, J. E., Forrest, J. K., Stafford, D. M., Moyer, B. D., Cheng, J., Guggino, W. B., Stanton, B. A., and Cutting, G. R. (2001) *J. Cell Sci.* **114**, 719-726
21. Swiatecka-Urban, A., Duhaime, M., Coutermarsh, B., Karlson, K. H., Collawn, J., Milewski, M., Cutting, G. R., Guggino, W. B., Langford, G., and Stanton, B. A. (2002) *J. Biol. Chem.* **277**, 40099-40105
22. Ostedgaard, L. S., Randak, C., Rokhlina, T., Karp, P., Vermeer, D., Ashbourne Excoffon, K. J., and Welsh, M. J. (2003) *Proc. Natl. Acad. Sci. USA* **100**, 1937-1942
23. Zambrowicz, B. P., Friedrich, G. A., Buxton, E. C., Lilleberg, S. L., Person, C., and Sands, A. T. (1998) *Nature* **392**, 608-611
24. Shenolikar, S., Voltz, J. W., Minkoff, C. M., Wade, J. B., and Weinman, E. J. (2002) *Proc. Natl. Acad. Sci. USA* **99**, 11470-11475
25. Ratcliff, R., Evans, M. J., Cuthbert, A. W., MacVinish, L. J., Foster, D., Anderson, J. R., and Colledge, W. H. (1993) *Nat. Genet.* **4**, 35-41
26. Vaandrager, A. B., Bajnath, R., Groot, J. A., Bot, A. G., and De Jonge, H. R. (1991) *Am. J. Physiol.* **261**, G958-965
27. Bijvelds, M. J., Jorna, H., Verkade, H. J., Bot, A. G., Hofmann, F., Agellon, L. B., Sinaasappel, M., and de Jonge, H. R. (2005) *Am. J. Physiol. Gastrointest. Liver Physiol.* **289**, G870-879
28. Markert, T., Vaandrager, A. B., Gambaryan, S., Pohler, D., Hausler, C., Walter, U., De Jonge, H. R., Jarchau, T., and Lohmann, S. M. (1995) *J. Clin. Invest.* **96**, 822-830
29. Van Dommelen, F. S., Hamer, C. M., and De Jonge, H. R. (1986) *Biochem J.* **236**, 771-778
30. French, P. J., van Doorninck, J. H., Peters, R. H., Verbeek, E., Ameen, N. A., Marino, C. R., de Jonge, H. R., Bijman, J., and Scholte, B. J. (1996) *J. Clin. Invest.* **98**, 1304-1312
31. Weinman, E. J., Steplock, D., Tate, K., Hall, R. A., Spurney, R. F., and Shenolikar, S. (1998) *J. Clin. Invest.* **101**, 2199-2206
32. Hwang, J. I., Heo, K., Shin, K. J., Kim, E., Yun, C., Ryu, S. H., Shin, H. S., and Suh, P. G. (2000) *J. Biol. Chem.* **275**, 16632-16637
33. Cha, B., Kim, J. H., Hut, H., Hogema, B. M., Nadarja, J., Zizak, M., Cavet, M., Lee-Kwon, W., Lohmann, S. M., Smolenski, A., Tse, C. M., Yun, C., de Jonge, H. R., and Donowitz, M. (2005) *J. Biol. Chem.* **280**, 16642-16650

34. Barrett, K. E., and Keely, S. J. (2000) *Annu. Rev. Physiol.* **62**, 535-572
35. Thiagarajah, J. R., and Verkman, A. S. (2003) *Curr. Opin. Pharmacol.* **3**, 594-599
36. Seidler, U., Bachmann, O., Jacob, P., Christiani, S., Blumenstein, I., and Rossmann, H. (2001) *J.O.P.* **2**, 247-256
37. Lee, J. H., Richter, W., Namkung, W., Kim, K. H., Kim, E., Conti, M., and Lee, M. G. (2007) *J. Biol. Chem.* **282**, 10414-10422
38. Cheng, J., Moyer, B. D., Milewski, M., Loffing, J., Ikeda, M., Mickle, J. E., Cutting, G. R., Li, M., Stanton, B. A., and Guggino, W. B. (2002) *J. Biol. Chem.* **277**, 3520-3529
39. Reddy, M. M., and Quinton, P. M. (1994) *J. Membr. Biol.* **140**, 57-67
40. Knowles, M. R., Paradiso, A. M., and Boucher, R. C. (1995) *Hum. Gene Ther.* **6**, 445-455
41. Weinman, E. J., Steplock, D., and Shenolikar, S. (2003) *FEBS Lett.* **536**, 141-144
42. Claass, A., Sommer, M., De Jonge, H. R., Kalin, N., and Tummler, B. (2000) *J. Histochem. Cytochem.* **48**, 831-837
43. Prince, L. S., Workman, R. B., Jr., and Marchase, R. B. (1994) *Proc. Natl. Acad. Sci. USA* **91**, 5192-5196
44. Haggie, P. M., Stanton, B. A., and Verkman, A. S. (2004) *J. Biol. Chem.* **279**, 5494-5500
45. Morales, F. C., Takahashi, Y., Kreimann, E. L., and Georgescu, M. M. (2004) *Proc. Natl. Acad. Sci. USA* **101**, 17705-17710
46. Li, C., Dandridge, K. S., Di, A., Marrs, K. L., Harris, E. L., Roy, K., Jackson, J. S., Makarova, N. V., Fujiwara, Y., Farrar, P. L., Nelson, D. J., Tigyi, G. J., and Naren, A. P. (2005) *J Exp. Med.* **202**, 975-986
47. Yun, C. C., Chen, Y., and Lang, F. (2002) *J. Biol. Chem.* **277**, 7676-7683
48. Hillesheim, J., Riederer, B., Tuo, B., Chen, M., Manns, M., Biber, J., Yun, C., Kocher, O., and Seidler, U. (2007) *Pflügers Arch.* **454**(4):575-86.
49. Gisler, S. M., Pribanic, S., Bacic, D., Forrer, P., Gantenbein, A., Sabourin, L. A., Tsuji, A., Zhao, Z. S., Manser, E., Biber, J., and Murer, H. (2003) *Kidney Int.* **64**, 1733-1745
50. Capuano, P., Bacic, D., Stange, G., Hernando, N., Kaissling, B., Pal, R., Kocher, O., Biber, J., Wagner, C. A., and Murer, H. (2005) *Pflügers Arch.* **449**, 392-402
51. Fujii, N., Haresco, J. J., Novak, K. A., Gage, R. M., Pedemonte, N., Stokoe, D., Kuntz, I. D., and Kiplin Guy, R. (2007) *Bioorg. Med. Chem. Lett.* **17**, 549-552

CHAPTER 3

Defective jejunal and colonic salt absorption and altered NHE3 regulation in PDZ-adapter protein NHERF-1 deficient mice

N. Broere[1*], M. Chen[2*], A. Cinar[2], A. K. Singh[2], J. Hillesheim[2], B. Biederer[2], M. Lünnemann[2], I. Rottinghaus[2], A. Krabbenhöft[2], R. Engelhardt[2], B. Rausch[2], E. J. Weinman[3], M. Donowitz[4], A. Hubbard[5], O. Kocher[6], H. R. de Jonge[1], B. M. Hogema[1], U. Seidler[2]

[1]Dept. of Biochemistry, Erasmus University Medical Center, Rotterdam,
[2]Dept. of Gastroenterology, Hannover Medical School, Hannover,
[3]Departments of Medicine and Physiology, University of Maryland School of Medicine;
[4]Departments of Medicine, Physiology, and
[5]Dept of Cell Biology, Johns Hopkins University School of Medicine, Baltimore
[6]Department of Pathology, Beth Israel Deaconess Medical Center and Harvard Medical School, Boston, MA

[*] these two authors share first authorship and are listed in alphabetical order

Manuscript in preparation

Abstract

Background and aims: We investigated the effect of genetic ablation of the NHE3-binding PDZ adapter protein NHERF-1 on intestinal salt and water absorption, NHE3 mRNA expression, NHE3 protein abundance, and transport activity in the murine intestine. **Results:** NHERF-1-deficient mice displayed reduced jejunal fluid absorption *in vivo*, as well as a attenuated Na^+ absorption in isolated mucosa of jejunal and colonic tissue but not of ileal mucosa. However, cAMP-mediated inhibition of both parameters remained intact. The acid-stimulated NHE3 transport rate was decreased in BCECF-loaded surface colonocytes, whereas inhibition by intracellular cAMP or cGMP was normal. Immunodetection of NHE3 revealed a normal NHE3 localization in the brush border membrane (BBM) of NHERF-1 null mice, but NHE3 abundance was significantly reduced as measured by Western blot analysis of isolated BBM from the small and large intestine. Additional knockout of PDZK1 (NHERF-3), another member of the NHERF family of adapter proteins, which binds to both NHE3 and NHERF-1, further reduced acid-activated NHE3 activity and caused a complete loss of cAMP-mediated NHE3 inhibition. However, NHERF-3 ablation did not further reduce NHE3 membrane abundance. An activator of the exchange protein activated by cAMP (EPAC) had no effect on jejunal fluid absorption *in vivo,* but slightly inhibited NHE3 activity in surface colonocytes *in vitro*. **Conclusion:** The absence of NHERF-1 has segment-specific effects on intestinal salt absorption, acid-activated NHE3 transport rates and NHE3 protein membrane abundance without affecting mRNA levels. However, in contrast to PDZK1, NHERF-1 is not required for NHE3 regulation by cyclic nucleotides.

Introduction

Electroneutral NaCl absorption is the major mechanism for intestinal salt and water absorption and is primarily mediated via the Na^+/H^+ exchanger NHE3 (1) and the Cl^-/HCO_3^- exchangers DRA (Slc26a3) (2) and PAT1 (Slc26a6) (3). The agonist-induced inhibition of this transport process causes diarrhea and is operative in diarrheal diseases of most etiologies. An increase in the enterocyte intracellular cyclic nucleotide levels, elicited by a multiple enterotoxins, hormones, and paracrine mediators, inhibits intestinal fluid absorption *in vivo* (4), and sodium as well as chloride absorption in isolated small and large intestinal mucosa *in vitro* in the presence but not in the absence of NHE3 (3). NHE3-binding proteins were identified as cofactors required for cAMP-mediated inhibition and were later called NHERF-1 (EBP50) and NHERF-2 (E3KARP) (reviewed in (5, 6)). It was shown that cAMP-mediated inhibition of NHE3 expressed in PS120 fibroblasts required co-expression of either NHERF-1 or NHERF-2 (7, 8).

These early studies were the first steps towards the understanding that NHE3, like many other transport proteins, is regulated within a multiprotein complex containing the ion transporter as well as anchoring proteins, the cytoskeleton, and the required protein kinases (5, 9, 10). It has since then been formulated that using drugs to target

the PDZ-domain interaction could theoretically be a highly efficient antidiarrheal strategy (5, 11). One cornerstone of future drug development targeting NHERF-mediated protein-protein interactions is an understanding of their function in different tissues of the living organism. In this study, we examined the effect of NHERF-1 ablation on fluid absorption in the intestine *in vivo* and observed a decreased fluid absorption in the jejunum of NHERF-1-deficient mice corresponding to a decreased sodium and chloride absorption in isolated jejunal mucosa. Furthermore, we studied the regulation of NHE3 activity in colonic and small intestinal enterocytes of NHERF-1-deficient mice and found decreased acid-activated NHE3 transport rates in surface enterocytes, whereas the inhibition of NHE3 transport rates by cyclic nucleotides was still intact in the absence of NHERF-1. NHE3 brush border membrane localization was unaffected by NHERF-1 deficiency, but the NHE3 brush border abundance was reduced. Because PDZK1 (NHERF-3) binds both NHERF-1 and NHE3 (12), we also studied the effect of combined NHERF-1 and PDZK1 ablation on intestinal salt and water transport, and the regulation of NHE3 transport rates. Absence of both PDZ proteins did not result in further reduction of jejunal fluid absorption or NHE3 abundance in the BBM, but it severely interfered with NHE3 regulation by acid and second messengers.

Material and methods

Animals - NHERF-1 null mice were generated in the laboratory of E.J. Weinman as described (13), and were bred for at least 6 generations into the FVB/N genetic background in the animal houses of the Erasmus University of Rotterdam and the Hannover Medical School. PDZK1 -/- mice were generated in the laboratory of O. Kocher at Harvard Medical School as described (14). For the purpose of this study, they were crossed into the FVB/N background and bred for several generations, before breeding NHERF-1/PDZK1 double-deficient mice. Wild-type control mice were bred from the same founders. Mice used in experiments were sex- and age-matched and were littermates in the case of the single-deficient mice, and no more than two generations apart (same great-grandparents) in the case of the double-deficient mice. Animal experiments followed approved protocols at the Medical School of Hannover and local authorities for the regulation of animal welfare (Regierungspräsidium) and the Dutch Animal Welfare Committee. Animals had *ad libitum* access to water and chow, but were fasted overnight before the *in vivo* perfusion experiments.

Single pass jejunal and ileal perfusion experiments *in vivo* - Induction of anaesthesia was achieved by the administration of 10 µL/g intraperitoneal (IP) haloperidol/midazolam/fentanyl cocktail (haloperidol 12.5 mg/Kg, fentanyl 0.325 mg/Kg and midazolam 5 mg/Kg body weight), and maintained using the cocktail at 20% of the initial dose every 30–45 minutes as indicated by respiratory rate and toe pinch reflex. The abdomen was opened by a small central incision, and approximately 10-15 cm of the jejunum or last part of the ileum, was exposed for the subsequent ligation. A polyethylene tube (PE100) with a distal flange was advanced to the jejunum (first incision 3-4 cm distal to the stomach, one PE200 tube was advanced into the proximal part to allow drainage of proximal secretions, then another PE100 tube was advanced into the mid jejunum (6-8 cm distal to pylorus) and secured by a ligature. The 10-15 cm isolated jejunal segment with intact blood supply was gently flushed and then perfused (Perfusor compact, BRAUN) at a rate of 3 mL/hr with 150

mmol/L NaCl. Effluents from the isolated segment were free of blood (visually and by haemocult test) throughout all experiments. Animals were maintained at 37°C using a heating pad controlled by a rectal thermistor probe. After an initial 30-minute washout, basal fluid absorption was measured for 30 minutes, followed by a 30 min perfusion with 150 mM NaCl containing 100 µM forskolin (FSK). At the end, mice were sacrificed by cervical dislocation and the length of the perfused jejunum was measured. The perfusate was collected in a pre-weighed 4.5 mL collecting tube. The amount of fluid absorbed was calculated by subtracting the amount of fluid recovered after 30 min from the amount perfused during the 30 min (1.5 ml) and absorption rates are expressed in millilitres of fluid absorbed per cm jejunum length per hour ($mL \cdot cm^{-1} \cdot hr^{-1}$).

Isolated loop experiments for *in vivo* measurement of intestinal fluid uptake - Fluid absorption was determined in mice (12-20 weeks) under ketamine/xylazine anesthesia (100 and 20 mg/Kg respectively, IP). An incision was made along the abdominal midline. The small intestine was rinsed with PBS (37°C) through a small distal incision and divided in three loops (10-12 cm each) which were closed by sutures and filled with isotonic PBS (37°C; ~90 µl/cm). The abdomen was closed with clips and animals were placed in a humidified 37°C incubator. After 1 h, mice were euthanized and the loop length and remaining fluid were measured. When indicated, 8-Br-cAMP (2 mM) or 8-Br-cGMP (0.5 mM) was added to the luminal solution; in that case the experiment was terminated after 2h instead of 1h. Absorption was determined as the difference between the amount of fluid injected and the remaining amount of fluid and expressed as $mL \cdot cm^{-1} \cdot hr^{-1}$.

$^{22}Na^+$ and $^{36}Cl^-$ flux studies in isolated mucosa *in vitro* - The preparation of the isolated jejunal mucosa and the $^{22}Na^+$ and $^{36}Cl^-$ flux studies were performed exactly as recently described (3). For the colonic flux measurements, the serosal to mucosal and the mucosal to serosal fluxes were determined in equivalent segments of proximal colon from two different mice, because the colon is too short to allow isolation of multiple pieces of tissue.

Preparation of colonic crypts and pH_i measurements - Murine colonic crypt preparation and fluorometric pH-measurements were performed exactly as recently described (15). The principle of the pH_i measurement method is that BCECF-loaded colonic crypts were acidified using an ammonium prepulse (40 mM NH_4Cl isotonically replacing NaCl) for 5 min, then perfused for 5 min with a Na^+-free buffer (TMA^+ isotonically replacing Na^+), until pH_i reached its lowest value plateau. Subsequently, 50 µM HOE642 and, if appropriate, 10^{-5} M forskolin was added to the Na^+-free buffer. 50 µM HOE642 has previously been shown to completely inhibit NHE1 and NHE2 (16). After 2-3 min, the buffer was switched to Na^+-containing buffer A, containing 50 µM HOE642 and forskolin or 8-Br-cGMP, if appropriate. Images were digitized every 1 (phase of rapid pH_i-recovery) -30 (plateau phases) seconds with a cooled CCD camera (CoolSnap ES, Roper Scientific, Ottobrunn, Germany) using the Metafluor software (Universal Imaging Corporation, Downington, PA, USA) during exposure of cells to alternating 440 and 495 nm light from a monochromator (Visichrome, Visitron Systems, Puchheim, Germany) with a 515 nm DCXR dichroic mirror and a 535 nm barrier filter (Chroma Technology Corp, Rockingham, VT, USA) in the emission pathway. Calibration of the 440/495 ratio was performed as described previously (17). Regions of interest (ROIs) were selected in the apical part of the crypts, where NHE3 is expressed. Intrinsic buffering capacity was determined for isolated murine colonic crypts using the protocol as described by Boyarsky et al. (18). $ß_i$ did not differ significantly between a variety of mouse genotypes and transgenes (15, 17) and has been published in graphic form before (17).

Immunohistochemistry and confocal microscopy - Formalin-fixed, paraffin-embedded tissue sections (5 µm) from mice with different genotypes were prepared on the same slide. After deparaffinization with xylene and treatment with 0.01M sodium citrate solutions, endogenous peroxidase activity was blocked with 0.6% H_2O_2 and 0.12% sodium azide. Sections were incubated with anti-NHE3 antibodies (1:100; NHE31-A, Alpha diagnostics Inc.) in PBS with 2% bovine albumin for 1 h at room temperature. Sections were subsequently incubated for 2 h with FITC-labeled secondary antibody (1:100; Nordic) and mounted with Vectashield (Vector). Immunofluorescence micrographs were captured using a Zeiss LSM510 confocal microscope equipped with a 25 mW Argon laser (488 nm). Fluorescence emission after excitation at 488 nm was detected using a 40x/1.3 numerical-aperture oil immersion lens, a dichroic beam splitter reflecting 488 nm excitation light and a 505-530 bandpass emission filter. Images were scanned using a 428µm (colon) and 703µm (jejunum) pinhole size. The same threshold was utilized for all images from one slide. Three age- and sex-matched mice of each genotype were analyzed.

Preparation of jejunal and colonic brush border membranes and Western blot analysis - NHE3 quantification was performed both in Hannover and in Rotterdam, using similar procedures. The preparation of small intestinal and colonic BBM vesicles and homogenate and the Western analysis were performed exactly as recently described (15, 19). Western blotting in Rotterdam was performed as described (6, 20).

Quantitative RT-PCR - PCR primers were designed using the computer programs "HUSAR PRIME" Sequence Analysis Software (STZ Genominformatik, Heidelberg) or with "Primer Express" (Applied Biosystems). Primer sequences were NHE3.for: 5'-AGGCCACCAACTATGAAGAG-3', NHE3.rev: 5'-AGGGGAGAACACGGGATTATC-3', PCR-product length 110 bp, (NHE3, NM_00108160); villin.for: 5'-TCATACTCAAGACTCCGTCC-3'; villin.rev: 5'-CACTTGTTTCTCCGTCC-3'; 119 bp; (Villin1, NM_009509.1); RPS9.for: 5'-AAGCACATCGACTTCTCCC-3'; RPS9.rev: 5'-ACAATCCTCCAGTTCAGCC-3', 150bp ; RPS9 (ribosomal protein 9, NM_ 029767.2). Real-time PCR reactions were carried out using SyberGreen PCR-Master-Mix (Applied Biosystems) in the Applied Biosystems 7300 Realtime PCR System. PCR extension was performed at 60°C with 40 repeats. Data were analysed using Sequence Detection Software 1.2.3 (Applied Biosystems) and exported to Microsoft Excel. Relative quantification was carried out using Villin and RPS9 as reference genes.

Statistical Analyses - Values are expressed as mean ± SE. Statistical analysis was performed using Student's *t*-test, Wilcoxon rank test, or ANOVA. P values <0.05 were considered statistically significant.

Results

In vivo fluid absorption rates in the NHERF-1 -/- and +/+ murine jejunum and ileum during single pass perfusion - Basal fluid absorption rates in the mid jejunum of anesthetized mice were significantly lower in NHERF-1 -/- mice compared to wild-type littermates (Figure 1A). Since fluid movement is secondary to electrolyte movements, this suggests net salt absorption is reduced in the jejunum in the absence of NHERF-1. Subsequent addition of 10^{-4} M forskolin to the luminal perfusate induced fluid secretion in both NHERF-1 -/- mice and control littermates, but the effect of forskolin was significantly lower in NHERF-1 -/- compared with +/+ littermates. In contrast, no significant difference in fluid absorption was observed in the distal ileum of NHERF-1-deficient mice (Figure 1B). In the proximal colon, similar experiments were not successful, because the colonic mucosa secreted fluid even in what we measure as the "basal period". We assume that the manipulation of the proximal colon to empty its fecal content elicits long-lasting secretory reflexes.

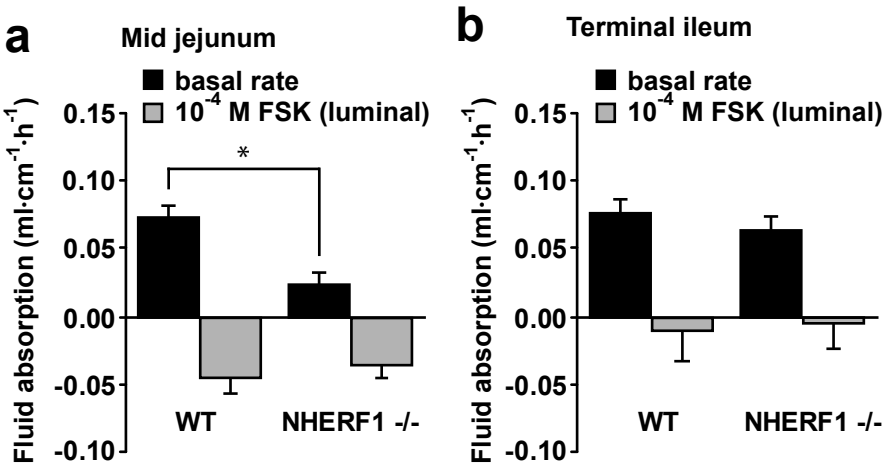

Figure 1. Fluid transport in the basal state and after FSK stimulation in the jejunum and ileum of anaesthetized NHERF-1 +/+ and -/- mice in vivo. Figure 1A: Jejunal fluid absorption rates in the basal state (black bars) and during luminal application of 10^{-4} M FSK (gray bars). Approximately 5 cm was perfused for 30 min and the amount of fluid absorbed was measured at the end of the experiment. Jejuna from NHERF-1-deficient mice absorbed significantly less fluid than WT littermates (* $P < 0.05$). In addition, the change in fluid transport from absorption to secretion was significantly less in the NHERF-deficient mice than the WT mice. This is likely due to the reduced CFTR activation (20). Data represent values from five independent experiments and are expressed as mean ± SE. Figure 1B: These differences were not observed in the terminal ileum of anesthetized NHERF-1-deficient and WT mice. n = 5.

Because the changes in fluid flux in this model are generated both by an inhibition of salt absorption and a stimulation of anion secretion, it cannot be said with certainty which process is primarily affected. This was clarified by performing isotope flux studies in isolated jejunal mucosa in Ussing-chamber setups.

$^{22}Na^+$ and $^{36}Cl^-$ fluxes in isolated jejunal and colonic mucosa of NHERF-1 -/- and WT mice - Net Na^+ and Cl^- absorption was measured in isolated jejunal mucosa by assessing bilateral $^{22}Na^+$ and $^{36}Cl^-$ fluxes, and subtracting the mucosal to serosal flux from the serosal to mucosal flux for each individual tissue pair. Basal net Na^+ absorption was significantly decreased in NHERF-1 -/- jejuna as compared to WT controls, but the inhibition by forskolin was intact in the absence of NHERF-1. In addition, stimulation of the Na^+/glucose cotransporter by addition of luminal glucose resulted in comparable increases in sodium flux (as well as the short circuit current), indicating that SGLT1 is unaffected by the absence of NHERF-1 (Figure 2A).

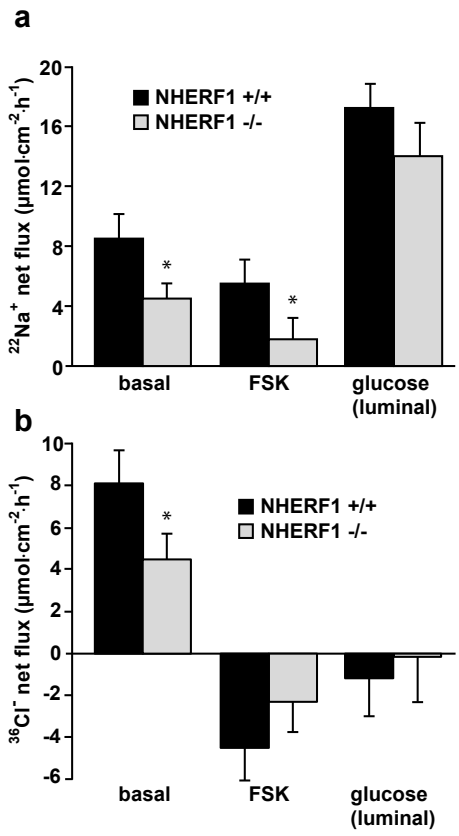

Figure 2. Net $^{22}Na^+$ and $^{36}Cl^-$ fluxes in isolated NHERF-1 +/+ and -/- jejunal mucosa. Figure 2A: Net $^{22}Na^+$ flux in mid-jejunal mucosa, as calculated by subtraction of the individual serosal to mucosal flux values from the mucosal to serosal flux values for each paired tissue sample were determined in NHERF-1 +/+ (black bars) and -/- mice (gray bars). A significant difference was observed in the basal Na^+ absorption between NHERF-1 +/+ and -/- mice (*, $P < 0.05$), but the relative inhibition by 10^{-5} M FSK applied to the serosal bath was similar. The response to 25 mM luminal glucose, added to stimulate the Na^+-glucose cotransporter, was similar; n = 9). Figure 2B: Net $^{36}Cl^-$ flux in mid jejunal mucosa, calculated similarly to the $^{22}Na^+$ flux experiments. A significant difference was observed in the basal absorption rates in NHERF-1 +/+ and -/- jejunum, similar to the decrease in net Na^+ absorption. In addition, there was a significant difference in the effect of FSK on the flux change (from the absorptive state to the secretory state), reflecting the defect in CFTR activation in the absence of NHERF-1 (20). I_{sc} values are given in the text. n = 8.

The net Cl^- absorption was also reduced in the absence of NHERF-1 (Figure 2B). In contrast to the comparable efficacy of cAMP in inhibiting Na^+ absorption in the absence vs. the presence of NHERF-1, there was a significant difference in the forskolin-stimulated net Cl^- secretion. This corresponded to a strong reduction in the FSK-stimulated short circuit current in the NHERF-1 -/- tissues compared to the WT tissues (ΔI_{sc} was 195±26 µA/cm^2 in WT vs. 102±12 µA/cm^2 in the NHERF-1-deficient jejunal mucosae), as has been observed before (20). The results suggest that the absence of NHERF-1 causes a significant reduction in the basal Na^+ absorption and a defect in cAMP-mediated stimulation of CFTR-dependent anion

secretion, but does not significantly affect cAMP-mediated inhibition of NHE3-dependent jejunal salt absorption.

The same experiments were performed in isolated proximal colonic mucosa. Because of the small size of the proximal colon, one section from the proximal colon was taken from two different mice to determine the unilateral fluxes. Again, the net Na^+ absorption rates were mildly, but significantly reduced in the NHERF-1 -/- mucosa, and inhibition by cAMP was observed (Figure 3). Because of the small size of the proximal colon and the necessity to perform many flux experiments to obtain significant results, we did not perform Cl^- fluxes.

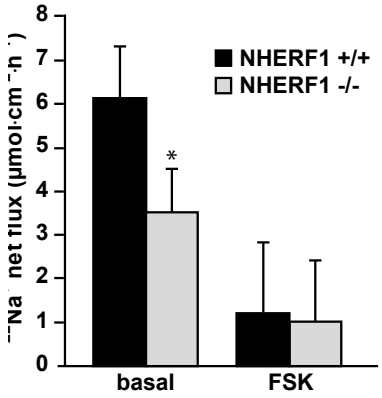

Figure 3. Net $^{22}Na^+$ flux in isolated NHERF-1 +/+ and -/- proximal colonic mucosa. The net $^{22}Na^+$ flux in colonic mucosa from NHERF-1 -/- mice (gray bar) was significantly reduced compared to +/+ littermates (black bar; * $P < 0.05$). 10^{-5} M FSK in the serosal compartment reduced the absorption in both NHERF-1 +/+ and -/- mucosa. (n = 9).

Segment-specific changes in fluid absorption assessed by ligated loop experiments - In addition to the single-pass perfusion experiments, the ligated loop technique was used for assessing fluid movements in the intestine *in vivo*. This method is able to measure fluid movements in different segments of the small intestine simultaneously. There was a significant difference in basal fluid absorption between NHERF-1-deficient jejunum, but not in the ileum (Figure 4).

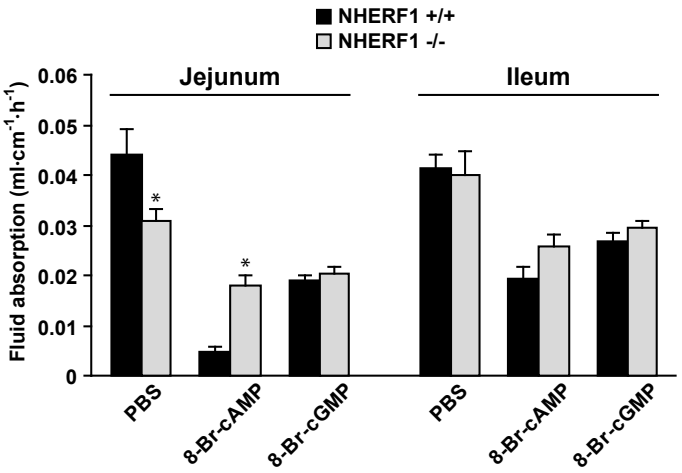

Figure 4. Closed loop experiments confirm segmental differences in absorptive rates in NHERF-1 +/+ and -/- mice. Fluid absorption was measured simultaneously in closed intestinal loops from the jejunum and ileum of the same mouse. In the jejunum, but not in ileum, fluid absorption was reduced in the NHERF-1-deficient mice, and the inhibition of absorption by the cAMP analogue was attenuated. n = 8; * $P < 0.05$.

Inhibition of fluid absorption by cyclic nucleotides was assessed by adding 8-Br-cAMP or 8-Br-cGMP. The effect of 8-Br-cAMP was less than the effect of forskolin (Figure 1), and the cyclic nucleotide-dependent inhibition of fluid absorption in the NHERF-1-deficient mice was significantly reduced in the jejunum but not in the ileum. This is similar to the results of the single pass perfusion experiments and also correlates with the finding of a significant decrease in CFTR-activation in NHERF-1-deficient jejunum but not ileum (20).

NHE3 transport activity in surface colonocytes from NHERF-1 -/- and +/+ intestine - In order to quantify NHE3 exchange activity in native NHE3-expressing enterocytes, we loaded isolated colonic crypts with the pH-sensitive dye BCECF and measured the acid-activated Na^+-dependent proton flux in the upper part of the glands in the presence of 50μM HOE642. At this concentration, HOE642 inhibits NHE1 and NHE2 but not NHE3 activity (16). In NHE3-deficient colonic crypts, acid-activated, Na^+-dependent, HOE642-insensitive proton fluxes were reduced by ~85%, validating the method for the measurement of NHE3 activity in native enterocytes (15). In the apical region of NHERF-1 -/- crypts, the acid activated, HOE642-insensitive Na^+-dependent proton flux was diminished by 30% compared to +/+ crypts (Figure 5A). This difference was abolished after treatment with 10^{-5} M of the NHE3 specific inhibitor Hoe S1611, indicating that it is due to a difference in NHE3 activity. In the presence of S1611, 10^{-5} M FSK had no further inhibitory effect, suggesting that NHE3 is the target for cAMP-dependent inhibition of the acid activated, HOE642-insensitive Na^+-dependent proton flux.

In order to study the regulation of NHE3 in NHERF-1-deficient colonocytes, we measured the acid activated, HOE642-insensitive Na^+-dependent proton flux in NHERF-1 -/- and +/+ surface colonocytes in the absence and presence of 10^{-5} M forskolin or 10^{-3} M 8-Br-cGMP (both at maximal inhibitory concentrations which were determined in experiments not shown). There was significant inhibition by both compounds in NHERF-1 -/- as well as +/+ crypts (Figure 5B), although the percentage of inhibition was slightly but significantly reduced in the NHERF-1 -/- mice ($p<0.05$). These experiments suggest that the inhibition of NHE3 activity by cyclic nucleotides remains intact in the NHERF-1-deficient colon.

Effect of EPAC activation on fluid absorption and NHE3 activity - It was recently shown that in addition to PKA, also the exchange protein activated by cAMP (EPAC) can cause cAMP-mediated inhibition of NHE3 in the proximal tubule of the kidney in a NHERF-1 dependent manner (21, 22). This protein is also expressed in the intestine (22). We investigated whether EPAC activation results in changes in ion- and fluid transport in the jejunum. In contrast to the PKA activator 8-pCPT-cAMP, which caused a dramatic decrease in fluid absorption (Figure 6A), addition of 200 μM of the structurally very similar but highly selective EPAC activator 8-pCPT-2'-O-Me-cAMP did not result in a significant change in fluid absorption (Figure 6B). This suggests that the pathway of NHE3 inhibition or CFTR activation via EPAC plays no role in the jejunum. We also tested the effect of EPAC activation on NHE3 activity in the surface cells of isolated colonic crypts (Figure 6C). In this segment, addition of the EPAC activator 8-pCPT-2'-O-Me-cAMP (100 μM) caused a slight but

significant inhibition of acid-activated NHE3 activity in NHERF-1 +/+ surface cells, whereas 10^{-5} M FSK caused a much stronger inhibition. Together, this indicates that EPAC is not a major pathway in the cAMP-mediated regulation of NHE3 in the intestine.

Western blot analysis of BBM from the small intestine and colon of NHERF-1-deficient mice and WT littermates - In order to search for the molecular mechanism causing the reduced sodium absorption and acid-activated NHE3 transport rate, we isolated brush border membranes from the small and large intestine and studied NHE3 abundance by Western analysis. A significant reduction in NHE3 abundance was found in the BBM but not in total homogenate of small intestinal epithelial cells (Figure 7A), as well in the BBM but not the total homogenate from the colon (Figure 7B)

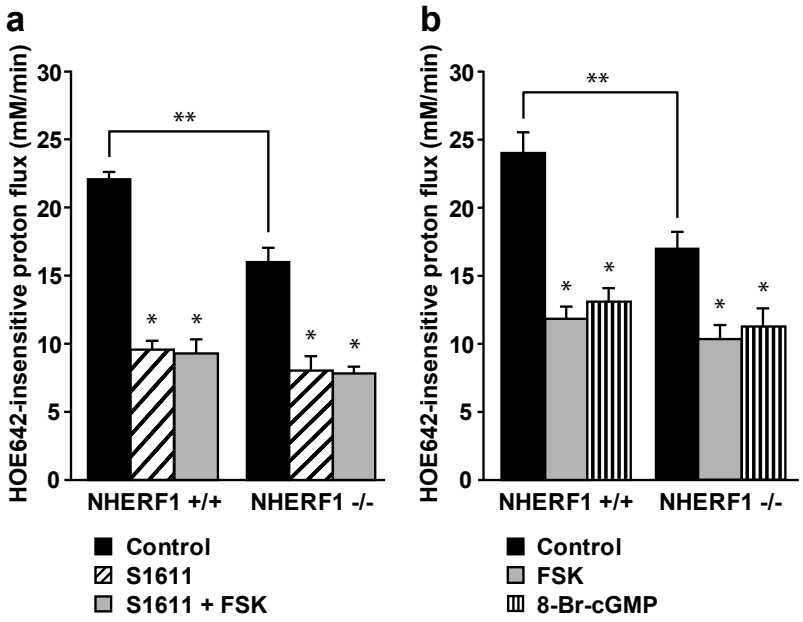

Figure 5. Fluorometric assessment of NHE3 activity in the surface enterocytes. The HOE642-insensitive, Na^+-dependent acid-activated proton flux was measured in the cells of the cryptal opening within isolated colonic crypts of NHERF-1 +/+ and -/- mice. Figure 5A: In NHERF-1 -/- surface enterocytes, the HOE642-insensitive proton flux was significantly reduced (**, $P < 0.05$). Furthermore, a significant reduction of the HOE642-insensitive, Na^+-dependent, acid-activated proton flux rates was observed in the absence but not the presence of 10 µM S1611 (* $P < 0.05$), indicating a reduction of NHE3 activity. In the presence of S1611, FSK did not exert an additional inhibitory effect, indicating that the inhibitory effect of FSK on the proton flux was due to NHE3 inhibition (n = 6). Figure 5B: Both 10^{-5} M FSK and 2 x10^{-4} M 8-Br-cGMP significantly inhibited acid-activated proton efflux rates to a similar extent in NHERF-1 +/+ and -/- colonocytes (* $P < 0.05$ versus control). There was, however, a mild but significant difference in the percentage of inhibition by FSK and 8-Br-cGMP between NHERF-1 +/+ and -/- colon (n = 6).

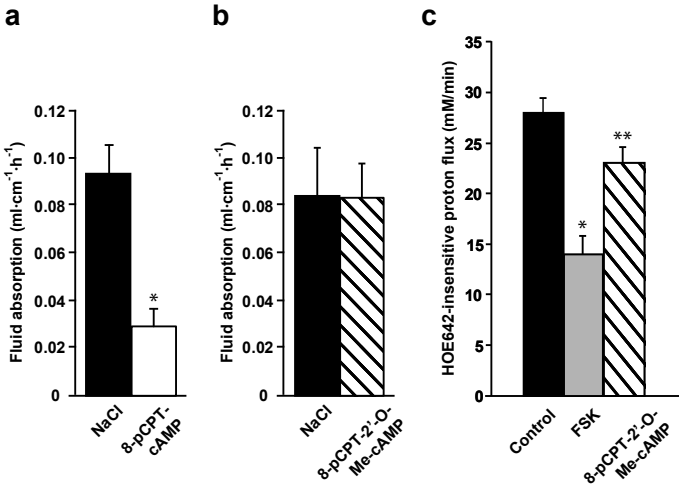

Figure 6. Effect of EPAC activation on jejunal fluid absorption and surface colonocyte NHE3 activity. Figure 6A and B: Whereas 200 µM 8-pCPT-cAMP caused a significant inhibition of jejunal fluid absorption (* $P < 0.05$), the same concentration of the structurally related selective EPAC activator 8-pCPT-2'-O-Me-cAMP had no effect (n = 5). Figure 6C: In surface colonocytes, 100 µM 8-pCPT-2'-O-Me-cAMP had a small but significant inhibitory effect on the proton flux (** $P < 0.05$), but full activation of adenylate cyclase by FSK caused a much more pronounced inhibition (* $P < 0.05$). Therefore, the NHERF-1 dependency of EPAC-mediated NHE3 inhibition, as observed in the proximal tubule (22), can only play a minor role in the colon (n = 6).

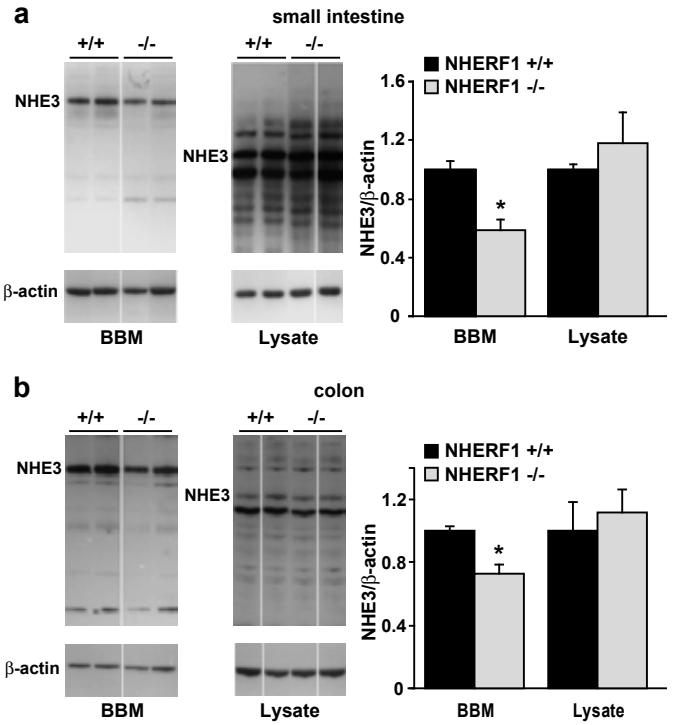

Figure 7. Western blot analysis of NHE3 protein in the brush border membrane and the enterocyte homogenate of small and large intestine of NHERF-1 +/+ and -/- mice. Figure 7A: NHE3 protein abundance was significantly reduced in BBM preparations from the small intestine from NHERF1 -/- mice (gray bar, n=11) compared to WT littermates (black bar, n = 19, *$P<0.05$), whereas no difference was seen in the enterocyte homogenate (n = 7). The amount of NHE3 is expressed relative to β-actin. Figure 7B: Similar results were obtained in the colon (n = 4-6).

Immunohistochemical staining and mRNA expression levels of NHE3 in the small and large intestine in NHERF-1 +/+ and -/- mice – Immuno-histochemical detection of NHE3 by confocal microscopy revealed a strong apical staining in small intestinal villus cells and colonic surface cells from both WT and NHERF-1-deficient mice (Figure 8). We observed a rather large variability of NHE3 staining in immunohistochemical experiments. Because of the lack of suitable control proteins to use for standardization, we therefore used immunohistochemistry in a qualitative fashion only.

NHE3 mRNA was measured by a quantitative PCR protocol using the villin gene as internal control. No significant change in NHE3 mRNA levels was detected in small and large intestinal epithelium of NHERF-1 -/- mice compared to WT littermates. Villin mRNA expression was not altered in the NHERF-1 -/- mice, when compared to the ribosomal protein RPS9 (Figure 9A, B).

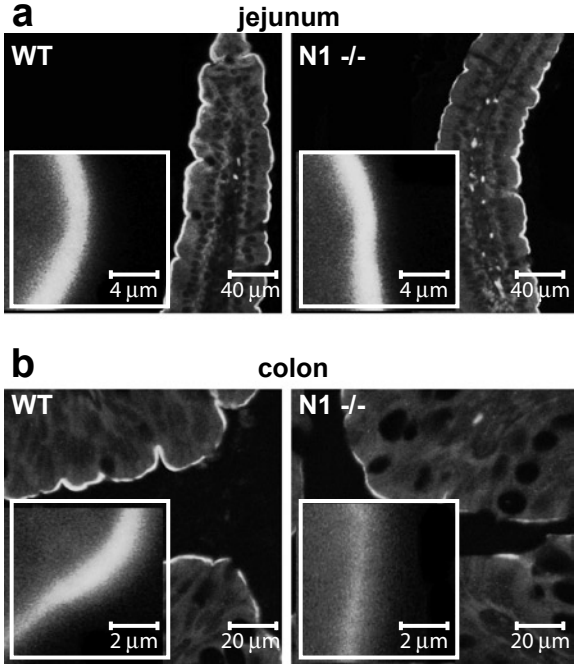

Figure 8. Immunohistochemical NHE3 staining reveals normal localization of NHE3 in the jejunal and colonic apical membrane of NHERF-1 -/- mice. The NHE3 localization at the apical border of the jejunum (Figure 8A) and colon (Figure 8B) was qualitatively similar in NHERF-1 +/+ and -/- mice, with considerable variability in the signal intensity within each group of mice. Images are representative examples from five independent experiments. Inserts show a 10x magnification of a part of the image shown in the larger panels.
(Color figure on page 168)

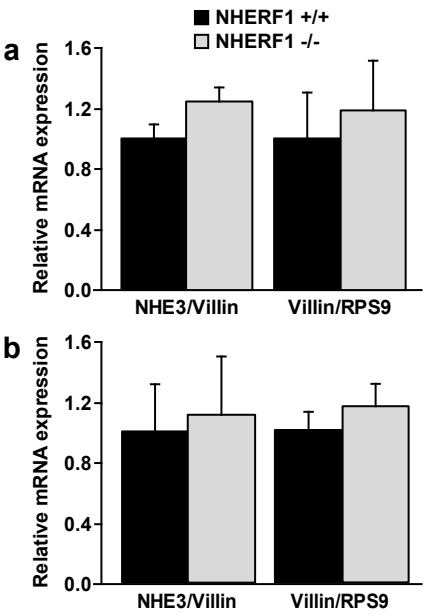

Figure 9. Expression of NHE3 and villin mRNA determined by quantitative real-time PCR. No changes in NHE3 mRNA expression levels (relative to the structural brush border protein villin) were observed between NHERF1 +/+ and -/- in the small (Figure 9A) and large (Figure 9B) intestine. In addition, no changes in villin expression levels (relative to the ribosomal protein RPS9) were observed in NHERF1 -/- mice as compared to WT mice. Data represent average values from three separate measurements in 3 pairs of +/+ and -/- mice. The results in the NHERF1 -/- tissues are relative to the WT expression level set at 1.

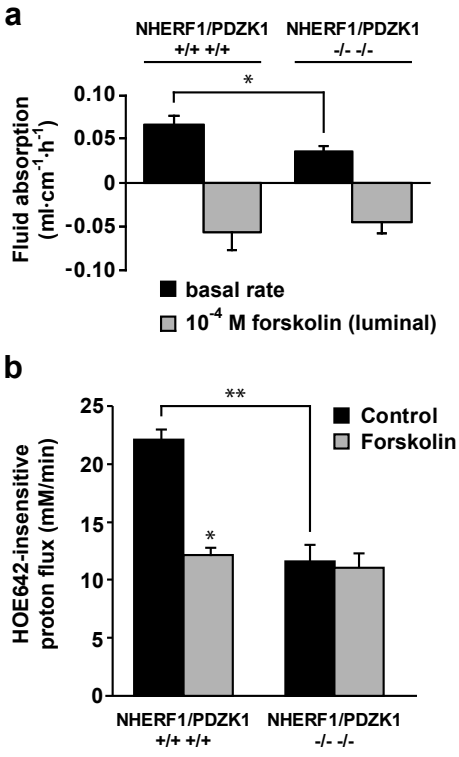

Figure 10. In vivo jejunal fluid movement and NHE3 activity in surface colonocytes in NHERF-1/PDZK1 double-deficient mice. Figure 10A: In NHERF-1/PDZK1 -/- jejunum, the basal fluid absorption (black bars) was significantly decreased ($P < 0.05$), and the response to FSK (gray bars) was diminished (n = 5). However, the changes did not significantly differ from those in the NHERF-1 -/- jejunum (see Figure 1A). Figure 10B: In contrast, the additional ablation of PDZK1 resulted in both a strong decrease in acid-activated NHE3 transport rates (black bars; ** $P < 0.05$) and abrogation of NHE3 inhibition by FSK (gray bars) in colonic surface cells compared to the WT animals (* $P < 0.05$) and to the NHERF-1 single-deficient animals shown in Figure 6C (n = 6).

Effect of NHERF-1/PDZK1 double deficiency on jejunal fluid absorption - The reduction in jejunal fluid absorption in NHERF-1/PDZK1 double-deficient mice compared to respective WT mice derived from the same founders and from the same generation (2^{nd} cousins) was similar to that observed in the NHERF-1-deficient mice (Figure 10A), and no significant further reduction in BBM NHE3 abundance was observed compared to the NHERF-1 -/- deficient mice (data not shown).

NHE3 activity and regulation in NHERF-1/PDZK1-deficient colonic surface cells - In contrast to the jejunal fluid absorption, the acid-activated NHE3 activity in colonic surface cells from NHERF-1/PDZK1 double-deficient mice was strongly reduced, and the NHE3 inhibition by forskolin was abolished. Thus, double deficient mice show a combination of the defects observed in NHERF-1 null mice (this paper), and the defects related to NHE3 transport rate regulation in PDZK1-deficient intestine (19).

Discussion

This work investigates the role of the NHE3-binding PDZ domain protein NHERF-1 on intestinal fluid and electrolyte absorption and studies the molecular mechanisms responsible for the observed reduced absorptive rates. In the absence of NHERF-1, jejunal, but not ileal, fluid absorption was significantly reduced *in vivo*, and the magnitude of change from absorption to secretion after the application of luminal forskolin was significantly diminished. While the reduced CFTR activation in the absence of NHERF-1 (20) can explain the latter observation, it cannot explain the former. Therefore, Na^+ and Cl^- transport was measured in isolated jejunal and colonic mucosa *in vitro*. Basal jejunal and colonic Na^+ absorptive rates were found to be significantly reduced, with intact inhibition of absorption by a rise in intracellular cAMP levels. In addition, acid-activated NHE3 transport rates were significantly reduced in colonic surface cells, but the inhibition of NHE3 activity by cyclic nucleotides was preserved. Western blot analysis revealed a reduction in the abundance of NHE3 in the jejunal and colonic BBM. Additional deficiency of PDZK1 abolished NHE3 inhibition by cAMP, without a further reduction in NHE3 BBM abundance or jejunal fluid absorption as compared to NHERF-1 null mice. Taken together, the results demonstrate an important, but segment-specific role for NHERF-1 in intestinal NHE3 membrane abundance, but no crucial role for the cAMP-dependent regulation of intestinal NHE3 activity.

NHERF-1 was the first PDZ-domain adapter proteins identified through its binding to NHE3 in the proximal tubule (23, 24). It enhanced the inhibitory effect of PKA on NHE3 in isolated renal brush border membranes (24), and established an inhibitory effect of cAMP on NHE3 when both proteins were coexpressed in PS120 and Caco-2 fibroblasts (7, 8, 25). Recently, mice have been generated that lack expression of NHERF-1 (13, 26), NHERF-2 (20), or PDZK1 (NHERF-3) (14), another PDZ-protein that binds to NHE3 (12). NHERF-1 null mice display a surprising variability in the phenotype in different tissues, and the current study demonstrates that NHERF-1 ablation even affects salt- and fluid transport

and NHE3 activity differently in various segments of the intestine. In isolated proximal tubules, NHE3 inhibition by cAMP was abolished in NHERF-1-deficient mice, which was explained by loss of cAMP-dependent phosphorylation of NHE3 (22, 27). In contrast, basal NHE3 activity as well as inhibition by 8-Br-cAMP was unaltered in ileal villi of NHERF-1-deficient mice (22). This was extended by our observation that basal and cAMP-inhibited fluid absorption rates are normal in the ileum of NHERF-1-deficient mice. The deletion of NHERF-3 (PDZK1), unexpectedly, resulted in reduction of jejunal Na^+ absorption and strong attenuation of its inhibition by an increase in intracellular cAMP (19), as well as abrogation of cAMP-mediated NHE3 inhibition in the large intestine, although PDZK1 is expressed at lower levels than NHERF-1 in this tissue (19, 28). Loss of NHERF-2, which is also expressed in the intestine and can substitute for NHERF-1 in PS120 fibroblasts with respect to cAMP-mediated inhibition of NHE3, did not impede cAMP-mediated NHE3 inhibition in enterocytes, although it did abolish Ca^{2+}-mediated inhibition (28), a feature also previously recognized in NHE3-transfected PS120 fibroblasts (29).

These results demonstrated that despite high structural homology within their PDZ domains, the biological functions of the three NHERF proteins are unique. In addition, the data are explicable only when accepting the hypothesis that for each transporter, the multiprotein complexes which mediate a similar function, i.e. cAMP-mediated inhibition of NHE3, are likely to be composed of different components in different epithelia. Thus far, much attention has been paid to the role of the PKA-anchoring protein ezrin in NHE3 inhibition. The formation of a complex containing NHE3, NHERF-1, ezrin and PKA appears crucial for cAMP-dependent inhibition of NHE3 in PS120 fibroblasts (8). In the proximal tubule, the affinity of PDZK1, another NHE3-binding PDZ-protein, for the kinase-anchoring protein D-AKAP-II was higher than its affinity for the kinase-anchoring protein ezrin, suggesting differences in the components of a multiprotein complex may be found at many levels (30). One conclusion from these observations was that more studies in native systems are required to better delineate the physiological significance of the NHERF adapter proteins in the regulation of ion transport in the different organ systems (5, 22, 31-33).

The first glimpse into this complexity was recently provided by the demonstration that in the kidney, an additional pathway exists for cAMP-mediated inhibition of NHE3 to the protein kinase A (PKA)-mediated phosphorylation, mediated though the exchange protein activated by cAMP (EPAC) (21), and that inhibition of NHE3 by both mechanisms was abolished in the kidney of NHERF-1 null mice (22). Because the protein EPAC is also expressed in the small and large intestinal mucosa, we tested the effect of EPAC activation on fluid movements in the jejunum and NHE3 regulation in colonic surface cells. The EPAC activator 8-pCPT-2'-O-Me-cAMP did not significantly affect jejunal fluid absorption. However, NHE3 activity was slightly but significantly inhibited in surface colonocytes (Figure 6C). Considering that NHERF-1 ablation has been shown to attenuate EPAC-dependent inhibition of NHE3 in the kidney, the reduced inhibition of NHE3 activity by FSK in NHERF-1-deficient

colonocytes (Figure 5) may in part be caused by loss of EPAC-dependent inhibition. Because the contribution of EPAC activation in relation to the overall effect of an increase in cAMP levels was small even in these cells, we did not attempt to prove this hypothesis. Why EPAC activation has different effects on renal, colonic and small intestinal NHE3 is unclear at this time. In fact, the molecular mechanism whereby EPAC affects NHE3 has not been elucidated yet.

Our study suggests that NHERF-1 is required for optimal BBM expression of NHE3 in small and large intestinal enterocytes. The abundance of NHE3 was reduced relative to the structural brush border membrane protein villin, and also relative to ß-actin, a major component of the subapical cytoskeletal network. Immunohistochemical staining of NHE3 located the protein only in the brush border both in WT and NHERF-1 null mice. The variability of the staining of tissue from different animals was relatively large and although we used it only in a qualitative fashion there was a trend towards lower signal intensity in the NHERF-1 null mice. Taken together, the decrease in NHE3 membrane abundance seems the best explanation for the significantly reduced fluid absorptive rates in the jejunum, and significant reductions in jejunal and proximal colonic net Na^+ absorptive rates. In line with this, no changes in fluid absorption (Figure 1 and 3) and NHE3 activity (22) were observed in the ileum of NHERF-1-deficient mice, which correlates with unaltered NHE3 abundance in the ileal brush border as determined by Western blotting (22). However, more work at the molecular level is needed to fully understand the changes in NHE3 activity caused by the absence of NHERF-1.

PDZK1-deficient mice display very different effects on NHE3 as compared to NHERF-1 null mice, namely a strong reduction in acid-activation of NHE3 transport rate as well as loss of inhibition by an elevation of cAMP or Ca^{2+} in colonic surface enterocytes, although NHE3 protein levels in the BBM were normal (15, 19). A molecular explanation for these findings, based on heterologous expression studies, is lacking. However, PDZK1-deficient mice displayed a strong increase in NHE3 mRNA expression levels in small and large intestine, suggesting that the turnover of NHE3 may be dramatically increased in the absence of PDZK1, even though we did not find evidence for a reduction in the amount of NHE3 protein present in the enterocyte cytoplasm or BBM (15, 19). Because PDZK1 binds to both NHE3 and NHERF-1, we wondered whether the combined ablation of NHERF-1 and PDZK1 would result in a potentiation of the defects observed in the single null mice. Surprisingly, we observed no further reduction in BBM NHE3 abundance, and no further reduction in basal fluid absorption in the jejunum *in vivo*. However, NHE3 regulation in surface colonic enterocytes of NHERF-1/PDZK1 double deficient mice was drastically changed compared to NHERF-1-deficient colonic enterocytes, with a strong reduction of acid-activated NHE3 transport rates, and a loss of cAMP-mediated inhibition of this acid-activated NHE3 rate. The severe reduction of acid-activated NHE3 activity and the lack of its inhibition by cAMP was identical in colonic surface enterocytes of the NHERF-1/PDZK1-deficient and the PDZK1 deficient mouse (15).

In comparison to PDZK1-deficient mice (15, 19), NHERF-1-deficient mice displayed a much higher acid-activated NHE3 transport rate in colonic surface cells and preserved regulation by cyclic nucleotides even in those segments of the intestinal tract where Na^+ absorption is affected (jejunum, colon). This may be one reason why the NHE3 mRNA upregulation that occurs in PDZK1 null mice was not observed in the small or large intestine of NHERF-1-deficient mice. Another reason may be the simultaneous reduction in CFTR-dependent anion secretion in the absence of NHERF-1, which is also seen *in vivo* (this study). Possibly, the decreased fluid secretion and decrease in absorption results in a balanced state. It will be important in future studies to assess the NHE3 membrane retention time in the absence of the different NHERF proteins and its potential effects on NHE3 regulation.

In summary, our results show that the absence of NHERF-1 results in segment-specific changes in intestinal salt absorption *in vivo*, correlating to a reduced Na^+ absorption in the isolated mucosa of these segments *in vitro*. In the colon, a correlation between this reduction in electroneutral Na^+ absorption and acid-activated NHE3 transport rates in the surface enterocytes was demonstrated. The membrane abundance of NHE3 was also reduced in the segments that displayed reduced absorptive rates, suggesting a causal relationship. In contrast to the deletion of PDZK1, intestinal NHERF-1 ablation leaves NHE3 regulation by cyclic nucleotides intact. Clearly, more detailed studies will be required to gain a full understanding and appreciation of the complexity of regulation of ion transport by the different NHERF proteins, but our studies suggest that the reduction in basal NHE3 activity observed in the jejunum and colon of NHERF-1 -/- mice may become an obstacle in using NHERF-1 as a target for anti-diarrheal action.

Acknowledgements

This work was supported by the Deutsche Forschungsgemeinschaft SFB621/C9 and by Support from the Lower Saxony Ministry of Science and education and the Volkswagen Stiftung. A part of this work was prepared in fulfillment with the requirements for the doctoral theses by Nellie Broere, Mingmin Chen, Anurag Singh and Jutta Hillesheim.

References

1. Schultheis, P. J., Clarke, L. L., Meneton, P., Miller, M. L., Soleimani, M., Gawenis, L. R., Riddle, T. M., Duffy, J. J., Doetschman, T., Wang, T., Giebisch, G., Aronson, P. S., Lorenz, J. N., and Shull, G. E. (1998) *Nat Genet* **19**, 282-285
2. Schweinfest, C. W., Spyropoulos, D. D., Henderson, K. W., Kim, J. H., Chapman, J. M., Barone, S., Worrell, R. T., Wang, Z., and Soleimani, M. (2006) *J Biol Chem* **281**, 37962-37971
3. Seidler, U., Rottinghaus, I., Hillesheim, J., Chen, M., Riederer, B., Krabbenhoft, A., Engelhardt, R., Wiemann, M., Wang, Z., Barone, S., Manns, M. P., and Soleimani, M. (2007) *Pflugers Arch*
4. Field, M. (2003) *J Clin Invest* **111**, 931-943
5. Lamprecht, G., and Seidler, U. (2006) *Am J Physiol Gastrointest Liver Physiol* **291**, G766-777
6. Donowitz, M., and Li, X. (2007) *Physiol Rev* **87**, 825-872
7. Zizak, M., Lamprecht, G., Steplock, D., Tariq, N., Shenolikar, S., Donowitz, M., Yun, C. H., and Weinman, E. J. (1999) *J Biol Chem* **274**, 24753-24758
8. Lamprecht, G., Weinman, E. J., and Yun, C. H. (1998) *J Biol Chem* **273**, 29972-29978
9. Shenolikar, S., Voltz, J. W., Cunningham, R., and Weinman, E. J. (2004) *Physiology (Bethesda)* **19**, 362-369
10. Sheng, M., and Sala, C. (2001) *Annu Rev Neurosci* **24**, 1-29
11. Lee, J. H., Richter, W., Namkung, W., Kim, K. H., Kim, E., Conti, M., and Lee, M. G. (2007) *J Biol Chem* **282**, 10414-10422
12. Gisler, S. M., Pribanic, S., Bacic, D., Forrer, P., Gantenbein, A., Sabourin, L. A., Tsuji, A., Zhao, Z. S., Manser, E., Biber, J., and Murer, H. (2003) *Kidney Int* **64**, 1733-1745
13. Shenolikar, S., Voltz, J. W., Minkoff, C. M., Wade, J. B., and Weinman, E. J. (2002) *Proc Natl Acad Sci U S A* **99**, 11470-11475
14. Kocher, O., Pal, R., Roberts, M., Cirovic, C., and Gilchrist, A. (2003) *Mol Cell Biol* **23**, 1175-1180
15. Cinar, A., Chen, M., Riederer, B., Bachmann, O., Wiemann, M., Manns, M., Kocher, O., and Seidler, U. (2007) *J Physiol* **581**, 1235-1246
16. Bachmann, O., Riederer, B., Rossmann, H., Groos, S., Schultheis, P. J., Shull, G. E., Gregor, M., Manns, M. P., and Seidler, U. (2004) *Am J Physiol Gastrointest Liver Physiol* **287**, G125-133
17. Bachmann, O., Rossmann, H., Berger, U. V., Colledge, W. H., Ratcliff, R., Evans, M. J., Gregor, M., and Seidler, U. (2003) *Am J Physiol Gastrointest Liver Physiol* **284**, G37-45
18. Boyarsky, G., Ganz, M. B., Sterzel, R. B., and Boron, W. F. (1988) *Am J Physiol* **255**, C857-869
19. Hillesheim, J., Riederer, B., Tuo, B., Chen, M., Manns, M., Biber, J., Yun, C., Kocher, O., and Seidler, U. (2007) *Pflugers Arch* **454**, 575-586
20. Broere, N., Hillesheim, J., Tuo, B., Jorna, H., Houtsmuller, A. B., Shenolikar, S., Weinman, E. J., Donowitz, M., Seidler, U., de Jonge, H. R., and Hogema, B. M. (2007) *J Biol Chem* **282**, 37575-37584
21. Honegger, K. J., Capuano, P., Winter, C., Bacic, D., Stange, G., Wagner, C. A., Biber, J., Murer, H., and Hernando, N. (2006) *Proc Natl Acad Sci U S A* **103**, 803-808
22. Murtazina, R., Kovbasnjuk, O., Zachos, N. C., Li, X., Chen, Y., Hubbard, A., Hogema, B. M., Steplock, D., Seidler, U., Hoque, K. M., Tse, C. M., De Jonge, H. R., Weinman, E. J., and Donowitz, M. (2007) *J Biol Chem* **282**, 25141-25151
23. Weinman, E. J., and Shenolikar, S. (1997) *Exp Nephrol* **5**, 449-452
24. Weinman, E. J., Steplock, D., Wang, Y., and Shenolikar, S. (1995) *J Clin Invest* **95**, 2143-214925. Yun, C. H., Oh, S., Zizak, M., Steplock, D., Tsao, S., Tse, C. M., Weinman, E. J., and Donowitz, M. (1997) *Proc Natl Acad Sci U S A* **94**, 3010-3015
26. Morales, F. C., Takahashi, Y., Kreimann, E. L., and Georgescu, M. M. (2004) *Proc Natl Acad Sci U S A* **101**, 17705-17710
27. Weinman, E. J., Steplock, D., and Shenolikar, S. (2003) *FEBS Lett* **536**, 141-144
28. Cinar, A., Chen, M., Riederer, B., Hogema, B. M., De Jonge, H., Donowitz, M., Weinman, E. J., Kocher, O., and Seidler, U. (2006) *gastroenterology, Abstract* **130**, A99
29. Lee-Kwon, W., Kim, J. H., Choi, J. W., Kawano, K., Cha, B., Dartt, D. A., Zoukhri, D., and Donowitz, M. (2003) *Am J Physiol Cell Physiol* **285**, C1527-1536
30. Gisler, S. M., Madjdpour, C., Bacic, D., Pribanic, S., Taylor, S. S., Biber, J., and Murer, H. (2003) *Kidney Int* **64**, 1746-1754
31. Zachos, N. C., Tse, M., and Donowitz, M. (2005) *Annu Rev Physiol* **67**, 411-443
32. Donowitz, M., Milgram, S., Murer, H., Yun, C., and Weinman, E. J. (2005) *J Physiol*
33. Donowitz, M., Cha, B., Zachos, N. C., Brett, C. L., Sharma, A., Tse, C. M., and Li, X. (2005) *J Physiol* **567**, 3-11

CHAPTER 4

NHERF-2 is required for cyclic GMP-dependent inhibition of NHE3 but not for cGMP-dependent stimulation of CFTR

Nellie Broere[1, a], Rafiquel I. Sarker[2, a], Vera Valkhoff[1, 2,], Albert P. Smolenski[3], Suzanne M. Lohmann[4], Hugo R. de Jonge[1], Mark Donowitz[2] and Boris M. Hogema[1]

[1]Department of Biochemistry, Erasmus University Medical Center, Dr. Molewaterplein 50, 3015 GE Rotterdam, The Netherlands
[2]Departments of Medicine and Physiology, Gastroenterology Division, The Johns Hopkins University School of Medicine, Baltimore, Maryland 21205, USA
[3]Institute for Biochemistry II, University of Frankfurt Medical School, Theodor-Stern-Kai 7, building 75, 60590 Frankfurt am Main, Germany
[4]Institute of Clinical Biochemistry and Pathobiochemistry, University of Würzburg Medical Clinic, Josef-Schneider-Str. 2, D-97080 Würzburg, Germany

[a] These authors contributed equally to this work

Manuscript in preparation

Abstract

The sodium/hydrogen exchanger 3 (NHE3) regulatory factors NHERF-1 and NHERF-2 bind to both NHE3 and the CFTR chloride channel. Functional consequences of this interaction for cGMP-dependent regulation were investigated using Caco-2/bbe and IEC-CF7 cells as models for intestinal villus and crypt cells, respectively. We demonstrate that siRNA-mediated gene silencing of NHERF-2 abolished cGMP/cGKII-dependent inhibition of NHE3, whereas CFTR activation was not affected by knockdown of NHERF-1 and NHERF-2. These findings suggest that NHERF-2 is required for targeting of cGKII to NHE3, whereas NHERF-1 and NHERF-2 are not required, or much less critical for, cGKII-mediated activation of CFTR.

Introduction

Cyclic guanosine monophosphate (cGMP) acts as a key regulator of intestinal epithelial ion transport by activating cGMP-dependent protein kinase II (cGKII), leading to simultaneous inhibition of NHE3-mediated electroneutral sodium absorption and activation of anion secretion by the cystic fibrosis transmembrane conductance regulator (CFTR) chloride channel. CFTR is the major anion channel responsible for cAMP/PKA- and cGMP/cGKII-regulated chloride conductance in epithelial tissues (1,2). NHE3, in conjunction with Cl^-/$HCO3^-$ exchangers Dra and PAT-1, is the major transporter mediating electroneutral salt uptake (3).

Inhibition of NHE3 by the cAMP/PKA pathway requires the presence of either NHERF-1 or NHERF-2. These structurally related proteins contain two PDZ domains and function as scaffolding proteins which place NHE3 in the vicinity PKA, leading to its efficient phosphorylation (and inhibition) by cAMP-dependent signaling (4,5). Whereas both NHERF-1 and NHERF-2 could fulfill this role in cAMP-mediated inhibition of NHE3, cGMP/cGKII-mediated inhibition of NHE3 was only detected in the presence of NHERF-2 (6). Because Na^+-absorption and Cl^- secretion are regulated in parallel, one might question whether the mechanism of cGMP-dependent CFTR regulation is similar to NHE3, requiring NHERF-2. Involvement of the NHERF proteins in cAMP-dependent regulation of CFTR activation has been described, but has also been the subject of debate in recent years, as recently reviewed by Guggiono and Stanton (see also the discussion section) (7).

The current study directly compares the role of the NHERF proteins in cGMP-dependent regulation of NHE3 and CFTR. siRNA-mediated gene silencing was used to reduce NHERF-1 and/or NHERF-2 expression in two polarized epithelial cell lines that serve as models

The abbreviations used are: NHE3, Na^+/H^+ exchanger isoform 3; NHERF, NHE3 regulatory factor ; CFTR, cystic fibrosis transmembrane conductance regulator ; cGKII, cGMP-dependent protein kinase isoform II; PKA, cAMP-dependent protein kinase; siRNA, small interfering RNA; PDZ, PDS95/Disks large/ZO-1.

for absorptive and secretory cells. Our data show that NHERF-2 is essential for cGMP-dependent inhibition of NHE3 in Caco-2/bbe cells, whereas NHERF-1 and NHERF-2 are not required, or are less critical, for CFTR activation in IEC-CF7 cells.

Materials and methods

Antibodies - Antibodies against NHERF-1, NHERF-2 (Ab2570) and cGKII have been described previously (2,4). Monoclonal mouse antibody directed to the HA epitope was obtained form Covance Research products, and HRP-conjugated donkey anti-rabbit IgG from Amersham.

Adenoviral constructs of NHE3 and NHERF-2 siRNA for viral infection of Caco-2/bbe cells - The Caco-2/bbe cell line, originally derived from a metastatic human adenocarcinoma, was a kind gift of Dr. M.S. Mooseker (Yale School of Medicine). HA-tagged NHE3 was cloned into the adenoviral shuttle vector ADLOX.HTM and transfected into CRE8 cells using lipofectamine 2000 (Invitrogen), followed by infection of the cells with helper virus (ψ5). siRNA constructs to downregulate NHERF-2 were designed using the program provided by OligoEngine (Seattle, WA). The selected sequences were 5'-GCTGGCAAGAAGGATGTCA-3' (Construct 2) and 5'-GCAAGATCCCTTCCAGGAG-3' (Construct 5). The hairpin constructs were transferred into the RNAi/Adeno transfer plasmid pPHA74243 and used for adenovirus production as described for NHE3. Cells were treated with 6 mM EGTA in serum-free medium for 2 h at 37°C prior to adenoviral infection (10^9–10^{10} particles/ml) at 37°C for 6h. Experiments were performed 40-48 hours post-infection.

Measurement of Na^+/H^+ exchange - Na^+/H^+-exchange activity of Caco-2/bbe cells was determined in confluent cells grown on filterslips (0.4 µm pore size, Corning) using the intracellular pH-sensitive dye 2',7'-bis(carboxyethyl)5-6-carboxyfluorescein (BCECF-AM; Molecular Probes, Eugene, OR) as described previously (6,8). Exposure to 8-pCPT-cGMP was during the last 30 minutes of the dye loading/NH_4Cl prepulse. Rates of Na^+-dependent intracellular alkalinization (efflux of H^+, in µM/s) were calculated as $\Delta pH/\Delta T$ for a given pH_i (within the linear phase, ~1 min of the initial rate of intracellular alkalinization). The activity could be blocked by the specific NHE3 inhibitor S3226 (data not shown).

Design of siRNA constructs and transfection of IEC-CF7 cells - IEC-CF7 cells (IEC-6 cells derived from rat small intestinal crypt stably expressing hCFTR) were cultured in 12-well plates and infected (10^9 particles/ml) with adenovirus expressing cGKII directly after plating as described previously (2). Four days after adenoviral infection, cells were transfected with siRNA (100 pmol/well) using Dharmafect™4 transfection reagent. The siRNAs N1 and N2 directed against NHERF-1 (5'-NNCCUGCACAGUGACAAAUCC-3') and NHERF-2 (5'-NNGGACAAUGAGGAUGGCAGU-3'), respectively, were obtained from Dharmacon (Lafayette, CO). Experiments were performed two days post-transfection.

Iodide ($^{125}I^-$) efflux - Iodide efflux was measured in confluent IEC-CF7 cells as described before (2). Cells were loaded with radioactive iodide (5 µCi/ml) for 2 h at 37°C and washed three times to remove extracellular isotope. Forskolin (10 µM), 8-Br-cAMP (500 µM) or 8-pCPT-cGMP (100 µM) were added 4.5 min. after the final washing step as indicated. Radiation was measured by γ-counting and expressed as fractional efflux per min as described previously (2).

Immunoblotting - Proteins were applied to SDS-PAGE and transferred onto nitrocellulose membranes. Primary antibodies NHERF-1 (1:3000), NHERF-2 (1:1000) and cGKII (1:3000) were

applied according to standard protocol. Fluorescently labeled IRDye^{TM}800, 680 secondary antibody was quantitated using the Odyssey system and Lycor software. HRP-conjugated secondary antibody was detected by chemiluminescence (Supersignal West Pico, Pierce) and quantitation of its signal on light-sensitive imaging film (Biomax XAR film, Kodak) using a calibrated GS-800 densitometer (Biorad) and Quantity-one software (Biorad).

RT-PCR - To quantify mRNA expression of NHERF-1 and NHERF-2, RNA was isolated from IEC-CF7 cells using Ultraspec (Biotecx Laboratories, Inc.), following the manufacturer's protocol. PCR of reverse-transcribed mRNA was performed using RedTaq DNA polymerase (Sigma) and the supplied buffer according to standard protocol. The following primers sets were used: 5'-AGAAGGAGAACAGCCGTGAA-3' and 5'-TGCTCAGAGGTTGCTGAAGA-3' for NHERF-1, and 5'-CTTCCCCCAGCCCACAA-3' and 5'-AGCCCCTCCACGTTCTGCCCATTC-3' for NHERF-2. The housekeeping gene PBGD (porphobilinogen deaminase) was used to standardize the amount of cDNA, using primers 5'-CGCGGAAGAAAACGGCTCAAT-3' and 5'-TGCAGATGGCTCCAATGGTAAAG-3'.

Results

siRNA-mediated genetic knockdown of NHERF-2 abolishes cGMP/cGKII-dependent inhibition of NHE3 in Caco-2/bbe cells – Until now, studies of the role of the NHERF proteins in cGMP-dependent NHE3 regulation have been performed using NHERF-2 and cGKII overexpression approaches in NHE3-transfected PS120 fibroblasts and opossum kidney (OK) cells (9). A recent study has shown that the mechanism of cAMP-dependent inhibition of NHE3 is different in the kidney and the ileum (10). In the current study we used two different epithelial cells lines to investigate whether cGMP-dependent regulation is dependent on the NHERF proteins in a similar way in Na^+-absorbing and Cl^--secreting intestinal cells. cGMP-dependent regulation of NHE3 was investigated in the human intestinal Caco-2/bbe cell line, which is characterized by endogenous expression of NHERF-1 and NHERF-2, and relatively low levels of NHE3. To allow for accurate measurements of NHE3 activity, cells were infected with adenovirus expressing HA-tagged NHE3. Initial experiments showed that addition of cGMP analog had no effect on NHE3 activity (Fig. 1A), probably due to the loss of cGKII expression which usually occurs in cultured cells (Fig. 1B). Consistent with this hypothesis, significant 8-pCPT-cGMP-dependent inhibition of NHE3 was observed following adenoviral transfer of cGKII (Fig. 1C).

To study the role of NHERF-2 in the regulation of NHE3 in the NHE3/cGKII-expressing Caco-2/bbe cells, an siRNA approach was used. Knock-down of NHERF-2 was achieved by infection with adenovirus containing pSUPER with siRNA (construct 2 and construct 5). The reduction of the NHERF-2 expression (~80%) did not affect NHERF-1 or NHE3 expression (data not shown) but resulted in complete loss of inhibition of of Na^+/H^+ exchange in response to 8-pCPT-cGMP (Fig. 2B). These results demonstrate that NHERF-2 is essential for the cGMP-regulated inhibition of NHE3 in human colonic epithelial cells, in addition to OK and PS120 cells.

siRNA-mediated knockdown of NHERF-1 and NHERF-2 in IEC-CF7 cells – In order to investigate whether NHERF-1 and/or NHERF-2 are required for cyclic nucleotide-dependent CFTR stimulation, as they are for the inhibition of NHE3, IEC-CF7 cells were examined. These have been used extensively in the past to study CFTR regulation by cGMP. NHERF-1 and NHERF-2 are endogenously expressed at high levels in this cell line (Fig. 3B). siRNAs were designed against rat NHERF-1 and NHERF-2 and transfection of IEC-CF7 cells with these duplexes successfully reduced each individually targeted NHERF protein (by ~70%) in an isoform-specific manner (Fig. 3C).

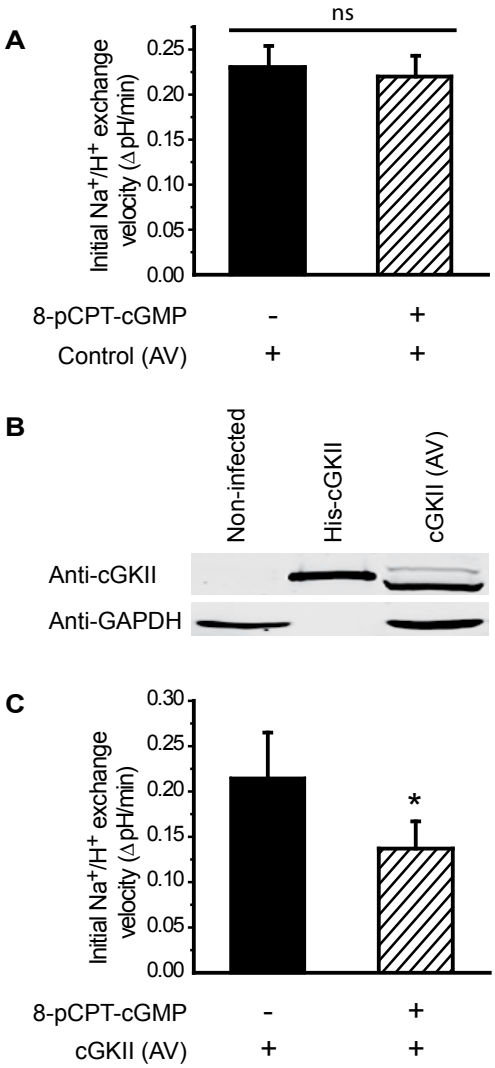

Figure 1. 8-pCPT-cGMP inhibits NHE3 activity in Caco-2/bbe cells expressing cGKII. (A) Na^+/H^+ exchange was not affected by 8-pCPT-cGMP in Caco-2/bbe cells infected with control adenovirus (n=4). (B) Infection with recombinant cGKII adenovirus induced expression of cGKII in Caco-2/bbe cells (lane 3). GAPDH was used as a loading control. The middle lane was loaded with purified his-tagged cGKII. Results are representative of three independent experiments. (C) Infection with cGKII adenovirus resulted in significant inhibition of the proton flux by 8-pCPT-cGMP (* $P<0.05$; n=4).

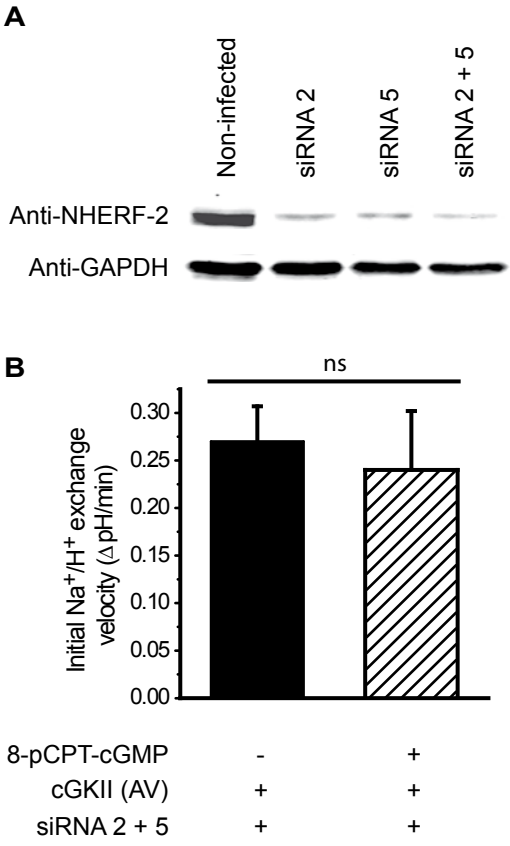

Figure 2. cGMP-mediated inhibition of NHE3 activity in Caco-2/bbe cells expressing cGKII requires NHERF-2. (A) Infection of cGKII-expressing Caco-2/bbe cells with NHERF-2 siRNA constructs (siRNA 2 and 5) strongly reduced NHERF-2 protein expression. The combination of the two constructs resulted in the strongest gene silencing (lane 4). GAPDH was used as loading control. (B) Reducing NHERF-2 expression resulted in loss of NHE3 inhibition by 8-pCPT-cGMP in cGKII-expressing cells (n = 3).

Effect of NHERF-1 and NHERF-2 knockdown on CFTR activation – Activation of CFTR in IEC-CF7 cells was determined by monitoring ^{125}I efflux. Addition of the adenylyl cyclase activator, forskolin, or the cell-permeable cAMP analog 8-Br-cAMP induced a large increase in the efflux (Fig. 4A-B). Knock-down of NHERF-1 and NHERF-2 did not reduce the activation of CFTR compared to mock-transfected cells (Fig. 4A, B). Because IEC-CF7 cells do not express cGKII, cGMP-mediated stimulation of CFTR was studied after infection with recombinant cGKII adenovirus (Fig. 5A). siRNA-mediated silencing of NHERF-1 and NHERF-2 did not significantly affect stimulation of iodide efflux by 8-pCPT-cGMP (Fig. 5B, C). Taken together, these findings show that NHERF-2 is essential for the cGMP-dependent inhibition of NHE3 in Caco-2/bbe cells, whereas no evidence was found for a requirement of NHERF-1 or NHERF-2 in the regulation of CFTR activity in the IEC-CF7 cell line.

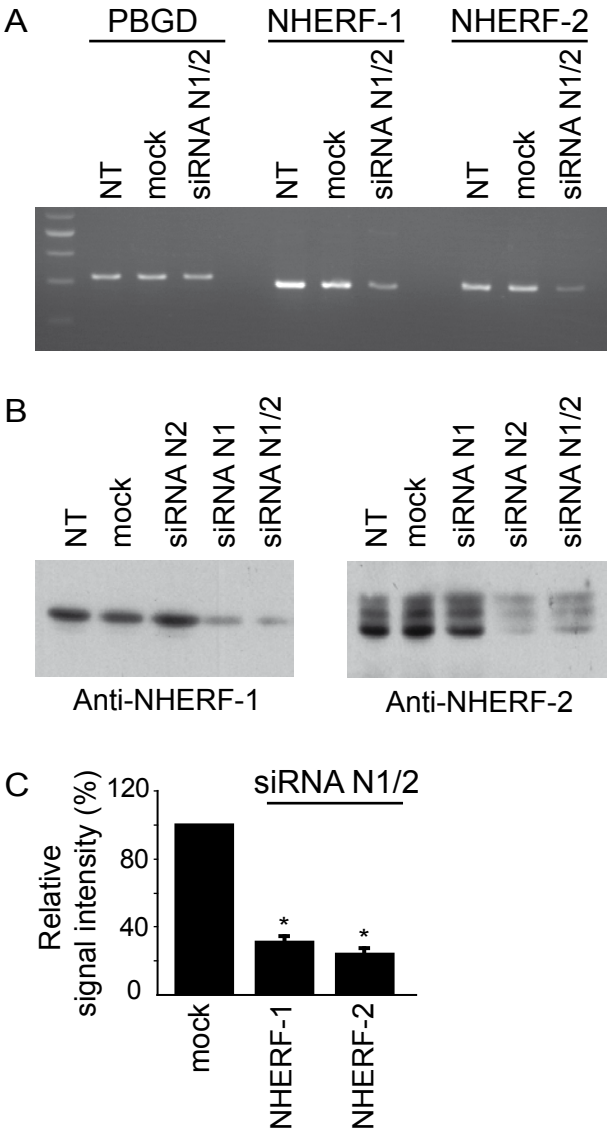

Figure 3. siRNA constructs specifically downregulate NHERF-1 or NHERF-2 expression in IEC-CF7 cells. (A) mRNA levels of NHERF-1 and NHERF-2 were strongly reduced in IEC-CF7 cells transfected with siRNA constructs N1 and N2, as compared to non-transfected (NT) and mock-transfected (mock) cells. PBGD was used as control for PCR input. (B) NHERF-1 and NHERF-2 protein levels were strongly and isoform-specifically reduced in IEC-CF7 cells transfected with siRNA N1 and/or siRNA N2, as compared to non-transfected (NT) and mock-transfected (mock) cells (10 μg per lane) (n=5). (C) Average NHERF-1 and NHERF-2 protein levels in siRNA-treated cells are shown relative to mock-transfected cells (designated as 100%). Data are means ± SEM (n=5).

Discussion

In this study we extended previous observations on the role of NHERF-2 in cGKII-dependent regulation of NHE3 to the more physiologically relevant intestinal epithelial cell line Caco-2/bbe. Furthermore, we investigated whether NHERF-1 and NHERF-2 are involved in the cAMP and/or cGMP-dependent regulation of CFTR in IEC-CF7 cells. Expression of NHERF-2 was found a prerequisite for cGMP-mediated inhibition of NHE3 in Caco-2/bbe cells. This is in line with previous findings in the PS120 fibroblast cell line in which NHERF-2

was shown to act as G-kinase anchoring protein which directly linked cGKII to NHE3. On the other hand, silencing of NHERF-1 and NHERF-2 did not affect cAMP- and cGMP-mediated regulation of CFTR activity in IEC-CF7 cells (Fig. 4 and 5), suggesting that cGKII anchoring to NHERF-2 is not required for cGMP-dependent regulation of CFTR, or that the requirement for NHERF-2 is less stringent than in case of cGMP-dependent inhibition of NHE3.

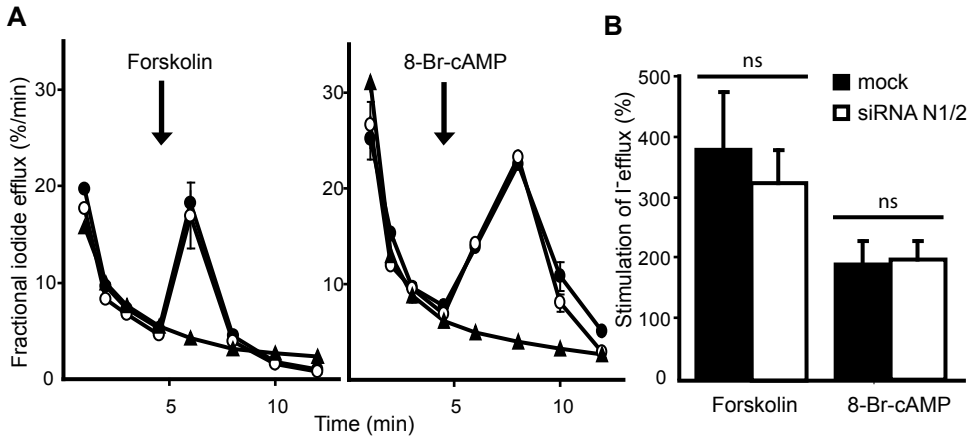

Figure 4. Knock-down of NHERF-1 and NHERF-2 does not significantly affect forskolin- and 8-Br-cAMP-stimulated iodide efflux in IEC-CF7 cells. (A) Stimulation of iodide efflux by forskolin (left panel) and 8-Br-cAMP (right panel) was not affected by downregulation of NHERF-1 and NHERF-2 expression by siRNA (○) compared to mock-transfected (●) controls. Efflux was compared with unstimulated N1/N2-transfected cells (▲). The fractional iodide efflux is expressed as mean ± SEM (n=3). Error bars are absent when the standard error was smaller than the symbol. (B) Average stimulation of iodide efflux (data from panel A). Data are expressed as means ±SEM of 4 independent experiments, each performed in triplicate. ns, not significant.

Interactions of CFTR with PDZ proteins (including NHERF-1 and NHERF-2) have been reported to affect CFTR activation in multiple ways, although the functional importance of these interactions is still rather controversial (7). Previous studies in which CFTR activation by cAMP was assessed directly showed variable effects of changes in NHERF expression and/or loss of interaction with PDZ domain proteins by C-terminal truncation of CFTR (11-15). Different levels of expression of the various CFTR-interacting PDZ domain proteins (which have stimulatory or inhibitory effects on CFTR) could potentially explain why the role of NHERF-1 and NHERF-2 in CFTR activation varies. Until now five PDZ domain proteins have been identified as CFTR binding partners. These proteins all have the ability to adhere to several binding partners simultaneously and therefore facilitate the formation of a plethora of different multiprotein complexes, which can be controlled in a dynamic way (for example by phosphorylation) (16). In addition to NHERF-1 and NHERF-2, CFTR has been shown to bind to the PDZ domains of NHERF-3 (also called PDZK1), CAL (CFTR Associated

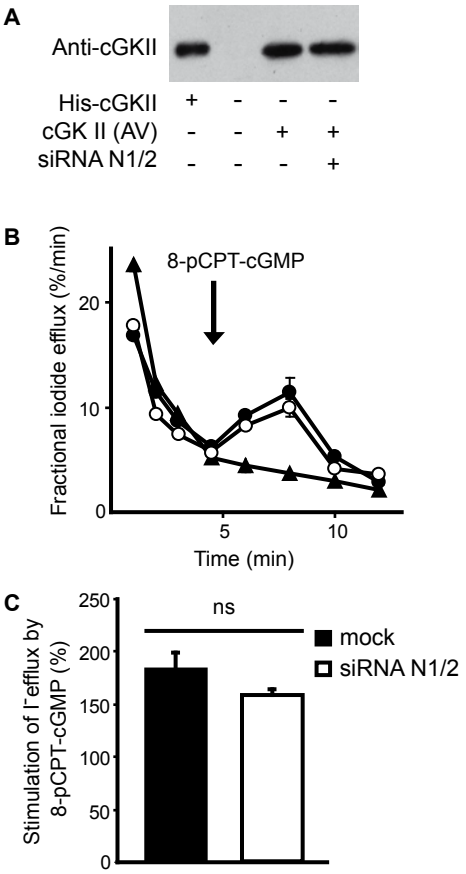

Fig. 5. siRNA-mediated silencing of NHERF-1 and NHERF-2 does not significantly affect 8-pCPT-cGMP-dependent iodide efflux. (A) cGKII expression (10 μg per lane) is not affected by transfection of IEC-CF7 cells with siRNAs (siRNA N1/2). Purified cGKII was used as a marker (His-cGKII, 3 ng). Results are representative of three independent experiments. (B) 8-pCPT-cGMP-stimulated iodide efflux was determined in cGKII-expressing, mock-transfected (●) and siRNA-transfected (○) cells and compared to unstimulated N1/N2-transfected cells controls (▲). Data are expressed as means ± SEM (n=3). Error bars are absent when the standard error was smaller than the symbol. (C) Quantitation of the data shown in panel B for n=4 experiments ± SEM.

Ligand) and Shank2 (SH3 and Ankyrin repeats containing protein 2) (14,17). Whereas NHERF-1, NHERF-2 and NHERF-3 positively affect CFTR function, CAL expression reduced CFTR surface expression (by enhancing lysosomal degradation) and Shank-2 reduced CFTR activation by cAMP (most likely by association with a phosphatase or by competition with NHERF-1) (13,14).

The siRNA treatment of IEC-CF7 cells resulted in strong reduction of NHERF-1 and NHERF-2, but not in a full deficiency for these proteins. The possibility cannot be excluded that small, residual amounts of NHERF-1 and NHERF-2 protein left in the siRNA-treated cells were sufficient for cAMP- and cGMP-mediated stimulation of CFTR. However, a similar reduction of NHERF-2 in Caco-2/bbe cells completely abolished inhibition of NHE3 by cGMP (Fig. 2). Furthermore, the extent of silencing of NHERF-1 and NHERF-2 in IEC-CF7 cells was comparable to that reported in other studies in which siRNA-mediated gene silencing affected various functions of the NHERF proteins (18-21). Taken together, our data support the notion that the NHERF proteins are involved in cGMP-dependent regulation of intestinal salt- and water homeostasis, but that their roles are remarkably different for NHE3 and CFTR regulation.

References

1. Riordan, J. R. (1993) *Annu Rev Physiol* **55**, 609-630
2. Vaandrager, A. B., Smolenski, A., Tilly, B. C., Houtsmuller, A. B., Ehlert, E. M., Bot, A. G., Edixhoven, M., Boomaars, W. E., Lohmann, S. M., and de Jonge, H. R. (1998) *Proc Natl Acad Sci U S A* **95**, 1466-1471
3. Field, M. (2003) *J Clin Invest* **111**, 931-943
4. Lamprecht, G., Weinman, E. J., and Yun, C. H. (1998) *J Biol Chem* **273**, 29972-29978
5. Donowitz, M., Cha, B., Zachos, N. C., Brett, C. L., Sharma, A., Tse, C. M., and Li, X. (2005) *J Physiol* **567**, 3-11
6. Cha, B., Kim, J. H., Hut, H., Hogema, B. M., Nadarja, J., Zizak, M., Cavet, M., Lee-Kwon, W., Lohmann, S. M., Smolenski, A., Tse, C. M., Yun, C., de Jonge, H. R., and Donowitz, M. (2005) *J Biol Chem* **280**, 16642-16650
7. Guggino, W. B., and Stanton, B. A. (2006) *Nat Rev Mol Cell Biol* **7**, 426-436
8. Kim, J. H., Lee-Kwon, W., Park, J. B., Ryu, S. H., Yun, C. H., and Donowitz, M. (2002) *J Biol Chem* **277**, 23714-23724
9. Yun, C. H., Oh, S., Zizak, M., Steplock, D., Tsao, S., Tse, C. M., Weinman, E. J., and Donowitz, M. (1997) *Proc Natl Acad Sci U S A* **94**, 3010-3015
10. Murtazina, R., Kovbasnjuk, O., Zachos, N. C., Li, X., Chen, Y., Hubbard, A., Hogema, B. M., Steplock, D., Seidler, U., Hoque, K. M., Tse, C. M., Dejonge, H. R., Weinman, E. J., and Donowitz, M. (2007) *J Biol Chem*, doi:10.1074/jbc.M701910200
11. Benharouga, M., Sharma, M., So, J., Haardt, M., Drzymala, L., Popov, M., Schwapach, B., Grinstein, S., Du, K., and Lukacs, G. L. (2003) *J Biol Chem* **278**, 22079-22089
12. Guerra, L., Fanelli, T., Favia, M., Riccardi, S. M., Busco, G., Cardone, R. A., Carrabino, S., Weinman, E. J., Reshkin, S. J., Conese, M., and Casavola, V. (2005) *J Biol Chem* **280**, 40925-40933
13. Lee, J. H., Richter, W., Namkung, W., Kim, K. H., Kim, E., Conti, M., and Lee, M. G. (2007) *J Biol Chem* **282**, 10414-10422
14. Cheng, J., Moyer, B. D., Milewski, M., Loffing, J., Ikeda, M., Mickle, J. E., Cutting, G. R., Li, M., Stanton, B. A., and Guggino, W. B. (2002) *J Biol Chem* **277**, 3520-3529
15. Naren, A. P., Cobb, B., Li, C., Roy, K., Nelson, D., Heda, G. D., Liao, J., Kirk, K. L., Sorscher, E. J., Hanrahan, J., and Clancy, J. P. (2003) *Proc Natl Acad Sci U S A* **100**, 342-346
16. Cao, T. T., Deacon, H. W., Reczek, D., Bretscher, A., and von Zastrow, M. (1999) *Nature* **401**, 286-290
17. Kim, J. Y., Han, W., Namkung, W., Lee, J. H., Kim, K. H., Shin, H., Kim, E., and Lee, M. G. (2004) *J Biol Chem* **279**, 10389-10396
18. Yun, C. C., Sun, H., Wang, D., Rusovici, R., Castleberry, A., Hall, R. A., and Shim, H. (2005) *Am J Physiol Cell Physiol* **289**, C2-11
19. Takahashi, Y., Morales, F. C., Kreimann, E. L., and Georgescu, M. M. (2006) *Embo J* **25**, 910-920
20. Oh, Y. S., Jo, N. W., Choi, J. W., Kim, H. S., Seo, S. W., Kang, K. O., Hwang, J. I., Heo, K., Kim, S. H., Kim, Y. H., Kim, I. H., Kim, J. H., Banno, Y., Ryu, S. H., and Suh, P. G. (2004) *Mol Cell Biol* **24**, 5069-5079
21. Hryciw, D. H., Ekberg, J., Ferguson, C., Lee, A., Wang, D., Parton, R. G., Pollock, C. A., Yun, C. C., and Poronnik, P. (2006) *J Biol Chem* **281**, 16068-16077

CHAPTER 5

Proteome of murine jejunal brush border membrane vesicles

Mark Donowitz[1,a], Siddharth Singh[1,a], Farah F. Salahuddin[1], Boris M. Hogema[2], Yueping Chen[1], Marjan Gucek[1], Robert N. Cole[1], Amy Ham[3], Nicholas C. Zachos[1], Olga Kovbasnjuk[1], Lynne A. Lapierre[3], Nellie Broere[2], James Goldenring[3], Hugo R. deJonge[2], and Xuhang Li[1]

[1]Johns Hopkins University School of Medicine and Hopkins Basic Research Digestive Diseases Development Core Center, Departments of Physiology and Medicine, GI Division
[2]Erasmus University Medical Center, Department of Biochemistry
[3]Vanderbilt University School of Medicine and Vanderbilt Digestive Diseases Core Center, Department of Surgery

[a] Co-first authors for equal contributions

Abstract

The first detailed description of the proteome of the mouse jejunal brush border membrane vesicle is presented here. This was obtained by a combination of purification via divalent (Mg^{2+}) cation precipitation starting with isolated cells plus strong cation exchange chromatography LC-MS/MS. Five hundred seventy proteins were identified including 45 transport proteins. Among the latter, 18 had either not been identified in the intestine in the past or there was a single unconfirmed report of their presence. Validation was accomplished by a combination of immunoblotting and immunofluorescence using mouse jejunum and previously described antibodies. The validated BB proteins were aquaporin 7, Glut 9b, $Na^{+}/^{-}$ symporter (NIS), and non-gastric H^{+}/K^{+}-ATPase. This study helps to further define the brush border membrane vesicle, a preparation which has been widely used to identify transport function of the small intestine.

Introduction

Identification of the proteome is a necessary step in defining unique aspects of the systems biology of GI epithelia. The structurally unique domain of all GI organs is the apical membrane and apical recycling compartment. In the small intestine, this is the brush border (BB), which is known to have distinct structural elements (glycocalyx, microvilli, actin core and rootlets, terminal web). The small intestinal BB is unique, even in comparison to the renal proximal tubule BB with different extents and perhaps mechanisms of endocytosis and proteins involved in endocytosis (caveolin, megalin, cubulin, etc).

Functional studies of intestinal absorptive function have recognized the unique contribution of the apical domain and techniques have been developed to isolate highly purified brush border membrane vesicles (BBMV) (1,2). BBMV form almost entirely right-side-out in a sealed form that allows uptake/concentrative studies. The current understanding of transport processes/ proteins present in the apical domain of the small intestine have been partially defined by such studies. These functional studies have concentrated on substrate uptake, which is generally linked to Na^{+} gradients generated by the basolateral membrane Na^{+}/K^{+}-ATPase, although some H^{+} gradient linked transporters have been identified. BBMV are typically obtained by divalent cation precipitation (and rarely free flow electrophoresis) and are highly enriched in microvillus membrane and include the supporting cytoskeleton and terminal web. In addition, they contain small but variable amounts of tight junctions, basolateral membrane “tags” and attached trafficking vesicles, making them a complex preparation. Attempts to localize proteins in the apical, basolateral membranes, and tight junctions of the small intestine have relied on enzymatic analyses in which changes in specific activities between the enriched fraction and initial lysates or total membranes were compared or similar comparisons were made by immunoblotting; another approach used was localization by microscopic identification in comparison to the location of proteins with known subcellular residence.

The current studies represent another way to identify proteins in BBMV and represent the initial detailed identification of the mouse jejunal BBMV proteome. Results will be compared to earlier definitions of the mouse renal proximal tubule (3) and rat inner medullary collecting duct BB proteome (4).

Methods

Cell Isolation and BBMV Preparation. Male FVB mice that were 12-20 weeks old were anesthetized by IP injection of ketamine (100 mg/kg) plus xylazine (20 mg/kg). The abdomens were opened, and the small intestine was rapidly removed. The segment starting from ~8 cm distal to the stomach to the beginning of the ileum (ileum is defined as distal half of the small intestine) was studied here as jejunum. Luminal contents were removed by washing with iced 154 mM NaCl, jejunum was everted, and epithelial cells were removed by vibration (Vibro-mixer model E1 from Chemap AG, Hännedorf, Switzerland) at a frequency of 50 Hz, amplitude 2 mm. After 1-2 min vibration in 150 mM NaCl to remove mucus and remaining luminal contents, cells were released by vibration for 25 min in 10 mM Tris, 150 mM NaCl, and 5 mM EDTA, pH 7.4, as previously described (5). This produced predominantly epithelial cells from all regions of the villus and a minority of crypt cells. Cells from 4-6 animals were combined for each preparation. The entire procedure was performed at 4 °C. Cells were centrifuged (750 x g, 5 min), washed twice in buffer I (298 mM mannitol, 12 mM Tris, pH 7.4), and frozen in the same buffer containing protease inhibitor ("Complete", Roche). After thawing slowly on ice, cells were homogenized by Teflon glass homogenization, and BBMV were prepared by Mg^{2+} precipitation, as described (6). After addition of 10 mM $MgCl_2$ and gentle mixing for 20 min at 4 °C, cell debris and large membrane fractions were removed by centrifugation (15 min, 2000 x g). Supernatant was centrifuged for 30 min at 30.000 x g to harvest BBMV. The pellet was dissolved in buffer I by Teflon glass homogenization, and the Mg^{2+} precipitation was repeated. The final pellet was dissolved in buffer consisting of 275 mM mannitol, 25 mM Tris, 1 mM Na_3VO_4, and protease inhibitor cocktail. Initial cell lysates were used for comparison of enrichment of the final BBMV preparation. Aliquots of cells were placed into buffer II (60 mM mannitol, 2.4 mM Tris, pH 7.1, 1 mM EGTA, 2 mM Na_3VO_4, 1 mM β-glyceropholPO_4, 1 mM phenylalanine with protease inhibitor cocktail (Sigma) 1:1000 plus phosphoramidon (1 µg/mL) and then homogenized at 4 °C with a Polytron (10 times for 10 s at setting 5 with a 20 s interval between each burst) followed by Teflon glass homogenization. The homogenates were centrifuged at 4000 rpm for 10 min at 4 °C to remove cell debris and nuclei. Supernatants were centrifuged at 40 000 rpm for 60 min, and total membrane (TM) pellets were collected and suspended in buffer I. Studies were performed on 3 separate BBMV preparations of mice of the same strain at 12, 13, and 20 weeks of age.

Characterization of BBMV by Enrichment of Marker Enzymes by IB; Antibodies Used and other Markers. Enrichment compared to total membrane preparations of the specific activities of marker enzymes known to reside in specific subcellular organelles was used to assess purification of the mouse jejunal BBMV. Initially, the total membranes and BBMV had protein concentrations estimated by Bichinoic acid assay (BioRad). To further match the amount of protein present, 20 µg of BB were separated on 1-dimensional SDS-PAGE gels (12%) and the total density of summed proteins was estimated by Ponceau S staining (See Figure 1A). About 20 µg of total membrane and

BBMV were then separated on several 12% SDS-PAGE and compared for marker enzyme density via IB. Proteins compared that are felt to localize to BB include intestinal alkaline phosphatase, NHE2 and NHE3 (although the latter is thought to have up to 20% in various aspects of the apical recycling system); basolateral membranes, Na/K-ATPase; ER, calnexin; Golgi, Golgin 84; and mitochondria, mitochondrial phosphate carrier (gift from P. Pedersen, JHUSOM).

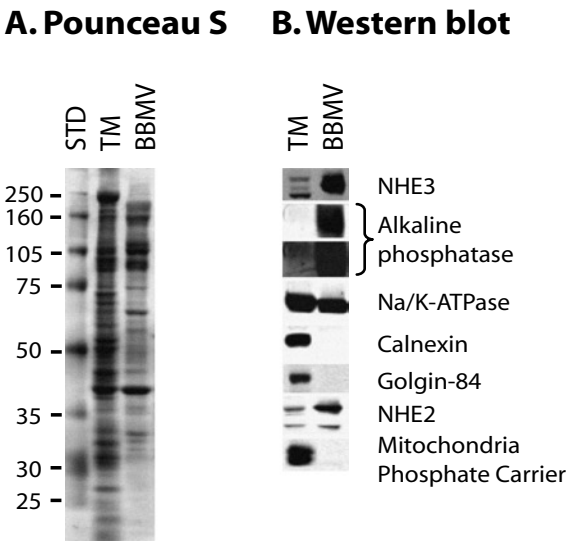

Figure 1. Enrichment in Mouse Jejunal BBMV Relative to Total Membranes (TM) Indicated by Immunoblotting. Total membrane and BBMV were separated by 12% SDS-PAGE stained with Ponceau S (A) with density estimated and used for normalization of IB data (B). Twenty micrograms of TM and BBMV were then separated by 12% SDS-PAGE gels and immunoblotted (IB) for the proteins shown. Odyssey fluorescence gel scanner was used to quantitate the IB signal and the ratio was used as an indication of enrichment after adjustment for differences in total proteins estimated from A. Markers of the BB were intestinal alkaline phosphatase (two exposures are shown with a darker exposure needed to show presence in TM), NHE3, NHE2; basolateral membranes, Na^+/K^+-ATPase; ER, calnexin; Golgi, Gogin-84; mitochondria, mitochondrial phosphate carrier. A representative experiment (12 week animals) which was repeated on the three BBMV preparations is shown.

Preparation of BBMV Fractions for LC-MS/MS Including Protein Digestion, iTRAQ Labeling, and Strong Cation Exchange Chromatography. Two techniques were used to generate results from 3 separate BBMV preparations (12, 13, and 20 week old animals), all using 2D LC-MS/MS with strong cation exchange chromatography (SCX). The BBMV (20 µg) from 12 week animals were also added to SDS-PAGE sample buffer (200 mM Tris pH 7.5, 0.9% SDS, 12 mM EDTA, 4% sucrose, 10 mM DTT, and Pyronin Y); the samples were heated for 5 min at 70 °C then applied to a 10% 1D SDS-PAGE gel with no stacking gel. Electrophoresis continued until the dye-front had migrated approximately 1-2 cm into the gel. The gel was then stained with Gel Code Blue (Pierce), and the stained protein band was excised from the gel, minced, and washed. The proteins were subjected to in-gel trypsin digestion (7), and the resulting peptides were eluted from the gel and submitted for LC-MS/MS analysis.

LC-MS/MS analysis of the resulting peptides was performed using a Thermo Finnigan LTQ ion trap mass spectrometer equipped with a Thermo MicroAS autosampler and Thermo Surveyor HPLC pump, Nanospray source, and Xcalibur 1.4 instrument control. The peptides were separated on a packed capillary tip, 100 µm x 11 cm, with C18 resin (Monitor C18, 5 micron, 100 angstrom, Column Engineering, Ontario, CA) using an inline solid-phase extraction column that was 100 µm x 6 cm packed with the same C18 resin (using a frit generated with liquid silicate Kasil 1 (8)) similar

to that previously described (9), except the flow from the HPLC pump was split prior to the injection valve. The flow rate during the solid-phase extraction phase of the gradient was 1 mL/min and during the separation phase was 700 nL/min. Mobile phase A was 0.1% formic acid; mobile phase B was acetonitrile with 0.1% formic acid. A 95 min gradient was performed with a 15 min washing period (100% A for the first 10 min followed by a gradient to 98% A at 15 min) to allow for solid-phase extraction and removal of any residual salts. After the initial washing period, a 60 min gradient was performed where the first 35 min was a slow, linear gradient from 98% A to 75% A, followed by a faster gradient to 10% A at 65 min and an isocratic phase at 10% A to 75 min. The MS/MS spectra of the peptides were performed using data-dependent scanning in which one full MS spectrum, using a full mass range of 400-2000 amu, was followed by 3 MS/MS spectra.

In addition to this 1D LC-MS analysis, the peptides were also subjected to 2D LC-MS/MS analysis in which the peptides were first fractionated using SCX (100 µm x 7 cm Luna SCX column, Phenomonex, Torrance, CA) using a 0-500 mM, pH 3.0-8.0 ammonium formate gradient in 25% acetonitrile as described previously (10), except a final salt bump of 0.5 M ammonium formate during the last 10 min of the 65 min was substituted for the KCl bump. After collection of the flowthrough fraction, each of 9 separate fractions were collected, the last three fractions were combined, and each fraction (including the flow-through fraction) was subjected to a reverse phase separation directly inline with the LTQ as described above. Proteins were identified using the cluster version of the SEQUEST algorithm (11) using the mouse subset of the Uniref 100 database (www.uniprot.org). The database was concatenated with the reverse sequences of all the proteins in the database to allow for the determination of false positive rates. Protein matches were preliminarily filtered using the following criteria: if the charge state of the peptide is 1, the xcorr is greater than or equal to 1, the RSp is less than or equal to 5, and the Sp is greater than or equal to 350. If the charge state is 2, the xcorr is greater than or equal to 1.8, the RSp is less than or equal to 5, and the Sp is greater than or equal to 350. If the charge state is 3, the xcorr is greater than or equal to 2.5, the RSp is less than or equal to 5, and the Sp is greater than or equal to 350. These filtering criteria achieved a false positive rate of less than 1% in all data sets.

BBMV samples from 13 and 20 week animals were analyzed twice. Each of the sets was digested, labeled with iTRAQ reagents (Isobaric Tagging for Relative and Absolute Quantitation), purified, and fractionated with SCX and analyzed on a QSTAR/Pulsar mass spectrometer. The iTRAQ technique was used to compare BBMV from wild type (reported here) with disease models, and the differences will be reported separately. The samples (75 µg each) were dissolved in 20 µL of 0.1% SDS in 500 mM TEAB (triethylammonium bicarbonate), reduced, alkylated, and digested with trypsin (Promega V5111) with a protein to enzyme ratio 20:1 at 37 °C overnight with iTRAQ reagent in ethanol then added to the digest. The mixture was incubated at room temperature for 1 h. The two BBMV samples were labeled with different iTRAQ agents. After labeling, the samples were mixed and dried down to a volume of 50 µL. The combined peptide mixture was fractionated by SCX on an UltiMate HPLC system (LC Packings) using a PolySulfoethyl A column (2.1 x 100 mm, 5 µm, 300 A, PolyLC, Columbia, U.S.A.). The sample was dissolved in 1 mL of SCX loading buffer (25% v/v acetonitrile, 10 mM KH_2PO_4, pH 2.8), and the pH was adjusted to 2.8 by adding 1 N phosphoric acid. The whole sample was loaded and washed isocratically for 30 min at 200 µL/min. Peptides were eluted with a gradient of 0-500 mM KCl (25% v/v acetonitrile, 10 mM KH_2PO_4, ph 2.8) over 40 min at a flow rate of 200 µL/min. The absorbance at 214 nm was monitored, and 32 SCX fractions were

collected along the gradient. Each SCX fraction was dried down and dissolved in 0.1% formic acid. The resulting fractions were analyzed on QSTAR Pulsar (Applied Biosystems-MDS Sciex) interfaced with an Eksigent nanoLC system. Peptides were separated on a reversephase column packed with 10 cm of C18 beads (360 x 75 µm, 5 µm, 120A, YMC ODS-AQ, waters, Milford, MA) with an emitter tip (New Objective, Woburn, MA) attached. The HPLC gradient was 5-40% B for 60 min (A, 0.1% formic acid; B, 90% acetonitrile in 0.1% formic acid) and the flow rate was 350 nL/ min. Survey scans were acquired from *m/z* 350-1200 with up to three precursors selected for MS/MS using a dynamic exclusion of 45 s. A rolling collision energy was used to promote fragmentation, and the collision energy range was ~20% higher than that used for unlabeled peptides due to iTRAQ tags.

The MS/MS spectra were extracted and searched against the SwissProt database using Protein Pilot software (Applied Biosystems) with the Paragon method and the following parameters: mouse as species, trypsin as enzyme (one missed cleavage allowed), cysteine static modification with methylmethanethiosulfate and iTRAQ (peptide labeled at N-terminal and Lysine) as sample type. Mass tolerance was set to 0.2 atomic mass units for precursor and 0.15 atomic mass units for fragmented ions. The raw peptide identification results from the Paragon Algorithm (Applied Biosystems) were parsed by Pro Group software (a component of Protein Pilot software) before they were displayed. The Pro Group uses the peptide identification results to determine the minimal set of proteins that can be reported for a given protein confidence threshold. The peptide confidence threshold cutoff for this study was at least 90% with maximum of 90.5% of total protein identified, including 2 or more peptide sequences identified. Proteins that were identified with one peptide with confidence more than 90% ("one hit wonders") were inspected manually. Such a protein was considered to have been acceptably identified if it was reported in Basic Local Alignment Search Tool (BLAST), the peptide was unique, and it represented >5% coverage, as determined by BLAST analysis.

The use of two different approaches for protein identification was meant to maximize protein identification on the hypothesis that different approaches were likely to identify different classes of proteins. However, the use of the two approaches on only one BBMV preparation precluded any meaningful comparison of differences in proteins identified.

Bioinformatic Analysis and Categorization of Identified Proteins. After the initial identification of proteins, they were searched in the ExPASy (Expert Protein Analysis System) proteomics server of the Swiss Institute of Bioinformatics (SIB), using the proteins' unique accession number, for their structure, function, distribution, and subcellular localization. Proteins that were inadequately described in ExPASy were further searched in Sanger Institute's collection of protein families and databases (Pfam: http://www.sanger.ac.uk/Software/Pfam/), European Bioinformatics Institute's database (InterPro: http://www.ebi.ac.uk/interpro/). The GeneLynx partial collection of gene databases (GeneLynx:http://www.genelynx.org/), Gene Ontology Consortium (http://www.geneontology.org/), and the National Library of Medicine and National Institute of Health's Entrez PubMed (http://www.ncbi.nlm.nih.gov/entrez/query.fcgi?DB=pubmed).

All identified proteins were classified into 5 Groups, some of which were subdivided to give 13 categories of proteins. The 5 Groups (with the subdivisions of each are) (1) Proteins predicted to be in the BBMV. These include: (i) apical plasma membrane transporters, (ii) known BB digestive enzymes, and (iii) cytoskeleton from the actin cores of the microvilli. However, BBMV are known to also contain tags of membrane attached to the BB and are likely to contain some (iv) tight junctional

and (v) basolateral membrane proteins. The presence of these tags in much smaller amounts than the BB explains the presence but de-enrichment of known basolateral membrane proteins. (2) Proteins that are part of basic cellular processes that are carried out by all cells or are carried out specifically by small intestinal absorptive cells and are not known to be present in the apical membrane. These include proteins involved in (vi) endosomal/membrane trafficking (since some trafficking vesicles are isolated with the BBMV, this category could alternatively been included with category i), (vii) signaling, (viii) metabolism, (ix) degradative proteins, and (x) stress-related proteins. (3) Proteins known to be resident in other organelles (mitochondria, nucleus, etc), and those involved in protein synthesis and assembly (considered category xi). (4) Proteins thought to be found specifically in immunologic cells (considered category xii). (5) Unknown proteins or proteins which have not been localized in mammalian cells or have not had their primary function defined (considered category xiii).

Validation. To validate a fraction of the proteins newly identified as being part of the jejunal BB, antibodies for the proteins were obtained by email solicitation or purchased. The antibodies were used for IB of total membranes and BBMV and for IF of mouse jejunum. We assume that validation of the presence of a protein in the BB is best established by demonstration of BB location by immunohistochemistry. The proteins studied included: aquaporin 7 (gift of S. Nielsen, Un of Aarhus, Denmar and Abcam, Inc); glucose transporter 9b (gift of K. Moley, Washington Un Sch of Med, St. Louis); NaI symporter (NIS) a (gift of N. Carrasco, Albert Einstein Un Sch of Med), non-gastric H^+/K^+-ATPase (gift of N. Modyanov, Un of Toledo) and major vault protein (gift of L. Rome, UCLA School of Med).

Results

BBMV Purification – Comparisons of enrichment of marker enzymes between total membranes and BBMV were performed normalizing to relative amount of total protein separated (Ponceau S staining). As shown in Figure 1, in which BBMV and total membranes of 12 week mice were compared, there was marked enrichment of the known BB proteins intestinal alkaline phosphatase, NHE2, and NHE3 and slight de-enrichment of the BLM protein Na/K-ATPase. Importantly, there was no signal by IB in BBMV for proteins found in mitochondria (mitochondrial phosphate transporter), the ER marker calnexin or the Golgi marker, Golgin-84, although all three were present in total membrane. These are characteristics of highly enriched BBMV in which proteins intrinsic to BB have markedly increased specific activities, whereas non-BB proteins, including proteins in the tight junctions and BLM, are not enriched or have somewhat reduced specific activities.

Proteome Identification – A total of 570 proteins were identified in the BBMV based on identification in at least one of the 3 separate BBMV preparations (Table 1 and Supplementary Table S for full list). Of these, 155 (27%) were present in 1 preparation, 278 (49%) in 2, and 137 (24%) in all 3. The protein categories that were present most in all 3 preparations were the BB digestive enzymes (50%) and tight junction proteins (40%). Shown in Table 1 is the number of proteins identified in each group and category and the percent

of the total number of proteins identified in the BBMV in each category. Figure 2A and B shows the percent of the BBMV proteome in each of the 13 categories (Figure 2A considers all BBMV proteins identified; Figure 2B considers all proteins excluding proteins known to be in other, non BBMV specific subcellular organelles or predominantly in immunologic cells).

One-hundred sixty-one (28%) proteins were from categories expected to be in the BBMV, 126 (22%) would not have been expected to be in BB (non-plasma membrane organelles and proteins found specifically in immunologic cells; Groups 3 plus 4), whereas 261 (46%) are felt to be in intracellular sites that are likely to have been trapped in closed vesicles, including cytosol. Only 22 (<5%) of the total BBMV proteins were not categorized sufficiently to predict subcellular localization. This attests to the advanced stage of classification/annotation of the human and mouse proteomes.

Table 1. Proteome of the mouse jejunal brush border membrane vesicles.

	category	number of proteins	percentage (%)	% detected in >1 prep	% detected in all 3 preps	group[a]
1.	transporters	45	8.1	65.2	28.3	1 (161)
2.	brush border digestive enzymes	20	3.5	90.0	50.0	
3.	tight junction	10	1.8	80.0	40.0	
4.	cytoskeleton	71	12.5	77.5	29.6	
5.	basolateral membrane proteins	15	2.4	78.6	21.4	
6.	endosomal/membrane trafficking	27	4.7	70.4	18.5	2 (261)
7.	signaling	105	18.4	77.1	33.3	
8.	metabolic	95	16.7	73.7	24.2	
9.	degradative proteins	19	3.3	84.2	5.3	
10.	stress-related proteins known residents of proteins	15	2.6	66.7	20.0	
11.	synthesis assembly,mitochondrion, nucleus and others	109	19.1	72.5	11.9	3 (109)
12.	immunologic	17	3.0	52.9	23.5	4 (17)
13.	unkown	22	4.9	40.9	9.1	5 (22)

[a] Group 1: Proteins predicted to be in the BBMV; Group 2: Proteins that are part of basic cellular processes which are carried out by all cells or are carried out specifically by small intestinal absorptive cells and are not known to be present in the apical membrane; Group 3: Proteins known to be resident in other organelles (mitochondria, nucleus, etc), and those involved in protein synthesis and assembly; Group 4: Proteins thought to be found specifically in immunologic cells; Group 5: Unknown proteins or proteins which have not been localized in mammalian cells or had their primary function defined.

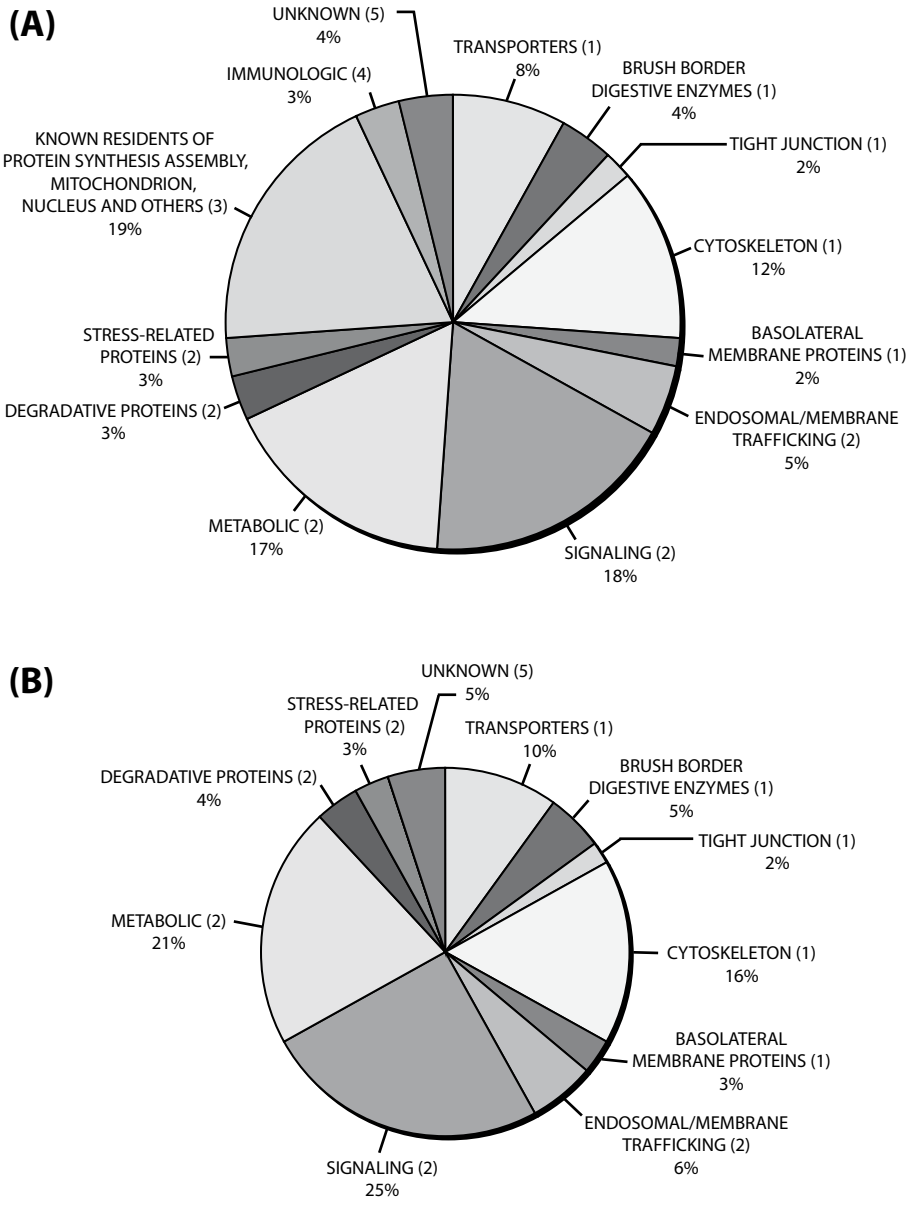

Figure 2. BBMV proteome expressed as pie charts. (A) Proteins identified in BBMV categorized into 5 Groups and 13 categories each expressed as a percent of total proteins identified. (B) Proteins identified in BBMV expressed as a percent of all proteins identified with exclusion of known residents of intracellular organelles and components of immunologic cells. Data from Table 1.

Table 2. Transporters in mouse jejunal brush border membrane vesicles and transporters in mouse jejunal brush border membrane vesicles not previously definitively identified there[a].

	A: Transporters in Mouse Jejunal Brush Border Membrane Vesicles
	Protein
1.	ATP-binding cassette sub-family G member 2
2.	ATP-binding cassette sub-family G member 5 (Sterolin-1)
3.	ATP-binding cassette sub-family G member 8
4.	B (0,+)-type amino acid transporter 1 (B(0,+)AT;Glycoprotein-associated amino acid transporter b0,+AT1)
5.	Canalicular multispecific organic anion transporter 1
6.	Intracellular chloride channel 1
7.	Intracellular chloride channel 5
8.	Calcium activated chloride channel 3
9.	Calcium activated chloride channel 6
10.	Calcium activated chloride channel 2
11.	Choline transporter-like protein 1 (Solute carrier family 44 member 1; CD92 antigen; CDw92)
12.	Choline transporter-like protein 4 (Solute carrier family 44 member 4)
13.	Cysteine-rich protein 1 (Cysteine-rich intestinal protein;CRIP)
14.	Glucose transporter 9b
15.	Large neutral amino acid transporter (LAT-1)
16.	L-type amino acid transporter 4 (LAT-4)
17.	Long-chain fatty acid transport protein 1 (EC 6.2.1.-;Fatty acid transport protein 1;FATP-1; Solute carrier family 27 member 1)
18.	Aquaporin 7
19.	Monocarboxylate transporter 1[MCT1]
20.	Microsomal triglyceride transfer protein
21.	Multidrug resistance protein 1[P-glycoprotein 1]
22.	Multidrug resistance protein 3[MDR1A]
23.	Bile salt export pump (Sister of P-glycoprotein)
24.	Na-I related cotransporter
25.	NBAT 1
26.	Niemann-Pick C1-like protein 1
27.	Oligopeptide transporter, small intestine isoform
28.	Organic cation/carnitine transporter (Could be 1 or 2)
29.	Putative organic anion transporter 5 (OAT5)
30.	Proton-coupled amino acid transporter 1
31.	Potassium-transporting ATPase alpha chain 2
32.	Potential phospholipid-transporting ATPase IC (EC 3.6.3.1) (Familial intrahepatic cholestasis type 1) (ATPase class I type 8B member 1) homolog
33.	Plasma membrane Ca^{2+} transporting ATPase 4 splice variant b
34.	SEC13-related protein
35.	Solute carrier family 13 member 2
36.	Solute carrier family 23 member (Could be 1 or 2)
37.	Solute carrier family 15 (oligopeptide transporter), member 1,
38.	Sodium-dependent phosphate transport protein 2B/Sodium/phosphate cotransporter 2B
39.	Sodium- and chloride-dependent taurine and beta-alanine transporter
40.	Sodium-dependent neutral amino acid transporter B(0)
41.	Sodium/glucose cotransporter 1
42.	KST1 sodium-solute cotransporter
43.	Transmembrane channel-like protein 5
44.	Trpm4 protein
45.	4F2 cell-surface antigen heavy chain

Table 2. (Continued).

B: Transporters in Mouse Jejunal Brush Border Membrane Vesicles Not Previously Definitively Identified There						previous characterization in small intestine					
Protein	**acc#**	**fam**	**cov%**	**pep**	**function**	**A**	**B**	**C**	**D**	**E**	**n**
Aquaporin 7 (Aquaglyceroporin 7)	O54794	Aqp7	25.30%	2	Forms a channel for water and glycerol		X[12]				1
Intracellular chloride channel 1 (Clic1)	Q3TIP8 Q9Z1Q5	Clic1	27.90%	9	Chloride channel		X[39]				2
Calcium activated chloride channel 6	Q6Q472	Clca6	11.60%	10	Chloride channel activity			X[40]			2
Calcium activated chloride channel 2	Q3UW98	Clca2	3.10%	3	Voltage-gated chloride channel			X[41]			1
Choline transporter-like protein 1 (CTL1; Solute carrier family 44 member 1;CD92 antigen)	Q6X893	Slc44a1	11.00%	2	Probable choline transporter			X[42]			2
Choline transporter-like protein 4 (Solute carrier family 44 member 4)	Q91VA1	Slc44a4	19.00%	1	Belongs to the choline transporter-like family			X[43]			2
Cysteine-rich protein 1(Cysteine-rich intestinal protein;CRIP)	P63254		68.40%	2	Role in zinc absorption and may function as an intra-cellular zinctransport protein			X[44]			2
Glucose transporter 9b Large neutral amino acid transporter (LAT2)	Q5ERC7 Q9QXW9	Slc2a9. Slc7a8	2.90% 9.40%	2 2	Glucose transport Sodium independent, high-affinity transport of large neutral amino acids		X[45]			X[27]	1 3
Long-chain fatty acid transport protein 1 (Fatty acid transport protein 1; FATP-1)	Q60714	Slc27a1	18.40%	1	Involved in translocation of long-chain fattyacids (LFCA) across the plasma membrane			X[46]			2
L-type amino acid transporter 4 (LAT4)	Q5CD76	Slc43a2	1.60%	2	L-amino acid transport			X[47]			1
Multidrug resistance protein 3[MDR1A]	P21447	ABC B1A	45.40%	32	Energy-dependent efflux pump responsible for decreased drug accumulation in multidrug resistant cells			X[48]			3
Na-I cotransporter	Q6A4K8	Slc5a12	3.50%	3	Sodium iodide transport	X*					1
Potassium-transporting ATPase alpha chain 2 (Non-gastric H/K ATPase)	Q9Z1W8	Atp12a	2.10%	2	Non-gastric H/K ATPase; catalyzes the hydrolysis of ATP coupled with the exchange of H^+ and K^+ ions across the plasma membrane. Responsible for K^+ absorption.				X[32]		2
Plasma membrane Ca^{++} transporting ATPase 4 splice variant b (PMCA4b)	Q6Q477	Atp2b4	2.90%	2	Calcium ion transport				X[49]		1
Putative organic anion transporter 5 (OAT5)	Q6A4K9	Slc22a19	11.30%	2	Renal organic anion/di-carboxylates exchanger					X[50]	1
Transmembrane channel like protein 5 (Tmc5)	Q7TN61	Tmc5	1.50%	3	Belongs to Trans-membrane Channel like protein family; could be a regulator					X[51]	1
Trpm4 protein (TRP-melastatin protein)	Q6PDM0	Trpm4	2.50%	2	Plasma membrane calcium channel activity		X[52]				1

[a] Previous characterization in small intestine: A- Physiologic role identified subsequently (*n*=1). B- Previous unconfirmed demonstration of protein in adult mammalian small intestinal brush border or apical domain (*n* =3). C- Present in adult mammalian small intestine (mRNA or protein) but brush border localization not demonstrated (*n* =9). D- Studied but not found in the adult mammalian small intestinal mucosa (mRNA or protein) (*n*) 2). E- Not studied in the adult mammalian small intestinal mucosa (mRNA or protein) (*n* =3). *-Personal Communication with N. Carrasco.

Tables 2A-6 list the proteins identified in several categories of BBMV, transporters (Table 2A), brush border digestive enzymes (Table 3), tight junctions (Table 4), cytoskeleton (Table 5), and basolateral membrane proteins (Table 6).

BBMV Transporters. Forty-five transport proteins were identified in the BBMV (Table 2A). There were 18 that had not previously been shown to be in the BB or their BB localization was based on a single study. These are listed in Table 2B. Validation of BB transporters not previously identified in intestinal BB was carried out by IB comparing total membrane and BBMV and IF studies of sections of mouse jejunum. Validation studies were performed on proteins for which antibodies were generously made available by other investigators who had prepared and tested the antibodies for specificity or purchased from commercial sources (immunoblotting, Figure 3, and immunofluorescence, Figure 4). This approach successfully identified as mouse jejunal BB proteins, aquaporin 7, glucose transporter 9b (small amount), NIS, and non-gastric H^+/K^+-ATPase. These studies failed to provide clear support that major vault protein was a BB protein. As shown in Figure 3, IB indicated enrichment in the BBMV compared to total membranes of aquaporin 7, glucose transporter 9b, NIS, and non-gastric H^+/K^+ ATPase, whereas there was de-enrichment of major vault protein which consequently is not listed in Table 2A or B, even though it was initially identified. IF localization of aquaporin 7 has been published from rat small bowel, confirming apical membrane localization at the tip of the villi (and colonocytes at the top of crypts and surface cells of rat left colon) (12). As shown in Figure 4, in histologic sections of mouse jejunum, there were significant amounts of non-gastric H^+/K^+-ATPase, NIS, and aquaporin 7. In addition, glucose transporter 9b was present in small amounts in the BB, although most was intracellular. Major vault protein had intracellular staining, some of which was near the apical membrane, but it could not be determined whether there was any BB localization.

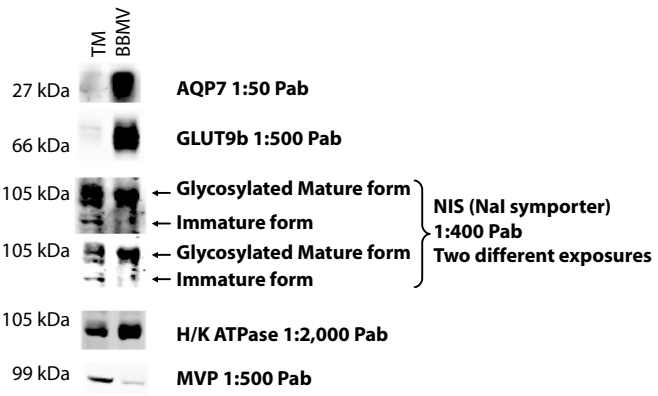

Figure 3. Validation of presence in the mouse jejunal BBMV of several transport proteins by enrichment by IB. The same mouse jejunal BBMV and total membrane preparations used in Figure 1 were IB for aquaporin 7 (antibody kindly provided by S. Nielsen), Glut 9b (kindly provided by K. Moley), NIS (kindly provided by N. Carrasco), non-gastric H+/K+-ATPase (kindly provided by N. Modyanov), and major vault protein (kindly provided by L. Rome). As in Figure 1, similar total protein was transferred to the TM and BBMV lanes. The antibody dilutions are shown in the figure. Enrichment is taken as indication that the protein is probably primarily present in the BBMV. (Pab, rabbit polyclonal antibodies.)

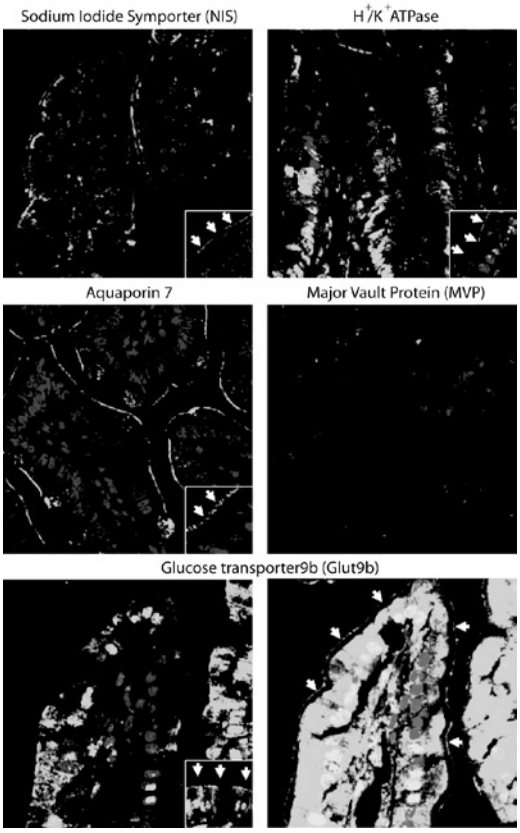

Figure 4. Validation of presence in mouse jejunal BBMV of several transport proteins using immunofluorescence/light microscopy for localization. Histologic sections (4 μm) of mouse jejunum were stained for localization of Na-I co-transporter, non-gastric H^+/K^+-ATPase, aquaporin 7, major vault protein (MVP), and Glut9b with Alexa 488 tagged secondary antibody (1:100). IF localization supported presence in the BB of NIS, non-gastric H^+/K^+-ATPase, aquaporin 7, and a low level of Glut 9b. Bottom right is overexposed to more clearly demonstrate BB Glut 9b (arrows) Major vault protein was intracellular with a small amount of apical signal that could not be definitely separated from edge artifact. Inserts represent higher power magnification (400x) of jejunal BB. Arrows indicate BB expression. Nuclei stained with Hoechst 350.
(Color figure on page 169.)

Table 3. Brush border digestive enzymes in mouse jejunal brush border membrane vesicles.

	Protein
1.	Alanyl (membrane) aminopeptidase
2.	Aminopeptidase B (EC 3.4.11.6; Arginyl aminopeptidase; Cytosol aminopeptidase IV)
3.	Dipeptidase 1
4.	Dipeptidyl peptidase 4
5.	Gamma-glutamyltranspeptidase 1
6.	Embryonic alkaline phosphatase
7.	Intestinal alkaline phosphatase
8.	Lactase
9.	Lactase-like protein [Precursor] (Klotho/lactase phlorizin hydrolase-related protein)
10.	Membrane-bound maltase-glucoamylase
11.	Membrane-bound aminopeptidase P /EC 3.4.11.9
12.	Neutral ceramidase
13.	Neprilysin/EC 3.4.24.11/Neutral endopeptidase
14.	N-acetylated-alpha-linked acidic dipeptidase-like protein
15.	Suppressor of tumorigenicity protein 14
16.	Soluble maltase-glucoamylase
17.	Similar to Hypothetical protein/Intestinal alkaline sphingomyelinase
18.	Rat lactase-phlorizin hydrolase homolog
19.	Trehalase
20.	Xaa-Pro dipeptidase

Table 3 lists the brush border digestive enzymes identified. These proteins were expected to be present in large amounts, and multiple disaccharidases and peptidases were identified as well as neutral ceramidase. Absence of identification of proteins know to be present in large amounts in BB, such as sucrase-isomaltase, could have several explanations and is not to be interpreted to indicate that it is not present in mouse jejunum (13). For instance, sucrase-isomaltase was not identified in these studies but was identified in a subsequent proteomic study of mouse jejunal BBMV (Donowitz, unpublished).

Table 4. Tight junctional proteins in mouse jejunal brush border membrane vesicles.

	Protein
1.	Claudin-3
2.	Claudin-7
3.	InaD-like protein (Pals1-associated tight junction (PATJ) protein; Protein associated to tight junctions; Channel-interacting PDZ domain-containing protein-CIPP)
4.	Junctional adhesion molecule A
5.	Junction plakoglobin
6.	MAGUK p55 subfamily member 5
7.	MFLJ00279 protein [
8.	Mucin and cadherin-like protein
9.	Partitioning defective 6 homolog beta (PAR-6 beta;PAR-6B)
10.	Tight junction protein ZO (Could be 1, 2 or 3)

Table 4 lists the tight junction proteins identified, and Table 5 lists the cytoskeleton proteins present. The tight junction proteins identified and not previously identified in the small intestinal tight junctions and/or the cytoskeleton include nexilin, myosin Vb, and myosin 1D. Myosin Vb has been assumed to be in the apical domain of all epithelial cells and has been shown to be localized there in the renal polarized cell model MDCK (14) and in a hepatocyte cell line, WIF-B9 (15). Nexilin is an F-actin binding protein localized at cell-matrix adherens junctions (16). Myosin 1d was previously called myr4 and has been implicated in endocytosis at a step between the early endosome and recycling endosome (17). No attempt was made to validate their presence in the BB. There were 15 proteins identified in the BBMV that are known to be basolateral membrane proteins. These are listed in Table 6. The presence of Na-K-ATPase alpha chains 1, 3, 4 and B-1 suggest that there is not a single Na^+-K^+-ATPase isoform in the mouse small intestine, although it is not clear whether a single cell has multiple isoforms or this reflects differences in cell types.

Table 5. Cytoskeletal Proteins in Mouse Jejunal Brush Border Membrane Vesicles.

	Protein
1.	Actin-like Protein 2
2.	Actin
3.	Actin, cytoplasmic 1
4.	Actin-like protein 3
5.	Actin-like protein 2 (Actin-related protein 2)
6.	Actin-related protein 2/3 complex subunit 1B (ARP2/3 complex 41 kDa subunit; p41-ARC)
7.	Actin-related protein 2/3 complex subunit 2 (ARP2/3 complex 34 kDa subunit; p34-ARC)
8.	Actin-related protein 2/3 complex subunit 4 (ARP2/3 complex 20 kDa subunit; p20-ARC)
9.	Adseverin/Scinderin/Gelsolin-like protein
10.	AI427122 protein
11.	Alpha-actin 1
12.	Alpha-actinin-1
13.	Alpha-actinin-4 (Non-muscle alpha-actinin 4) (F-actin cross linking protein)
14.	Alpha-adducin (Erythrocyte adducin subunit alpha)
15.	Cofilin 1, Non-muscle homolog
16.	Type VII collagen
17.	Coronin-1A
18.	Coronin-1B (Coronin-2)
19.	Coronin-1C (Coronin-3)
20.	Coronin-2A
21.	Destrin (Actin-depolymerizing factor) (ADF) (Sid 23)
22.	Dstn protein
23.	Dynein heavy chain (DYHC; Cytoplasmic dynein heavy chain 1; DHC1)
24.	Ezrin (p81; Cytovillin;Villin-2)
25.	Ezrin-radixin-moesin-binding phosphoprotein 50 (EBP50)
26.	Radixin
27.	F-actin capping protein alpha subunit
28.	F-actin capping protein subunit beta
29.	Filamin (could be A, B or C)
30.	Gamma actin-like protein
31.	Harmonin
32.	Keratin complex 2
33.	Keratin
34.	Keratin, type I cytoskeletal 10
35.	Keratin, type I cytoskeletal 13
36.	Keratin, type I cytoskeletal 19 (Cytokeratin-19; CK-19; Keratin-19; K19)
37.	Keratin, type II cytoskeletal 1
38.	Keratin, type II cytoskeletal 8
39.	Keratin complex 2, basic, gene 1
40.	Kinesin heavy chain (Ubiquitous kinesin heavy chain; UKHC)
41.	Mucin-13
42.	Myo5b protein
43.	Myosin Id
44.	Myosin If
45.	Myosin Ia
46.	Myosin-5A (Myosin Va; Dilute myosin heavy chain, non-muscle)
47.	Myosin-6
48.	Myosin VI homolog
49.	Myosin light polypeptide 6 (Smooth muscle and nonmuscle myosin light chain alkali 6;Myosin light chain 3;MLC-3;LC17)
50.	Myosin-7A (Myosin VIIa)
51.	Myosin-7B (Myosin VIIb)
52.	MFLJ00256 protein
53.	Myosin-9 (Myosin heavy chain, nonmuscle Iia; NMMHC-IIA; Cellular myosin heavy chain, type A; NMMHC-A)
54.	Myosin-14
55.	Nexilin
56.	Plastin-2 (L-plastin; Lymphocyte cytosolic protein 1; LCP-1;65 kDa macrophage protein;pp65)
57.	Plastin-3 (T-plastin)
58.	Protein diaphanous homolog 1 (Diaphanous-related formin-1; DRF1; mDIA1)
59.	Profilin 1
60.	Spectrin alpha chain
61.	Similar to beta actin
62.	Skeletal muscle alpha-actin mRNA.
63.	Tubulin alpha-4 chain (Alpha-tubulin 4; Alpha-tubulin isotype M-alpha-4)
64.	Tubulin beta-2C chain
65.	Tubulin beta-3 chain
66.	Tubulin beta-5 chain
67.	Transforming protein RhoA
68.	Tubulin beta-4 chain
69.	Tubulin alpha-6 chain
70.	Tubulin beta-3 chain
71.	Villin

Table 6. Basolateral Membrane Proteins in Mouse JejunalBrush Border Membrane Vesicles

	Protein
1.	Atp2b1 protein [Fragment]
2.	Hephaestin [Precursor]
3.	Integrin alpha-3
4.	Integrin beta-1
5.	Itgb4 protein
6.	Integrin alpha-6
7.	Integrin beta-1 [Precursor] (Fibronectin receptor subunit beta; Integrin VLA-4 subunit beta; CD29 antigen)
8.	Organic cation/carnitine transporter 3 (Solute carrier family 22 member 21; Solute carrier family 22 member 9)
9.	Solute carrier family 2, facilitated glucose transporter member 2, GLUT 2
10.	Solute carrier family 12 member 2 (Nkcc1)
11.	Sodium/potassium-transporting ATPase alpha-1 chain
12.	Sodium/potassium-transporting ATPase alpha-3 chain
13.	Sodium/potassium-transporting ATPase alpha-4 chain
14.	Sodium/potassium-transporting ATPase subunit beta-1
15.	Talin-1

Discussion

In studies of epithelial cell physiology, emphasis has been on the unique epithelial cell organelle, which is made up of the brush border, including the terminal web, plus the apical cytoplasm and components of the endosomal recycling system. The epithelial cells studied include the parietal cell, small intestine, and renal proximal tubule and inner medullary collecting duct. All have large apical domains, although dynamic regulation of the apical domain and their functions are different. The parietal cell, and its tubulovesicular system, was the model that was first used to establish that the V-Snare/T-snare hypothesis applied to epithelia in addition to neural synaptic junctions. The proximal tubule has a large endocytic function in reabsorbing solute filtered at the glomerulus. The collecting duct has dynamic concentrative conservation of water/Na^+ as a major function. The small intestine has massive nutrient absorption as its major function. One way to increase understanding of the apical organelles is by increasing information about their proteomes. In fact, in spite of extensive biochemical study of highly enriched membrane fractions of the apical compartment from these cells, a single proteomic study has been reported of the renal proximal tubule BB (3) and of the cortical collecting duct apical membrane (4). In addition, until now, definition of subcellular or organellar proteomes have otherwise emphasized studies of simple cells and brain (18). Nonetheless, the major conclusion from our study in addition to the identification of specific brush border proteins is that, though highly enriched for brush border proteins, the “highly purified preparation” of small intestinal

BBMV contains proteins from numerous cell compartments. This was the same conclusion reached from the proteomic studies of highly enriched apical membrane vesicles from renal proximal tubule using the free flow electrophoresis technique, which provides the greatest enrichment (3). In this study, the apical membrane preparations contained proteins from other cellular compartments including mitochondria, cytosol, nuclei, and basolateral membranes, as well as numerous proteins involved in signaling and trafficking. This was also the conclusion reached from proteomic studies using highly purified synaptic vesicles and clathrin coated vesicles from brain, which also identified the presence of proteins assumed to be in other compartments (18,19). The latter study, in addition, was interpreted to indicate that trafficking vesicles deliver membrane with lipids and proteins plus soluble material from the donor to the acceptor compartment. Importantly, in the synaptic vesicle studies, multiple SNAREs were identified which were involved not only in the expected exocytic process but also in all stages of early and late endosomes, which was interpreted to indicate that the isolated vesicle compartment had been in touch with all the other compartments involved in endocytosis and exocytosis. In addition, the studies revealed that the number of copies of each protein in synaptic vesicles was highly variable, from a few copies of the V-ATPase, to many copies of transporters involved in neurotransmitter uptake as well as in trafficking.

We now report the specific proteins identified in this initial detailed characterization of the proteome of highly enriched murine jejunal brush border membrane vesicles. The mouse small intestine contains multiple types of epithelial cells but also includes multiple types of inflammatory cells, including intraepithelial lymphocytes. Based on the technique of isolation, starting with vibration to free cells, the cell population obtained is largely from the villus and is greatly enriched in Na^+ absorptive epithelial cells but also contains a minor population of crypt cells, an unknown percentage of goblet cells, intraepithelial lymphocytes, and a few enteroendocrine cells. Contamination with cells from the lamina propria is predicted to be less. Based on the techniques of Mg^{2+} precipitation and differential centrifugation, there was the expected enrichment of the heavier BB due to the presence of the cytoskeletal core and de-enrichment (or failure to enrich) of the epithelial cell basolateral membranes and plasma membrane of nonpolarized cells (including lymphocytes, enteroendocrine cells) as well as intracellular membranes and cytosol. By conventional biochemical analysis, this preparation demonstrated marked enrichment of known apical markers such as intestinal alkaline phosphatase, NHE2, and NHE3 (the latter, even given that 10-20% of NHE3 is estimated to be intracellular in some aspect of the recycling compartment in small intestinal Na^+ absorptive cells (20,21). Please note that detailed biochemical analysis of this BBMV preparation has been reported (5,6) and it was previously reported to be relatively free of biochemical markers of contamination with Golgi, ER, or mitochondria. Nonetheless, the presence of some of the multiple categories of proteins we identified was anticipated because the BBMV is not made up only of the apical membrane, apical cytoskeleton, and terminal web but includes an unknown amount

of apical endocytic and recycling vesicles in various stages of attachment to the apical domain, tags of tight junctions, and small amounts of basolateral membrane proteins. Also, given that these vesicles seal right-side-out in a large percent of the vesicles, trapping of cytosol and other intracellular organelles was predicted. Thus, although this preparation is highly enriched in Na^+ absorptive cell brush borders, it contains, other than BB, proteins which were identified due to the sensitivity of the strong cation chromatography LC-MS/MS technique. Moreover, identification by itself gives no insights into the stoichiometry of proteins present. Thus, the proteome of the BBMV should be used to interpret the function of the BBMV, which has been used for many transport studies and has helped identify the transport process carried out by the small intestine.

The technique used for proteomic identification was strong cation exchange chromatography followed by LC-MS/MS. This approach of multidimensional chromatography was chosen because our goal was to identify membrane proteins. This approach is easier to handle and allows detection of more membrane proteins than the approaches which start with 1D or 2D gel separations. It is worth noting, however, that there appears to be surprisingly little overlap of proteins detected by 2D gels vs 2D chromatography, and future use of 2D gel approaches are likely to identify additional proteins. The number of proteins identified, 570, was in the range of other organelle proteomes determined by multidimensional LC-MS/MS, including studies of renal proximal tubule BB (268) (3), collecting duct (241) (4) (IMCD online database, http://dir.nhlbi.nih.gov/papers/lkem/imp/Default.aspx), Arabidopsis plasma membrane (100 and 174 proteins in two studies) (22,23), synaptic vesicles (~200 proteins) (18), and clathrin coated vesicles (~200 proteins) (19), among others.

Of the proteins shown to be part of the jejunal BBMV proteome, there were 45 transporters identified, of which we classified 18 as not previously being shown to be in intestinal cells (Table 2B). These 18 proteins were further classified (see Table 2B) as never studied for localization or presence in the adult mammalian small intestine; studied and claimed not to be in small intestine; previously shown to be present in small intestine but BB localization not demonstrated; or there was a single unconfirmed report of the presence of the protein in the small intestinal BB. An example of the latter is aquaporin 7 (12) although, message was also previously described as present in the intestine (24,25). In addition, there is a single example of a protein not previously thought to be in the intestinal BB, but following our identification, the protein was studied and shown to have a physiologic function in the small intestine. This is NIS and is described below.

While 20 BB digestive enzymes were identified, all had previously been shown to be in the intestinal BB. Similarly, although 71 cytoskeletal proteins were identified, only 3 had not been shown to be in small intestine in the past (myosin Vb, nexilin, myosin 1d) (14,17); and the 10 tight junctional proteins and 15 basolateral membrane proteins identified had been recognized in the past.

Several of the newly identified apical membrane transporters were confirmed as

present in mouse BBMV by IB and shown to be apical by immunocytochemistry. We feel that the latter is the most definitive way to localize a protein to the BB and even then, subapical localization cannot be eliminated by light microscopy. The decision of which to study was based on availability of characterized antibodies from other laboratories who kindly provided them or commercial sources. Confirmed were aquaporin 7 (12), an aquaglyceroporin, and the newly identified BBMV proteins include glucose transporter 9b, NIS, and non-gastric H^+/K^+-ATPase. Major vault protein, which was identified as present in the BBMV by the proteomic analysis, was not found by either IB or IF. Although initially it was suggested that no intestinal epithelial cells contained plasma membrane aquaporins, several have now been identified. These include aquaporin 3, 7, 10, (12,25,26) with recent demonstration by immunocytochemistry that aquaporin 7 was present in the apical membrane of rat duodenum, jejunum, ileum, cecum, colon, and rectum, with highest expression in the surface epithelial cell (12). Glucose transporter 9b is a splice variant of glucose transporter 9 (Glut family protein of the Glut 5, 7, 11 subclass), which was cloned from human liver and shown to be expressed in kidney and placenta where it is called Glut9DeltaN (27,28). This human protein is expressed in proximal tubule, and when expressed in the distal tubule renal cell line, MDCK cells, was present on the apical membrane. This is different than glucose transporter 9, which though also present in proximal tubule, was on the basolateral membrane (28). Interestingly, mouse Glut 9b trafficked to the basolateral membrane in MDCK cells. There was no previous report of Glut 9b (Glut9DeltaN) being present in mammalian small intestine. The physiologic function of Glut 9b is not known, although it does transport the nonmetabolized deoxyglucose with low affinity compared to Glut4. Its role in the intestine has not been established. However, its expression in mouse kidney and liver increases in the streptozotocin model of diabetes, suggesting a role in glucose transport in diabetes (27,29). NIS, is the protein that mediates iodide uptake in the thyroid gland, which is the initial step in biosynthesis of T3 and T4. This protein has been examined in most detail in the thyroid, not only as the source of iodide for thyroid hormone synthesis, but more recently for treatment of thyroid cancer and other thyroid diseases. In this function, this transporter is on the basolateral membane and allows uptake from the blood of ^{131}I. NIS is in the same gene family as SGLT1 and has been shown to be in the basolateral membrane of breast epithelial cells (30). Subsequent to our identification of its BB location in small intestine, a role in the small intestinal apical membrane has been experimentally determined. NIS appears to be the major transporter involved in intestinal iodide absorption, accounting for Na^+-dependent iodide absorption, a process that had not been previously examined in detail (31) (N. Carrasco, personel communication). The non-gastric H^+/K^+-ATPase which was identified in the jejunal BBMV was known to be present in the apical surface of distal colon, particularly in surface colonocytes, kidney and prostate, where it seems to be involved in K^+ absorption (32-34). It was not thought to be present in the rat small intestine based on Northern analyses although small amounts of message were present in rat embryo intestine at least

at day 4.5; with no detailed studies in adult mouse small intestine reported. There were studies, however, of H^+/K^+-ATPase in mouse prostate, which showed that this pump was present on the apical membrane and functioned to secrete H^+ with results not allowing determination whether this protein had a role in K^+ absorption (35). Interestingly, in rat inner medullary collecting duct, H^+/K^+-ATPase is present, although it was interpreted as being the gastric isoform (4,36). Studies are required to determine the physiologic role of the non-gastric H^+/K^+-ATPase in small intestine, especially its role in K^+ absorption and as an acid extruder.

The presence of multiple transporters not yet identified as present in the small intestine is not surprising given other recent proteomic and localization studies that have created the concept that many transport proteins predicted as being in limited numbers of cells and in restricted domains may be present in additional cells and locations. For instance, though the Na^+-linked D-glucose transporters SGLT1 is generally considered to be restricted to the small intestine and renal proximal tubule, SGLT1 has been shown to be present in synaptic vesicles (18). Also in kidney, SGLT1 not only is present in proximal tubule especially the S3 segment but also appears to be present in smooth muscles of blood vessels and renal capsule; and SGLT1 message is present in addition in liver, lung, and cardiomyocytes (37,38). Also, Na^+/H^+ exchangers NHE 6 and 9, which had been thought to be restricted to intracellular organelles, were recently shown to be present on the plasma membrane of hair cells of the inner ear (38). Much more detailed studies of proteins suggested as present in BBMV must be carried out to evaluate not only their presence but functional significance.

This is the initial description of the mouse small intestinal BBMV proteome. A similar study was carried out in rat renal proximal tubule BB(3) in which a similar divalent cation (Mg^{2+}) precipitation/differential centrifugation technique was compared to purification with free flow electrophoresis with the purified membranes then either separated by SDS-PAGE gels, cut into 19 fractions for in-gel trypsin digestion or strong cationic chromatography with separation into 20 fractions for solution trypsin digestion with both techniques followed by peptide separation by LC-MS/MS. Both methods of apical membrane separation gave similar conclusions, that highly enriched membrane preparations could be obtained that allowed identification of large number of proteins (in the Mg^{2+} precipitation method for BB preparation there were 251 proteins identified in the SDS-PAGE approach and 148 by the strong cationic chromatography; and in the free flow electrophoresis method plus strong cationic chromatography method there were 268 proteins identified). The authors concluded that in-solution trypsinization was more efficient than in-gel trypsinization which is why we used in-solution trypsinization. Similar to the studies in mouse jejunal BBMV, a large number of transporters were identified (44 in the apical membrane) in the rat cortical apical membrane (3). One important difference was the much higher number of unidentified proteins in the renal proximal tubule, which we attribute to the fact that even now, 2 years after that publication, rat databases are not as complete as mouse

databases and the fact that many more proteins have been annotated in the past 2 years. Also similarly, the proteome of the inner medullary collecting duct identified 241 proteins, which included 57 transporters (4). Although this is the initial detailed characterization of the mouse jejunal BBMV proteome, a recent publication studied a related area of the mouse intestine (duodenum and upper jejunum) but used IP of aminopeptidase and separation by blue native gels to isolate intact aminopeptidase containing complexes (12). Not surprisingly, much fewer proteins were identified, but there was also identification of several proteins that we did not find.

Acknowledgment

Supported in part by the National Institutes of Health, NIDDK Grants RO1-DK26523, RO1-DK61765, KO1-DK62264, PO1-DK44484, PO1-DK72084, R01-DK070856 and the Vanderbilt Venture Capital Fund, R24- The Hopkins Basic Research Digestive Diseases Development Core Center (R24-DK64388), the Vanderbilt Center for Molecular and Cellular Biology for Digestive Diseases (P30-DK058404), and the Vanderbilt Proteomics Laboratory and Protein Mass Spectrometry Research Center. We acknowledge the expert editorial assistance of H. McCann.

Supporting Information Available

Supplemental Table. This material is available free of charge via the Internet at http://pubs.acs.org.

References

1. Murer, H. (1988) *Comp Biochem Physiol A* **90**, 749-755
2. Murer, H., Ahearn, G., Biber, J., Cassano, G., Gmaj, P., and Stieger, B. (1983) *J Exp Biol* **106**, 163-180
3. Cutillas, P. R., Biber, J., Marks, J., Jacob, R., Stieger, B., Cramer, R., Waterfield, M., Burlingame, A. L., and Unwin, R. J. (2005) *Proteomics* **5**, 101-112
4. Yu, M. J., Pisitkun, T., Wang, G., Shen, R. F., and Knepper, M. A. (2006) *Mol Cell Proteomics* **5**, 2131-2145
5. Vaandrager, A. B., Bot, A. G., De Vente, J., and De Jonge, H. R. (1992) *Gastroenterology* **102**, 1161-1169
6. van Dommelen, F. S., Hamer, C. M., and De Jonge, H. R. (1986) *Biochem J* **236**, 771-778
7. Ham, A.-J. L. (2005) *Proteolytic Digestion Protocols*. Biological Applications Part A: Peptides and Proteins, Elsevier Ltd., Oxford, UK
8. Cortes, H. J., Pfeiffer, C. D., Richter, B. E., and Stevens, T. (1987) *J. High Res. Chromatogr. Commun.* **10**, 446-448
9. Licklider, L. J., Thoreen, C. C., Peng, J., and Gygi, S. P. (2002) *Anal Chem* **74**, 3076-3083
10. Adkins, J. N., Varnum, S. M., Auberry, K. J., Moore, R. J., Angell, N. H., Smith, R. D., Springer, D. L., and Pounds, J. G. (2002) *Mol Cell Proteomics* **1**, 947-955
11. Yates, J. R., 3rd, Eng, J. K., and McCormack, A. L. (1995) *Anal Chem* **67**, 3202-3210
12. Laforenza, U., Gastaldi, G., Grazioli, M., Cova, E., Tritto, S., Faelli, A., Calamita, G., and Ventura, U. (2005) *Biol Cell* **97**, 605-613

13. Babusiak, M., Man, P., Petrak, J., and Vyoral, D. (2007) *Proteomics* **7**, 121-129
14. Lapierre, L. A., Kumar, R., Hales, C. M., Navarre, J., Bhartur, S. G., Burnette, J. O., Provance, D. W., Jr., Mercer, J. A., Bahler, M., and Goldenring, J. R. (2001) *Mol Biol Cell* **12**, 1843-1857
15. Wakabayashi, Y., Dutt, P., Lippincott-Schwartz, J., and Arias, I. M. (2005) *Proc Natl Acad Sci U S A* **102**, 15087-15092
16. Ohtsuka, T., Nakanishi, H., Ikeda, W., Satoh, A., Momose, Y., Nishioka, H., and Takai, Y. (1998) *J Cell Biol* **143**, 1227-1238
17. Huber, L. A., Fialka, I., Paiha, K., Hunziker, W., Sacks, D. B., Bahler, M., Way, M., Gagescu, R., and Gruenberg, J. (2000) *Traffic* **1**, 494-503
18. Takamori, S., Holt, M., Stenius, K., Lemke, E. A., Gronborg, M., Riedel, D., Urlaub, H., Schenck, S., Brugger, B., Ringler, P., Muller, S. A., Rammner, B., Grater, F., Hub, J. S., De Groot, B. L., Mieskes, G., Moriyama, Y., Klingauf, J., Grubmuller, H., Heuser, J., Wieland, F., and Jahn, R. (2006) *Cell* **127**, 831-846
19. Blondeau, F., Ritter, B., Allaire, P. D., Wasiak, S., Girard, M., Hussain, N. K., Angers, A., Legendre-Guillemin, V., Roy, L., Boismenu, D., Kearney, R. E., Bell, A. W., Bergeron, J. J., and McPherson, P. S. (2004) *Proc Natl Acad Sci U S A* **101**, 3833-3838
20. Janecki, A. J., Montrose, M. H., Zimniak, P., Zweibaum, A., Tse, C. M., Khurana, S., and Donowitz, M. (1998) *J Biol Chem* **273**, 8790-8798
21. Donowitz, M., Janecki, A., Akhter, S., Cavet, M. E., Sanchez, F., Lamprecht, G., Zizak, M., Kwon, W. L., Khurana, S., Yun, C. H., and Tse, C. M. (2000) *Ann N Y Acad Sci* **915**, 30-42
22. Marmagne, A., Rouet, M. A., Ferro, M., Rolland, N., Alcon, C., Joyard, J., Garin, J., Barbier-Brygoo, H., and Ephritikhine, G. (2004) *Mol Cell Proteomics* **3**, 675-691
23. Nelson, C. J., Hegeman, A. D., Harms, A. C., and Sussman, M. R. (2006) *Mol Cell Proteomics* **5**, 1382-1395
24. Ishibashi, K., Yamauchi, K., Kageyama, Y., Saito-Ohara, F., Ikeuchi, T., Marumo, F., and Sasaki, S. (1998) *Biochim Biophys Acta* **1399**, 62-66
25. Kuriyama, H., Kawamoto, S., Ishida, N., Ohno, I., Mita, S., Matsuzawa, Y., Matsubara, K., and Okubo, K. (1997) *Biochem Biophys Res Commun* **241**, 53-58
26. Lignot, J. H., Cutler, C. P., Hazon, N., and Cramb, G. (2002) *J Exp Biol* **205**, 2653-2663
27. Mobasheri, A., Shakibaei, M., and Marples, D. (2004) *Histochem Cell Biol* **121**, 463-471
28. Augustin, R., Carayannopoulos, M. O., Dowd, L. O., Phay, J. E., Moley, J. F., and Moley, K. H. (2004) *J Biol Chem* **279**, 16229-16236
29. Keembiyehetty, C., Augustin, R., Carayannopoulos, M. O., Steer, S., Manolescu, A., Cheeseman, C. I., and Moley, K. H. (2006) *Mol Endocrinol* **20**, 686-697
30. Riesco-Eizaguirre, G., and Santisteban, P. (2006) *Eur J Endocrinol* **155**, 495-512
31. Ilundain, A., Larralde, J., and Toval, M. (1987) *J Physiol* **393**, 19-27
32. Spicer, Z., Clarke, L. L., Gawenis, L. R., and Shull, G. E. (2001) *Am J Physiol Gastrointest Liver Physiol* **281**, G1369-1377
33. Pestov, N. B., Korneenko, T. V., Adams, G., Tillekeratne, M., Shakhparonov, M. I., and Modyanov, N. N. (2002) *Am J Physiol Cell Physiol* **282**, C907-916
34. Pestov, N. B., Korneenko, T. V., Shakhparonov, M. I., Shull, G. E., and Modyanov, N. N. (2006) *Am J Physiol Cell Physiol* **291**, C366-374
35. Fejes-Toth, G., and Naray-Fejes-Toth, A. (2001) *Am J Physiol Renal Physiol* **281**, F318-325
36. Ahn, K. Y., and Kone, B. C. (1995) *Am J Physiol* **268**, F99-109
37. Lee, W. S., Kanai, Y., Wells, R. G., and Hediger, M. A. (1994) *J Biol Chem* **269**, 12032-12039
38. Hill, J. K., Brett, C. L., Chyou, A., Kallay, L. M., Sakaguchi, M., Rao, R., and Gillespie, P. G. (2006) *J Neurosci* **26**, 9944-9955

CHAPTER 6

Identification of glial fibrillary acidic protein (GFAP) as binding partner of cGMP-dependent protein kinase II

Boris M. Hogema, Nellie Broere, Marcel Edixhoven, Sietske Rensen, and Hugo R. de Jonge

Department of Biochemistry, Erasmus University Medical Center, Rotterdam, The Netherlands.

Manuscript in preparation.

Abstract

Cyclic nucleotide dependent protein kinases associate with anchoring proteins that affect subcellular targeting and may contribute to the high specificity of the kinase-mediated responses. Two-hybrid screening of a mouse brain cDNA library using cyclic cGMP-dependent protein kinase isoform II (cGKII) as a bait resulted in the identification of glial fibrillary acidic protein (GFAP) as a cGKII binding partner. The interaction was confirmed by overlay and pulldown assays. Deletion mapping confined the interacting regions to the N-terminal regulatory domain of cGKII and the coil 2B domain of GFAP. Expression of cGKII in a glioblastomal cell line resulted in increased GFAP protein abundance whereas the mRNA expression level was unaffected. However, a catalytically inactive mutant of cGKII did not affect GFAP abundance in these cells, suggesting that phosphorylation by cGKII serves to protect GFAP against degradation in intact glial cells.

Introduction

Because the substrate specificity of cyclic nucleotide-dependent protein kinases is rather limited, an additional level of specificity is provided by targeting of the kinases to their relevant substrates by means of anchoring proteins which are located at discrete intracellular locations. The regulatory subunits of cAMP-dependent protein kinase (PKA) bind to A-kinase anchoring proteins (AKAPs) of which more than 50 have been identified (1). Similarly, cGMP-dependent protein kinases (cGKs) were found to bind to several GKAPs, which can improve the efficiency and specificity of target protein phosphorylation (2-6). Whereas the regulatory and catalytic domains of PKA are separate subunits, the cGKs consist of one polypeptide, implying that its catalytic domain is not released from the complex upon cGMP activation. In most cases, therefore, the GKAPs themselves serve as the target for cGK-dependent phosphorylation. Most proteins that have thus far been identified as cGK-interacting proteins bind to the N-terminal domain, which also contains a leucine zipper required for dimerization and an autoinhibitory region which suppresses kinase activity in the absence of cGMP (7). Binding of cGMP to the two binding sites in the regulatory domain induces a large conformational change and releases the catalytic domain from the autoinhibitory domain, allowing the phosphorylation of serine/threonine residues in substrate proteins. Two types of cGK (cGKI and cGKII) have been identified that are encoded by *Prkg1* and *Prkg2* (8, 9). Alternative splicing of the *Prkg1* gene leads to the production of two different cGKI isoforms, cGKIα and cGKIβ which only differ in their N-terminal 90-100 amino acid residues (8). Consequently, binding to GKAPs is often isoform specific (e.g. (10, 11)).

The cGKs regulate a broad range of processes in various cell types (7, 12). cGKI functions include smooth muscle relaxation, vascular remodeling and platelet aggregation. cGKII affects renin secretion, bone growth, resetting of the circadian clock, and is required for salt- and water homeostasis in the intestinal tract (12). To date, 11 proteins that

bind to cGKIα and/or cGKIβ have been identified, but the binding of cGKII to anchoring proteins has received less attention. The subcellular localization of cGKII is determined by myristoylation of the N-terminal Gly2 residue, leading to its translocation to the membrane (13). This is essential for the cGMP-dependent stimulation of the cystic fibrosis transmembrane conductance regulator (CFTR) chloride channel (14).

The first cGKII-interacting protein identified was myosin. The functional relevance of this interaction was not investigated and it was not clear whether myristoylation of cGKII is sufficient to target cGKII to its substrates or whether additional binding to GKAPs are required. Recently however, binding of the PDZ domain protein NHE3 regulatory factor 2 (NHERF-2) was shown to be required for the cGMP-dependent inhibition of the sodium/proton exchanger NHE3 in different cell lines (15). NHERF-2 is the first known broad specificity GKAP which binds to cGKIα, cGKIβ and to cGKII, albeit with relatively low affinity. The highly homologous protein NHERF-1 did not bind to cGKII and its expression in PS120 fibroblasts did not facilitate cGMP-dependent NHE3 inhibition (15). The identification of this GKAP for cGKII prompted us to search for other cGKII-interacting proteins by using the yeast two-hybrid system. During this search, we identified glial fibrillary acidic protein (GFAP) as a novel binding partner of cGKII. GFAP is specifically expressed in astrocytes in the CNS where it is the major intermediate filament present. Intermediate filaments are cytoskeletal structures that form fibers with a diameter of ~10 nm. The interaction between GFAP and cGKII was confirmed by overlay and pulldown. Furthermore, we showed that the N-terminal 108 aa of cGKII was sufficient for binding and that GFAP is phosphorylated by cGKII *in vitro*. Expression of cGKII in a gliablastomal cell line did not affect the GFAP mRNA expression level, but induced an increase in the abundance of the GFAP protein as detected by Western blotting. A catalytically inactive cGKII mutant had no effect on the protein abundance, suggesting that phosphorylation of GFAP by cGKII serves to reduce GFAP turnover.

Materials and methods

Yeast two-hybrid screening for cGKII binding proteins - Full-length mouse cGKII was cloned into the two-hybrid vectors pGADT7 and pGBKT7, which encode fusion proteins of the GAL4 activation domain and binding domain, respectively (Clonetech, CA, USA). RT-PCR amplification of mouse jejunal cDNA was performed using primers 5'-CCCTGAGCCATATGGGAAATGGTTCAGTG-3' and 5'-CATGAATTCGTCAGAAGTCTTTATCCCAGCCTG-3' and the PCR product was cloned exploiting the *Nde*I and *EcoR*I restriction sites present in the primers. These and all other cloned PCR fragments were verified by sequence analysis. The resulting bait construct was co-transformed with the mouse brain matchmaker cDNA library (Clonetech, CA, USA) to the *S. cerevisiae* strain AH109 from the matchmaker GAL4 yeast-two hybrid system 3 (Clonetech, CA, USA) using standard protocols. 254 positive clones were obtained using the medium-stringency selection medium (SD/-His/-Leu/-Trp). Plasmids from positive clones were isolated and amplified in *E. coli*. Because most clones encoded

Na^+/K^+-ATPase (isoform β-1 and β-2), clones were screened by PCR, using the primers forward 5'-TATTATCCCTACTACGGCAAACTC-3' and reverse-5'-GTCCCTGAAAACGGTCTT-3' for β-1, and forward 5'-TCCAAGCACAGAAGAATGATG-3' and reverse 5'-GGCTGCCCGGTGCTGTAA-3' for the β-2 isoform. All other clones were re-screened for false positive hits by transformation to yeast in combination with the empty bait vector and with the plasmid containing cGKII. Na^+/K^+-ATPase was classified as a false-positive hit (although growth in the presence of cGKII was somewhat faster). After this re-screening, only one positive clone was obtained, which encoded the C-terminal part (aa 139-430) of glial fibrillary acidic protein.

Other plasmids used for yeast two-hybrid assays and production of recombinant proteins - To identify which regions of cGKII and GFAP are important for the interaction, several fragments of the genes were subcloned in pGBKT7 and pGADT7. Some fragments were also subcloned into pET28a (Novagen) and/or pGEX-2T (Amersham) in order to generate his-tagged and GST-tagged fusion proteins in *E. coli*. A novel multiple cloning site (5'-GGATCCCATATGGCCATGGAGGCCGAATTC-3') was introduced in pGEX-2T by inserting annealed oligonucleotides with *Bam*HI and *Eco*RI overhangs, to enable us to exchange the various restriction fragments between all plasmids used. The GFAP clone obtained in the two-hybrid screen encoded aa 139-430. The insert (without the linker sequence used for making the cDNA library) was amplified by PCR using primers forward 5'-GCGGGATCCATATGGACAACTTTGCACAG-3' and reverse 5'-CCAGGTGGTCGACCTCACATCACCA-3' and was ligated into the two-hybrid vector pGBKT7 after digestion of plasmid and PCR product with *Bam*HI and *Sal*I. The *Nde*I/*Pst*I or *Nde*I/*Sal*I insert encoding GFAP aa 139-430 was subsequently excised and subcloned into pGADT7, pET28a and pGEX-2T. Because no clone encoding full-length GFAP was recovered from the cDNA library, the 5' end of GFAP was amplified by PCR of genomic mouse DNA from a tail clip using primers 5'-AGGCAGGGCCATATGGAGCGGAGAC-3' and 5'-CCGATCATATTAGGGAACAAAGA-3'. The start codon was incorporated in a *Nde*I site and after digestion of plasmid and PCR fragment by *Nde*I and *Ppu*MI the PCR fragment was cloned into pGEX-2T containing GFAP aa 139-430. To generate full-length his-tagged GFAP, the *Nde*I/*Afl*I fragment from the resulting plasmid was transferred to pET28a containing the GFAP fragment encoding aa 139-140, digested with *Nde*I/*Afl*I. Various GFAP fragments (indicated in Fig. 1) were subcloned by PCR. Fragments were generated using different combinations of primers containing novel start- or stopcodons. The following primers, all containing a startcodon incorporated in a *Nde*I restriction site at the indicated amino acid position, were used for amplification at the 5' end of the required insert: 139 forward (5'-GCGGGATCCATATGGACAACTTTGCACAG-3'), 249 forward (5'-CTAGAGCGGCATATGCGCGAAC-3'), 309 forward (5'-CTAGAGCGGCATATGCGCGAAC-3') and 337 forward (5'-CCAAAGCCATATGGAGGAGATGGCC-3'). Reverse primers containing novel stopcodons were: 430 reverse (5'-CCAGGTGGTCGACCTCACATCACCA-3'), 398 reverse (5'-GGTGGAATTCTTACACGGATTTG-3') and 283 reverse (5'-CTGGAATTCGCGGCGTTAGTCGT TAG-3').

Various fragments encoding cGKII domains were subcloned in a similar way. The fragment encoding the N-terminal fragment (aa 1-108) was amplified from mouse jejunal cDNA using primers forward 5'-CCCTGAGCCATATGGGAAATGGTTCAGTG-3' and reverse 5'-ATGGGATCCCTATCTTGCGGTGAACATCCAGAG-3' and cloned into pGADT7, pGBKT7 and pGEX-2T using the *Nde*I and *Bam*HI restriction sites. The fragments encoding the cGMP

binding domains (aa 100-436), the catalytic domain (aa 385-762) and the combination of the two (aa 100-762) were generated by subcloning fragments generated by PCR of rat cGKII (using the pRc/CMV-cGKII plasmid as a template (9)) into pGBKT7 and pGBKT7. The primers used were 100 foreward (5'-AGGCCTCTCATATGAAAGTGCCTCTGGATGTTCA-3', containing a *Nde*I site), 385 forward (5'-TCGTGATCCATATGGAAACATTCAACCAA-3', containing a *Nde*I site), 762 reverse (5'-ATGGAATTCCGATCCTCACGGTCCTCT-3', containing a *Eco*RI site) and 436 reverse (5'-GTCGACGGATCCCCCTGAATCATCTCCAG-3', containing a *Bam*HI site). A mutation rendering cGKII catalytically inactive (K482M) was introduced into pGBKT7 containing the entire mouse cGKII coding region with the Quickchange™ site directed mutagenesis kit (Stratagene) using primers foreward 5'-ATGTTGCTTTTGCCATGATGTGTATAAGGAAGAAGCA-3' and reverse 5'-TGCTTCTTCCTTATACACATCATGGCAAAAGCAACAT-3'.

Fragments from the intermediate fiber proteins desmin, lamin A and vimentin which are homologous to the GFAP fragment originally identified (aa 139-430) were cloned into the various expression plasmids by PCR amplification from mouse total small intestine cDNA employing primers forward (5'-GGTCGGGATCCATATGGACAACCTGATAGACGACCT-3', *Nde*I site) and reverse (5'-ACGGGGCCAGTCGACTGAATTCCTGG-3', *Sal*I site) for desmin (aa 180-469); forward (5'-CAAAGTGCATATGGAGTTCAAGGAGC-3', *Nde*I site) and reverse (5'-TGAGACTGGGAATTCTAGGAGGAGGC-3', *Eco*RI site) for lamin A (aa 111-404) and forward (5'-GTCGGGATCCATATGGACAACCTGGCCGAGGACATCAT-3', *Nde*I site) and reverse (5'-ACTGCACTGGTCGACCAAGTGTGTG-3', *Sal*I site) for vimentin (aa 176-466). Two hybrid assays were performed by co-transforming constructs expressing the GAL4-AD and BD fusion proteins to yeast and comparing the growth rate on medium- and high stringency selection plates with cells transformed with the individual fusion proteins in combination with the empty vectors pGADT7 or pGBKT7. α-galactosidase activity was determined using X-α-Gal indicator plates.

Expression of recombinant proteins - GST-tagged and his-tagged recombinant proteins were expressed in the *E. coli* Rosetta™ strain (Novagen). 1 mM IPTG was added in the mid-log phase. Bacteria were harvested 4 hours later by centrifugation, resuspended in Dulbecco's PBS containing protease inhibitors (Complete, Roche) and lysed by snap-freezing. After thawing on ice, samples were homogenized by sonication and centrifuged at 23.000 x g for 30 min at 4°C . For purification of his-tagged proteins, the supernatants were added to pre-equilibrated nickel beads (Qiagen) for 1 h, washed with PBS containing 20mM imidazole and 0.5% Triton X-100 and eluted by increasing the imidazole concentration to 500mM. The GST fusion proteins were purified using Glutatione Sepharose 4B beads (Amersham). Beads were washed with PBS containing 0.5% Triton X-100, and protein was subsequently eluted with 50 mM Tris pH 8.0 containing 10 mM glutathione, and 0.5% Triton X-100. Full-length human his-tagged cGKII was purified from Sf9 insect cells as described previously (16).

Gel overlay assay - Recombinant proteins (1 µg/lane) were resolved by SDS-PAGE and transferred to nitrocellulose membranes as described. Purified cGKII was radiolabeled by autophosphorylation in the presence of ^{32}P-ATP. To this end, 6.25 µg of purified cGKII was incubated for 10 min at 30°C in 20 mM Tris/HCl, pH 7.4 containing 10 mM $MgCl_2$, 5mM β-mercaptoethanol, 20 µM cGMP, 12 µM ATP and 10 µM [γ-^{32}P]ATP (0.3 µCi/nmol). The reaction was stopped by diluting the samples in PBS containing 1mM EDTA and 1% Triton X-100. Excess ^{32}P-ATP was removed using a PD10 desalting column and cGKII was eluted in PBS containing 0.1 mM EDTA and 1% Triton

X-100. Labeled cGKII was added to the Western blot membrane and incubated overnight at room temperature on a rotator. Membranes were washed five times with PBS containing 1% Triton X-100, dried and exposed to Biomax MR film (Kodak).

Pulldown and immunoprecipitation assays - 1 µg of purified GST or GST-tagged cGKII (aa 1-108) was bound to gluthathione-Sepharose beads (Glutathion 4B Sepharose, Pharmacia) and incubated with PBS containing 0.2% Triton X-100. 1 µg purified his-tagged GFAP (aa 139-430) was added for 1 h at room temperature. After spinning down and washing the beads twice with PBS containing 0.2% Triton X-100, proteins were eluted by boiling in SDS sample buffer and analyzed by immunoblot using the GFAP antibody.

Binding of cGKII to GFAP was also assessed in a reversed mode by coupling GFAP antibody (14.5 µg) to Rabbit ExactaCruzF IP matrix (Santa Cruz) for 1 h at 4°C. After washing three times with PBS containing 0.2% Triton X-100, 4 µg of purified his-tagged GFAP (aa 139-430) was added and incubated for 1 h at room temperature. Beads were washed twice with PBS/0.2% Triton X-100, and 1 µg of purified his-tagged full-length human cGKII or his-tagged mouse cGKII (aa 1-108) was added and incubated for 2 h. After washing five times, the samples were subjected to SDS-PAGE and immunoblot analysis using antibody to cGKII. Studies were repeated at least three times.

***In vitro* phosphorylation** - Purified his-tagged GFAP fragment (aa 139-430; 7 µg) was incubated with purified cGKII (0.4 µg) for 6 min in 20 mM Tris/HCl, 13 mM MgCl2 and 0.4 mM ^{32}P-ATP (0.3 µCi/nmol). The reaction was terminated by addition of SDS-PAGE sample buffer and boiling (3 min). Samples were resolved by SDS-PAGE, after which the gels were dried and exposed to film.

SNB19 cell culture and infection with cGKII recombinant adenovirus - SNB19 human glioblastoma cells were obtained from the Deutsche Sammlung von Microorganismen und Zellkulturen (DSMZ) and were cultured in Dulbecco's modified Eagle's medium supplemented with 10% fetal bovine serum, 0.1 mg/ml streptomycin and 0.04 mg/ml penicillin. Cells were infected with previously described recombinant adenovirus expressing rat cGKII (17), a catalytically inactive cGKII mutant (PKGII K482A) (18) or the parent vector (pJM17) (17). Virus was added to the cells at a MOI of 1200 directly after plating. Cells were cultured in a 5% CO_2 atmosphere at 37°C for two days. Medium was then refreshed daily for five days after which cells were harvested by scraping and low speed centrifugation.

Determination of GFAP mRNA expression level - SNB19 cells cultured under various conditions were harvested and resuspended in Ultraspec (Biotecx Laboratories, Inc.) containing 8% β-mercaptoethanol following the manufacturer's protocol. The RNA pellet was dissolved in TE buffer containing RNAsin (Promega). 2 µg of RNA was reverse transcribed using 0.5 µg random primers, 0.5 mM dNTPs, and 200 units of reverse transcriptase in the presence of 30 units RNAsin (all obtained from Promega). The reaction was performed at 37°C for 60 min and stopped by incubating for 15 min at 95°C. PCR primers used were GFAP forward 5'-GCGCCCGGCTGGAGGTTG-3' and reverse 5'-CTGGCGCCGGTAGTCGTT-3'. The reaction was performed using 0.4 µM of each primer, 1.8 mM $MgCl_2$, 0.2 mM dNTPs (Promega), 0.3 units RedTaq DNA polymerase (Sigma), and the supplied buffer. The PCR was performed for 25 cycles, with denaturation for 45 s at 94 °C, annealing for 45 s at 45 min and elongation for 40 s at 72 °C. Expression was normalized with respect to the amount of actin and GAPDH

cDNA which were detected using primers actin_forward 5'-TGGCACCACACCTTCTACAA-3', actin_reverse 5'-CGTCATACTCCTGCTTGCTG-3', GAPDH_forward 5'-CAGTCAGCCGCATCTTCTTT-3' and GAPDH_reverse 5'-GTCTTCTGGGTGGCAGTGAT-3'.

Western blot analysis - The effect of cGKII expression in SNB19 cells on the amount of GFAP protein was analyzed by Western blot. Cells were grown and infected with adenovirus as described, and cell pellets were lysed by snap-freezing and resuspended in PBS containing 1% Triton X-100 and protease inhibitors. Laemmli sample buffer was added to the supernatants and samples (2 µg/lane) were separated by SDS-PAGE and transferred to nitrocellulose membrane (Schleicher and Schuell Bioscience). Membranes were blocked with 2.5% non-fat dried milk for 1 h at room temperature and incubated overnight with primary antibody at 4°C. The primary antibodies used were directed against GFAP (1:5000; DakoCytomation Z0334), cGKII (1:500; (14)) and β-actin (1:15000; Chemicon MAB1501). HRP-conjugated secondary antibodies were used for detection of primary antibodies (donkey anti-rabbit IgG from Amersham Bioscience and goat anti-mouse IgG-HRP from Biosource international). Secondary antibody was detected by chemiluminescence (Supersignal West Pico substrate, Pierce) by exposing to light-sensitive imaging film (Biomax MR, Kodak). Imaged bands were quantified using a calibrated GS-800 densitometer and Quantity-One software (Biorad).

Immunocytochemistry - GFAP and cGKII localization was determined in SNB19 cells cultured on glass slides in 6 wells plates, infected as described above and fixed for 10 min with acetone 48 h post-infection. Slides were treated with an advidin/biotin blocking kit (Vector laboratories) and incubated for 1 h with primary GFAP (1:300; DakoCytomation Z0334) or cGKII (1:100; (14)) antibody. Subsequently, the slides were incubated for 1 h with FITC-labeled anti-rabbit secondary antibody (1:100, Jackson Immunoresearch Laboratory, West Grove, PA). The sections were mounted with Vectashield (Vector Laboratories Inc., Burlingame, CA) and immunofluorescent emission was examined using an inverted Olympus IX50 microscope (Olympus, the Netherlands). Images were acquired and analyzed using AnalySiS imaging software (Soft Imaging Systems, Münster, Germany). Confocal microscopy was used to determine GFAP abundance and localization, using a Zeiss LSM510 confocal microscope equipped with a Plan-Neofluar 30x/1.3 oil immersion lens. A 488 nm argon laser was used for excitation and emission was detected using a 505-530 nm bandpass filter. Images were analyzed using KS400 Zeiss software.

Results

Identification of GFAP as a cGKII-interacting protein and mapping of the interacting regions - To identify novel cGKII interaction proteins, full-length cGKII was used as a bait in a yeast two-hybrid screening of a cDNA library derived from pooled mouse brains. Approximately 200,000 clones were screened, and 254 positive clones were obtained using the medium-stringency selection medium (SD/-His/-Leu/-Trp). Positive clones were re-transformed to yeast in combination with the regular cGKII bait and with the empty bait plasmid. Clones that supported growth of yeast cells in combination with the empty bait vector were discarded as false-positive hits. Finally, only one positive clone was obtained,

which contained the C-terminal part (aa 139-430) of glial fibrillary acidic protein (GenBank Accession No.: NM_010277.2). GFAP is a type III intermediate filament protein which is specifically expressed in astrocytes and although it is widely used as an astrocyte marker, relatively little is known about its function. The interaction with cGKII was further verified by exchanging the inserts from the 'bait' and 'prey' vectors, transforming the resulting constructs to AH109 and determining growth in the different media and α-galactosidase activity.

To determine which regions of GFAP and cGKII are important for the interaction, we subcloned various fragments of both genes and used the yeast two-hybrid method to assess whether the fragments interacted. Constructs encoding GFAP aa 139-430, 139-398, 139-283, 249-398, 309-398 and 337-430 were co-expressed in yeast with the prey vector encoding the full-length cGKII (aa 1-762). Interaction was observed only when the GFAP region aa 249-398 was present in the bait constructs (Fig. 1A). Similarly, various deletion constructs of cGKII were made and expressed with the originally isolated GFAP clone. The N-terminal 108 aa proved to be necessary and sufficient for the interaction (Fig. 1B). We therefore conclude that the N-terminal part of cGKII binds to the coil 2 domain of GFAP.

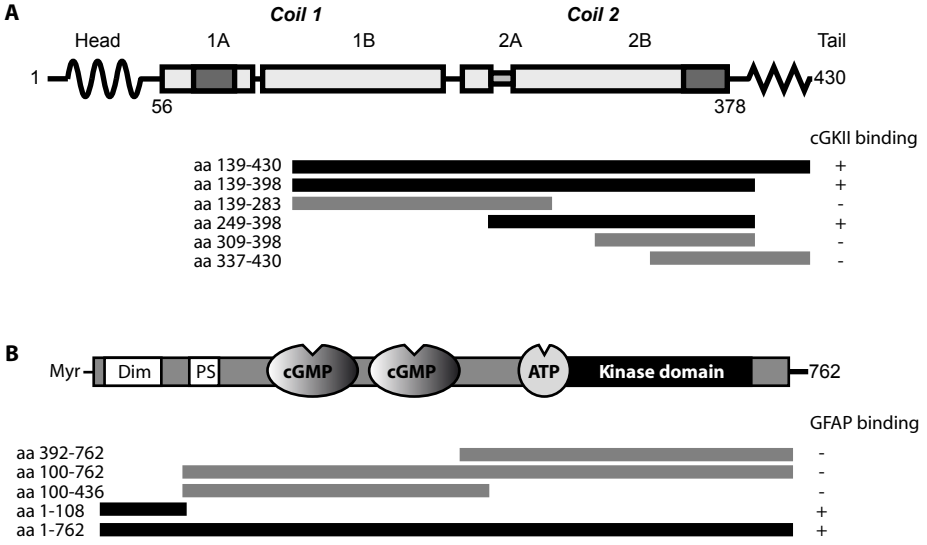

Figure 1. cGKII association with GFAP requires the N-terminal domain of cGKII and the Coil2 region of GFAP. The yeast two-hybrid screening employing full length mouse cGKII as a bait initially identified GFAP (aa 139-430) from a mouse brain cDNA library. The structures of GFAP *(A)* and cGKII *(B)* are shown schematically and the various fragments of GFAP and cGKII that were cloned in the yeast prey and/or bait vectors are indicated. Binding to GFAP and cGKII was assessed by comparing growth rates of yeast cells transformed with the indicated protein fragments co-transformed with full length cGKII (A) or GFAP aa 139-430 (B) with controls transformed with one fusion construct and the empty pGADT7 or pGBKT7 plasmid. Only the GFAP fragments that contain the aa 249-398 region were found to bind cGKII. Similarly, the N-terminal 108 amino acids cGKII bind to GFAP.

Interestingly, another type III intermediate filament protein, vimentin, is a known binding partner of cGKIα (19). Because vimentin and GFAP are highly homologous (77% homology and 55% identical amino acids) we investigated whether cGKII also binds to vimentin and whether cGKIα binds to GFAP using a yeast two-hybrid assay. As shown in Table 1, co-transformation of the N-terminal fragment of cGKIα (aa 1-94) and GFAP (aa 127-418) in the AH109 yeast strain supported growth in selective media. No evidence was obtained for an interaction between GFAP and cGKIβ. We confirmed that cGKIα binds to vimentin and in addition showed that vimentin can also bind to the N-terminus of cGKII. To investigate whether binding to intermediate filaments is a general property of cGMP-dependent protein kinases, interaction with two more IF proteins was tested. Desmin was chosen because it is highly homologous to GFAP and vimentin (60% and 69% identity, respectively), and lamin A represents a type V intermediate filament which displays 48% homology and 28% identity in the region that was cloned. Whereas no binding to the N-terminus of any of the cGK proteins was observed (Table 1), the use of full-length cGKII in two-hybrid assays showed that desmin may weakly interact with cGKII (data not shown). However, growth was only observed when desmin was fused to the activation domain of pGADT7 and not when desmin was subcloned in pGBKT7 (data not shown). Furthermore, the yeast colonies were substantially smaller than with vimentin or desmin. No evidence was obtained for an interaction between one of the cGKs and Lamin A. The functionality of the lamin A expression constructs was confirmed by cloning the lamin A fragment in both the bait and prey vector. When both lamin A fusion constructs were co-transformed, yeast growth was observed showing that the cloned fragments are expressed and interact as expected.

Table 1. Interactions between cGK proteins and intermediate fibers, as determined by 2-hybrid analysis.

cGK isoform	Intermediate fibers			
	GFAP	Vimentin	Desmin	Lamin A
cGKIα (aa 1-59)	-	-	-	nd
cGKIα (aa 1-94)	+*	+	-	-
cGKIβ (aa 1-75)	-	-	-	nd
cGKIβ (aa 1-109)	-	+	-	-
cGKII (aa 1-108)	+	+	-	-

Note: Interactions were determined qualitatively using medium and high-stringency selection media and are presented as negative (-) or positive (+); growth on high-stringency media after 5 days was scored as positive. GFAP (aa 139-430) and the homologous domains from vimentin, desmin and lamin A were subcloned in both pGADT7 and pGBKT7 and were co-transformed to yeast with the kinase domains in the appropriate vector. Transformation of every combination of inserts was performed twice (with the inserts from pGADT7 and pGBKT7 'swapped'). Results were identical for both combinations of inserts with one exception: * the combination of cGKIα (aa 1-94) and GFAP resulted in cell growth only when the GFAP insert was in the DNA binding domain vector (pGBKT7). nd: not determined.

Confirmation of cGKII-GFAP interaction and phosphorylation of GFAP by cGKII - To confirm the interactions observed in the yeast two-hybrid system, overlay and pulldown assays were performed using purified recombinant proteins. Purified his-tagged fragments of GFAP (aa 139-430), vimentin (aa 176-466) and desmin (aa 180-469) were resolved by SDS-PAGE and overlayed with ^{32}P-labelled purified cGKII. Binding to all three intermediate filaments was observed, but not to GST which was used as a negative control (Fig. 2). Similarly, the N-terminal domain of GST-tagged cGKII (aa 1-108) immobilized on glutathione-Sepharose beads was able to bind his-tagged GFAP (aa 139-430), but GST alone was not (Fig. 2B). The originally isolated GFAP fragment (and the homologous parts of vimentin and desmin) was used in these experiments, because production of full-length GFAP in *E. coli* resulted in expression of a protein that spontaneously formed fibers and precipitated (data not shown).

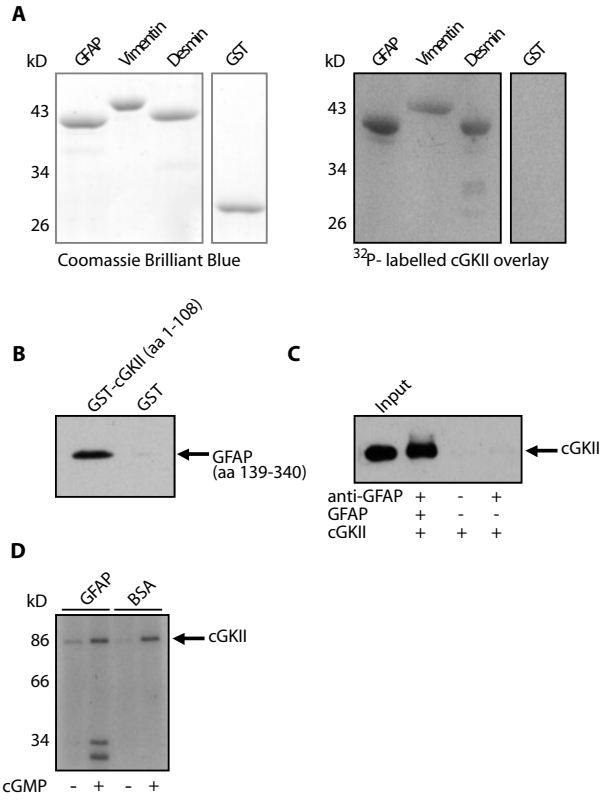

Figure 2. Direct interaction of cGKII with intermediate filaments GFAP, vimentin and desmin. *A*. Purified his-tagged GFAP (aa 139-430) and the corresponding fragments of vimentin (aa 176-466) and desmin (aa 180-469) and purified GST were separated by SDS-PAGE and stained by Coomassie Brilliant Blue (left panel) or transferred to nitrocellulose and overlayed with ^{32}P-labeled cGKII. All fragments from the intermediate filaments were shown to bind cGKII, whereas no interaction with GST was detected. *B*. Pull down assay. Purfied his-tagged GFAP (aa 139-430) was incubated with GST-cGKII (aa 1-108) or GST control protein, immobilized on Glutathione-Sepharose. After washing, bound protein was detected by immunoblotting using a rabbit anti-GFAP antibody. *C*. cGKII bound to purified GFAP (aa 139-430) which was retrieved using GFAP antibody immobilized on ExactaCruz IP matrix. *D*. GFAP (aa 139-430) was phosphorylated *in vitro* by cGKII. Purified his-tagged GFAP was incubated with cGKII and ^{32}P-ATP in the absence and presence of cGMP. Only when cGMP was present, two bands at the position of GFAP were observed in addition to the autophosphorylated cGKII (86 kD) band. The double GFAP band was also observed on gels stained with Coomassie Brilliant Blue and was therefore not related to the phosphorylation of the protein (data not shown). No phosphorylated BSA was detected.

Because cGKII is membrane-localized, solubilization with detergent at high salt concentrations is required to generate protein extracts (13). This interfered with regular co-immunoprecipitation experiments. Therefore, 'reversed' pulldown was performed by coupling purified GFAP (aa 139-430) to GFAP antibody and adding full-length cGKII. After extensive washing, Western blotting showed that cGKII binds to the GFAP fragment.

To investigate whether GFAP can be phosphorylated by cGKII, purified his-tagged GFAP (aa 139-430) was incubated with purified cGKII in the presence of ^{32}P-labelled ATP in the presence or absence of cGMP. After SDS-PAGE and exposure of the gel to film, the incorporation of ATP into proteins could be monitored. The expected band at the position of (autophosphorylated) cGKII was visible as well as two bands at the position of purified his-tagged GFAP (Fig. 4D). Coomassie staining also showed that expression of his-tagged GFAP yielded two separate bands after purification. Under the experimental conditions used, phosphorylation of albumin by cGKII was undetectable.

GFAP protein abundance in glioblastomal cells is upregulated by cGKII expression - Because nitric oxide (NO) had been shown to increase the expression of GFAP mRNA via a cGMP/cGK-dependent signaling pathway in mouse primary astrocytes (20), we investigated the role of cGKII in GFAP expression in cultured human SNB19 glioblastoma cells. As shown in figure 3A, endogenous levels of cGKII expression in the glioblastomal cells were below the detection level, as is common in cultured cells (21). Cells were subsequently infected with recombinant adenovirus expressing rat cGKII or a catalytically inactive mutant of cGKII (K482A). Cells infected with the parent vector (PV) or non-infected (NI) cells were used as controls. After infection with the adenoviral constructs, comparable levels of catalytically inactive and active cGKII proteins were expressed. cGKII was localized predominantly in the membrane and in the perinuclear area (Fig 3B). Densitometric scanning of Western blots showed that the GFAP abundance was increased ~4-fold in cGKII-expressing cells compared to non-infected cells and cells infected with parent vector or catalytically inactive cGKII (Figure 4B). This was confirmed by immunostaining of GFAP in SNB19 cells, showing that GFAP protein expression is increased in cells infected with cGKII compared to cGKII K482A infected cells (Fig. 4C). Semi-quantative PCR was used to check whether the increase in GFAP abundance was caused by upregulation of the gene expression. As shown in figure 4A, GFAP mRNA expression (relative to actin and GAPDH mRNA expression) was not significantly altered in cells infected with cGKII showing that the increase in GFAP protein is caused by post-translational events, most likely by phosphorylation by cGKII.

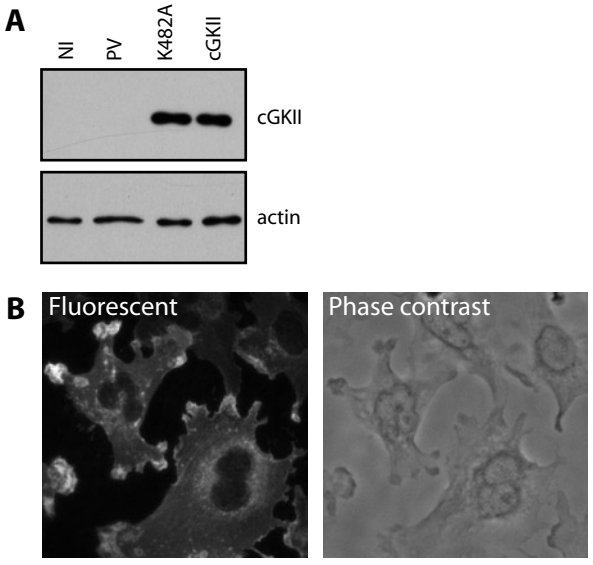

Figure 3. cGKII is expressed in SNB19 glioblastomal cells after adenoviral infection. *A.* Western blot of SNB19 cells harvested 5 days post-infection. No detectable cGKII protein was detected in non-infected cells (NI) and cells infected with the parent vector (PV). Cells infected with recombinant adenovirus encoding the catalytically inactive (cGKII K482A) and wild-type cGKII displayed comparable levels of cGKII protein. Actin was used as loading control (bottom panel). *B.* cGKII localization was determined in SNB19 cells infected with cGKII adenovirus using fluorescent microscopy. cGKII was detected predominantly in the cell membrane and around the nucleus (left panel). The right panel shows the phase contrast image of the cells.

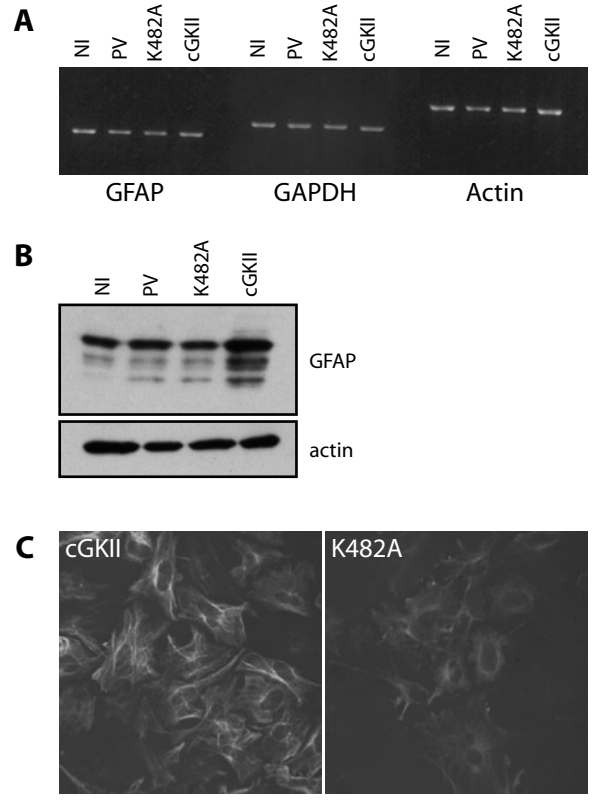

Figure 4. GFAP expression and abundance is upregulated in cells expressing active cGKII. *A.* Semi-quantitative PCR of cDNA from SNB19 cells showed that GFAP mRNA expression is unaltered in cells that were infected with the catalytically active cGKII (cGKII) compared to non-infected (NI), parent vector (PV) or catalytically inactive cGKII (K482A) infected cells. GAPDH and actin were used to normalize the cDNA input for the PCR reactions. *B.* The amount of GFAP protein is ~4-fold increased in cells that were infected with adenovirus encoding cGKII (cGKII) compared to non-infected (NI), parent vector (PV) or catalytically inactive cGKII (K482A) infected cells. Actin was used as a loading control. *C.* Confocal images of SNB19 cells infected with adenovirus encoding cGKII (cGKII; left panel) display a strong increase in GFAP abundance compared to cells expressing catalytically inactive cGKII (cGKII K482A; right panel). Images are representative examples of four independently performed experiments.
(Color figure on page 172.)

Discussion

Although *in vitro* substrate specificity provides a good prediction of *in vivo* specificity, co-localization of kinase and substrate is at least as important (1). Thus far, 11 different binding partners of cGKI have been identified. These proteins have a wide range of functions, but in most cases, the binding was required for efficient phosphorylation of the binding protein itself. The major exception is the IP3 receptor associated G-kinase protein (IRAG) which simultaneously binds to the IP3 receptor and to cGKIβ, resulting in targeting of cGKI to the receptor which is important for smooth muscle relaxation.

Binding of the type II isoform of cGK to anchoring proteins has received less attention. Correct localization of cGKII critically depends on myristoylation of a glycine residue, leading to insertion in the membrane in HEK293 and COS-1 cells (13). Non-myristoylated cGKII was predominantly localized in the cytosol and was impaired in the activation of the CFTR chloride channel in intestinal cells and inhibition of Ca^{2+} absorption in cultured kidney cells (14, 21). Whether membrane targeting is sufficient for cGKII action or whether additional binding to GKAPs is required for efficient substrate phosphorylation is not fully clear yet. The observation that a membrane-targeted cGKI chimera composed of the N-terminal myristoylation sequence of cGKII fused to cGKIβ was able to stimulate CFTR, similar to cGKII, but showed no effect on cGMP-dependent calcium reabsorption in cultured kidney cells suggests that additional factors may be involved (14, 21). The first indication that the cGKII can specifically bind to other proteins came from protein overlay assays using labeled cGKII, which showed binding to several proteins in a tissue-specific manner (3). Myosin was the only binding partner identified in this study, but the functional relevance of the binding was not investigated. Binding was mapped to the N-terminal regulatory domain, hence the term GKAP was introduced in analogy with the A-kinase anchoring proteins (3). More recently, NHERF-2 was shown to bind to cGKII (as well as to cGKI α and cGKIβ) and serves as a 'classical' anchoring protein which is not phosphorylated itself, but is required to position cGKII near the sodium/proton exchanger NHE3 which is inhibited by cGMP only when NHERF-2 is present (15). The third known binding partner of cGKII is the glutamate receptor GluR1. Phosphorylation of GluR1 by cGKII increases the cell surface expression of the receptor and was shown to be required for long-term potentiation (LTP) in hippocampal slices (22). Unlike the previously identified GKAPs, the binding domain was mapped to the catalytic domain of cGKII. Interestingly, the fragment of GluR1 that binds to cGKII displayed significant homology to the autoinhibitory domain of cGKII which suggests cGKII can bind only in the presence of cGMP (22). Because GluR1 does not bind to the regulatory domain of cGKII, the term 'anchoring' protein is debatable and the more general term 'GKIP' (G-kinase interacting protein) seems to be more appropriate in this case (23).

In the present study, we have searched for novel binding partners of cGKII and identified the intermediate fiber protein GFAP using the yeast two-hybrid method. The interaction was verified by several standard methods, and deletion mapping showed

that the N-terminal fragment (aa 1-108) of cGKII can bind to the second coil region (aa 249-398) of GFAP. GFAP is the major intermediate filament protein expressed in astrocytes in the central nervous system and is thought to be important for control of cell shape and movement (24). Although GFAP has been studied extensively and is widely used as an astrocyte marker, relatively little is known about its exact functions. GFAP deficient mice display no detectable anatomical abnormalities but are deficient in long-term depression at distinct sites in the brain as well as in eyeblink conditioning (25). The only specific function of GFAP currently known is the formation of a multiprotein complex containing GFAP, ezrin, NHERF-1 and the glutamate transporter GLAST (26, 27). Expression of GFAP is essential for retaining GLAST in the plasma membrane of astrocytes. Moreover, transport of the glutamate analog D-aspartate was significantly increased in the presence of GFAP and NHERF-1 (26). Taken together, this suggests that GFAP may have a role in preventing glutamate excitotoxicity.

Similar to other IF proteins, formation of GFAP fibers is largely controlled by phosphorylation. Polymerized GFAP exists in a dynamic equilibrium with a small pool of soluble GFAP and the assembly/disassembly cycle is modulated by phosphorylation of amino acids in the N-terminal domain. GFAP is a known substrate of various protein kinases, including cAMP-dependent protein kinase (PKA), Ca^{2+}/calmodulin-dependent protein kinase II (CaMK II), protein kinase C (PKC), cdc-2 kinase and Rho-associated kinase (28, 29), and it can be dephosphorylated by protein phosphatase 1 (PP1) in the rat hippocampus (30, 31). cGMP-dependent phosphorylation of GFAP has not been described previously. However, cGKIα is a known binding partner of the highly homologous intermediate filament vimentin. Stimulation of cGKI was shown to induce a transient co-localization of cGKI and vimentin and resulted in vimentin phosphorylation and fiber formation in cultured human neutrophils (19, 32). Using the two-hybrid system, we confirmed that the N-terminus of cGKIα (aa 1-94) binds to vimentin and showed that also cGKIβ (aa 1-109) and cGKII (aa 1-108) can bind to vimentin (the latter was confirmed in gel overlay assays). Surprisingly, a smaller cGKIα fragment (aa 1-59) did not support growth although this was the fragment that interacts with several known GKAPs both in two-hybrid and pulldown assays (10, 11, 33). A similar observation was made previously with the Formin Homology Domain protein 1 (FHOD1) which binds to the N-terminus of cGKIα (23). Although the N-terminal 59 aa of cGKIα were sufficient for interaction with FHOD1 (in pull-down and 2-hybrid assays), a larger fragment (236 aa) interacted much more strongly, showing that not only the leucine zipper is important for interaction (23).

One might expect that the function of the binding of cGKII to GFAP would resemble the function of the interaction between vimentin and cGKIα. We investigated whether cGKII in the glioblastomal cell line SNB19 affects fiber formation and GFAP abundance. No cGKII was detected in SNB19 as is usually the case after repeated passage of cultured cells (21). However, when cGKII was introduced by adenoviral infection, a strong increase in GFAP abundance was observed by Western blotting and confocal microscopy. No obvious

effect on GFAP localization was noted. Since expression of cGKII did not affect the GFAP mRNA expression levels in SNB19 cells, we conclude that GFAP protein is stabilized by cGKII expression. An inactive cGKII mutant, which was expressed at similar levels, had no effect on the amount of GFAP in SNB19 cells. We tested whether the mutation rendering cGKII inactive affects binding to GFAP in a two-hybrid assay and observed no difference with normal cGKII, as was expected considering that the N-terminal part is required for the binding (data not shown). The effect of expression of active cGKII on GFAP abundance (without stimulation of the cGMP pathway) suggests that a tonus of cGMP-elevating agents exists in cultured cells, similar to what was observed in murine intestine and in cultured smooth muscle cells (34, 35).

Addition of cGMP analogs resulted in highly variable effects on fiber formation in cGKII-expressing SNB19 cells (data not shown). However, in primary cultures of astrocytes, stimulation of the cGMP pathway was recently shown to induce a major reorganization of the GFAP and actin cytoskeleton (36). Stimulation of guanylate cyclase or addition of cell-permeable cGMP analogs resulted in elongation and branching of astrocytes and a redistribution of GFAP and actin filaments, as well as increased migration of astrocytes in an *in vitro* scratch-wound assay. The cytoskeletal rearrangements were prevented by addition of a specific cGK inhibitor (36). Although it was not investigated which of the cGK isoforms was present in these primary cultures, cGKII is the most likely candidate, because this isoform was detected in many types of cells in the brain, including astrocytes, whereas no cGKI was detected in GFAP-expressing cells (37, 38).

The most plausible explanation for GFAP stabilization by cGKII is direct phosphorylation. Phosphorylation of GFAP has previously been shown to increase protein stability *in vivo*. Mice carrying serine to alanine substitutions at several phosphorylation sites in the N-terminal head domain displayed reduced amounts of GFAP, which also shows that GFAP is phosphorylated under basal conditions (39). These residues are phosphorylated by several kinases, but their phosphorylation by cGKI or cGKII have not been studied sofar. Preliminary data show that cGKII was able to phosphorylate a purified GFAP fragment (aa 139-430) *in vitro,* but additional studies are needed to map the cGKII phosphorylation sites *in vivo*. Although full-length GFAP could be produced in *E. coli*, the investigation of its properties were unfortunately hampered by spontaneous precipitation.

In our experiments, cGKII expression had no effect on the GFAP mRNA expression level. Brahmachari *et al*. (2006), on the other hand showed that elevated cGMP leads to an increase in the expression level of GFAP mRNA in cultured primary astrocytes in a cGK-dependent manner (20). The mechanism that causes the kinase-dependent upregulation of GFAP mRNA in the primary astrocytes is still unknown, but appeared not to be operative in the SNB19 cells or may require stronger stimulation of cGKII. cGMP-dependent effects on expression levels of intermediate fibers may be a more general phenomenon, since down-regulation of cGKI expression levels by hypoxia or using small interfering RNA resulted in reduced levels of vimentin in cultured vascular smooth muscle cells (40). It was not

investigated whether this reduction was caused by altered mRNA expression levels or by post-transcriptional events.

In conclusion, we have identified GFAP as a novel binding partner of cGKII and determined that expression of cGKII in an astroglial cell line promotes the stability of the GFAP protein. Inflammatory compounds are known to stimulate the cGMP pathway in astrocytes, leading to rearrangement of the intermediate fiber and actin cytoskeleton and increased astrocyte migration (36). Our data indicates that the various (patho)physiological responses to cGMP stimulation in astrocytes may include a direct effect of cGKII on GFAP phosphorylation and protein abundance.

References

1. Beene, D. L., and Scott, J. D. (2007) *Curr Opin Cell Biol* **19**, 192-198
2. Murthy, K. S., and Zhou, H. (2003) *Am J Physiol Gastrointest Liver Physiol* **284**, G221-230
3. Vo, N. K., Gettemy, J. M., and Coghlan, V. M. (1998) *Biochem Biophys Res Commun* **246**, 831-835
4. Yuasa, K., Omori, K., and Yanaka, N. (2000) *J Biol Chem* **275**, 4897-4905
5. Yuasa, K., Michibata, H., Omori, K., and Yanaka, N. (1999) *J Biol Chem* **274**, 37429-37434
6. Schlossmann, J., Ammendola, A., Ashman, K., Zong, X., Huber, A., Neubauer, G., Wang, G. X., Allescher, H. D., Korth, M., Wilm, M., Hofmann, F., and Ruth, P. (2000) *Nature* **404**, 197-201
7. Vaandrager, A. B., Hogema, B. M., and de Jonge, H. R. (2005) *Front Biosci* **10**, 2150-2164
8. Orstavik, S., Natarajan, V., Tasken, K., Jahnsen, T., and Sandberg, M. (1997) *Genomics* **42**, 311-318
9. Jarchau, T., Hausler, C., Markert, T., Pohler, D., Vanderkerckhove, J., De Jonge, H. R., Lohmann, S. M., and Walter, U. (1994) *Proc Natl Acad Sci U S A* **91**, 9426-9430
10. Surks, H. K., Mochizuki, N., Kasai, Y., Georgescu, S. P., Tang, K. M., Ito, M., Lincoln, T. M., and Mendelsohn, M. E. (1999) *Science* **286**, 1583-1587
11. Ammendola, A., Geiselhoringer, A., Hofmann, F., and Schlossmann, J. (2001) *J Biol Chem* **276**, 24153-24159
12. Hofmann, F., Feil, R., Kleppisch, T., and Schlossmann, J. (2006) *Physiol Rev* **86**, 1-23
13. Vaandrager, A. B., Ehlert, E. M., Jarchau, T., Lohmann, S. M., and de Jonge, H. R. (1996) *J Biol Chem* **271**, 7025-7029
14. Vaandrager, A. B., Smolenski, A., Tilly, B. C., Houtsmuller, A. B., Ehlert, E. M., Bot, A. G., Edixhoven, M., Boomaars, W. E., Lohmann, S. M., and de Jonge, H. R. (1998) *Proc Natl Acad Sci U S A* **95**, 1466-1471
15. Cha, B., Kim, J. H., Hut, H., Hogema, B. M., Nadarja, J., Zizak, M., Cavet, M., Lee-Kwon, W., Lohmann, S. M., Smolenski, A., Tse, C. M., Yun, C., de Jonge, H. R., and Donowitz, M. (2005) *J Biol Chem* **280**, 16642-16650
16. Vaandrager, A. B., Hogema, B. M., Edixhoven, M., van den Burg, C. M., Bot, A. G., Klatt, P., Ruth, P., Hofmann, F., Van Damme, J., Vandekerckhove, J., and de Jonge, H. R. (2003) *J Biol Chem* **278**, 28651-28658
17. Vaandrager, A. B., Tilly, B. C., Smolenski, A., Schneider-Rasp, S., Bot, A. G., Edixhoven, M., Scholte, B. J., Jarchau, T., Walter, U., Lohmann, S. M., Poller, W. C., and de Jonge, H. R. (1997) *J Biol Chem* **272**, 4195-4200
18. Gambaryan, S., Butt, E., Marcus, K., Glazova, M., Palmetshofer, A., Guillon, G., and Smolenski, A. (2003) *J Biol Chem* **278**, 29640-29648
19. MacMillan-Crow, L. A., and Lincoln, T. M. (1994) *Biochemistry* **33**, 8035-8043
20. Brahmachari, S., Fung, Y. K., and Pahan, K. (2006) *J Neurosci* **26**, 4930-4939
21. Hoenderop, J. G., Vaandrager, A. B., Dijkink, L., Smolenski, A., Gambaryan, S., Lohmann, S. M., de Jonge, H. R., Willems, P. H., and Bindels, R. J. (1999) *Proc Natl Acad Sci U S A* **96**, 6084-6089
22. Serulle, Y., Zhang, S., Ninan, I., Puzzo, D., McCarthy, M., Khatri, L., Arancio, O., and Ziff, E. B. (2007) *Neuron* **56**, 670-688

23. Wang, Y., El-Zaru, M. R., Surks, H. K., and Mendelsohn, M. E. (2004) *J Biol Chem* **279**, 24420-24426
24. Eng, L. F., Ghirnikar, R. S., and Lee, Y. L. (2000) *Neurochem Res* **25**, 1439-1451
25. Shibuki, K., Gomi, H., Chen, L., Bao, S., Kim, J. J., Wakatsuki, H., Fujisaki, T., Fujimoto, K., Katoh, A., Ikeda, T., Chen, C., Thompson, R. F., and Itohara, S. (1996) *Neuron* **16**, 587-599
26. Sullivan, S. M., Lee, A., Bjorkman, S. T., Miller, S. M., Sullivan, R. K., Poronnik, P., Colditz, P. B., and Pow, D. V. (2007) *J Biol Chem*
27. Hughes, E. G., Maguire, J. L., McMinn, M. T., Scholz, R. E., and Sutherland, M. L. (2004) *Brain Res Mol Brain Res* **124**, 114-123
28. Tsujimura, K., Tanaka, J., Ando, S., Matsuoka, Y., Kusubata, M., Sugiura, H., Yamauchi, T., and Inagaki, M. (1994) *J Biochem (Tokyo)* **116**, 426-434
29. Schroder, N., de Mattos-Dutra, A., Sampaio de Freitas, M., Fogaca Lisboa, C. S., Zilles, A. C., Pessoa-Pureur, R., and Izquierdo, I. (1997) *Brain Res* **749**, 275-282
30. Vinade, L., and Rodnight, R. (1996) *Brain Res* **732**, 195-200
31. Kosako, H., Amano, M., Yanagida, M., Tanabe, K., Nishi, Y., Kaibuchi, K., and Inagaki, M. (1997) *J Biol Chem* **272**, 10333-10336
32. Wyatt, T. A., Lincoln, T. M., and Pryzwansky, K. B. (1991) *J Biol Chem* **266**, 21274-21280
33. Tang, K. M., Wang, G. R., Lu, P., Karas, R. H., Aronovitz, M., Heximer, S. P., Kaltenbronn, K. M., Blumer, K. J., Siderovski, D. P., Zhu, Y., and Mendelsohn, M. E. (2003) *Nat Med* **9**, 1506-1512
34. Vaandrager, A. B., Bot, A. G., Ruth, P., Pfeifer, A., Hofmann, F., and De Jonge, H. R. (2000) *Gastroenterology* **118**, 108-114
35. Brophy, C. M., Woodrum, D. A., Pollock, J., Dickinson, M., Komalavilas, P., Cornwell, T. L., and Lincoln, T. M. (2002) *J Vasc Res* **39**, 95-103
36. Boran, M. S., and Garcia, A. (2007) *J Neurochem* **102**, 216-230
37. de Vente, J., Asan, E., Gambaryan, S., Markerink-van Ittersum, M., Axer, H., Gallatz, K., Lohmann, S. M., and Palkovits, M. (2001) *Neuroscience* **108**, 27-49
38. Feil, S., Zimmermann, P., Knorn, A., Brummer, S., Schlossmann, J., Hofmann, F., and Feil, R. (2005) *Neuroscience* **135**, 863-868
39. Takemura, M., Gomi, H., Colucci-Guyon, E., and Itohara, S. (2002) *J Neurosci* **22**, 6972-6979
40. Zhou, W., Dasgupta, C., Negash, S., and Raj, J. U. (2007) *Am J Physiol Lung Cell Mol Physiol* **292**, L1459-1466

CHAPTER 7

Discussion

Correct localization and regulation of ion transporters is essential for maintaining salt- and fluid homeostasis in epithelial tissues. Members of the NHERF family of proteins interact with various ion transporters and signaling proteins, thereby facilitating the formation of large protein complexes in a correct spatial organization. The major goal of the studies described in this thesis was to further understand the physiological role of NHERF-1 and NHERF-2 in the regulation of intestinal ion transport. Most attention was paid to the regulation of the key transporter proteins mediating intestinal salt and water secretion and absorption, i.e. the CFTR chloride channel and the sodium/proton exchanger NHE3, respectively.

Our work unequivocally shows that the NHERF proteins are required for normal function of both CFTR and NHE3 in the intestinal tract, and provides information on the various mechanisms whereby the NHERF proteins may regulate CFTR in native epithelial cells. Surprisingly, the effect of NHERF-1 ablation on CFTR and NHE3 function differed strongly between various segments of the small intestine. Furthermore, the mechanism whereby NHE3 is regulated by NHERF-1 is different in the kidney and the intestinal tract. These differences are summarized in Tables 1 - 3 and are discussed in detail later in this chapter. In addition to the experiments performed in NHERF-deficient mice, the role of the NHERF proteins in the regulation of NHE3 and CFTR was investigated in polarized epithelial cell lines. These studies confirmed previous reports showing that NHERF-2 is required for cGMP-dependent inhibition of NHE3 by acting as a 'G-kinase anchoring protein' (GKAP) which facilitates formation of a complex containing NHERF-2, the cGMP-dependent protein kinase isoform II (cGKII) and NHE3. A search for other GKAP proteins binding to cGKII resulted in the identification of glial fibrillary acidic protein (GFAP), which, however, is not expressed in epithelial cells. Finally, an analysis of the proteome of the brush border of murine jejunum is presented. This work may serve as a starting point for future studies of changes in brush border membrane composition as a consequence of absence of one or more of the NHERF scaffolding proteins.

Functions of NHERF-1 and NHERF-2 in regulation of CFTR activity (Chapters 2 and 4)

The PDZ domain containing proteins NHERF-1 and NHERF-2 are present in various epithelial tissues, including the epithelial cells of the intestinal tract. To function as a chloride channel, CFTR needs to be localized in the apical membrane and activated by phosphorylation by cyclic nucleotide dependent kinases. The NHERF proteins may be important components of the following CFTR regulating mechanisms:

1. Targeting of CFTR to the apical membrane – In polarized epithelial cells CFTR is located in the apical membrane. Correct sorting (or targeting) of CFTR from the Golgi apparatus to the apical membrane is crucial for its function. The role of the binding of the C terminus to several PDZ proteins in the intracellular targeting of CFTR has been subject of debate for a long time and remains controversial. Several studies suggest that the C-terminal PDZ binding motif of CFTR is required for its localization in the apical

membrane. Deletion or mutation of the PDZ binding motif resulted in aberrant targeting of CFTR in MDCK cells (1, 2). Similarly, in human airway and kidney cells, a CFTR mutant (lacking the last 26 amino acids) was located in the basolateral membrane (3). In contrast, several studies using a very similar approach, showed no effect of C-terminal mutations for sorting of CFTR to the apical membrane in several cell lines, even in the same cell line in which the effect was first shown (4-6). Why comparable mutations in the PDZ binding domain of CFTR resulted in an opposite effect on CFTR targeting remains unknown. Therefore, we studied the effect of the absence of CFTR/PDZ protein binding on CFTR in a more physiological context and in a more specific manner by using NHERF deficient mice.

In the NHERF-1, NHERF-2, and NHERF-1/-2 deficient mice, CFTR staining remained confined to the apical border of the jejunal crypt cells and no evidence was found for its redistribution to the basolateral membrane. Furthermore, double staining of CFTR and villin (a microvillus marker) in jejunal crypts from wild-type and in NHERF-1 deficient mice showed that CFTR was concentrated almost completely in the microvillar region (Figure 5 of Chapter 2). Together, these results demonstrate that binding of CFTR to NHERF-1 or NHERF-2 is not required for its targeting to the apical border of epithelial cells in the jejunal crypts. However, the finding of normal apical targeting of CFTR in NHERF-1 and/or NHERF-2 deficient mice does not exclude a role for its C terminus in this process. It remains possible that the C terminus of CFTR binds to other PDZ proteins, and that binding to these alternative partners is required for apical targeting.

2. Localization and abundance of CFTR - At the apical border, CFTR can be localized in the membrane itself or in small subapical vesicles just below the apical membrane. CFTR is endocytosed and recycled back to the plasma membrane continuously, and PDZ proteins affect these processes. Only the pool of CFTR molecules present in the apical membrane is able to function in transepithelial chloride transport. We demonstrated that in NHERF-1 and NHERF-2 deficient mice the total amount of CFTR in the brush borders of epithelial cells, as measured by Western blotting, was unaltered (Table 1). In contrast, based on analysis of CFTR localization and abundance in jejunal crypts by confocal microscopy, we estimate that the mean fluorescence intensity as well as the total amount of fluorescence per crypt was reduced by ~35% in NHERF-1 and NHERF-1/-2 deficient mice (Figure 5 of Chapter 2). One possible way to explain this reduced fluorescence intensity is a more diffuse CFTR distribution in the apical region resulting in reduced local concentrations of CFTR that may drop below the detection limit.

3. Anchoring of CFTR to the cytoskeleton - NHERF-1 is known to anchor CFTR (via ezrin) to the actin cytoskeleton (7). Disruption of CFTR/cytoskeleton binding in cultured cells (using C-terminally mutated CFTR) resulted in an increased mobility of CFTR in the membrane, as measured by FRAP (fluorescence recovery after photobleaching) and by single particle tracking of individual CFTR molecules labeled with quantum dots (8, 9). An increased mobility might result in a more diffuse distribution of CFTR in the membrane as

shown in our NHERF-1 deficient mice. Uncoupling of CFTR from the cytoskeleton might also lead to an altered turnover of the channel. In MDCK cells, CFTR showed a strongly reduced half-life time in the membrane after removal of the functional PDZ binding domain (5). A higher endocytosis rate may exist also in the jejunal crypts form our NHERF-1 deficient mice and may provide a potential explanation for the more diffuse distribution of CFTR observed in this epithelial compartment.

Table 1. Summary of the ablation of the different NHERF isoforms on the localization and abundance of CFTR and NHE3

Tissue	NHERF isoform	Effect of NHERF ablation on:			
		Apical CFTR localization	CFTR abundance	Apical NHE3 localization	NHE3 abundance
Jejunum	NHERF-1	Unaltered (Chapter 2)	Unaltered (but altered distribution) (Chapter 2)	Unaltered (Chapter 3)	~40% reduced (Chapter 3)
	NHERF-2	Unaltered[1]	Unaltered (Chapter 2)		
	NHERF-3			Unaltered (10)	Unaltered (10), but mRNA level was increased (10)
Ileum	NHERF-1			Unaltered (11)	Unaltered (11)
Colon	NHERF-1			Unaltered (Chapter 3)	Reduced (Chapter 3)
	NHERF-3			Unaltered (12)	Unaltered (10,12) but mRNA level was increased (10)
Kidney	NHERF-1			Unaltered (13)	Unaltered (11,13,14)

[1] Unpublished data.

4. Phosphorylation and activation of CFTR – Opening of the CFTR chloride channel is controlled by the activity of kinases and phosphatases. Multiple kinases (e.g. PKA and cGKII) can activate CFTR by phosporylating its R domain.

PKA is anchored at specific subcellular sites by A kinase anchoring proteins (AKAPs) (15). Binding of an AKAP to PKA is important for the cAMP-dependent activation of CFTR and ezrin was shown to be an AKAP which could promote cAMP-mediated phosphorylation of CFTR (16). Since NHERF-1 and NHERF-2 are able to bind CFTR and ezrin, they can tether PKA (bound to ezrin) in close vicinity of CFTR, thereby regulating its phosphorylation and activation. Overexpression of NHERF-1 in BHK cells resulted in a ~30% increase in cAMP-mediated CFTR currents (4), whereas silencing of NHERF-1 expression

(using antisense oligonucleotides) resulted in reduced cAMP-activated currents in M-1 mouse cortical collecting duct cells (17).

In NHERF-1 deficient mice we observed a ~30% decreased cAMP-mediated activation of CFTR in the duodenum and jejunum (see Table 2).This ~30% reduction may well be a strong underestimation of the actual contribution of NHERF-1 to the activation of the total pool of CFTR present in the cell, since the amount of CFTR in ileum of wild-type mice is not a rate-limiting factor for the anion current. Based on CFTR-mediated transepithelial current measurements in mice with reduced expression levels of CFTR, it is estimated that in ileum approximately 20% of the amount of CFTR present in wild-type mice is sufficient to allow for normal CFTR-dependent chloride currents (18). This notion has been confirmed in differentiated epithelial cells in culture (19). Thus, a reduction of *functional* CFTR of more than 80% would be required to account for the seemingly moderate effect of NHERF-1 and NHERF-1/-2 deficiency that we observed in jejunal epithelial tissue.

Table 2. Summary of the effects of NHERF ablation on CFTR and NHE3 activity in murine intestinal segments, results are organized per NHERF isoform

Tissue	NHERF isoform	Effect of NHERF ablation on:			
		cAMP-/cGMP-dependent CFTR activation*	Basal NHE3 activity**	cAMP-dependent NHE3 inhibition	Ca^{2+}-dependent NHE3 inhibition
Duodenum	NHERF-1	~30% reduced HCO_3^-secretion (Chapter 2)			
	NHERF-2	Unaltered HCO_3^- secretion (Chapter 2)			
	NHERF-3	~20% reduced[1] (10)			
Jejunum	NHERF-1	~30% reduced (Chapter 2)	~45% reduced Na^+ flux (Chapter 3)	Unaltered (Chapter 3)	
	NHERF-2	Unaltered (Chapter 2)			
	NHERF-3	Unaltered[1] (10)	~50% reduced Na^+ flux (10)	Loss of inhibition (10)	
Ileum	NHERF-1	Unaltered (Chapter 2)	Unaltered (11)	Unaltered (11)	
	NHERF-2	Unaltered (Chapter 2)			
Colon	NHERF-1	Slightly (30%) but not significantly reduced[2]	~40% reduced Na^+ flux (Chapter 3)	Slightly reduced inhibition (Chapter 3)	
	NHERF-2	Unaltered[2]		Unaltered[1] (20)	Loss of inhibition (20,21)
	NHERF-3		~50% reduced (12)	Loss of inhibition (12)	Loss of inhibition (12)
Kidney	NHERF-1		Unaltered (14)	Loss of inhibition (14)	

*CFTR activity is measured by I_{sc} and/or (if mentioned) by HCO_3^- secretion. Bicarbonate secretion may not directly reflect CFTR activity (in duodenum also Slc26a6 and Slc26a3 can secrete HCO_3^-), but it is estimated that in mouse duodenum 50% of bicarbonate secretion is directly mediated by CFTR (22-24).

** NHE3 activity is measured by HOE642-insensitive Na^+-dependent acid-activated proton flux (in colon) and/or by $^{22}Na^+$ flux.

[1] cGMP-activated I_{sc} change was not measured.

[2] Only forskolin-mediated CFTR activation was measured (n=6 mice), unpublished data.

Table 3. Summary of the effects of NHERF ablation on intestinal fluid absorption

Tissue	NHERF isoform	Effect of NHERF ablation on:		
		Basal fluid absorption	cAMP-dependent fluid absorption	cGMP-dependent fluid absorption
Jejunum	NHERF-1	strongly reduced (Fig. 1 and 4 of Chapter 3)	strongly reduced inhibition (Fig. 1 and 4 of Chapter 3)	~25% reduced inhibition (Chapter 3)
	NHERF-2	Unaltered[1]	~30% reduced inhibition[1,2]	Unaltered[1]
Ileum	NHERF-1	Unaltered (Chapter 3)	Unaltered (Chapter 3)	Unaltered (Chapter 3)
	NHERF-2	~20% increased[1]	Unaltered[1]	Unaltered[1]

[1] Unpublished data.
[2] Inhibition of fluid absorption was reduced in the proximal part of the jejunum only; the other measurements summarized in this table were performed in the distal part of jejunum.

As described above (under 1.), the reduced cAMP-stimulated transepithelial chloride current in jejunum of NHERF-1 deficient mice was not due to defective targeting of CFTR. Most likely, it was caused by a reduction of functional CFTR in the apical membrane, or by an indirect effect of NHERF-1 ablation on the electrochemical driving force for chloride exit across the apical membrane. In order to discriminate between these possibilities, we measured CFTR activation in the apical membrane more directly following the permeabilization of the basolateral membrane by nystatin. Surprisingly, not the cAMP-activated, but the basically active pool of CFTR was reduced in nystatin-permeabilized jejunum from NHERF-1 deficient mice (Figure 3 of Chapter 2). These results, together with the finding that NHERF-1 ablation equally affected cAMP- and cGMP-dependent stimulation of CFTR, suggest that the reduced CFTR activation by cAMP in the absence of NHERF-1 is not due to aberrant targeting of PKA (via ezrin) to CFTR.

Ablation of NHERF-1 and/or NHERF-2 did not significantly affect CFTR activity in mouse ileum, in contrast to our findings in the jejunum (Table 2 and Figure 2 of Chapter 2). Although it could be that the mechanism of CFTR activation is different and completely independent of NHERF-1, we consider it more plausible that the reduction in functional CFTR in this compartment does not drop below the critical level (~20% of the wild-type level) that is required to maintain normal transepithelial chloride currents. This is in line with recent preliminary measurements of CFTR activity in NHERF-1 deficient/dF508 CFTR mice. In these mice the amount of dF508 CFTR is rate-limiting for the chloride current and the CFTR-mediated transepithelial chloride currents in these double transgenic mice was reduced substantially in both the jejunum and the ileum as compared to dF508 mice containing NHERF-1. Alternatively, the mechanism of CFTR activation and the role of other PDZ proteins may differ between ileum and jejunum. Several PDZ proteins compete for binding to CFTR and may affect its activity in different ways. As described in Chapter 1, CFTR activity is negatively regulated by Shank2 and CAL binding (17, 25, 26). In contrast,

NHERF-3 (like NHERF-1) may stimulate CFTR activity by crosslinking 2 CFTR molecules, which leads to an increased open probability of the channels (27-29). Future measurements of the abundance and localization of Shank2 and CAL in the different segments of the intestine of NHERF-1 null vs. wild-type mice, would be helpful in delineating a possible role for these PDZ proteins in intestinal CFTR-regulation, and whether differences observed between the segments might be mediated by these proteins. Interestingly, ablation of NHERF-1 also strongly reduced NHERF-3 abundance in jejunal epithelial cell extracts (Figure 7 of Chapter 2). This reduction in NHERF-3 protein expression is post-transcriptional, since semi-quantitative RT-PCR showed that the mRNA expression level of NHERF-3 was not changed in NHERF-1 deficient mice (unpublished results). Therefore, NHERF-1 might be important for the stabilization of NHERF-3, possibly via the formation of an NHERF-1/NHERF-3 complex demonstrated *in vitro*. (30).

Finally, the differences in NHERF-1 dependent regulation of CFTR in jejunum and ileum may also be explained by the presence of other (yet unknown) binding partner(s). Analysis of endogenous binding partners for CFTR in epithelial cells from ileum and jejunum might provide novel information about the composition of CFTR containing protein complexes. Analysis of the CFTR interactome by immunoprecipitation of CFTR and its binding partners from intestinal brush borders, followed by analysis of the complex using proteomics, might be a useful approach for such a study. Furthermore, as will be discussed later, comparing the proteomes of brush border membrane vesicles from wild-type and NHERF-1 deficient mice might render some new information about proteins that are directly or indirectly affected by NHERF-1 ablation.

The work described in this thesis addresses, for the first time, the possible roles of NHERF-1 and NHERF-2 in the cGMP-dependent, cGKII-mediated, regulation of CFTR. cGMP-dependent stimulation of CFTR in mouse jejunum was only affected by NHERF-1, but not by NHERF-2 ablation (Table 2 and Chapter 2). In contrast, cGMP-dependent inhibition of NHE3 in PS120, OK and Caco-2/bbe cells appeared NHERF-2, but not NHERF-1 dependent (31)(Chapter 3). These results indicate that the role of NHERF-1 and NHERF-2 is different for the cGMP/cGKII-dependent phosphorylation of CFTR and NHE3 (see Table 1 for an overview).

Roles of NHERF-1 and NHERF-2 in the regulation of NHE3 (Chapters 3 and 4)

NHERF-1 and NHERF-2 bind to NHE3 and are involved in the regulation of its inhibition (32, 33). NHE3 activity is inhibited by cAMP-, cGMP- and calcium-mediated phosphorylation. The role of NHERF-1 and NHERF-2 in cAMP-dependent inhibition of NHE3 activity was first established in PS120 fibroblasts. These cells lack endogenous expression of NHERF-2, have low levels of NHERF-1 protein, and failed to show cAMP-dependent inhibition of NHE3. Stable transfection of the PS120 cells with NHERF-1 or NHERF-2 restored the cAMP-dependent inhibition of NHE3 (34). Since then, the role of the NHERF proteins in cAMP-, cGMP- or Ca^{2+}-dependent NHE3 inhibition was established further in different cell lines

and in NHERF-1 null mice. In the kidney of these mice, the basal activity was unaltered, whereas the cAMP-dependent inhibition of NHE3 was lost (Table 2) (14). Lack of inhibition was probably due to loss of PKA-mediated phosphorylation in these NHERF-1 null mice (13, 14). This confirmed the model in which NHERF-1 brings PKA (bound to ezrin) in the close proximity of NHE3, stimulating its phosphorylation and inhibition.

cGMP-dependent inhibition of NHE3 in cell lines - NHERF-2 binds to cGKII and functions as a cGMP-dependent protein kinase anchoring protein (GKAP). By binding both cGKII and NHE3, NHERF-2 targets cGKII to NHE3, thereby stimulating phosphorylation and inhibition of NHE3 (31). NHE3 was acutely inhibited by the addition of cGMP in PS120 cells expressing cGKII and NHERF-2 (but not NHERF-1) (31). The specific role for NHERF-2 in cGMP-dependent inhibition of NHE3 was further confirmed in OK cells. OK cells express NHERF-1, NHERF-3 and NHERF-4, but lack (or have very low amounts of) NHERF-2 protein (35, 36). In these cells, NHE3 activity was only inhibited by cGMP after stable co-transfection with cGKII and NHERF-2 (31). These studies clearly demonstrated that NHERF-2 is required for the cGKII-mediated inhibition of NHE3, but were all performed in cells that do not express NHERF-2 endogenously. In complementary experiments, we observed that downregulation of endogenous NHERF-2 expression in Caco-2/bbe cells (by using siRNA) completely abolished cGMP/cGKII-dependent inhibition of NHE3 (Figure 2 of Chapter 4), confirming that NHERF-2 is required and sufficient for inhibition. Other studies examined the molecular mechanisms by which NHERF-2 allowed cGKII to inhibit NHE3. Pull-down and overlay experiments showed that NHERF-2 directly binds to cGKII, while NHERF-1 failed to bind with similar affinity. Furthermore, it was demonstrated that cGKII must be attached to the plasma membrane by a N-terminal myristoyl group to phosphorylate and inhibit NHE3 (31). Myristoylation of cGKII is also important for cGKII-mediated phosphorylation and stimulation of CFTR (37, 38). However, NHERF-2 is not required for cGMP-dependent phosphorylation of CFTR, since ablation of NHERF-2 in the small intestine of mice did not affect cGMP-dependent activation of CFTR (see above). This indicates that CFTR and NHE3 have a different mode of regulation. NHE3 requires an AKAP and a GKAP for cAMP- and cGMP-dependent phosphorylation respectively, whereas CFTR does not.

Regulation of NHE3 in NHERF deficient mice - From studies of the phenotype of NHERF-1 deficient mice it now becomes increasingly clear that the role of NHERF-1 in the regulation of NHE3 activity is highly tissue specific, and even the mechanisms of NHERF-1-dependent regulation may differ (see Table 1). By measuring $^{22}Na^{+}$ flux and acid-activated NHE3 transport rates, we found a decreased basal activity of NHE3 in jejunum and colon of NHERF-1 deficient mice. These results might explain the reduced basal fluid absorption rates that we observed in the jejunum of NHERF-1 null mice. However, although NHERF-1 is important for basal NHE3 activity, it did not affect the cyclic nucleotide-triggered inhibition of NHE3 in jejunum and colon. In kidney, on the other hand, basal activity of NHE3 was unchanged in the NHERF-1 null mice, whereas cAMP failed to inhibit NHE3 (Table 2) (11, 13, 14). A plausible hypothesis that may at least partially explain the tissue

specific effect of NHERF-1 on the regulation of NHE3 activity, is the assumption that the multiprotein complexes which mediate the regulation of NHE3 are composed of different proteins in different epithelia. Another prominent example of tissue-specific regulation of NHE3 is the NHE3 inhibition by EPAC (exchange protein activated by cAMP) (39). In kidney, the EPAC-mediated inhibition of NHE3 was abolished in the absence of NHERF-1 (11). We showed that the jejunal fluid absorption of both wild-type and NHERF-1 null mice remained unaffected by the EPAC-activator 8-pCPT-2'O-Me-cAMP, and the effect of this activator on colonic NHE3 activity was small, indicating that EPAC has no important role in NHE3 regulation in the intestinal tract. Why EPAC activation has a different effect on renal and intestinal NHE3 activity is still unclear.

Unlike our findings in jejunum, basal fluid absorption remained unaffected in the ileum of NHERF-1 deficient mice. Furthermore, the cAMP- and cGMP- dependent inhibition of fluid absorption was comparable in wild-type and NHERF-1 null mice, indicating that ileal fluid- and ion transport is regulated independently of NHERF-1 (Table 3). These results are in line with studies that show that increased levels of cAMP and/or cGMP affects CFTR and NHE3 activity similarly in the ileum of NHERF-1 deficient and wild-type mice (11) (Table 2 and Chapter 2).

Similar to CFTR, several PDZ proteins can compete for binding to NHE3 and may affect the regulation of NHE3 in different ways in the different segments of the intestine. It was shown previously that in NHERF-3 deficient mice the basal NHE3 activity was unaltered whereas the cAMP and Ca^{2+}-dependent inhibition of NHE3 was lost in the large intestine (Table 2) (10,12). Because NHERF-1 and NHERF-3 both bind NHE3, and because the absence of these proteins affected NHE3 inhibition in different ways, we also tested intestinal fluid transport in NHERF-1/-3 double deficient mice. The phenotype of the double deficient mice was a combination of the changes observed in the NHERF-1 and NHERF-3 single null mice. Like in the NHERF-1 single null mice, the basal fluid absorption in the jejunum as well as the basal HOE642-insensitive acid-activated proton flux in the colon were reduced in the NHERF-1/-3 null mice. Furthermore, the cAMP-dependent inhibition of NHE3 was completely absent in the double deficient mice, similar to what was observed in the NHERF-3 single null mice (12). Because the absence of both NHERF-1 and NHERF-3 did not result in an additional phenotype this suggests that NHERF-1 and NHERF-3 are involved in NHE3 regulation via different processes, although these processes might be interconnected. We showed that the NHERF-3 abundance in jejunum is reduced in NHERF-1 deficient mice, suggesting that these proteins form a complex *in vivo* (Figure 7 of Chapter 2). It is still unknown via which mechanism NHERF-3 can affect NHE3 inhibition and why the role of NHERF-1 in NHE3 regulation is different in kidney compared to jejunum and colon (see Table 1).

There is no indication that NHERF-1 is involved in the targeting of NHE3 to the apical membrane. Truncated mutants of NHE3 (which can not bind PDZ proteins) were targeted normally to the plasma membrane of OK cells (40). Furthermore, in NHERF-1

deficient mice, NHE3 was correctly localized at the apical surface of proximal tubule cells in the kidney (13). Likewise in the jejunum and colon of our NHERF-1 null mice, NHE3 was localized in (or near) the apical membrane (Figure 9 of Chapter 3). However, the NHE3 abundance in BBMVs of these intestinal segments was on average reduced by ~40%. This decrease in NHE3 protein was post-transcriptional, because the intestinal NHE3 mRNA levels were not changed in NHERF-1 null mice. We assume that the turnover of NHE3 in the apical membrane was affected by NHERF-1 ablation, which may explain the reduced basal NHE3 activity and fluid absorption rates in the intestine of NHERF-1 null mice (Chapter 3). However, more work at the molecular level is needed to fully understand the role of NHERF-1 and NHERF-3 in regulation of NHE3.

Proteome of murine jejunal brush border membrane vesicles (Chapter 5)

To understand the transport function of the small intestine in more detail at the molecular level, identification of the proteome of the brush border compartment is a helpful step. The brush border is comprised of both the apical membrane and apical recycling compartment. Highly purified brush border membrane vesicles (BBMVs) have been used previously to study the transport processes and proteins present in the apical membrane of the small intestine. In Chapter 5 of this thesis, a detailed description of the mouse jejunal brush border membrane proteome is presented. This proteome description further defines the content and composition of BBMV preparations, and identifies several novel transport proteins that were never described before as genuine constituents of the intestinal brush border. This study provides an important basis for future analysis of the quantitative composition of BBMVs from wild-type and NHERF-1 deficient mice, which will learn us more about the function of NHERF-1 in the expression, localization and stabilization of other BBM proteins.

Identification of GFAP as a cGKII binding partner (Chapter 6)

As described before, NHERF-2 can act as a cGMP-dependent protein kinase anchoring protein (GKAP), and is required for the cGKII-mediated inhibition of NHE3. Eleven binding partners of cGKI (the cytosolic cGMP-dependent protein kinase) have been identified and research of these binding partners has yielded much information about the functions of cGKI. For example, the cGKIβ binding protein IRAG ($InsP_3R$-associated cGMP kinase substrate) is required for the inhibition of $InsP_3$-dependent calcium release and the subsequent smooth muscle relaxation. cGKI-mediated smooth muscle relaxation in the intestine is crucial for the maintenance of normal gut function (41, 42).

However, binding of cGKII to anchoring proteins has received less attention. Thus far only 3 binding partners for cGKII have been identified, namely myosin, NHERF-2 and the glutamate transporter GluR1 (31, 43, 44). To find novel proteins that bind to cGKII and might function as a GKAP, we screened a mouse brain cDNA library for cGKII binding partners, using the yeast two-hybrid method. The only “hit” in this screen was GFAP (glial

fibrillary acidic protein). GFAP is a member of the intermediate filament (IF) proteins and is abundantly expressed in astrocytes. We confirmed its binding to cGKII using pull-down and overlay techniques. Furthermore, we showed that cGKII is able to phosphorylate GFAP *in vitro*. Polymerized GFAP exists in a dynamic equilibrium with a small pool of soluble GFAP. The assembly/disassembly cycle is modulated by phosphorylation of N-terminal sites. Mice that express GFAP with mutated phosphorylation sites (Ser/Thr were replaced by Ala) showed a reduced GFAP abundance suggesting that phosphorylation protects GFAP against degradation (45). In line with these results we observed that in intact SNB19 glioblastoma cells, GFAP abundance was increased after adenoviral infection with cGKII. Only catalytically active cGKII was able to affect GFAP abundance in these cells: neither the introduction of a catalytically inactive mutant of cGKII, nor the adenoviral parent vector affected GFAP protein expression (Figure 4 of Chapter 6). Semi-quantitative RT-PCR experiments showed that the mRNA expression level in SNB19 cells was not affected by adenoviral infection.

Together, these results indicate that phosphorylation of GFAP by cGKII plays an important role in the stabilization of the protein in astroglial cells. It has been shown before that increased levels of intracellular cGMP (induced by inflammatory compounds) in astrocytes affect the arrangement of intermediate filaments (including GFAP) and actin. Our data indicates that these cGMP-dependent rearrangements may depend on direct effects of cGKII on GFAP phosphorylation and stabilization.

References

1. Moyer, B. D., Duhaime, M., Shaw, C., Denton, J., Reynolds, D., Karlson, K. H., Pfeiffer, J., Wang, S., Mickle, J. E., Milewski, M., Cutting, G. R., Guggino, W. B., Li, M., and Stanton, B. A. (2000) *J Biol Chem* **275**(35), 27069-27074
2. Milewski, M. I., Mickle, J. E., Forrest, J. K., Stafford, D. M., Moyer, B. D., Cheng, J., Guggino, W. B., Stanton, B. A., and Cutting, G. R. (2001) *J Cell Sci* **114**(Pt 4), 719-726
3. Moyer, B. D., Denton, J., Karlson, K. H., Reynolds, D., Wang, S., Mickle, J. E., Milewski, M., Cutting, G. R., Guggino, W. B., Li, M., and Stanton, B. A. (1999) *J Clin Invest* **104**(10), 1353-1361
4. Benharouga, M., Sharma, M., So, J., Haardt, M., Drzymala, L., Popov, M., Schwapach, B., Grinstein, S., Du, K., and Lukacs, G. L. (2003) *J Biol Chem* **278**(24), 22079-22089
5. Swiatecka-Urban, A., Duhaime, M., Coutermarsh, B., Karlson, K. H., Collawn, J., Milewski, M., Cutting, G. R., Guggino, W. B., Langford, G., and Stanton, B. A. (2002) *J Biol Chem* **277**(42), 40099-40105
6. Ostedgaard, L. S., Randak, C., Rokhlina, T., Karp, P., Vermeer, D., Ashbourne Excoffon, K. J., and Welsh, M. J. (2003) *Proc Natl Acad Sci U S A* **100**(4), 1937-1942
7. Short, D. B., Trotter, K. W., Reczek, D., Kreda, S. M., Bretscher, A., Boucher, R. C., Stutts, M. J., and Milgram, S. L. (1998) *J Biol Chem* **273**(31), 19797-19801
8. Haggie, P. M., Stanton, B. A., and Verkman, A. S. (2004) *J Biol Chem* **279**(7), 5494-5500
9. Haggie, P. M., Kim, J. K., Lukacs, G. L., and Verkman, A. S. (2006) *Mol Biol Cell* **17**(12), 4937-4945
10. Hillesheim, J., Riederer, B., Tuo, B., Chen, M., Manns, M., Biber, J., Yun, C., Kocher, O., and Seidler, U. (2007) *Pflugers Arch* **454**(4), 575-586
11. Murtazina, R., Kovbasnjuk, O., Zachos, N. C., Li, X., Chen, Y., Hubbard, A., Hogema, B. M., Steplock, D., Seidler, U., Hoque, K. M., Tse, C. M., De Jonge, H. R., Weinman, E. J., and Donowitz, M. (2007) *J Biol Chem* **282**(34), 25141-25151

12. Cinar, A., Chen, M., Riederer, B., Bachmann, O., Wiemann, M., Manns, M., Kocher, O., and Seidler, U. (2007) *J Physiol* **581**(Pt 3), 1235-1246
13. Shenolikar, S., Voltz, J. W., Minkoff, C. M., Wade, J. B., and Weinman, E. J. (2002) *Proc Natl Acad Sci U S A* **99**(17), 11470-11475
14. Weinman, E. J., Steplock, D., and Shenolikar, S. (2003) *FEBS Lett* **536**(1-3), 141-144
15. Huang, P., Trotter, K., Boucher, R. C., Milgram, S. L., and Stutts, M. J. (2000) *Am J Physiol Cell Physiol* **278**(2), C417-422
16. Sun, F., Hug, M. J., Bradbury, N. A., and Frizzell, R. A. (2000) *J Biol Chem* **275**(19), 14360-14366
17. Lee, J. H., Richter, W., Namkung, W., Kim, K. H., Kim, E., Conti, M., and Lee, M. G. (2007) *J Biol Chem* **282**(14), 10414-10422
18. Charizopoulou, N., Wilke, M., Dorsch, M., Bot, A., Jorna, H., Jansen, S., Stanke, F., Hedrich, H. J., de Jonge, H. R., and Tummler, B. (2006) *BMC Genet* **7**, 18
19. Farmen, S. L., Karp, P. H., Ng, P., Palmer, D. J., Koehler, D. R., Hu, J., Beaudet, A. L., Zabner, J., and Welsh, M. J. (2005) *Am J Physiol Lung Cell Mol Physiol* **289**(6), L1123-1130
20. Cinar, A., Chen, M., Riederer, B., Hogema, B. M., De Jonge, H., Donowitz, M., Weinman, E. J., Kocher, O., and Seidler, U. (2006) *Pflugers Arch 2006*, http://www.physiologische-gesellschaft.de/kongress/abstracts/2006/12899
21. Lamprecht, G., and Seidler, U. (2006) *Am J Physiol Gastrointest Liver Physiol* **291**(5), G766-777
22. Schreiber, R., Boucherot, A., Murle, B., Sun, J., and Kunzelmann, K. (2004) *J Membr Biol* **199**(2), 85-98
23. Thiagarajah, J. R., and Verkman, A. S. (2003) *Curr Opin Pharmacol* **3**(6), 594-599
24. Seidler, U., Bachmann, O., Jacob, P., Christiani, S., Blumenstein, I., and Rossmann, H. (2001) *Jop* **2**(4 Suppl), 247-256
25. Kim, J. Y., Han, W., Namkung, W., Lee, J. H., Kim, K. H., Shin, H., Kim, E., and Lee, M. G. (2004) *J Biol Chem* **279**(11), 10389-10396
26. Cheng, J., Wang, H., and Guggino, W. B. (2004) *J Biol Chem* **279**(3), 1892-1898
27. Li, J., Dai, Z., Jana, D., Callaway, D. J., and Bu, Z. (2005) *J Biol Chem* **280**(45), 37634-37643
28. Wang, S., Yue, H., Derin, R. B., Guggino, W. B., and Li, M. (2000) *Cell* **103**(1), 169-179
29. Raghuram, V., Mak, D. D., and Foskett, J. K. (2001) *Proc Natl Acad Sci U S A* **98**(3), 1300-1305
30. Gisler, S. M., Pribanic, S., Bacic, D., Forrer, P., Gantenbein, A., Sabourin, L. A., Tsuji, A., Zhao, Z. S., Manser, E., Biber, J., and Murer, H. (2003) *Kidney Int* **64**(5), 1733-1745
31. Cha, B., Kim, J. H., Hut, H., Hogema, B. M., Nadarja, J., Zizak, M., Cavet, M., Lee-Kwon, W., Lohmann, S. M., Smolenski, A., Tse, C. M., Yun, C., de Jonge, H. R., and Donowitz, M. (2005) *J Biol Chem* **280**(17), 16642-16650
32. Yun, C. H., Lamprecht, G., Forster, D. V., and Sidor, A. (1998) *J Biol Chem* **273**(40), 25856-25863
33. Lamprecht, G., Weinman, E. J., and Yun, C. H. (1998) *J Biol Chem* **273**(45), 29972-29978
34. Yun, C. H., Oh, S., Zizak, M., Steplock, D., Tsao, S., Tse, C. M., Weinman, E. J., and Donowitz, M. (1997) *Proc Natl Acad Sci U S A* **94**(7), 3010-3015
35. Hryciw, D. H., Ekberg, J., Ferguson, C., Lee, A., Wang, D., Parton, R. G., Pollock, C. A., Yun, C. C., and Poronnik, P. (2006) *J Biol Chem* **281**(23), 16068-16077
36. Yun, C. C., Chen, Y., and Lang, F. (2002) *J Biol Chem* **277**(10), 7676-7683
37. Vaandrager, A. B., Smolenski, A., Tilly, B. C., Houtsmuller, A. B., Ehlert, E. M., Bot, A. G., Edixhoven, M., Boomaars, W. E., Lohmann, S. M., and de Jonge, H. R. (1998) *Proc Natl Acad Sci U S A* **95**(4), 1466-1471
38. Vaandrager, A. B., Ehlert, E. M., Jarchau, T., Lohmann, S. M., and de Jonge, H. R. (1996) *J Biol Chem* **271**(12), 7025-7029
39. Honegger, K. J., Capuano, P., Winter, C., Bacic, D., Stange, G., Wagner, C. A., Biber, J., Murer, H., and Hernando, N. (2006) *Proc Natl Acad Sci U S A* **103**(3), 803-808
40. Cha, B., Kenworthy, A., Murtazina, R., and Donowitz, M. (2004) *J Cell Sci* **117**(Pt 15), 3353-3365
41. Fritsch, R. M., Saur, D., Kurjak, M., Oesterle, D., Schlossmann, J., Geiselhoringer, A., Hofmann, F., and Allescher, H. D. (2004) *J Biol Chem* **279**(13), 12551-12559
42. Schlossmann, J., Ammendola, A., Ashman, K., Zong, X., Huber, A., Neubauer, G., Wang, G. X., Allescher, H. D., Korth, M., Wilm, M., Hofmann, F., and Ruth, P. (2000) *Nature* **404**(6774), 197-201
43. Vo, N. K., Gettemy, J. M., and Coghlan, V. M. (1998) *Biochem Biophys Res Commun* **246**(3), 831-835
44. Serulle, Y., Zhang, S., Ninan, I., Puzzo, D., McCarthy, M., Khatri, L., Arancio, O., and Ziff, E. B. (2007) *Neuron* **56**(4), 670-688
45. Takemura, M., Gomi, H., Colucci-Guyon, E., and Itohara, S. (2002) *J Neurosci* **22**(16), 6972-6979

SUMMARY

The chloride channel CFTR (cystic fibrosis transmembrane conductance regulator) and the sodium/proton exchanger NHE3 are key proteins involved in transepithelial ion and water transport in several epithelial tissues, including the intestine. To ensure proper localization and function of CFTR and NHE3 several processes are of crucial importance, including 1) the production and folding of these proteins, 2) targeting of the proteins to the apical membrane, 3) their half-life time in the membrane, and 4) the regulation of their activity by phosphorylation. In this thesis we mainly focus on the role of the NHERF (NHE3 Regulatory Factor) proteins as regulators of CFTR and NHE3 activity. The members of the NHERF family of proteins (NHERF-1, -2, -3 and -4) contain PDZ protein-protein interaction domains and mediate the formation of large protein complexes, thereby affecting the localization and/or activation of their binding partners.

The role of the NHERF proteins in the regulation of CFTR is controversial. To date, most studies have been performed in cultured cells in which the NHERF proteins and/or the studied ion transporters were overexpressed or mutated to prevent binding. In contrast, our studies have been performed mainly in native murine intestine, in which the role of individual NHERF proteins in the regulation of ion transport was studied by using "knockout" mice.

Functions of NHERF-1 and NHERF-2 in CFTR regulation and localization is described in **Chapter 2**. Here we show that, in jejunal crypts of NHERF-1 and NHERF-2 deficient mice, all detectable CFTR was localized apically, indicating that the trafficking of CFTR to the apical membrane is not dependent on the presence of NHERF-1 and/or NHERF-2. Moreover, Western blot analysis showed that the total abundance of CFTR in the intestine of NHERF-1 and NHERF-2 deficient mice was unaltered. However, the local abundance of CFTR in the crypts, as detected by confocal microscopy, was reduced by ~30% in NHERF-1 deficient mice. To account for these seemingly discrepant findings, we postulate that NHERF-1 ablation results in a more diffuse distribution of CFTR in the apical membrane and/or subapical vesicles.

Protein kinase A (PKA) and cGMP dependent kinase II (cGKII) are known to phosphorylate and activate CFTR in response to increased levels of cAMP and cGMP, respectively. We found that cAMP- and cGMP-dependent activation of CFTR was moderately reduced in the duodenum and jejunum (but not in ileum) of NHERF-1 deficient mice. No changes were observed in NHERF-2 deficient mice. The reduced activation of CFTR in NHERF-1 null mice may be explained by the altered distribution of CFTR in the NHERF-1 deficient mice. We found no evidence for a model in which CFTR targeting of PKA is mediated by NHERF-1.

The role of NHERF-1 in the regulation of NHE3 was examined in **Chapter 3**. NHERF-1 deficient mice displayed a decreased basal fluid absorption and a reduced sodium absorption in the jejunum. In addition, basal (acid-activated) NHE3 activity was decreased in the colon of NHERF-1 null mice. These observations may be explained by the

reduced NHE3 protein level that we observed in the brush border membrane fraction of jejunum and colon of these mice. In contrast to the basal activity, the cAMP- and/or cGMP-dependent inhibition of NHE3 was not appreciably affected in NHERF-1 deficient mice. Ablation of both NHERF-1 and NHERF-3 resulted in both a decreased basal fluid absorption and a loss of cAMP-dependent inhibition of NHE3, which was also observed in NHERF-3 single-deficient mice. Unexpectedly, in ileum (in contrast to jejunum) NHERF-1 ablation neither affected fluid absorption nor cyclic nucleotide dependent CFTR-mediated chloride secretion (Chapter 2).

In **Chapter 4** we describe the effects of NHERF-1 and/or NHERF-2 gene knockdown on cGKII-mediated regulation of NHE3 and CFTR activity in polarized epithelial cell lines. Based on measurements of Na^+/H^+ exchange rates in Caco-2/bbe cells, NHERF-2 was shown to be required for cGMP-dependent inhibition of NHE3. In contrast, knock-down of NHERF-1 and NHERF-2 did not affect cGMP-stimulated iodide efflux (a specific indicator for CFTR activity) in IEC-CF7 cells. Taken together, the results indicate that in these cells NHERF-2 is required for cGKII-dependent regulation of NHE3, but not of CFTR.

An overview of the proteome of the jejunal brush border of the mouse is presented in **Chapter 5**. A total of 570 proteins were identified, including 45 known transporters. Eighteen of these transporters were not previously identified in intestinal cells. The presence of aquaporin 7, Glut9b (glucose transporter 9b), NIS (Na^+/I^- symporter), non-gastric H^+/K^+-ATPase and MPV (major vault protein) in the apical membrane was confirmed by immunoblotting and immunofluorescence microscopy.

Finally, the experiments described in **Chapter 6** show that the glial fibrillary acidic protein (GFAP) is a specific binding partner for cGKII. cGMP dependent kinase anchoring proteins (GKAPs) bind the kinases, thereby increasing the efficiency of phosphorylation of the target proteins. Using the yeast two-hybrid system, we searched for novel cGKII binding partners and found an interaction with GFAP. GFAP is a member of the intermediate filament protein family (IF) and is present in astrocytes of the central nervous system. The N-terminal part of cGKII was shown to bind to the coil 2 region of GFAP. Binding of GFAP to cGKII was confirmed by pull-down and gel overlay experiments. cGKII was able to phosphorylate GFAP *in vitro*. In addition, expression of active cGKII in cultured glioblastoma cells (using adenoviral infection), but not of a catalytically inactive form, increased GFAP abundance. In contrast, mRNA levels of GFAP were not affected by cGKII expression. From our data we propose that cGKII-mediated phosphorylation of GFAP in the intracellular environment results in a more stable configuration and a prolonged half-life of this glial cell specific intermediate filament protein.

SAMENVATTING

Het chloride kanaal CFTR ('cystic fibrosis transmembrane conductance regulator') en de natrium/proton uitwisselaar NHE3 vervullen een sleutelrol in transepitheliaal ionen- en water transport in verschillende weefsels, inclusief de darm. Voor een correct functioneren van CFTR en NHE3 is een aantal processen cruciaal: 1) de productie en vouwing van deze eiwitten, 2) transport van de eiwitten naar, en lokalisatie in het apicale membraan, 3) de verblijftijd van de eiwitten in het membraan en 4) de regulatie van CFTR en NHE3 activiteit door middel van eiwit fosforylering. In dit proefschrift staat voornamelijk de rol van de NHERF ('NHE3 regulatory factor') eiwitten als regulatoren van CFTR en NHE3 activiteit centraal. De NHERF eiwitten (NHERF-1, -2, -3 en -4) bevatten PDZ eiwit-eiwit interactie domeinen en verzorgen de vorming van eiwitcomplexen, waardoor de lokalisatie en/of activiteit van hun bindingspartners wordt beïnvloed.

De rol van de NHERF eiwitten in de regulatie van CFTR is controversieel. De bestaande studies waren meestal uitgevoerd in gekweekte cellen waarin die de NHERF eiwitten en/of the ionen transporteurs tot overexpressie waren gebracht, of waarin de binding tussen de transporteurs en de NHERF eiwitten was verbroken door een mutatie. Onze studies zijn daarentegen grotendeels uitgevoerd in natief darmepitheel, waarbij we de rol van de NHERF eiwitten in de regulatie van ion transport bestudeerden in normale en in NHERF "knockout" muizen.

De rol van NHERF-1 en NHERF-2 in CFTR regulatie en lokalisatie is beschreven in **hoofdstuk 2**. Hierin hebben we aangetoond dat al het detecteerbare CFTR eiwit apicaal gelocaliseerd bleef in de crypten van het jejunum van NHERF-1 en NHERF-2 deficiënte muizen. Dit impliceert dat het transport van CFTR naar het apicale membraan niet door de afwezigheid van NHERF-1 en/of NHERF-2 gestoord werd. Daarnaast toonden we met behulp van Western blots aan dat ook de totale hoeveelheid CFTR eiwit niet veranderd was in NHERF-1 en/of NHERF-2 knockout muizen. Confocale immunofluorescentie microscopie liet daarentegen zien dat de locale expressie van CFTR eiwit in de crypten van het jejunum met ~30% verlaagd was in NHERF-1 deficiënte muizen. We interprteren deze verschillende waarnemingen als een aanwijzing voor een meer diffuse distributie van CFTR in het apicale membraan en/of het sub-apicale compartiment als gevolg van het ontbreken van de CFTR-NHERF-1 interactie.

Het is bekend dat de eiwitkinasen PKA (proteïne kinase A) en cGKII (cGMP afhankelijk eiwitkinase type II) CFTR door middel van fosforylering kunnen activeren na een verhoging van respectievelijk de cAMP en cGMP niveaus in de cel. Wij hebben gevonden dat cAMP- en cGMP-afhankelijke CFTR activiteit verminderd is in het duodenum en jejunum (maar niet in het ileum) van NHERF-1 deficiënte muizen. Deze veranderingen werden niet waargenomen in NHERF-2 deficiënte muizen. De verminderde activiteit van CFTR in NHERF-1 deficiënte muizen zou een gevolg kunnen zijn van de veranderde distributie van CFTR in het apicale compartiment van de enterocyt. Wij hebben geen aanwijzingen

gevonden voor een alternatief model waarbij NHERF-1 nodig is om PKA in de buurt van het CFTR te verankeren en fosforylering van CFTR te bevorderren.

De rol van NHERF-1 in de regulatie van NHE3 is onderzocht in **hoofdstuk 3.** NHERF-1 deficiënte muizen vertoonden in het jejunum een verlaagde basale vloeistofabsorptie en een verminderde natrium absorptie. Daarnaast was in het colon van deze NHERF-1 knockout muizen de basale NHE3 activiteit verlaagd. Deze effecten van NHERF-1 deficïentie konden worden verklaard door een afname van de hoeveelheid NHE3 eiwit in de borstelzoom membraan van het jejunum en colon van deze muizen. In tegenstelling tot de basale NHE3 activiteit waren de cAMP- en de cGMP-afhankelijke remming van NHE3 activiteit niet aantoonbaar veranderd in NHERF-1 deficiënte muizen. Afwezigheid van zowel NHERF-1 als NHERF-3 (in NHERF-1-/NHERF-3-dubbel-deficiënte muizen) resulteerde echter in verlaagde basale vloeistofabsorptie alsmede in verlies van de cAMP-afhankelijke remming van NHE3. Dit verlies van cAMP remming van NHE3 was al eerder aangetoond in NHERF-3 deficiënte muizen, en is dus NHERF-3 specifiek. Tegen onze verwachting in vonden we in het ileum van NHERF-1 deficiënte muizen geen aanwijzingen voor een veranderde vloeistofabsorptie (hoofdstuk 3) of cAMP-/cGMP-afhankelijk chloride transport via CFTR (hoofdstuk 2).

In **hoofdstuk 4** beschrijven we de effecten van NHERF-1 en/of NHERF-2 gen "knock-down" op cGKII-afhankelijke regulatie van NHE3 en CFTR activiteit in gepolariseerde epitheliale cellijnen. Op basis van meting van Na^+/H^+-uitwisseling in Caco-2/bbe cellen konden we laten zien dat NHERF-2 noodzakelijk was voor de cGMP-afhankelijke remming van NHE3 in deze humane colon cellijn. Daarentegen had een verlaagde expressie van NHERF-1 en NHERF-2 in IEC-CF7 cellen geen effect op de cGMP-afhankelijke CFTR activiteit, gemeten met behulp van jodide efflux. Tezamen suggereren deze resultaten dat NHERF-2 noodzakelijk is voor cGKII-afhankelijke regulatie van NHE3, maar niet van CFTR.

In **hoofdstuk 5** wordt een analyse van het proteoom van de brush border membraan van het jejunum van de muis gepresenteerd. In totaal werden 570 eiwitten geïdentificeerd, waaronder 45 transport eiwitten. Achttien van deze transport eiwitten waren nog nooit eerder aangetoond in darmepitheel. Door middel van immunoblots en immunofluorescentie microscopie kon de aanwezigheid van de eiwitten aquaporine 7, Glut9b ('glucose transporter 9b'), NIS ('Na^+/I^- symporter'), non-gastric H^+/K^+-ATPase en MPV ('major vault protein') in het apicale membraan bevestigd worden.

Tenslotte laten we met de experimenten die beschreven staan in **hoofdstuk 6** zien dat GFAP ('glial fibrillary acidic protein') een specifieke bindingspartner is van cGKII. 'Verankerings' eiwitten (GKAPs) voor cGMP afhankelijke kinases positioneren deze kinases in de nabijheid van hun substraat en verhogen de efficiëntie van de fosforylering van deze substraat eiwitten. Met behulp van het gist 'two-hybrid' systeem hebben we gezocht naar nieuwe bindingpartners voor cGKII. Hierbij werd GFAP als een nieuwe GKAP geïdentificeerd. GFAP is een lid van de familie van intermediaire filament (IF) eiwitten en is aanwezig in astrocyten van het centrale zenuwstelsel. Het amino-uiteinde van cGKII bleek te binden aan de 'coil 2' regio van GFAP. De binding van GFAP aan cGKII kon bevestigd worden met

behulp van ‘pull-down’ en ‘gel overlay’ experimenten. cGKII bleek ook in staat om GFAP *in vitro* te fosforyleren. Expressie van katalytisch actief cGKII (middels adenovirale infectie in gekweekte glioblastoom cellen) resulteerde in een verhoging van de endogene hoeveelheid GFAP eiwit. Een katalytisch inactieve cGKII mutant had dit effect niet. De mRNA expressie van GFAP werd niet beïnvloed door de adenovirale infecties. Deze resultaten passen in een model waarin de cGKII-afhankelijke fosforylering van GFAP in de gliacellen resulteert in een stabielere configuratie en een verhoogde halfwaardetijd van dit astrocyt-specifieke intermediaire filament eiwit.

Curriculum Vitae

Nellie Broere werd geboren op 17 juni 1982 te Rotterdam en groeide op in Capelle aan den IJssel. In 1999 behaalde zij haar Hoger Algemeen Voortgezet Onderwijs diploma aan het Wartburg College te Rotterdam. In september van hetzelfde jaar begon zij aan de opleiding Biologie en Medisch laboratorium onderzoek aan de Hogeschool Rotterdam. Tijdens de opleiding werden de onderzoeksstages doorlopen aan de Erasmus Universiteit binnen de afdeling Biochemie onder begeleiding van Dr. B.M. Hogema en Dr. H.R. de Jonge. Na het behalen van het afsluitend examen in juli 2003 startte zij in september als Assistent in Opleiding op de afdeling Biochemie, Faculteit der Geneeskunde van de Erasmus Universiteit Rotterdam. Het project betrof: “The role of the tandem PDZ proteins NHERF-1 and NHERF-2 as regulators of the CFTR chloride channel” en werd wederom uitgevoerd onder leiding van Dr. B.M. Hogema en Dr. H.R. de Jonge. Sinds maart 2008 is zij via Quintiles te Hoofdorp gedetacheerd als clinical research associate (CRA) bij de firma Pfizer bv.

Dankwoord / Acknowledgements

Een promotie doe je niet alleen!

Daarom zijn deze laatste pagina's van mijn proefschrift misschien wel de belangrijkste van dit boekje. Zonder de hulp en steun van vele mensen was mijn promotie nooit een feit geworden. Voor mij is promoveren veel meer dan het schrijven van een proefschrift. Het is een proces, met mooie momenten en leerpunten (zowel wetenschappelijk als niet-wetenschappelijk), een wijze levensles. Ik wil dan ook *een ieder*, die op welke wijze dan ook, heeft bijgedragen aan deze levensles hartelijk bedanken! Ik voel me bevoorrecht dat ik dit alles heb mogen meemaken en dat er zoveel mooie mensen om mij heen stonden!

Graag wil ik toch nog enkele mensen persoonlijk bedanken:

Prof.dr. J.P. Verrijzer, hartelijk dank dat u mijn promotor wilt zijn en dat u mij de ruimte en vrijheid hebt geboden om dit onderzoek te doen.
De co-promotoren Dr. H.R. de Jonge en Dr. B.M. Hogema, beste Hugo en Boris, jullie hadden beiden een onmisbaar en onfeilbaar vertrouwen in het project, de experimenten, maar bovenal in de goede afloop van mijn promotieonderzoek en daar wil ik jullie hartelijk voor danken! Hugo, je passie voor wetenschap en bijna oneindige kennis van de vakliteratuur hebben steeds weer een grote indruk op mij gemaakt. Wat er ook uit een experiment kwam, jij zag altijd de positieve kanten. Bedankt voor al je waardevolle bijdragen aan de interpretatie en verwoording van de resultaten, maar bovenal dank dat je mij de kans hebt geboden om binnen "lab 1" mijn promotieonderzoek te mogen doen! Boris, mijn directe begeleider en "partner" op het NHERF project, onze samenwerking begon al toen ik als HLO-stagiaire op lab 1 kwam. Sindsdien hebben we vele uren samen gepipetteerd, gekloneerd, DNA en sequence gelen gerund, gekweekt, cellen getrild en BBMV's gemaakt, bij de ussing kamers gezeten, naar Western blots gestaard, nieuwe experimenten bedacht en tenslotte teksten geschreven en herschreven. Ik ben je dankbaar voor alles wat je me geleerd hebt, voor je vertrouwen, nauwkeurigheid en geduld. Toen ik je als stagiaire voor het eerst de hand schudde had ik nooit kunnen denken of dromen dat ik nu, een paar jaar later, de laatste alinea's van dit proefschrift zou schrijven!

Graag wil ik de leden van de promotiecommissie bedanken voor hun inzet, belangstelling en tijd: Prof.dr. J.A. Grootegoed, Prof.dr. F.G. Grosveld, Prof.dr. J.P.T.M van Leeuwen, Prof.dr. W.H. Moolenaar, Prof.dr. M. Donowitz en Prof.dr. U. Seidler.
Prof.dr. M. Donowitz, dear Mark, I want to thank you for carefully reading the manuscript of this thesis, for your enthusiastic and positive personal and scientific input, and for the great and inspiring collaboration with you and the people from your lab. It is a great honor to me that you came all the way from Baltimore, to take part in the opposition during my thesis defence.

Liebe Frau Prof.dr. U. Seidler, an dieser Stelle möchte ich mich recht herzlich bei Ihnen für die enge, erfolgreiche Zusammenarbeit bedanken. Ich bewundere Ihre Arbeit sehr und fühle mich geehrt, daß Sie extra aus Hannover kommen, um als Mitglied der Prüfungskommission an meiner Promotion teil zu nehmen.

Alle mensen van 'lab 1' hartelijk dank voor jullie hulp, input en de fijne tijd. Alice, Martina en Marcel Bijvelds bedankt voor al de keren dat jullie insprongen bij de ussing kamer experimenten (als er op de meest cruciale momenten weer eens een storing was) en voor de gezellige thee-uurtjes. Marcel Edixhoven, bedankt voor je intensieve betrokkenheid bij het 'GFAP project'. Huub, bedankt voor je hulp bij het microscoopwerk, maar vooral voor alle leuke gesprekken en lunches. Ben, bedankt voor je heldere blik op en input tijdens de werkbesprekingen. Sietske, al ben je al jaren vertrokken naar Leiden toch wil ik je graag bedanken want ik heb veel van je geleerd. Ik heb warme herinneringen aan al die uren dat we samen gisten hebben uitgeplaat, terwijl we over van alles en nog wat kletsten. Christina, samen hebben we de 'AIO-kamer' omgebouwd van 'een kamer voor papieropslag' tot een werkkamer met posters en planten. Bedankt voor alles wat we de afgelopen jaren hebben doorgemaakt en besproken, bij jou kon ik altijd mijn verhaal kwijt. Ik wens je veel succes met het afronden van je eigen promotie en ik vind het heel fijn dat je, in deze voor jou zo drukke tijd, mijn paranimf wilt zijn!

Hartelijk dank ook aan alle stagiaires die de afgelopen jaren de afdeling kwamen versterken: Suaad, Alex, Patrick, Paulette, Joost, Samira, Vera, Natasha, Salim, Richard en Aryandi. Vera, ik wil jou bijzonder bedanken voor onze nauwe samenwerking en de gezellige tijd. Ik hoop dat je het naar je zin hebt in Malawi en wens je heel veel succes met het promotieonderzoek waar je binnenkort aan gaat beginnen.

Uiteraard wil ik ook de andere mensen van de afdeling biochemie bedanken voor hun hulp, belangstelling en het creëren van een fijne werkomgeving. In het bijzonder wil ik mijn 'kamergenootjes' Diederik van Deursen en Diederik Kuster bedanken! Diederik van Deursen, ik wens je heel veel succes met de afronding van je eigen proefschrift, de laatste loodjes wegen het zwaarst maar zijn de moeite meer dan waard! Diederik Kuster, ik ken weinig mensen die zo'n positieve levenshouding hebben als jij, bedankt voor alle gezelligheid en belangstelling! Ik wens je veel succes met de tweede helft van je promotieonderzoek.

Graag wil ik Tom de Vries Lentsch bedanken voor zijn enorme hulp bij de grafische opmaak van het proefschrift. Tom, zonder jouw hulp en precisie was het zeker niet zo mooi geworden!

Ook buiten de muren van de universiteit en wetenschap zijn er veel mensen te bedanken:

Lieve familie, vrienden en vriendinnen, ik realiseer me dat ik vaak onbegrijpelijke verhalen heb verteld over het lab en mijn proeven. Ondanks mijn pogingen heb ik velen van jullie nooit echt goed uit kunnen leggen waar ik nu precies mee bezig was. Toch zijn jullie nooit opgehouden om mee te leven met het wel en wee van mijn 'lab leven'. Ik noem jullie niet allemaal bij naam, maar dat doet niets af aan mijn dank. Jullie onafgebroken belangstelling en steun waren voor mij onmisbaar!

In het bijzonder wil ik wel mijn oma's noemen. Lieve oma's, ik weet dat jullie opkijken naar dit proefschrift. Maar dit proefschrift vertegenwoordigd slechts kennis, geen wijsheid. Ik hoop ooit uw (levens)wijsheid te bezitten!

Arie, mijn lieve broer, ik ben ongelofelijk trots dat jij mijn paranimf wil zijn! Bedankt voor de fijne band die we hebben. Onze samenwerking heeft al heel wat succesvolle resultaten opgeleverd. Dat zie ik iedere dag in mijn huis en ook het 'brainstormen' voor de kaft van dit proefschrift is daar een mooi voorbeeld van.

Lieve pap en mam, jullie komen dan wel op de laatste, maar zeker niet op de minste plaats in dit dankwoord. Dankzij jullie ben ik gekomen waar ik nu sta! Jullie hebben me niet alleen geleerd maar vooral ook voorgeleefd dat 'geloof, hoop en liefde' de fundamenten voor dit leven zijn. Bedankt dat jullie er altijd voor me zijn om vreugde en verdriet te delen, om me te steunen en te adviseren. Ik ben ontzettend trots en dankbaar om jullie dochter te mogen zijn!

Bedankt !

Nellie

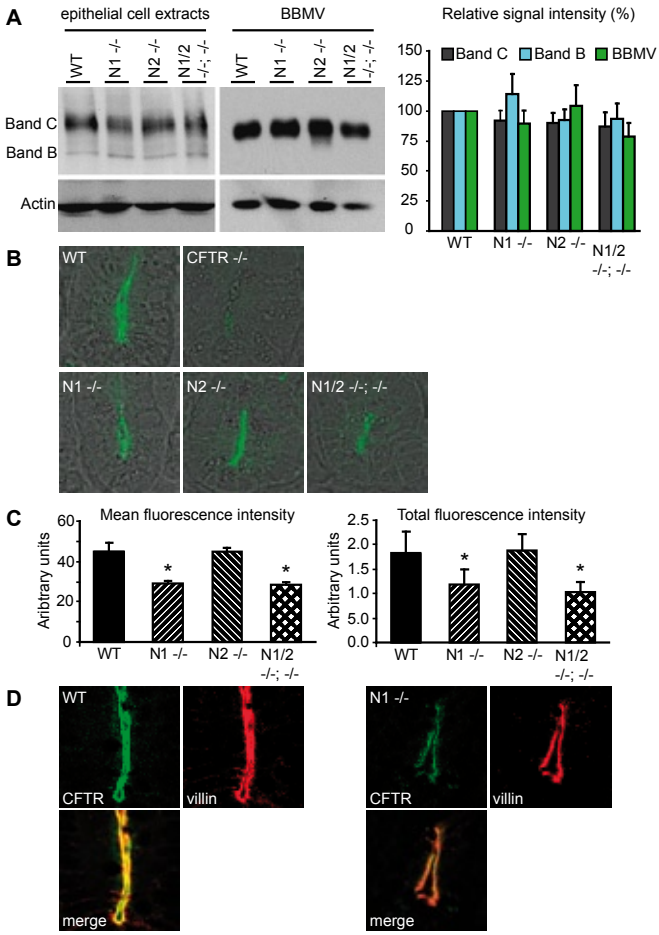

Chapter 2, figure 5. Western blot analysis of CFTR expression in jejunal epithelium and immunocytochemical detection of CFTR in jejunal crypt cells from WT, NHERF-1-deficient (N1-/-), NHERF-2-deficient (N2-/-), and NHERF-1/2-deficient (N1/2-/-) mice. *A*, Western blot analysis of CFTR in jejunal epithelial cell extracts (20 μg/lane) and BBMVs from jejunum (5 μg/lane) displayed no significant difference in the amounts of CFTR protein among mice of the different genotypes. The positions of *band B* (immature CFTR) and *band C* (mature, complex glycosylated CFTR) are indicated. Actin was used as a loading control. Representative Western blots from at least five independently isolated samples are shown at the *left*, and the average amounts of CFTR levels relative to wild type mice are shown in the *right panel*. The data represent relative signal intensity of at least eight Western blots. The *error bars* indicate the S.E. *B*, confocal microscopic analysis of CFTR abundance and localization in jejunal crypts of wild type, NHERF-1-deficient, NHERF-2-deficient, NHERF-1/2-deficient, and CFTR-deficient (CFTR-/-) mice. CFTR-dependent fluorescence was significantly ($p<0.05$) reduced in NHERF-1-and NHERF-1/2-deficient mice. No signal was detected in sections from CFTR-deficient mice, demonstrating the high specificity of the antibody. *C*, quantitative analysis of confocal microscope datasets of three sex- and age-matched couples of wild type, NHERF-1-, NHERF-2-, and NHERF-1/2-deficient mice. Three jejunal crypts from each section were analyzed, and the total and average intensities from all Z-stacks with detectable CFTR signal were calculated for each individual crypt. The average intensity was significantly lower in NHERF-1 and NHERF-1/2 null mice compared with wild type (*left panel*). Likewise, the total intensity per crypt was reduced in NHERF-1 and NHERF-1/2 but not in NHERF-2-deficient mice (*right panel*). *, $p<0.05$ *versus* wild type. *D*, CFTR and villin abundance in jejunal crypts was studied by confocal microscopy in wild type (*left three images*) and NHERF-1-deficient mice(*right three images*). CFTR (shown in *green*) colocalization with villin (shown in *red*) in the apical border is unaltered in NHERF-1 null mice compared with wild type control.

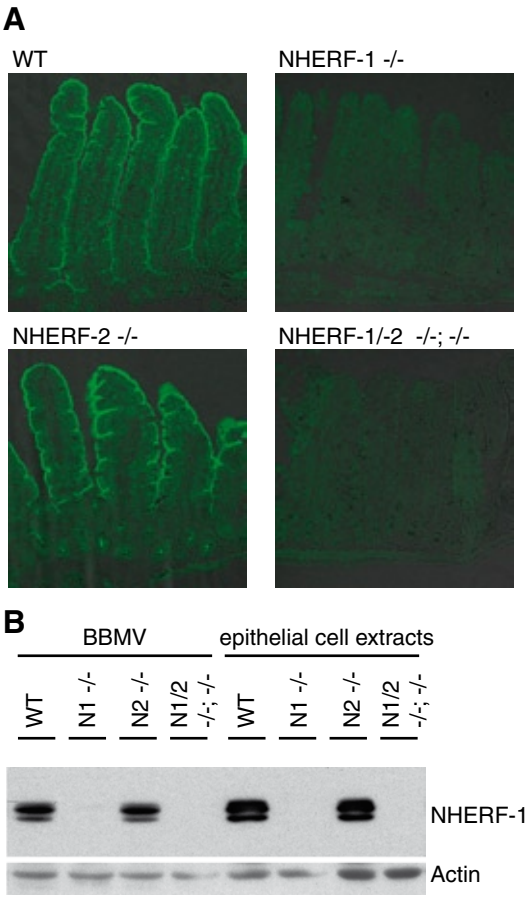

Chapter 2, figure 6. Localization and quantification of NHERF-1 in jejunum by immunocytochemical and Western blot analysis. *A*, immunocytochemical staining shows that NHERF-1 lines the apical border of epithelial cells along the entire crypt-villus axis. No alterations were observed in NHERF-2-deficient (N2-/-) mice. No staining was detected in tissue sections from NHERF-1-deficient (N1-/-) and NHERF-1/2 double deficient (N1/2-/-) mice. *B*, Western blot analysis of NHERF-1 in pooled BBMV extracts from jejunum (5 μg/lane) and pooled jejunal epithelial cell extracts (10 μg/lane). NHERF-1 expression was not significantly altered in NHERF-2-deficient mice. Actin was used as a loading control.

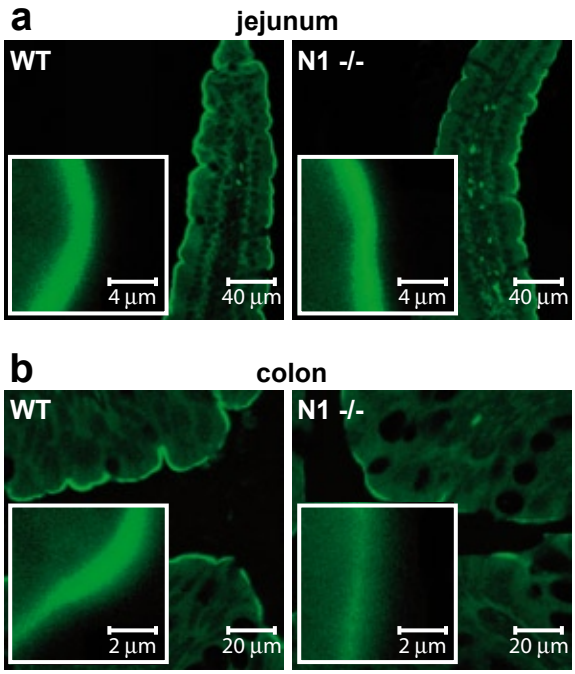

Chapter 3, figure 8. Immunohistochemical NHE3 staining reveals normal localization of NHE3 in the jejunal and colonic apical membrane of NHERF-1 -/- mice. The NHE3 localization at the apical border of the jejunum (Figure 8A) and colon (Figure 8B) was qualitatively similar in NHERF-1 +/+ and -/- mice, with considerable variability in the signal intensity within each group of mice. Images are representative examples from five independent experiments. Inserts show a 10x magnification of a part of the image shown in the larger panels.

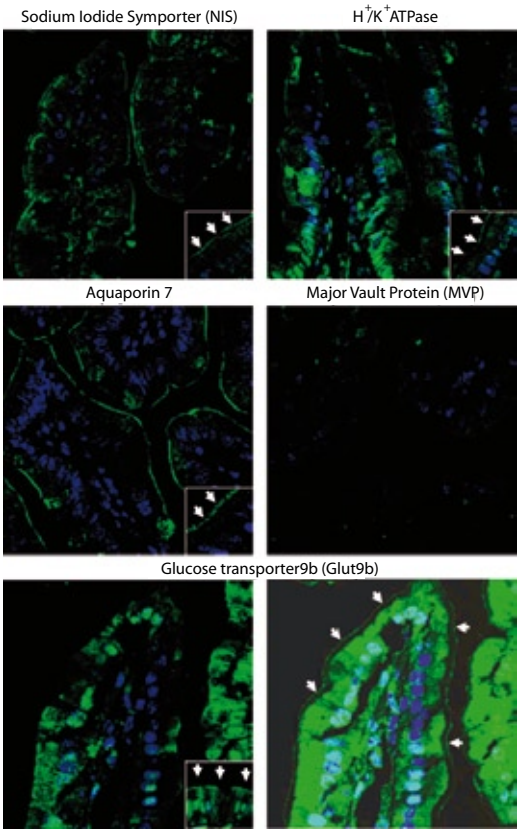

Chapter 5, figure 4. Validation of presence in mouse jejunal BBMV of several transport proteins using immunofluorescence/light microscopy for localization. Histologic sections (4 μm) of mouse jejunum were stained for localization of Na-I co-transporter, non-gastric H^+/K^+-ATPase, aquaporin 7, major vault protein (MVP), and Glut9b with Alexa 488 tagged secondary antibody (1:100). IF localization supported presence in the BB of NIS, non-gastric H^+/K^+-ATPase, aquaporin 7, and a low level of Glut 9b. Bottom right is overexposed to more clearly demonstrate BB Glut 9b (arrows) Major vault protein was intracellular with a small amount of apical signal that could not be definitely separated from edge artifact. Inserts represent higher power magnification (400x) of jejunal BB. Arrows indicate BB expression. Nuclei stained with Hoechst 350.

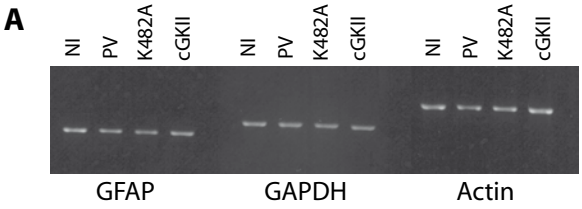

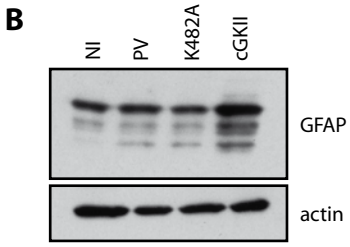

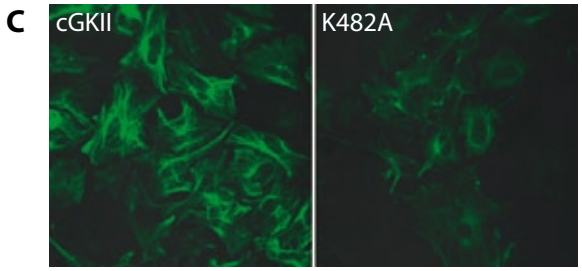

Chapter 6, figure 4. GFAP expression and abundance is upregulated in cells expressing active cGKII. *A.* Semi-quantitative PCR of cDNA from SNB19 cells showed that GFAP mRNA expression is unaltered in cells that were infected with the catalytically active cGKII (cGKII) compared to non-infected (NI), parent vector (PV) or catalytically inactive cGKII (K482A) infected cells. GAPDH and actin were used to normalize the cDNA input for the PCR reactions. *B.* The amount of GFAP protein is ~4-fold increased in cells that were infected with adenovirus encoding cGKII (cGKII) compared to non-infected (NI), parent vector (PV) or catalytically inactive cGKII (K482A) infected cells. Actin was used as a loading control. *C.* Confocal images of SNB19 cells infected with adenovirus encoding cGKII (cGKII; left panel) display a strong increase in GFAP abundance compared to cells expressing catalytically inactive cGKII (cGKII K482A; right panel). Images are representative examples of four independently performed experiments.